THESIS

DEVELOPMENT OF AN ULTRASENSITIVE ELISA FOR THE DETECTION OF *MYCOBACTERIUM TUBERCULOSIS* ANTIGENS: AN IMPOSSIBLE CHALLENGE OR A PROMISING FEAT?

Submitted by

Kala Early

Department of Microbiology, Immunology, and Pathology

In partial fulfillment of the requirements

For the Degree of Master of Science

Colorado State University

Fort Collins, Colorado

Summer 2022

Master's Committee:

Advisor: Karen Dobos
Co-Advisor: Carolina Mehaffy

Alan Schenkel
Charles Henry

ABSTRACT

DEVELOPMENT OF AN ULTRASENSITIVE ELISA FOR THE DETECTION OF *MYCOBACTERIUM TUBERCULOSIS* ANTIGENS: AN IMPOSSIBLE CHALLENGE OR A PROMISING FEAT?

Tuberculosis (TB) has been classically characterized as a two-state disease with active and latent phases. Latent TB infection (LTBI) is diagnosed by either the tuberculin skin test (TST) or the Interferon Gamma Release Assay (IGRA) test. However, both diagnostic tests are unable to differentially diagnose active TB and LTBI and perform poorly in immunocompromised patients. The TST is further complicated by cross-reactivity with BCG vaccination. Therefore, further diagnostic discovery for LTBI is needed for differential diagnosis and to identify those at risk of progression to active TB for subsequent treatment. Extracellular vesicles (EVs) are nanovesicles released by eukaryotic cells. EVs from TB patients contain *Mycobacterium tuberculosis (Mtb)* proteins, and these protein biomarkers show promise for TB and LTBI diagnostics. Our lab previously identified 31 *Mtb* peptides in trypsin-treated serum EVs isolated from patients with LTBI using multiple reaction monitoring-mass spectrometry (MRM-MS) methods. MRM-MS is a highly sensitive technology but is not feasible for widespread use as a diagnostic. The goal of this study was to develop an ultrasensitive ELISA against *Mtb* proteins for potential use as a point-of-care diagnostic.

A sandwich ELISA was initially developed against *Mtb* proteins DnaK, Mpt32, and GroES. Reagent development for the sandwich ELISA included polyclonal antibody production using a rabbit model, murine monoclonal antibody purification and biotinylation from an existing collection of hybridoma cell lines for each antigen, and detection using a streptavidin-

HRP system with a chemiluminescent substrate for signal expansion. We observed that the sandwich ELISA was complicated by non-specific binding of the DnaK and GroES antigens to the BSA block. We hypothesized that the chaperone function of these two proteins influenced them to bind to BSA. This non-specific interaction was further characterized using SPR technology and demonstrated a concentration dependent binding of DnaK to BSA.

A direct-biotinylated ELISA was subsequently developed and optimized. Limit of detection (LOD) and limit of quantification (LOQ) of the direct-biotinylated ELISA was determined for each antigen: 1) GroES had an LOD of 1.959 ng/mL and an LOQ of 6.531 ng/mL, 2) Mpt32 had an LOD of 1.884 ng/mL and an LOQ of 6.278 ng/mL, and 3) DnaK had an LOD of 6.310 ng/mL and an LOQ of 21.032 ng/mL. This direct-biotinylated ELISA platform demonstrated high sensitivity with low background for all three antigens. Thus, we successfully developed and optimized an ultrasensitive ELISA for the detection of *Mtb* antigens.

ACKNOWLEDGMENTS

First and foremost, thank you Lord Jesus for the breath in my lungs and the opportunity to witness Your majesty in this world.

"*Whoever dwells in the shelter of the Most High will rest in the shadow of the Almighty*"

Psalms 91:1 NIV

Thank you to Colorado Clinical and Translational Sciences Institute at CU Anschutz and the Dobos lab for funding for this project.

Thank you, Dr. Carolina Mehaffy for not only teaching me how to be a better scientist but for also being a role model for me in and out of the lab. I also want to thank Dr. Karen Dobos for taking a chance on me when I joined her lab as a naïve, bright-eyed and bushy-tailed undergraduate. I am forever a better scientist for joining your lab. Thank you for doing all you could for me when times were difficult.

A big thank you to all of those who helped with this project: David DeSimone and Briana Marsico for your work with the exosome purification side of this project, Dr. Mollie Burton for your help with the (fun) rabbit side of this project, and Dr. Erika Orban for your help and wisdom for all things Biacore.

I want to thank my family and friends who have been there for me throughout this whole process. I don't know how many times I have changed my mind about what I want to be, where I want to go, or what I want to do. Thank you for being there through the roller coaster and supporting my crazy dreams.

DEDICATION

For Hunter Jay

To my beloved boy, thank you for showing me that angels come wrapped in four paws. I am so grateful and honored that you and God both agreed to let me be your human. I love you always big guy.

TABLE OF CONTENTS

ABSTRACT……... ii
ACKNOWLEDGMENTS…… iv
DEDICATION……... v
CHAPTER 1 – INTRODUCTION…… 1
CHAPTER 2 – ELISA REAGENT DEVELOPMENT AND QUALIFICATION…… 15
CHAPTER 3 – THE ROLE OF *MYCOBACTERIUM TUBERCULSIS* ANTIGENS IN ELISA DEVELOPMENT…… 68
CHAPTER 4 – FUTURE DIRECTIONS & CONCLUDING REMARKS……... 120
REFERENCES……... 127
APPENDIX…… 143

CHAPTER ONE: INTRODUCTION

1.1 Tuberculosis

According to the most recent World Health Organization (WHO) report, approximately 1.3 million people died in 2020 from Tuberculosis (TB) alone and an additional ~200,000 people with an HIV co-infection [1]. The same WHO report also estimated that approximately "one-quarter of the world's population has been infected with *Mycobacterium tuberculosis* (*Mtb*)" [1]. *Mtb* is the causative agent of TB [1]. TB was the global leader for "deaths by an infectious agent" prior to the COVID-19 pandemic [1]. However, if and when COVID-19 subsides, TB may well in fact resume its role at the top of the podium.

Mtb is a "facultative intracellular bacteri[um]" and a strict "obligate aerobe" [2]. *Mtb* is a member of the MTB complex alongside *Mycobacterium canettii*, *Mycobacterium microti*, *Mycobacterium bovis*, and *Mycobacterium africanum* [3–5,2], all with matching "16s rRNA sequences" [6]. The mycobacterial species in this complex can infect different mammals [6] but *Mtb* selectively infects humans [2], and is not ubiquitous in the environment [7]. Due to this fact, *Mtb* has acquired certain characteristics that allow it to co-exist with humans [7]. This is both beneficial and troublesome. Since *Mtb* has acquired adaptations that allow it to evade detection [7], the ability of the host to control infection (or clear it completely) and the bacteria to survive host system attacks becomes an intricate dance that can make diagnosis and treatment difficult. However, since *Mtb* is a human-specific pathogen, diagnostics and treatment can be highly targeted.

TB disease can have both pulmonary and extrapulmonary forms [2]. Pulmonary TB comprises the majority of cases, where aerosolization of *Mtb* is the most common route of infection [2]. TB is often depicted as a black and white, two-state disease with active and latent

phases [8]. In the past, this two-disease state model was used to "simplify classification of TB pathogenesis" [9]. However, more recent research has suggested that TB disease is more of a "spectrum," by taking into account the fluid state of pathogen and host responses to infection [8].

1.2 Active Tuberculosis Disease

Active TB is often characterized by clinical evidence (symptoms), microbiological identification [9], and "radiographical abnormalities" [8]. Characteristic clinical symptoms of active TB disease are a "productive cough" [2] that persists for " > 3 weeks, coughing up blood, night sweats, and weight loss" [10]. During the active phase of disease, *Mtb* bacteria are in a state of replication [10].

Approximately one-quarter of those that come in close contact with a person with active TB will become infected themselves [11,9]. From here, a smaller percentage ("5-10%") of those infected will progress to the active phase of disease relatively quickly [11,9]. The vast majority of infected people will be able to control the infection with a robust immune response [9]. However, this does not equate to complete elimination of the bacteria [12] and oftentimes, *Mtb* will simply regress into a more quiet state for survival [13].

1.3 Active Tuberculosis Diagnostics

Currently, the diagnostic tests used for active TB disease utilize sputum as the clinical sample [14]. These diagnostic tests include sputum smear microscopy, sputum culturing, and nucleic acid amplification testing (NAAT) [15].

Sputum smear microscopy utilizes acid-fast staining [15]. The sputum smear microscopy test remains the most utilized diagnostic for active TB diagnosis in "resource-limited settings" [16]. However, sputum smear microscopy has a wide range of sensitivity [16,17] and cannot differentiate between *Mycobacterium* species [15].

Sputum culturing is considered to be the "gold standard" for active TB disease diagnostics, using both solid and liquid growth media [2]. These different media offer variations in growth time as well as sensitivity, with the liquid growth media showing superiority for both [16]. Sputum culturing can be used to test for drug resistance as well [16]. However, the ability to contain and manipulate these cultures safely can be a challenge in resource-limited areas [18,19].

NAA tests such as the Xpert MTB/RIF assay have shown promise when compared to sputum culturing [20]. Helb et al. was the first to develop an *Mtb*-specific assay with the GeneXpert (Cepheid) instrument [20]. From sample preparation to detection, this assay was performed in only a couple of hours [20]. The sputum samples are added to an assay-specific reagent for pretreatment and then added to a cartridge where *Mtb* DNA is extracted [21]. A PCR reaction is performed in the GeneXpert instrument [22,20] for amplification of a specific gene sequence (*rpoB*) that can identify "members of the MTB complex" as well as "rifampin resistance mutations" [20]. Assay sensitivity (detection limit) was comparable to sputum culturing [21,23] and produced a high degree of specificity for both detection of *Mtb* DNA and rifampin resistance in clinical samples [20,21].

The Tuberculin skin test (TST) and the interferon-gamma release assays (IGRAs) are two additional tests [2] but are generally not recommended for active TB due to the inability of both to differentially diagnose active TB and LTBI [24,25].

1.4 The Subclinical Spectrum of Tuberculosis

The majority of TB cases fall within the latent phase of disease, also known as latent tuberculosis infection or LTBI. Immunosuppression from human immunodeficiency virus (HIV) infection, diabetes, and malnutrition can all disrupt the delicate host immune control of *Mtb* during dormancy [25]. Reactivation of primary active TB disease occurs in approximately 10% of LTBI cases and often leads to silent transmission [26].

Due to the dynamic nature of TB, a "spectrum" of disease has been proposed in an attempt to represent the oscillation of pathogen and host control during disease progression [27,28,8]. During infection, the host will protect itself by creating granulomas, a mass of different immune cells surrounding the macrophages that harbor the *Mtb* bacteria [29]. Even though *Mtb* faces survival challenges in these environments, like limited resource accessibility [8], the bacteria have evolved mechanisms to take advantage of this host response. Although these trapped bacteria are not as active, *Mtb* can induce host cellular changes within the local granuloma environment to sequester nutrients [30–32,29]. Therefore, the granuloma is still a source of "viable" bacteria [29] and can break down when the host becomes immunocompromised [33]. This host-pathogen dynamic has been proposed to shift across different subclinical states [8].

In recent years, researchers have sought to characterize two more subclinical states, incipient and subclinical [8]. These two substates are classified using clinical, radiographical, and microbiological evidence, or lack thereof [8]. Characterization is often challenging due to limited knowledge of how or when individuals progress through these substates [8]. However, these subclinical states offer some insight into different "pathways" through TB disease progression [8]. These pathways may progress directly to active TB disease or may "cycle through" different substates [8]. After establishment of latency, individuals are proposed to progress from LTBI to incipient infection then to subclinical TB disease [8]. Each subclinical state has viable bacteria [9]. The incipient infection stage lacks clinical presentation whilst the subclinical TB disease stage may manifest "unidentifiable" symptoms [9] that do not quite match "TB-related symptoms" [8]. Microbiological and radiographical evidence can be determined for subclinical TB disease [8]. Transmission events are not likely during the incipient infection stage but are more likely during subclinical TB disease due to the increase in bacterial activity [9].

Many of the same microbiological and radiographical tests for active TB can be utilized for subclinical TB disease [34,8]. However, sputum smear microscopy is complicated by a decreased bacterial burden in subclinical TB disease [34]. Similar to LTBI, incipient infection is difficult to diagnose because *Mtb* is not actively replicating at high enough numbers to detect pathogen-specific antigens [35]. Therefore, diagnostic tests for LTBI and incipient infection have to rely on the host mounting a robust immune response [35].

1.5 Latent Tuberculosis Infection Diagnostics

Currently, there is not a standard diagnostic test for LTBI [36,35]. However, the TST and IGRA tests are used to tentatively diagnose LTBI [35].

The TST measures an individual's immune response to purified protein derivative (PPD), "a mixture of protein[s] precipitated of mycobacterial culture filtrates" that have been steamed [37,35]. The PPD is "injected intradermally into the forearm" and a delayed-type hypersensitivity (DTH) response is measured 48-72 hr post-injection [35]. Localized inflammation ("induration" or a wheel) created by an immunological memory response is indicative of a DTH response [38]. Different risk factors like age, HIV status, and working with *Mtb* influence positivity baselines [39]. The TST is useful in identifying "past or present infections" [35] and can be used in surveillance for LTBI [37]. The TST remains one of the cheaper and lower-tech options for LTBI diagnostics [35]. However, the TST is complicated by Bacille Calmette–Guérin (BCG) vaccination and infections with non-tuberculous mycobacteria (NTM) [35].

The IGRAs are a type of blood test that measures an individual's immune response based on key host cell inflammatory markers [35]. There are different variations of IGRAs, some using whole blood or separated blood (peripheral blood mononuclear cells, PBMCs) for assay samples [35,40]. *Mtb* antigens ESAT-6 and CFP-10 are added to the blood samples for T cell stimulation [35,41].

The sensitized T cells then release the interferon-gamma (IFN-γ) cytokine [42]. The IFN-γ response is then quantified by enzyme-linked immunosorbent assays (ELISAs) or enzyme-linked immunosorbent spot (ELISPOT) immunoassays [42]. The most prominent IGRA assays available today are the T-Spot.TB or the QuantiFERON (QFT) and QuantiFERON TB Gold [42].

The IGRAs hold a few more advantages over the TST. The IGRAs are not complicated by BCG vaccination [9] and infections with most NTM species [43,44] due to the specific antigens used [9]. IGRA quantification allows for "less bias" in results [45]. IGRAs also have the added benefit of assay controls [45]. However, IGRAs are more expensive and a higher-tech diagnostic [25].

The TST and IGRAs have a few of the same pitfalls. Neither test can differentially diagnose active TB disease and LTBI and both tests generally perform poorly in the immunocompromised [35]. Additionally, both tests have poor positive predictive values for progression to active TB and testing in different risk groups is limited [46].

1.6 TB Diagnostic Challenges

Many challenges face current TB diagnostics. The diagnosis of active TB relies on sputum as the clinical sample [47]. However, the use of sputum presents a challenge for immunocompromised individuals as well as children, due to the inability of these groups to produce sputum [48–51]. Sputum-based diagnostics are complicated by latent infection, as bacillary loads tend to be much lower [52,53]. Therefore, other types of clinical samples may be needed to develop more specific and sensitive diagnostics.

There are currently no diagnostic tests that can differentially diagnose active TB and LTBI, let alone any of the subclinical states [47]. As previously mentioned, LTBI cases are only tentatively diagnosed with the TST and IGRA tests due to the lack of a gold standard [36,35] and the reliance on the host mounting a robust immune response during infection [54]. The challenge with

relying on the host response is two-fold: 1) immunocompromised individuals, such as those with HIV, have too few CD4+ T cells to produce an adequate immune response [55,54] and 2) it is difficult to determine if a response is due to a past or present infection [54].

A final hurdle for TB diagnostics is the ability to implement highly sensitive and high-tech instrumentation into resource-limited areas at the point-of-care (POC). Currently there are no TB diagnostics that have been successfully implemented at the POC [47]. The WHO laid out a set of priorities for POC TB diagnostics. POC tests should: 1) …identify biomarkers in non-sputum samples to differentially diagnose TB disease states, 2) be "simple, cost effective", and implemented at the point-of-contact with the healthcare system, 3) utilize sputum as a sample for "microscopy replacement", and 4) be able to test for drug resistance at a lower care setting [56]. POCs are implemented to decrease the time between results and the start of treatment [57].

1.7 Pathogen-Based Biomarker Discovery

Biomarker discovery could help resolve some of the issues facing TB diagnostics. Non-sputum based clinical samples such as blood, serum, and urine can all be sources of both host and pathogen-specific biomarkers [14]. Biomarkers from both host and pathogen have been utilized for development of potential TB diagnostics [14]. Biomarker discovery could not only aid in differential diagnosis but also identify those at risk of progression from LTBI to active TB [58].

One of the most popular and promising pathogen-based biomarkers for active TB is the mycobacterial cell wall component LAM (lipoarabinomannan) [47]. A previous study identified LAM in urine samples of active TB individuals [59]. This research was based off the finding that mice, injected with the *Mtb* cell wall subcellular fraction, were able to process LAM and "excrete the intact form" in their urine [59]. A lateral flow assay to detect LAM in urine was subsequently developed and commercialized as the Alere Determine™ TB LAM Ag assay

(Abbott Diagnostics, Santa Clara California, USA) that is low-cost and works well in advanced HIV positive patients [60–63]. This is a true POC test in that it offers a simple collection platform, uses a more accessible, safer clinical sample, and has quick turnaround time for results and subsequent "treatment initiation" [63]. However, in a study performed on samples from multiple African countries, the sensitivity and positive predictive values for this test (when used alone) was low (~ 38% and 60%, respectively) in HIV-negative individuals who were suspected of having TB disease (clinical symptoms and hospitalization criteria) [63]. Both parameters increased in HIV-positive samples [63]. This LAM lateral flow assay is highly recommended for the use in HIV-positive populations [61–63] where a sputum clinical sample is hard to produce [64,65]. However, specificity was high for the HIV-negative samples but decreased slightly with the HIV-positive samples [63] and therefore this test requires additional optimization. Currently, this test remains as an active TB diagnostic only. A search in the ClinicalTrials.gov database using key words "LAM TB" in the advanced search "condition or disease" resulted in three clinical trials (many others with "unknown status" or "withdrawn"), including two using the urine lateral flow assay (Determine) [66].

The Xpert MTB/RIF assay is another popular diagnostic based on pathogen-specific biomarkers. As mentioned previously, this assay detects *Mtb* DNA in sputum samples via a PCR reaction [22,20]. The original version of this assay had sensitivity levels that fell between sputum culturing and sputum smear microscopy [67]. However, a newer version of the Xpert MTB/RIF (Ultra) lowered the detection limit further, even closer to the range of sputum culturing [67]. The increased sensitivity was a result of identification of an additional two genetic signatures within the same gene sequence used (*rpoB*) [67]. The original studies were performed in "reference labs" [68] but subsequent studies looked at implementing this technology in resource-limited countries [68].

Boehme et al. implemented The Xpert MTB/RIF assay at a point of healthcare contact setting in resource-limited countries around the world [68]. This group demonstrated that the Xpert MTB/RIF assay was able to maintain high sensitivity and specificity and had a quicker turnaround time for diagnosis than both sputum culturing and smear microscopy [68]. Boehme et al. also found that unlike sputum smear microscopy, the Xpert MTB/RIF assay results were not swayed by HIV status [68]. However, this test has been shown to produce false positive results for rifampicin resistance [21] and is not as sensitive for "smear-negative sputum" samples [69]. This technology also requires a somewhat stable infrastructure to run [68] and is more expensive than sputum smear microscopy [21]. A search in the ClinicalTrials.gov database using key words "Xpert MTB/RIF" in the advanced search "condition or disease" resulted in 16 clinical trials, including one in current phase 4 trials [66].

1.8 Host-Based Biomarker Discovery

The dynamic relationship between *Mtb* and the host creates a challenge for developing diagnostic tests that are based on the host immune response [70]. Serological testing, detection of anti-*Mtb* antigen antibodies in serum, can be complicated by a lack of complete understanding of the immune response during *Mtb* infection [70]. A meta-analysis review compiled sensitivity and specificity results for different serological assays for pulmonary and extrapulmonary TB [71]. This analysis demonstrated that serological assays have a wide range of sensitivity and specificity for both pulmonary and extrapulmonary TB and therefore, "do not provide an accurate diagnosis of tuberculosis" [71]. In 2011, the WHO recommended against the use of serological diagnostics for TB [72,70].

IP-10, the interferon-gamma inducible protein-10, has potential as a host-based biomarker for active TB and LTBI [73]. This chemokine is released from macrophages during

times of inflammation [74–77]. IP-10 has been shown to participate in stimulating pro-inflammatory DTH responses [78,79,77]. An *in vitro* study demonstrated a significant production of IP-10 in IGRA (QFT) test supernatants stimulated with *Mtb* antigens (ESAT-6, CFP-10, and TB7.7) from active TB patients ("confirmed or clinically assessed") when compared to healthy controls [76]. This test may not offer much improvement for children, compared to an IGRA, and may only be slightly better with use in HIV-positive individuals [76]. This test also relies on the use of TST and IGRA tests as a baseline for LTBI determination [77] due to the lack of a gold standard for LTBI. Many clinical studies have been conducted [76] with this assay but no clinical trials.

The C-Tb skin test is a cross between the TST and the IGRAs. *Mtb*-specific proteins ESAT-6 and CFP10 are used for the intradermal injection [80]. The DTH response is then measured [80]. There is no cross-reaction with BCG vaccination [81]. One clinical trial (phase 3) demonstrated that the C-Tb test is comparable to both TST and IGRA sensitivity in children and HIV-positive individuals, both in groups with active TB (defined by clinical TB symptoms, positive sputum culturing and Xpert MTB/RIF) and non-TB (LTBI suspect defined by clinical TB symptoms, negative sputum culturing and Xpert MTB/RIF) [80]. However, due to the lack of a gold standard diagnostic for LTBI, this clinical trial had to rely on a positivity baseline for LTBI based on negative sputum culturing and Xpert MTB/RIF results [80]. This trial used samples from a high burden [82] setting (South Africa) [80]. C-Tb would be a simple, low-cost alternative test [83,80]. A search in the ClinicalTrials.gov database using key words "C-TB" in the advanced search "condition or disease" resulted in six clinical trials, two focusing on comparison of C-Tb to the QuantiFERON IGRA [66].

Gene expression transcriptional profiling has also been utilized to identify host genetic biomarkers for active TB and LTBI. One study was able to identify fives genes in PBMCs,

stimulated with PPD, cultures from individuals with active TB (clinical symptoms, positive sputum smear microscopy and/or sputum culture), LTBI (positive IGRA T-SPOT.TB test, household contact, negative chest X-ray), and healthy donor controls (negative IGRA T-SPOT.TB, negative chest X-ray, no clinical symptoms, household contact) that were able to differentiate individuals with active TB and LTBI [84]. Three of the genes paired together had high predictive performances to classify each individual for active TB vs LTBI [84]. Gene expression profiling technology shows promise as a means to identify biomarkers for active TB and LTBI. However, this type of technologically is advanced, costly, and not practical as a POC [84].

1.9 Master's Thesis Background

As technology has become increasingly more sensitive, the world of "omics" has opened a new avenue for TB biomarker discovery [67]. "Omics" has shifted science away from serodiagnostics and toward "molecular biology-based diagnostics" [67]. Both host and pathogen-specific biomarkers have been discovered using "genomics, proteomics, transcriptomics, and metabolomics" [67].

Detection of *Mtb* proteins in serum extracellular vesicles (EVs) using multiple reaction monitoring-mass spectrometry (MRM-MS) is an example of pathogen-specific biomarker discovery using targeted proteomics. EVs are a population of nanovesicles released by most eukaryotic cells [51,85]. EVs include "exosomes, microvesicles, and apoptotic bodies" [85,86]. Due to the lack of specific identifying markers for exosomes, the nomenclature was changed to "extracellular vesicles" [87]. These smaller EVs ("30-100 nm in size") [51] are produced via external cellular release of multivesicular bodies (MVB) and contain host cell components (i.e. "proteins, lipids, nucleic acids") [85]. EV composition is a reflection of the state of the cell [88,51]. Thus, EVs could be a source of *Mtb* biomarkers due to the intracellular nature of the pathogen [89,51]. In fact,

Mtb infected macrophages were shown to produce EVs that contained *Mtb* antigens [90,91]. Immunization of a naïve murine model using EVs from *Mtb* culture filtrate treated macrophage cultures demonstrated 1) that EVs contained *Mtb* products and 2) these EVs were able to stimulate pathogen-specific T cell responses [91]. This study also utilized shotgun proteomic analysis to identify 41 *Mtb*-specific proteins in the EVs isolated from infected macrophage cultures [91]. These studies highlighted the potential of EVs to act as a reservoir for potential *Mtb* biomarkers.

As mentioned previously, one hurdle with TB diagnostics is the use of sputum as the clinical sample. Serum on the other hand is a more readily available, safer clinical sample [92]. A couple of studies have sought to use serum as a source of EVs for TB biomarker discovery. Purification of serum allows for concentration of these low abundance *Mtb* biomarkers for a higher chance of detection [51]. One study sought to use shotgun and targeted proteomics to identify a slew of potential protein peptide candidates from serum EVs of individuals with active TB either pulmonary or extrapulmonary (symptoms, sputum smear microscopy and sputum culture positive), and LTBI (sputum smear microscopy and sputum culture negative) in Uganda [51]. This study created a foundation for *Mtb* biomarker discovery using purified serum EVs but fell short in creating a refined targeted proteomics method where peptides could be quantified with a high level of confidence [86].

Therefore, Mehaffy, et al. built upon these targeted methods by adding "additional peptide targets, synthetically labeled peptides for quantification, and healthy donor serum EV samples as controls" [92]. The refinement of the MRM-MS methods allowed for detection of low abundance peptides in serum EV samples from individuals with active pulmonary TB (sputum culture positive) and TB negative suspect (possibility of LTBI, no smear microscopy results) [92].

The refined targeted proteomic methods were then used on serum EV samples from individuals with LTBI (TST positive, household contact, TST conversion from negative to positive in < 2 years) compared to healthy donor controls (TST and/or IGRA negative) from the United States [86]. Since pathogen-based biomarkers are lacking for LTBI, this study provided support for potential use of these MRM-MS methods to detect LTBI-specific *Mtb* antigens. The MRM-MS methods were able to identify 31 peptides in LTBI samples [86]. Some of the peptides identified in the Mehaffy et al., 2020 study for LTBI were also identified in TB+ samples in the Kruh-Garcia et al., 2014 study. This discrepancy could have been due to "unrefined methodologies" and/or were a "reflection" of the dynamic TB disease state with differing peptide abundance in active TB and LTBI samples [86]. Future studies using larger, better characterized cohorts of TB+, LTBI, and healthy donor samples from different countries (high burden) are needed for identification of additional disease state-specific biomarkers [86]. However, these proteomics-based tools identified potential biomarkers for LTBI that could aid in creation of more sensitive and specific diagnostic tests.

1.9.1 Master's Thesis Project Specific Goals

The targeted proteomics approach in the Mehaffy et al., 2020 study provided identification of potential *Mtb*-specific biomarkers for LTBI. The top six peptides identified in LTBI serum EV samples belonged to proteins GlnA, GroES, DnaK, AcpM, GarA, and Mpt32, from most to least hits detected, respectively [86]. A peptide for GlnA1 was detected in 82% of the LTBI serum EV samples [86]. Mass spectrometry is a highly sensitive tool. However, POC diagnostics are needed so that a sensitive and specific assay can be created in a simple platform for implementation in resource-limited settings. For this reason, mass spectrometry is not a

feasible diagnostic tool in resource-limited areas due to its high cost and high degree of technological difficulty.

Therefore, for this master's thesis project, we attempted to use the targeted proteomics results to develop an enzyme-linked immunosorbent assay (ELISA) as a potential diagnostic tool to detect *Mtb* proteins. For the first leg of this project, the original goal was to develop an ultrasensitive sandwich ELISA using purified native GroES, native Mpt32, and recombinant DnaK. Development of the ELISA would involve reagent production and qualification, followed by extensive assay optimization. The optimized sandwich ELISA would then be tested on complex fluids, such as serum and purified serum EVs.

The overall goal of this project is to provide a proof-of-concept for a potential POC diagnostic ELISA for individuals with LTBI. This project and the previous targeted mass spectrometry studies could thus satisfy the first two WHO priorities for POC TB diagnostics, that they should: "1) …identify biomarkers in non-sputum samples to differentially diagnose TB disease states and 2) be "simple, cost effective", and implemented at the point-of-contact with the healthcare system " [56].

CHAPTER 2: ELISA REAGENT DEVELOPMENT AND QUALIFICATION

2.1 Introduction

During the early stages of immunoassay development, sample analytes were quantified using radioisotope labels [93,94]. One of the earliest examples of this radioactive immunoassay (RIA) technique was used as a means to detect human insulin [93,94]. An RIA assay was developed where unlabeled human insulin and radioactively-labeled beef insulin competed for binding to α-beef insulin guinea pig serum antibodies [93]. The ability of the human insulin to out-compete the radioactively labeled beef insulin for binding to the beef insulin α-serum allowed for quantitation of the antibody-bound human insulin [93]. The subsequent enzyme linked immunosorbent assay (ELISA) eliminated the need of radioisotope labeling [94] and instead, utilized horseradish peroxidase (HRP) [95,94] and alkaline phosphatase (AP) enzyme conjugates [96]. Enzyme conjugates were regularly used for labeling histological tissue samples [96]. However, this concept was adapted for the ELISA plate-based platform for the quantification of sample "antigens and antibodies" [96]. More than 50 years later, the ELISA technique has been improved upon to increase both sensitivity and specificity of the assay.

Four different types of ELISAs have been developed, depending on desired levels of sensitivity and specificity [97] as well as availability of reagents. Direct ELISAs offer the lowest specificity but are not as laborious and require less reagents [97,98]. Antigens (antibodies or other protein antigens) are coated on microtiter plates (microplates) that offer different adsorbent matrices for specific analytes (i.e. hydrophobic or hydrophilic microplate surfaces) that aid in "passive adsorption" or pulldown of the antigens [98]. Generally, an enzyme-labeled antibody specific for the antigen of interest is then incubated with the microplate-bound antigen and developed using an AP or HRP specific substrate.

The indirect and sandwich ELISAs offer robust signal expansion but at a cost of non-specific interactions from the enzyme-labeled secondary/detection antibody [97]. The secondary antibodies, produced in different species from the primary antibody, can often be "sticky", especially at a concentrated dilution, and can create false positive signals [99]. Indirect ELISAs differ slightly from the direct ELISAs with the additional layer of the enzyme-labeled secondary antibody. Sandwich ELISAs are the most "sensitive and specific" of the four types due to the "sandwiching" of the antigen between two antibodies [98]. However, sandwich ELISAs are more prone to cross-reactivity with multiple reagents [98]. Sandwich ELISAs are more expensive as well as time consuming [97]. Extensive optimization is needed for sandwich ELISAs to find the optimal reagent pairings. These three ELISA types can utilize biotinylated antibodies and HRP conjugate enzymes (streptavidin or avidin) for signal expansion [100]. Streptavidin and avidin proteins both form strong interactions with biotin and have four biotin binding sites per streptavidin/avidin "tetrameric molecule" [100]. Competitive ELISAs are often used for smaller analytes and include a labeled and unlabeled analyte that compete for antibody/antigen binding [98]. Concentration of the unlabeled analyte of interest corresponds with a lower signal output [98].

There is a variety of commercially available reagents for each different type of ELISA. However, many laboratories will resort to making in-house reagents due to lack of availability. While many different species can be used for polyclonal antibody (PAB) production, rabbits are a popular animal model [101,102]. Rabbits offer multiple advantages over other species: 1) the shear surface area of their ears allows for quick and almost painless blood collection, 2) they are big enough to produce a sufficient amount of PAB serum but are small enough for cheaper housing (group housing), 3) they can be easily manipulated for procedures, and 4) α-rabbit reagents are readily available [101,102]. However, PAB production using a rabbit model is not a renewable

resource. Rabbit titers will eventually wane without constant boosting and the cost to keep rabbits around for many years is steep. Rabbit PAB serum can vary from lot-to-lot but does offer a diverse repertoire of antibodies [103]. Rabbit housing may be cheaper than larger animal housing, but it is by no means a low-cost expense. Chickens are sometimes used as a PAB production animal model due to a more renewable source of PAB antibodies in chicken eggs [102,104]. However, housing chickens is still costly in the long run.

Monoclonal antibody (MAB) production is a different story. Whereas many different species of animals can be used for PAB production, MAB production is limited to animal models that have an immortalized myeloma cell line available [102]. Thus, most MAB production studies use a murine model [102]. B cells taken from the animal are fused with the corresponding species-specific myeloma cell line [102]. The fused cells are then subcloned to monoclonality and upscaled for antibody production [102]. MABs are produced to recognize a single epitope, are a "renewable resource" [105,102], and are more consistent lot-to-lot, but the MAB production process is costly and laborious [103].

After PAB and MAB production, purification of serum and hybridoma cell culture supernatant, respectively, can often be a difficult task, requiring multiple reagents and methods. The goal behind purification of these complex matrices would be to increase sensitivity and lower background noise in assays such as ELISAs. Purification methods such as ammonium sulfate (AS) precipitation allow for a crude purification of large molecular weight proteins [106]. Other purification methods, such as protein A and G beads and columns are more specific for pull-down of immunoglobulins as well as purification of different isotypes but often include "harsh elution conditions" (buffers) [106]. One study tested different purification methods on rabbit and human serum, including Protein G and Protein A/G columns as well as polyethylene glycol

(PEG) and caprylic acid/ammonium sulfate precipitations [106]. The study demonstrated that different purification methods may yield a final product with variable purity and quality depending on the "species of origin" [106]. This study also alluded to the fact that purification method conditions using harsher reagents could possibly affect the "quality, integrity and function of the purified antibody molecules" [106].

Another purification method, the Melon gel column, uses a "proprietary ligand" on the resin "to bind serum proteins" and any immunoglobulins other than IgG, according to the manufacturer [107]. The flow through of the column contains the purified IgG antibodies [107]. Melon gel purification is quick and has the added benefit of ditching the "harsh low pH elution conditions [buffers]" [108]. Choosing a purification method, or methods in tandem, is important depending on the purpose of purification, whether that is to simply eliminate large contaminating proteins (AS or PEG precipitation) [106,109] or to have a purified sample with a single isotype of immunoglobulins (Melon gel).

For this master's thesis project, the original goal was to create an ultrasensitive sandwich ELISA to detect *Mtb* antigens. This ELISA would utilize polyclonal antibodies (PAB) from rabbit serum as the capture antibodies and monoclonal antibodies (MAB) from murine hybridoma cell culture supernatant as the detection antibodies. The use of a PAB serum for the capture antibody would theoretically allow for greater pull down of the antigen, as multiple epitopes would be recognized. The MABs would be purified and biotinylated for use with an HRP system alongside a chemiluminescent substrate for detection. MAB purification would include: 1) concentration of the antibodies in the cell culture supernatant (growth of hybridoma cells until complete cell death), 2) ammonium sulfate precipitation (50% cut), and 3) a Melon gel

purification column. Since all the MABs used for this study had IgG isotypes, the Melon gel column seemed the most promising and efficient method for purification.

In order to create an ultrasensitive sandwich ELISA, the first step in this process was reagent development and qualification. This chapter highlights the key reagents created for this project.

2.2 Methods

2.2.1 Polyclonal Antibody Production

All rabbit work was performed in accordance with the protocol (#1323 Polyclonal Antibody Production) established and accepted by the Institutional Animal Care and Use Committee at Colorado State University. The Principal Investigator of the protocol was notified of modifications.

Two female New Zealand White rabbits were immunized subcutaneously against native and/or recombinant *Mtb* (strain H37Rv) antigens. All mycobacteria-specific reagents were provided through BEI resources unless otherwise stated. One rabbit (R1) was immunized against purified recombinant GlnA (kindly provided by the Dobos laboratory), and the second rabbit (R2) was immunized against four purified antigens: native Mpt32 (NR-14862), native GroES (NR-14861), recombinant DnaK (kindly provided by the Dobos laboratory), and recombinant GlnA (kindly provided by the Dobos laboratory). DnaK and GlnA recombinant proteins were produced from plasmids, NR-13279 and NR-13314, respectively, and followed protocols offered through BEI resources. A naïve bleed of ~ 5 mL was performed before the start of immunizations to test for non-specific reactivity to culture filtrate protein (CFP, NR-14825) and whole cell lysate (WCL, NR-14822) of *Mtb* strain H37Rv origin (kindly provided by the Dobos laboratory). Three immunizations per rabbit were administered. The second immunization was

administered ~ 3.5 weeks post first immunization. The third immunization was administered ~ 6 weeks post second immunization. For the first and second immunizations, rabbit R1 was immunized with 500 µg of recGlnA and rabbit R2 was immunized with a combined mixture of 125 µg native Mpt32, 125 µg native GroES, 125 µg recombinant DnaK, and 125 µg recombinant GlnA. For the third immunization, rabbit R1 was immunized with ~320 µg recGlnA and rabbit R2 was immunized with 50 µg recGlnA, 50 µg recDnaK, 200 µg nMpt32, and 200 µg nGroES. For the first immunization, the antigens were emulsified with TiterMax Gold (MilliporeSigma) at a 1:1 *antigen: emulsifier* ratio. For the two subsequent immunizations, the antigens were emulsified with Incomplete Freund's Adjuvant (MilliporeSigma) at a 1:1 *antigen: emulsifier* ratio. Significant loss of emulsified antigen product was seen for all immunizations due to loss of volume in the emulsifier. Approximately 5 mL of blood were collected from each rabbit after the second immunization to check for sufficient reactivity to purified native or recombinant antigens, as well as the *Mtb* crude CFP fraction. Rabbit R2 was bled for a second test bleed after the third injection due to insufficient reactivity following the second immunization. Both rabbits were subjected to three production bleeds where 1 % of their body weight in blood was collected four weeks or more apart. However, for rabbit R2, there was a two-week rest between the second and third production bleeds due to lower volumes taken each time. This was still in accordance with CSU policy. Intramuscular injections (IM) of acepromazine (VetOne) at 0.95mg/kg-1mg/kg, depending on rabbits' weight, were given for sedation when needed for larger blood collections. All bleeds were performed using either the central artery or the peripheral veins of the ears. Different needles and blood collection tubes were used to optimize the blood collection process. Wintergreen essential oil (Healing Solutions, LLC) and Lidocaine 2.5% and Prilocaine 2.5%

cream (AKORN) were used topically on the rabbits' ears to aid in vasodilation and comfort (respectively) during blood collections.

Blood processing was as such: briefly, after collection, blood was incubated at 37°C for 1hr to 1.5 hr. Tubes were flicked to release clots and incubated at 4°C overnight to shrink clots. Approximately 24 hr later, the blood was spun down twice at 10,000 *x g* for 10 min, at 4°C. After the first spin, the serum supernatant was collected and transferred to a new tube. After the second spin, the serum supernatant was collected, transferred to a new tube, aliquoted, and frozen at -70°C for long term storage. Qualification of the ***un***purified PAB serum aliquots was performed at a later time (see *section 2.2.3 Qualification of Polyclonal Antibody Reagents*).

Some deviations from the blood processing protocol were carried out: 1) the first test bleed had one spin at 3,000 *x* g, 5 min at 4°C and two subsequent spins at 10,000 *x g*, 10 min each at 4°C and 2) rabbit R1 production bleed #1 and rabbit R2 test bleed #2 included three, 3,500 *x g* spins, 5-15 min each at 4°C followed by two, 10,000 *x g* spins, 10 min each at 4°C carried out a day after the first spins.

2.2.2 Polyclonal Antibody Serum Purification

Ammonium sulfate (AS) precipitation was carried out on combined aliquots of PAB serum (~ 4-5 mL final volume) from the first production bleed of rabbit R2. An appropriate amount of AS reagent (MilliporeSigma) was added for a final AS saturation of 50% weight/volume [110]. The AS reagent was added slowly to the serum sample at room temperature and inverted to mix. AS precipitation was carried out overnight at 4°C, rocking. The AS precipitation cut was collected the next day and divided into smaller tubes for centrifugation at 10,000 x g for 30 min, at 4°C. The subsequent AS precipitation cut supernatant was decanted, saved, and stored at 4°C. The AS precipitation cut pellets were re-suspended in 1X Melon gel

purification buffer, pH 6.7 from the Melon™ Gel IgG Purification Kit (ThermoFisher) and combined for a final volume of ~12 mL. Melon gel reagents were pre-mixed according to the manufacturer's protocol. The re-suspended AS precipitation cut pellet samples were dialyzed against 1X Melon gel purification buffer, pH 6.7 using equilibrated 3500 MWCO dialysis tubing (Fisher Scientific). Two buffer exchanges, one after 6-7 hr and one overnight, were performed at 4°C. After dialysis, the samples were collected and dialysis membranes were washed with 1X Melon gel purification buffer, pH 6.7 and added to the samples.

Subsequent purification of the PAB serum, using the Melon gel column kit, was performed following the manufacturer's protocol, with some modifications for optimization. Briefly, all Melon gel reagents were equilibrated to room temperature (~30 min) prior to starting column. Plastic columns were rinsed thoroughly with 20% ethanol, followed by ultrapure (Milli-Q) water, and finally with 1X Melon gel purification buffer, pH 6.7. Next, enough Melon gel slurry was used for a final packed column volume (CV) of 5 mL (packed column was approximately 20% of the slurry volume). The Melon gel slurry drip packed via gravity flow. If needed, pressure from a syringe was used to aid in the drip packing steps when flow slowed. 1X Melon gel purification buffer, pH 6.7 was added to wash the packed column at 10 times the packed CV. Enough buffer remained at top of column, as to keep the column from drying out. The packed, washed column was purposely perturbed by addition of sample. The sample slurry was then rocked manually at room temperature for 10 min. Next, the sample slurry was allowed to settle before drip packing via gravity flow. The initial flow through was collected separately. The packed column was then washed with 50 times the packed CV with 1X Melon gel purification buffer, pH 6.7. The washes were collected in batches. The sample flow through and wash batches were stored at 4°C until further processing and analysis.

Each flow through and wash batches were concentrated separately using equilibrated 10,000 MWCO ultrafiltration amicons (MilliporeSigma). The sample amicons were centrifuged at 3,500 *x g*, 4°C, ~ 40 min each spin. The amicons were washed thrice with ~15 mL of 1X PBS (Fisher Scientific) with the same centrifugation parameters. The final concentrated, washed 10,000 MWCO retentate was collected and the amicon membranes were washed thrice with ~1 mL of 1X PBS (Fisher Scientific). The amicon membrane washes were added to the concentrated retentate of the respective sample batch and aliquoted into smaller tubes. The diluted retentates were frozen at -70°C and subsequently dried on a speed vacuum concentrator. The concentrated samples were combined into a single tube, respective of the specific batch (flow through or wash batches). The collection tubes were rinsed with a small volume of 1X PBS (Fisher Scientific), vortexed, spun down and added to final respective sample tube. The samples were frozen at -70°C until further qualification and analysis (*section 2.2.3.3 Purified Polyclonal Antibody Protein Concentration and SimplyBlue Staining Protocol)*. The final purified PAB serum product will be denoted as PR2-1 (rabbit R2, second production bleed serum batch).

2.2.3 Qualification of Polyclonal Antibody Reagents

The rabbit PAB serum collected from naïve, test, and production bleeds were qualified via Western blotting and colorimetric indirect ELISAs against purified *Mtb* native or recombinant proteins, and crude CFP and/or WCL fractions (depending on rabbit), with some modifications to the protocols.

2.2.3.1 Western blotting

Briefly, 1 µg of purified recombinant and/or native protein(s) and/or 5 µg crude *Mtb* fractions CFP and WCL were mixed with 4X LDS sample buffer (Fisher Scientific) and loaded on NuPAGE Novex 4-12% Bis-tris gels (Fisher Scientific). The sample buffer included a

reducing agent for a denaturing SDS-PAGE gel. The SDS-PAGE gels were run at 200 V for 35 min. Protein gels were transferred to nitrocellulose membrane at 50 V for 1 hr in a blotting transfer chamber. From here on, all incubation steps were performed continuously shaking on an orbital shaker at room temperature, unless otherwise specified. All wash steps involved 5 min rocking incubations with TBST or TBS followed by removal of the liquid. Blots were then blocked with a blocking solution of 3% bovine serum albumin (BSA) in TBST (Tris-base with 0.05% v/v Tween®20, pH 7.4) and incubated for 1 hr or overnight at 4°C. Blots were rinsed with TBST. Rabbit PAB serum was diluted appropriately in TBST, and blots were incubated for 1 hr. Blots were rinsed with TBST. Secondary α-rabbit antibody (Abcam, alkaline phosphatase conjugated) was diluted in TBS (Tris-base without Tween®20, pH 7.45) and blots were incubated for 35 min. Blots were rinsed with TBS. The blots were developed for no more than 5 min using SigmaFast Tabs (MilliporeSigma) for an alkaline phosphatase system development. For the substrate solution, one SigmaFast tablet was dissolved in 10 mL of deionized water. For Western blot analysis, a PAB serum dilution of 1:1,000 with a dark band signal indicated sufficient immunization. Rabbit serum (unpurified and purified) are denoted as dilutions, as the concentrations were determined.

2.2.3.2 Indirect ELISA

TBST and TBS recipes can be found in *section 2.2.3.1 Western blotting*. All ELISA incubation steps were performed continuously shaking at 200 rpm using a titer plate shaker (Lab-Line Instruments, Inc., Model # 4625) at room temperature, unless otherwise specified. All liquids were decanted and tapped on a towel 3-4 times to remove excess liquid. All wash steps included three, brief washes with 200 µL/well of TBST (or TBS) using a multichannel pipet.

Briefly, Immulon 4 HBX clear, flat bottom 96-well microplates were coated with 1 μg/100 μL (10,000 ng/mL) purified native or recombinant proteins and 5 μg/100 μL (50,000 ng/mL) *Mtb* crude fractions CFP and WCL in a 49 mM sodium carbonate/sodium bicarbonate coating buffer (pH 9.60, in ultrapure water) [111]. The coating buffer was subsequently filtered and stored at room temperature for no more than one month. The coated microplate was sealed with a plate sealer and placed at 4°C overnight, rocking. The following day, the liquid was removed, and the microplate was washed. A 3% bovine serum albumin (BSA) in TBST solution was plated at 300 μL/well and incubated for 1 hr. The microplate was washed. Rabbit PAB serum was diluted appropriately in TBST. The rabbit PAB serum was plated at 100 μL/well an incubated for 1 hr or overnight at 4°C. The microplate was washed. Secondary α-rabbit antibody (Abcam, alkaline phosphatase conjugated) was diluted appropriately in TBS. The secondary antibody was plated at 100 μL/well and incubated for 35 min. The microplates were washed (this time using TBS). The colorimetric indirect ELISAs were developed using a solution of Pierce™ 5X Diethanolamine Substrate Buffer (ThermoFisher) and p-Nitrophenyl phosphate (pNpp) tablets (Sigma). Briefly, two pNpp tablets were dissolved in 8 mL of distilled water, 2 mL of the diethanolamine solution was added, and the substrate solution mixed well. The substrate solution was plated at 100 μL/well. The microplate was then read at 405 nm on a microplate reader (Synergy HTX) using the Gen5 software. The microplate reader was set to shake continuously at 365 cpm and performed a kinetic read with three reads total at 15, 30, and 45 min. No stop solution was added for development of the colorimetric substrate.

For data analysis, the 30 min development time was used. An OD405 value of ≥ 1.0 indicated sufficient immunization (for test bleeds) and dilutions (for production bleeds) for the corresponding data. An OD405 value > 4.0 had an output value of "OVRFLW". A value of 4.01

will be given to these data for analysis purposes. Data for ELISAs (samples, positive controls, or negative controls) were represented as the average of duplicate values, unless otherwise noted.

The term "sample" is used to indicate a full ELISA that included all reagents to distinguish these signals from the negative control signals. For the negative control, all incubation steps remained the same, but instead of the addition of the PAB serum, TBST buffer was added and incubated for 1hr, shaking at room temperature. The negative control will be denoted as "NO PAB".

Standard deviations (SD) for "samples" and NO PAB negative were graphed. The positive and negative SD were entered. SD for the OVRFLW values could not be calculated and received an asterisk in the data table and above the corresponding column in the graphs.

2.2.3.3 Purified Polyclonal Antibody Protein Concentration and SimplyBlue Staining

The purified R2-1 PAB serum was qualified by first determining the total protein concentration for each flow through and wash batch using the Pierce™ BCA Protein Assay kit (ThermoFisher). Aliquots of different steps during purification were taken for analysis but protein concentration could not be determined for some of them due to variable buffers and possible buffer interference with the BCA kit. For visualization, 5 µg of each purified flow through and wash batch, 1 & 5 µg of a separate aliquot of ***un***purified R2-1 PAB serum, and 7.5 µL of different purification step aliquots, for which no concentration could be obtained, were run on SDS-PAGE gel for SimplyBlue staining. Briefly, samples were mixed with 4X LDS sample buffer (Fisher Scientific) and loaded on NuPAGE™ Novex 4-12% Bis-tris gels (Fisher Scientific). The sample buffer (NuPAGE™ LDS Sample Buffer, ThermoFisher) included a reducing agent for a denaturing SDS-PAGE. The SDS-PAGE gels were run at 200 V for 35 min. Gels were then washed briefly in water. Gels were incubated for 1 hr, room temperature, rocking

in a generous amount of SimplyBlue stain (Fisher Scientific). The gels were destained in water at room temperature, rocking until gels could be dried properly. After qualification, purified flow through and wash batches were combined, tubes were washed and added to respective samples, aliquoted, and stored at -70°C.

2.2.4 Monoclonal Antibody Purification

Monoclonal antibody (MAB) producing hybridoma cell lines previously established for Mpt32 (Clone B, 3D11-G7, kindly provided by the Dobos laboratory), DnaK (Clone A, NRC-49679), α-GroES (SA-12, Clone IT-3, NR-49223), and GlnA (both Clone A (NRC-49687) and Clone B (NRC-50108)) were thawed, upscaled, and grown to complete cell death. Cell line base media (DMEM/F12+ Glutamax (FisherScientific), IMDM (Sigma-Aldrich), or RPMI-1640 (FisherScientific, ATCC modified)) varied but all contained at least: 10% fetal bovine serum (FBS – Sigma), 1X antimycotic/antibiotic (Fisher Scientific), 0.055 mM 2-Mercaptoethanol (ThermoFisher Scientific), and 1X HT supplement (Fisher Scientific). Tissue culture supernatants from concentrated MAB producing cultures were collected and sterile filtered using a 0.22 μm PES membrane filter unit (Fisher Scientific). Filtered supernatants were frozen and stored at -20°C if they could not be processed right away.

The purification for the MAB supernatants follows the same protocols as the PAB serum purification (*section 2.2.2 Polyclonal Antibody Serum Purification*), with some modifications. The procedure was adjusted to accommodate larger starting volumes of samples. The conditions were optimized using Mpt32 MAB. This section will address these modifications. After AS precipitation, the supernatant was decanted (saved) and the pellet re-suspended in 25-32 mL of 1X Melon gel purification buffer, pH 6.7 from the Melon™ Gel IgG Purification Kit (ThermoFisher) for dialysis. Two buffer exchanges, one after 3-5 hr and the second overnight,

were carried out at 4°C. The samples were then collected, the dialysis membrane washed and added to sample, and sample was processed immediately after or stored at 4°C until Melon gel purification column could be performed.

The Melon gel purification column followed the same procedure as *section 2.2.2 Polyclonal Antibody Serum Purification*, with some modifications. The following address these modifications. The procedure was adjusted to accommodate larger starting volumes. For Mpt32, a regenerated column from a previous antigen was used and an additional 10 mL of the Melon gel slurry was added. Enough Melon gel slurry was used for a final packed column volume (CV) of 5-6 mL (packed column was approximately 20% of the slurry volume). The sample slurry was rocked manually at room temperature for 5 min. If the sample volume was more than the column could hold (as was the case for α-GroES MAB), the sample was allowed to flow through (collected) and another incubation of the sample with the slurry was repeated. The initial sample flow through(s) and subsequent washes were collected into the same container. It is important to note that when we began optimizing the Melon gel protocol, we did not know how many washes were needed to extract all the IgG antibodies nor which washes were pure. Therefore, Mpt32 was collected in three separate fractions: flow through (FT), washes 1+2, and wash 3. Mpt32 column wash steps were also less extensive (3 x 30 mL washes) than DnaK and GroES column wash steps (10 x 25 mL). The diluted purified flow through(s)/washes were concentrated using equilibrated 10,000 MWCO ultrafiltration amicons (MilliporeSigma). The sample amicons were centrifuged at 3,500 *x g*, 4°C, ~15-40 min each spin. The concentrated sample amicons were washed thrice with ~15 mL of 1X PBS (Fisher Scientific) with the same centrifugation parameters. The final, concentrated, washed 10,000 MWCO retentate was collected and the amicon membranes were washed thoroughly with 1X PBS (Fisher Scientific). Some MABs

remained in wash buffer in the amicons overnight (DnaK and GroES) or over the weekend (Mpt32). The membrane washes were added to the concentrated retentate and aliquoted into smaller tubes. Samples were dried on a speed vacuum concentrator and stored at -70°C until MAB biotinylation.

2.2.5 Monoclonal Antibody Biotinylation

Dried, purified MABs were re-suspended in ~1 mL of 1X PBS (Fisher Scientific) and subsequently biotinylated using an EZ-Link™ NHS-Biotin reagent (ThermoFisher) [112]. Biotinylation followed the manufacturer's instruction manual, under *section* **"***Procedure for Biotinylating Proteins"* [112]. Briefly, volume of biotinylation reagent needed was calculated for an excess molarity of biotin molecules. The biotin molar excess for each MAB biotinylation was as follows: 1) DnaK MAB was at 15mmol biotin /1 mmol protein (IgG, 15-fold excess), SA-12 (α-GroES) was at 20mmol biotin/1mmol protein (IgG, 20-fold excess), and both Mpt32 MAB fractions (both FT/washes 1+2 and wash 3, kept separate) were at 20mmol biotin/1mmol protein (IgG, 20-fold excess). The biotin molar excess for each antigen was chosen by the guidelines found in the manufacturer's instruction manual under *section* **"***Procedure for Biotinylating Proteins"*: proteins at a "10 mg/mL concentration should have a ≥ 12-fold molar excess and proteins at a 2 mg/mL concentration should have a ≥ 20-fold molar excess" [112]. Concentrations of purified MABs were determined using the Pierce™ BCA Protein Assay kit (ThermoFisher). The purified DnaK MAB had a final purified protein concentration of 9.292 mg/mL. The purified α-GroES (SA-12) MAB fraction had a final purified protein concentration of 2.672 mg/mL. For purified Mpt32 MABs, the "FT/washes 1+2" fraction had a final purified protein concentration of 1.469 mg/mL and the "wash 3" fraction had a final purified protein concentration of 1.232 mg/mL.

A 10 mM biotin reagent solution was made by dissolving 2 mg of EZ-LinkTM NHS-Biotin reagent in 590 μL of dimethyl sulfoxide (MilliporeSigma). The 10 mM biotin reagent solution was made fresh for each MAB biotinylation. The corresponding amount of 10 mM biotin reagent solution calculated was added to the 1 mL MAB samples, using manufacturer's protocol (user guide) equation *section* "*Procedure for Biotinylating Proteins*" [112]. The MAB samples were incubated at room temperature for 30 min, rocking. The Mpt32 biotinylated MAB samples remained at 4°C (~30-45 min) after biotinylation but the DnaK and α-GroES MAB samples were processed immediately after biotinylation. The biotinylated MAB samples were concentrated using equilibrated 50,000 MWCO ultrafiltration amicons (MilliporeSigma). The concentrated samples were washed five times with ~4.5-5 mL of 1X PBS (Fisher Scientific). Mpt32 MAB samples remained in wash steps in the amicons overnight at 4°C. DnaK and α-GroES MAB samples were concentrated and washed in the same day. The sample amicons were centrifuged at 3,500 x g at 4°C, ~ 15 min each spin. The concentrated, washed retentate was collected for each sample and the amicon membranes were washed five times with 0.5 mL of 1X PBS (Fisher Scientific) and added to respective samples. The diluted samples were then aliquoted and frozen at -70°C. The final washed, Mpt32 MAB retentate samples remained at 4°C overnight until they could be aliquoted and frozen at -70°C. The frozen samples were then concentrated on a speed vacuum concentrator and immediately re-suspended for qualification purposes or stored dry at -70°C until further qualification. The EZ-Link™ NHS-Biotin reagent (dry) was appropriately stored at room temperature for repeated use of all purified MABs.

2.2.6 Qualification of Monoclonal Antibody Reagents

2.2.6.1 Purified Monoclonal Antibodies

The dilutions and reactivity of the purified MABs were qualified via Western blotting (see *section 2.2.3.1 Western blotting*) and colorimetric indirect ELISAs (see *section 2.2.3.2 Indirect ELISA*), with some modifications. Both immunoassays were performed using purified *Mtb* native or recombinant proteins, and crude CFP and/or WCL fractions. An α-mouse secondary antibody (Abcam) was used at a 1:2,500 dilution in TBS. For both immunoassay analyses, purified MABs will be compared to the ***un***purified MAB positive controls against the respective antigens. These ***un***purified MAB positive controls were filtered hybridoma cell culture supernatants (kindly provided by Dobos laboratory). The ***un***purified MABs had been previously qualified for appropriate Western blot and ELISA dilutions. The term "sample" is used to indicate a full ELISA that included all reagents to distinguish these signals from the negative control signals. All incubation steps remained the same, but instead of the addition of the MAB, TBST buffer was added and incubate for 1 hr, shaking at room temperature. The negative control will be denoted as "NO MAB".

Standard deviations (SD) for "samples", positive control, and NO MAB were graphed. The positive and negative SD were entered. SD for the OVRFLW values could not be calculated and received an asterisk in the data table and above the corresponding column in the graphs.

For visualization of the purified MABs using Western blotting, 1 & 5 μg of each purified MAB and 4 μL (or 7.5 μL) of aliquots taken from different purification steps during the entire purification process were quantified and run on an SDS-PAGE gel (Fisher Scientific) for SimplyBlue staining (Fisher Scientific) (see *section 2.2.3.3 Purified Polyclonal Antibody Protein Concentration and SimplyBlue Staining*).

2.2.6.2 Biotinylated Monoclonal Antibodies

For qualification, the dried biotinylated MABs were re-suspended in 1 mL ultrapure (Milli-Q) water. Re-suspended biotinylated MABs were subsequently aliquoted and re-frozen at -70°C for ease of future use. The biotinylated MABs were qualified via Western blotting (see *section 2.2.3.1 Western blotting*) against purified *Mtb* native or recombinant proteins, and crude fractions CFP and/or WCL, with some modifications to the Western blotting protocol. One modification included the use of a streptavidin-HRP conjugate (Sigma, denoted as "strep-HRP") in lieu of a secondary α-mouse antibody. The streptavidin-HRP conjugate was incubated for 1 hr, room temperature, rocking. After incubation, the blots were washed once with TBS for 5 min. A second modification included the use of a TMB substrate (Sigma) for blot development (according to manufacturer's protocol) [113]. Briefly, enough TMB substrate was added to cover the entire blot. The blots were allowed to develop until sufficient reactivity was observed. The manufacturer called for development for 5-15 min, but the blots developed in < 1 min (blew out blots quickly). The substrate was then discarded, and the blots were rinsed quickly then washed for 4 min in ultrapure (Milli-Q) water (1 min rocking). Scans of the blots were taken once blots were dry enough to ensure no loss of signal. Mpt32 MABs (both fractions) were qualified twice, second time with a more dilute biotinylated MAB dilution. These second-round Mpt32 blots are shown in Figure 20.

2.3 Results and Discussion

2.3.1 Polyclonal Antibody Production: Naïve Bleeds (R1 & R2)

Western blot analysis indicated that the naïve rabbit serum, from both rabbits, was reactive against a slew of *Mtb* antigens in crude CFP and WCL = fractions at dilutions of 1:500 and 1:1,000 (Figure 1). However, we observed low to no reactivity via ELISA against purified antigens or crude fractions for both rabbits' serum (Figure 2, A & B). Rabbit R1 may have

shown some non-specific reactivity against recombinant DnaK more so than the other antigens on the ELISA. It is important to note that we were not able to compare the "samples" to the negative control due to the use of an incorrect secondary antibody (α-mouse instead of α-rabbit used). Rabbit serum for a positive control was not available, so reactivity was solely based on the "sample" OD405 signal for the ELISAs.

One hypothesis for this reactivity, although not tested, was that the rabbits could have been exposed to NTM species in their water or housing units and thus, showed cross-reactivity to *Mtb* antigens. Laboratory animals are potentially exposed to different microbes whether airborne in the rabbit caging areas [114] or in their water [115]. The rabbits were allowed to free drink from a bowl of water (source unknown). We cannot be certain that this was what created the cross-reactivity of their naïve serum to the crude *Mtb* fractions.

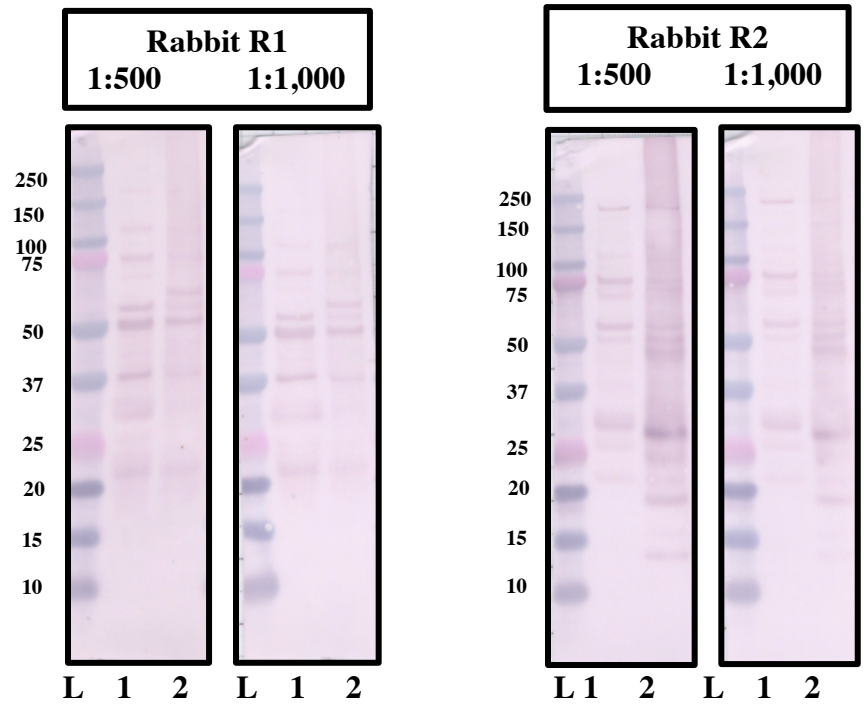

FIGURE 1: Rabbit R1 & R2 Naïve Bleed Western blots

Western blot analysis of rabbits' R1 and R2 naïve serum. Description of antigens loaded on blots: (**lane L**) 2 µL protein ladder, (**lane 1**) 5 µg CFP, and (**lane 2**) 5 µg WCL. Naïve rabbit serum was tested at dilutions of 1:500 and 1:1,000 as indicated above the corresponding blots.

A. Rabbit R1 Naïve Bleed ELISA

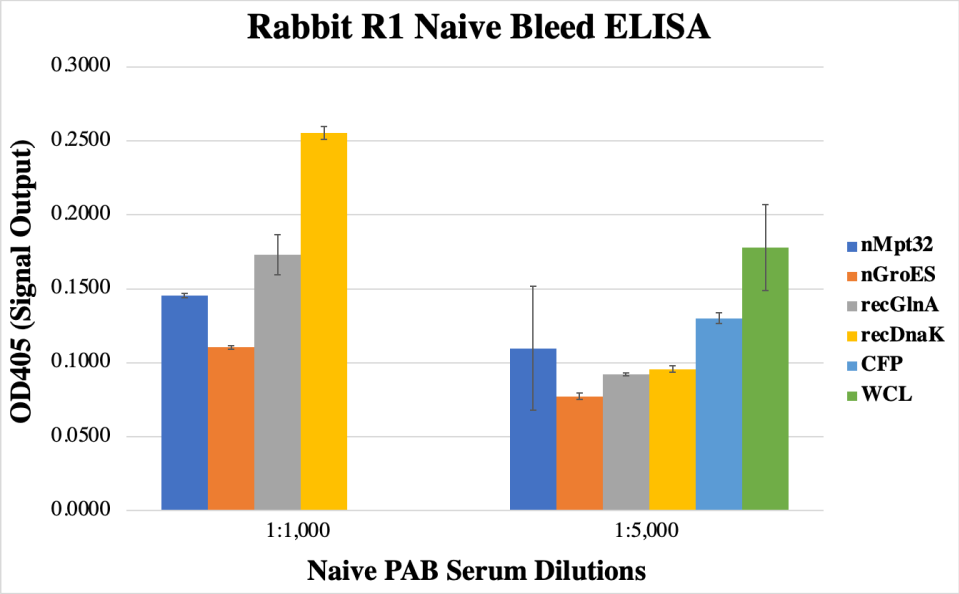

B. Rabbit R2 Naïve Bleed Sera ELISA

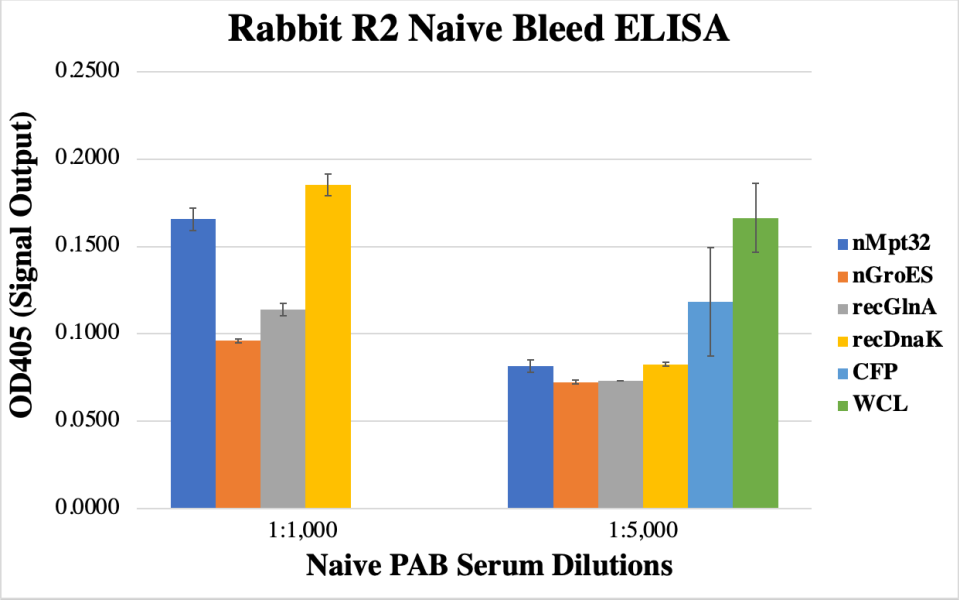

FIGURE 2: Rabbit R1 & R2 Naïve Bleed ELISA

ELISA analysis of rabbits' R1 & R2 naïve serum. **Graph A)** data from naïve bleed ELISA for rabbit R1. **Graph B)** data from naïve bleed ELISA for rabbit R2. Averaged *triplicate* OD405 output signals are graphed on the *Y-axis*. PAB serum dilutions are graphed on *X-axis*. The colors correspond to the different antigens. The purified antigens (nMpt32, nGroES, recGlnA, recDnaK) were plated at a concentration of 1 µg/100 µL (10,000 ng/mL). The crude *Mtb* fractions CFP and WCL were plated at a concentration of 5 µg/100 µL (50,000 ng/mL). The

naïve PAB serum was tested at dilutions of 1:1,000 and 1:5,000 for the purified antigens. Crude fractions were only tested against a naïve PAB serum dilution of 1:5,000.

2.3.2 Polyclonal Antibody Production: Test Bleeds (R1 & R2)

Western blot analysis for the first test bleed demonstrated successful immunization of rabbit R1. Rabbit R1 showed reactivity to both native GlnA (CFP) and recGlnA at a dilution of 1:1,000 (Figure 3). These results mirrored the ELISA data which showed sufficient reactivity to recGlnA as well as both crude CFP and WCL fractions (Figure 4). A third immunization for rabbit R1 was not necessary, but we decided to move forward with one last boost with the remaining antigen. Instead of performing a second test bleed post third immunization, rabbit R1 was deemed ready to start production bleeds (~ 2 weeks post third immunization).

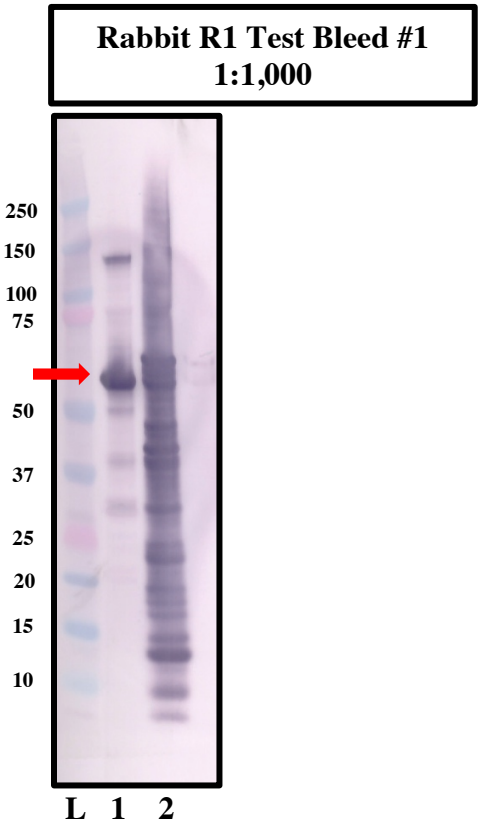

FIGURE 3: Rabbit R1 Test Bleed #1 Serum Western blot
Western blot analysis of rabbit R1 test bleed #1 serum. Description of antigens loaded on blot: (**lane L**) 2 µL protein ladder, (**lane 1**) 5 µg CFP, and (**lane 2**) 1 µg recGlnA. The PAB serum was tested at a dilution of 1:1,000. GlnA protein band (~53 kDa) is indicated by red arrow.

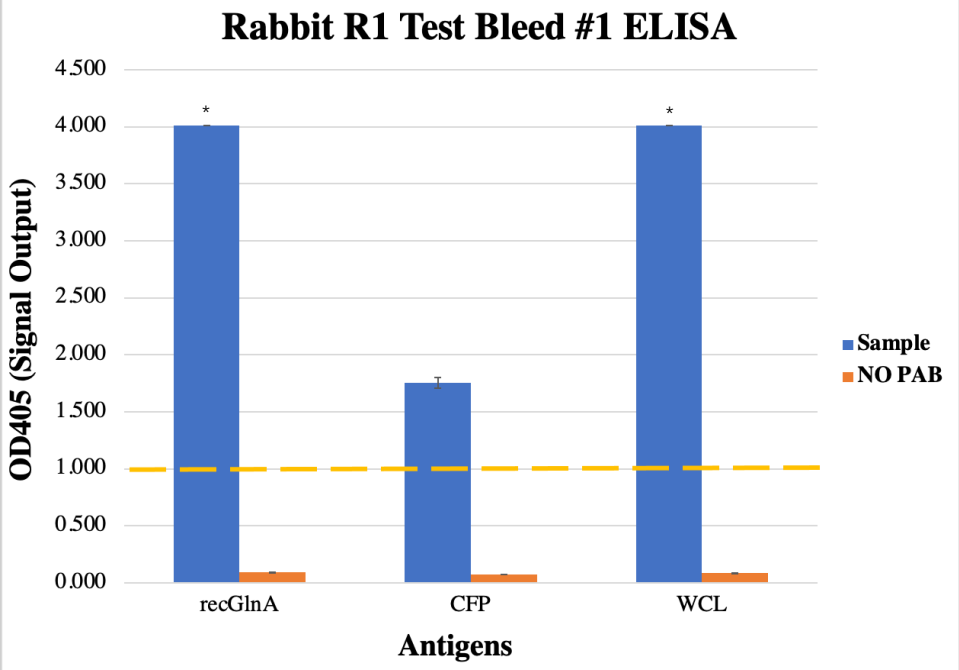

FIGURE 4: Rabbit R1 Test Bleed #1 Serum ELISA
ELISA analysis of rabbit R1 test bleed #1 sera. Averaged *duplicate* OD405 output signals are graphed on the *Y-axis*. The "samples" (blue) and NO PAB negative control (orange) are grouped according to the different antigens tested and are graphed on *X-axis*. The purified recGlnA antigen was plated at a concentration of 1 μg/100 μL (10,000 ng/mL). The crude *Mtb* fractions CFP and WCL were plated at a concentration of 5 μg/100 μL (50,000 ng/mL). A PAB serum dilution of 1:1,000 was tested for the "samples". A dashed-yellow line indicates an OD405 signal of 1.

Western blot data for the first test bleed for rabbit R2 demonstrated decent reactivity to both recombinant proteins (DnaK and GlnA) at a dilution of 1:1,000. However, rabbit R2 demonstrated poor reactivity to both native proteins (GroES and Mpt32) at a dilution of 1:1,000 (Figure 5). ELISA results demonstrated that all but nMpt32 were at an OD405 of ≥ 1 at 30 min development (Figure 6), which was reflected in the raw data OD405 readings (data not shown). However, the SD negative value would put nGroES under this cut off. Both immunoassay analyses indicated that rabbit R2 was not sufficiently immunized against the two native proteins. This was surprising as both nMpt32 and nGroES are highly immunogenic [17,116,117]. Therefore, for the third immunization, we decided to increase the concentration of both native proteins from 125 μg to 200 μg each antigen and decrease the concentration of both recombinant proteins from 125 μg to 50 μg each antigen.

Western blot (Figure 5) and ELISA (Figure 6) data for the second test bleed of rabbit R2 demonstrated an increase in reactivity for both nGroES and nMpt32 antigens at a dilution of 1:1,000. Western blots showed a darkening of the band signal for nGroES (10 kDa) and a slight darkening of the band signal for nMpt32 (45kDa, typical "hamburger bun" pattern) when comparing test bleed #1 to test bleed #2 (Figure 5). For nGroES, ELISA data demonstrated an increase to an OVRFLW signal for test bleed #2 (Figure 6). For nMpt32, ELISA data demonstrated an increase of OD405 reading from < 1 for test bleed #1 to an OD405 reading of ~ 3.3 for test bleed #2 (Figure 6). Recombinant proteins DnaK and GlnA showed an increase in

reactivity as well in both Western blot and ELISA analyses (Figures 5 & 6, respectively). Crude CFP and WCL fractions had an increase in reactivity on ELISA from test bleed #1 to test bleed #2 as well (Figure 6). An OD405 of ≥ 1 at 30 min development on ELISA and a darker signal on the Western blots, both immunoassays with a PAB serum dilution of 1:1,000, for all four antigens indicated successful immunization and rabbit R2 was deemed ready to start production bleeds (2 weeks post third immunization).

The lack of sufficient immunization after the second injection (first test bleed) could have been due to the loss of emulsified antigen product. A significant amount of product was lost in the emulsifier and the volume was greatly decreased from the intended final injection volume of 1 mL. However, a loss of product would mean equal loss among all four antigens. Increasing the concentration of the two native proteins in the final third immunization greatly increased reactivity in test bleed #2 for rabbit R2, even with loss of antigen product during antigen preparations. It seems that rabbit R2 mounted a more robust immune response against the recombinant proteins after the first two immunizations and was able to mount a more robust immune response against the native proteins only after the native protein concentrations increased.

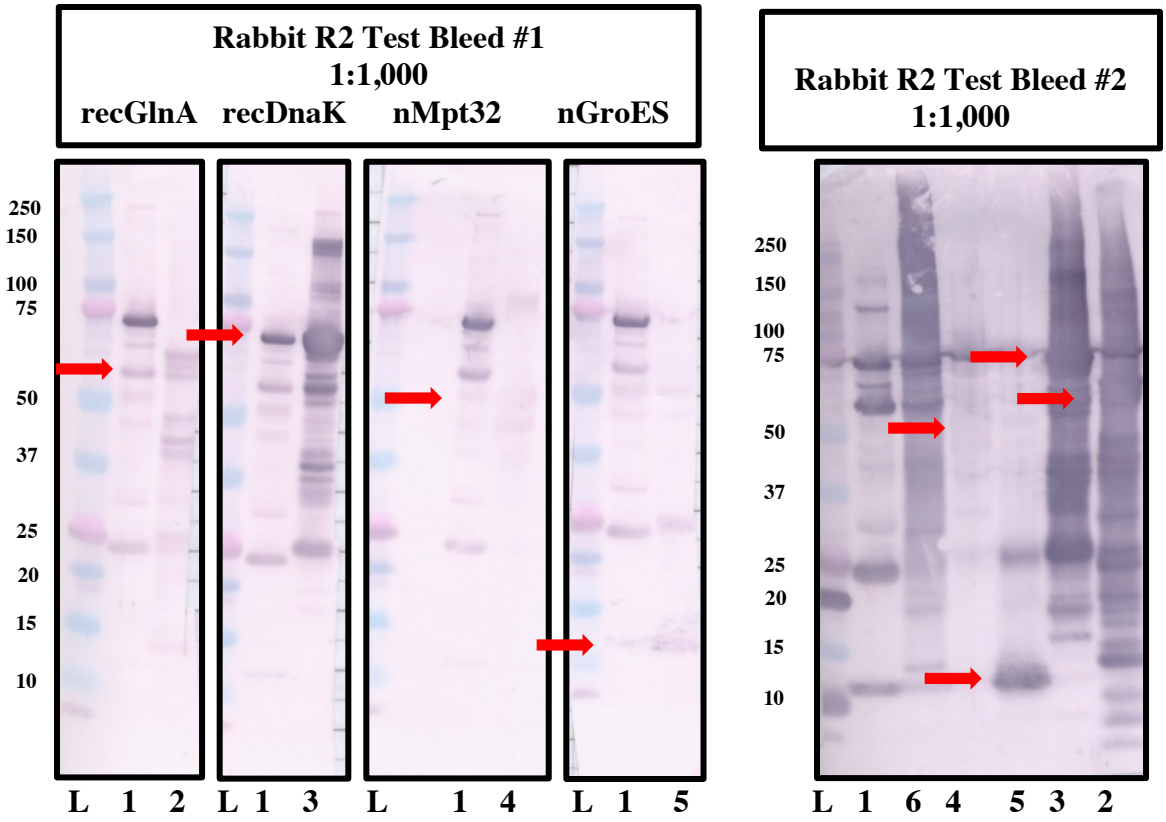

FIGURE 5: Rabbit R2 Test Bleeds #1 & #2 Serum Western blots
Western blot analysis of rabbit R2 test bleeds #1 & #2 serum. Description of antigens loaded on blots: (**lane L**) 2 µL protein ladder, (**lane 1**) 5 µg CFP, (**lane 2**) 1 µg recGlnA, (**lane 3**) 1 µg recDnaK, (**lane 4**) 1 µg nMpt32, (**lane 5**) 1 µg nGroES, and (**lane 6**) 5 µg WCL. PAB sera for test bleeds #1 & #2 were tested at a dilution of 1:1,000 (for both blots). *The test bleed #2 blot lanes were run in a different order and is represented in the description*. Mpt32 (45 kDa, typical "hamburger bun" pattern), GroES (10 kDa), DnaK (~67 kDa), and GlnA (~53 kDa) protein bands are indicated by red arrows.

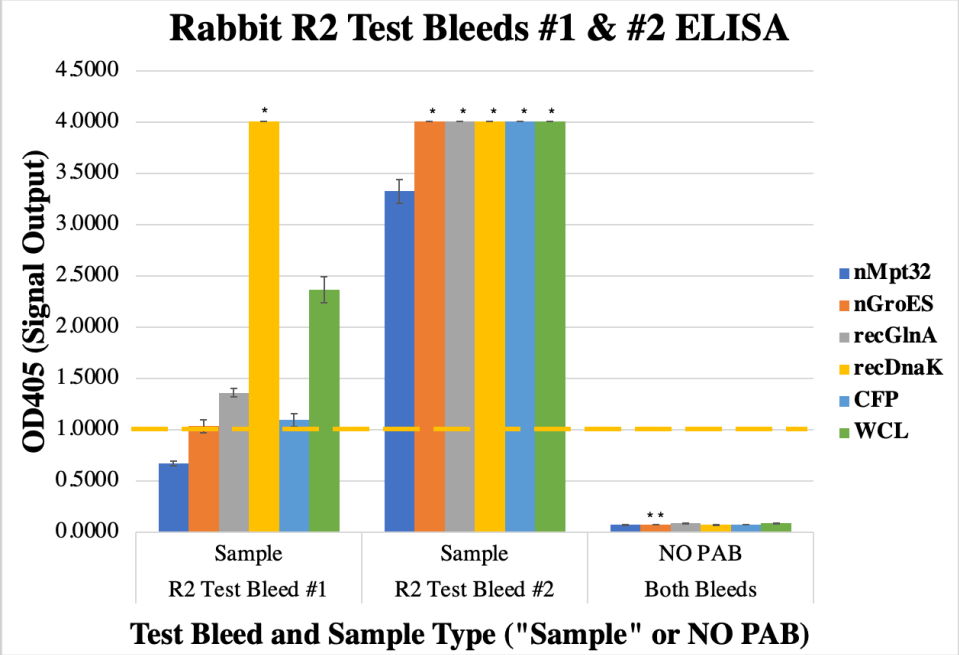

FIGURE 6: Rabbit R2 Test Bleeds #1 & #2 Serum ELISA
ELISA analysis of rabbit R2 test bleeds #1 &#2 serum. Averaged *duplicate* OD405 output signals (for "samples" and NO PAB negative control) are graphed on *Y-axis*. Antigens are graphed on *X-axis* and are grouped according to test bleed #1 or #2 as well as NO PAB negative control (same for both bleeds). The different colors correspond to the different antigens. The purified antigens (nMpt32, nGroES, recGlnA, recDnaK) were plated at a concentration of 1 µg/100 µL (10,000 ng/mL). The crude *Mtb* fractions CFP and WCL were plated at a concentration of 5 µg/100 µL (50,000 ng/mL). A PAB serum dilution of 1:1,000 was tested for both test bleeds #1 & #2. A double asterisk indicates nGroES with only one signal value (no duplicates). A dashed-yellow line indicates an OD405 signal of 1.

2.3.3 Polyclonal Antibody Production: Production Bleeds (R1)

For the first and second production bleeds of rabbit R1, the Western blot analysis (Figure 7) demonstrated sufficient reactivity at a PAB serum dilution of 1:40,000 against recGlnA. There could be some slight decrease in reactivity for both crude fractions at the 1:40,000 dilution, but both remained highly reactive. The third production bleed demonstrated a waning of PAB serum dilution to 1:20,000 against recGlnA. However, band signal intensity did not seem to wane for the crude CFP and WCL fractions for any of the dilutions. The Western blots also demonstrated that the PAB serum was reactive to only a couple of protein bands for the crude fractions. Only

data for production bleeds #1 and #3 are shown due to production bleed #2 looking similar in dilution and signal strength (*Appendix: Figure 36*).

Figure 8 demonstrates nicely a decreasing signal trend as dilutions decreased for each antigen (for each production bleed) for the ELISAs. The NO PAB negative control signals remained very low for each antigen (for each production bleed). We observed that the signals for the corresponding dilution for recGlnA were above the dashed-yellow line. However, the signals for the crude CFP and WCL fractions fell below this line for almost all the dilutions. The crude fractions would have needed more testing to find the correct dilutions for the ELISA. However, this indicated that PAB serum was less reactive against the native GlnA in these crude fractions. The reactivity for these crude fractions waned from production bleed to production bleed. ELISA data also demonstrated a PAB serum dilution of 1:40,000 against recGlnA for the first and second production bleeds.

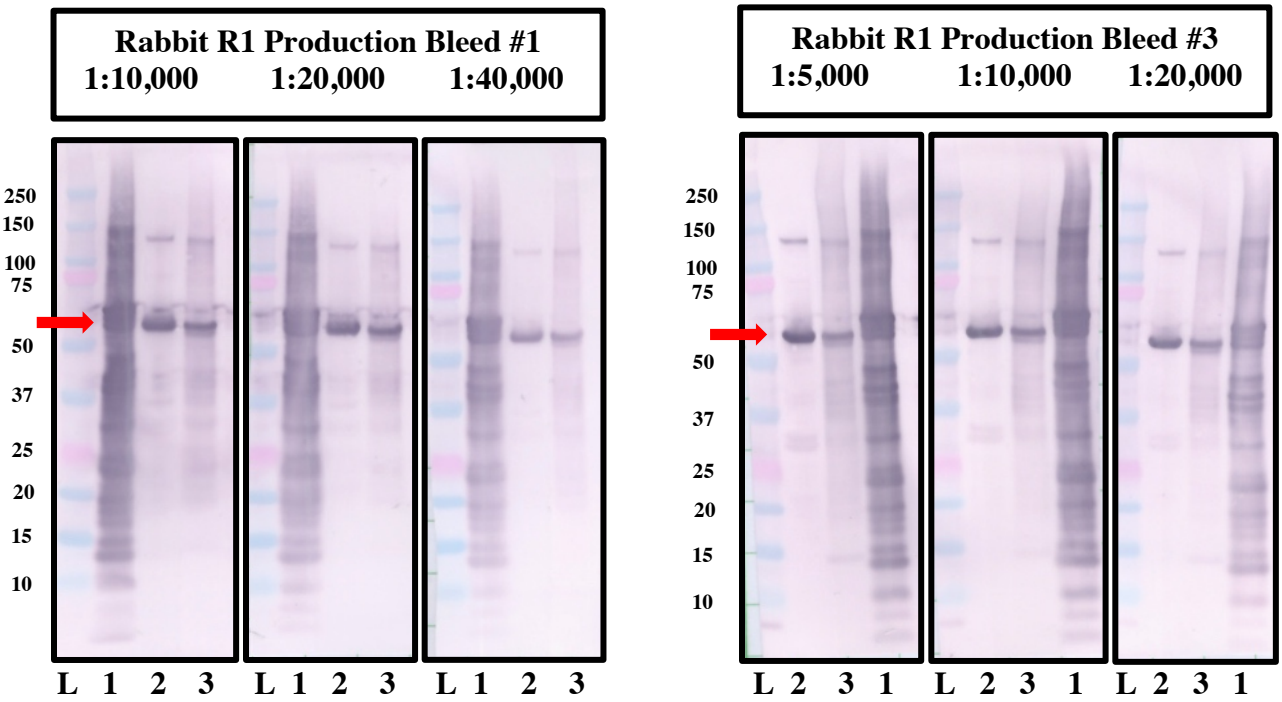

FIGURE 7: Rabbit R1 Production Bleeds #1 & #3 serum Western blots
Western blot analysis of rabbit R1 production bleeds #1 & #3 serum. Description of antigens loaded on blots: (**lane L**) 2 µL protein ladder, (**lane 1**) 1 µg recGlnA, (**lane 2**) 5 µg CFP, and (**lane 3**) 5 µg WCL. PAB serum for production bleed #1 was tested at dilutions of 1:10,000, 1:20,000, and 1:40,000. PAB serum for production bleed #2 was tested at dilutions of 1,5000, 1:10,000, and 1:20,000. Dilutions tested are labeled above the corresponding blots. GlnA protein band (~53 kDa) is indicated by red arrows.

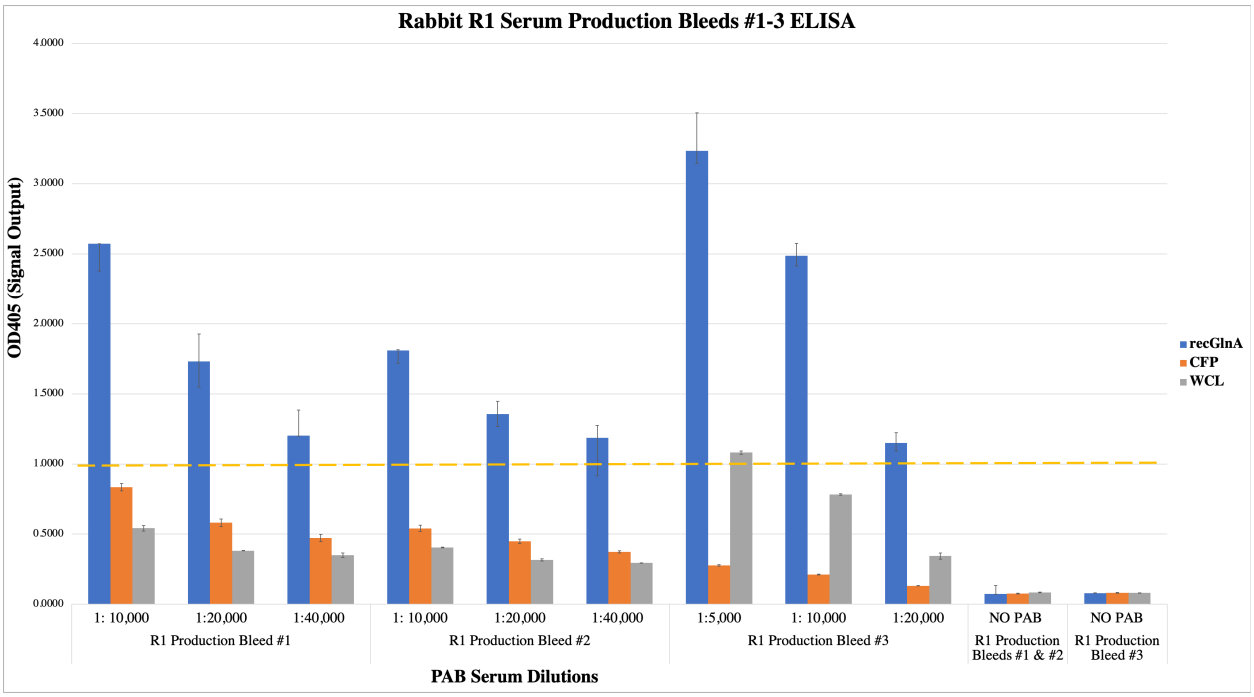

FIGURE 8: Rabbit R1 Production Bleeds #1-3 Serum ELISA
ELISA analysis of rabbit R1 production bleeds #1-3 serum. Production bleeds #1 & #2 were run on the same microplate using the same NO PAB negative controls ("*NO PAB R1 Production Bleeds #1 & #2*" on graph). Production bleed #3 was run on a separate microplate with its own NO PAB negative controls ("*NO PAB R1 Production Bleed #3*" on graph). Averaged *duplicate* OD405 output signals (for "samples" and NO PAB negative controls) are graphed on *Y-axis*. PAB sera dilutions are graphed on the *X-axis*. The colors correspond to the different antigens. The recGlnA antigen (blue) was plated at a concentration of 1 µg/100 µL (10,000 ng/mL). The crude *Mtb* fractions CFP (orange) and WCL (grey) were plated at a concentration of 5 µg/100 µL (50,000 ng/mL). PAB serum was tested at dilutions of 1:10,000, 20,000, and 40,000 for production bleeds #1 and #2 and at dilutions of 1:5,000, 1:10,000, and 1:20,000 for production bleed #3. A dashed-yellow line indicates an OD405 signal of 1.

2.3.4 Polyclonal Antibody Production: Production Bleeds (R2)

For the first production bleed of rabbit R2, Western blot analysis demonstrated a PAB serum dilution of < 1:5,000 for nMpt32 (more concentrated dilutions not tested) and a dilution of 1:10,000 for nGroES, recDnaK, and recGlnA (Figure 9). We saw waning in band signal intensities for both recombinant proteins and nGroES when tested at a dilution of 1:20,000 (Figure 9).

For the second production bleed of rabbit R2, Western blot analysis demonstrated an increase in reactivity to nMpt32, with a dilution of 1:10,000 with an argument for 1:20,000. Both recombinant proteins' reactivity increased to a dilution of 1:20,000 as well. The second production bleed demonstrated a decrease in reactivity against nGroES with a more concentrated dilution of 1:5,000 (Figure 9).

By the third production bleed of rabbit R2, we observed waning in band signal intensity on the Western blots for all four antigens. RecDnaK, recGlnA, and nMpt32 all demonstrated a dilution of 1:5,000 and nGroES a dilution of 1:2,500 (Figure 9). For the crude CFP and WCL fractions, the reactivity seemed generally lower, but it was difficult to distinguish all four antigen bands. DnaK and GlnA seemed to have the most intense band signals for both crude fractions. GroES bands were better visualized in the CFP fraction for production bleed #3. However, it is difficult to discern the typical Mpt32 "hamburger bun" pattern for any of the crude fractions.

Figure 10 demonstrates nicely a decreasing signal trend as dilutions decreased for each antigen, for each production bleed for the ELISAs. The NO PAB negative control signals remained very low for each antigen (for each production bleed). The yellow-dashed line demonstrated that recDnaK was the only antigen that remained at an OD405 $\geq$ 1 for all dilutions, for all production bleeds.

By the third production bleed of rabbit R2, ELISA data demonstrated a dramatic increase in reactivity for all antigens. At this point, all antigens increased above the OD405 $\geq$ 1 yellow-dashed line. This was interesting because the third production bleed was performed ~ 3 months post third immunization. This could have been the result of repeated exposure to *Mtb* antigens as mentioned in *section 2.3.1 Polyclonal Antibody Production: Naïve Bleeds (R1 & R2).*

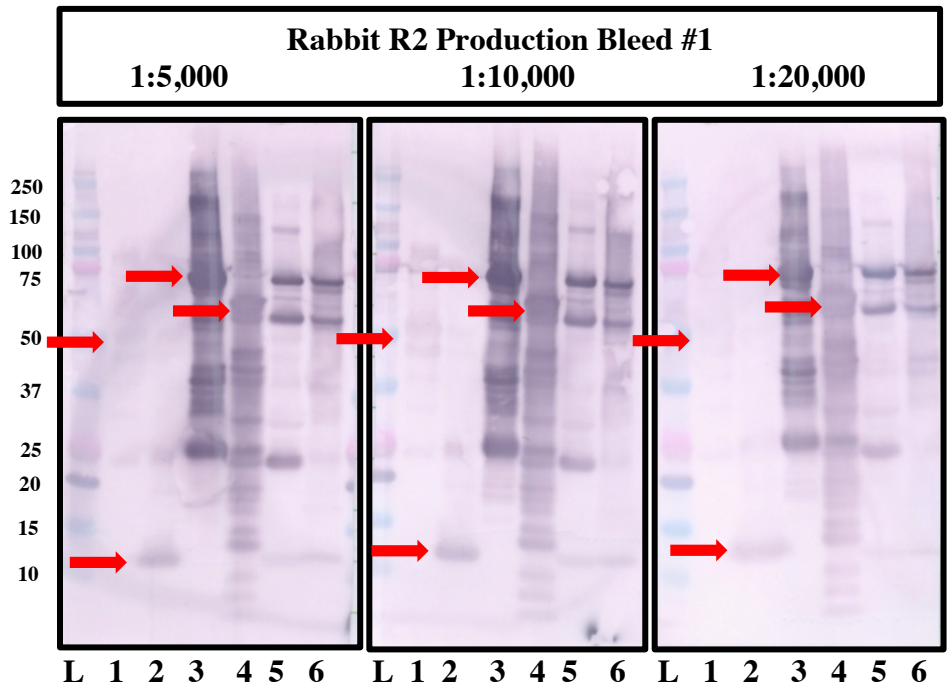
Rabbit R2 Production Bleed #1
1:5,000
1:10,000
1:20,000
250
150
100
75
50
37
25
20
15
10
L 1 2 3 4 5 6
L 1 2 3 4 5 6
L 1 2 3 4 5 6

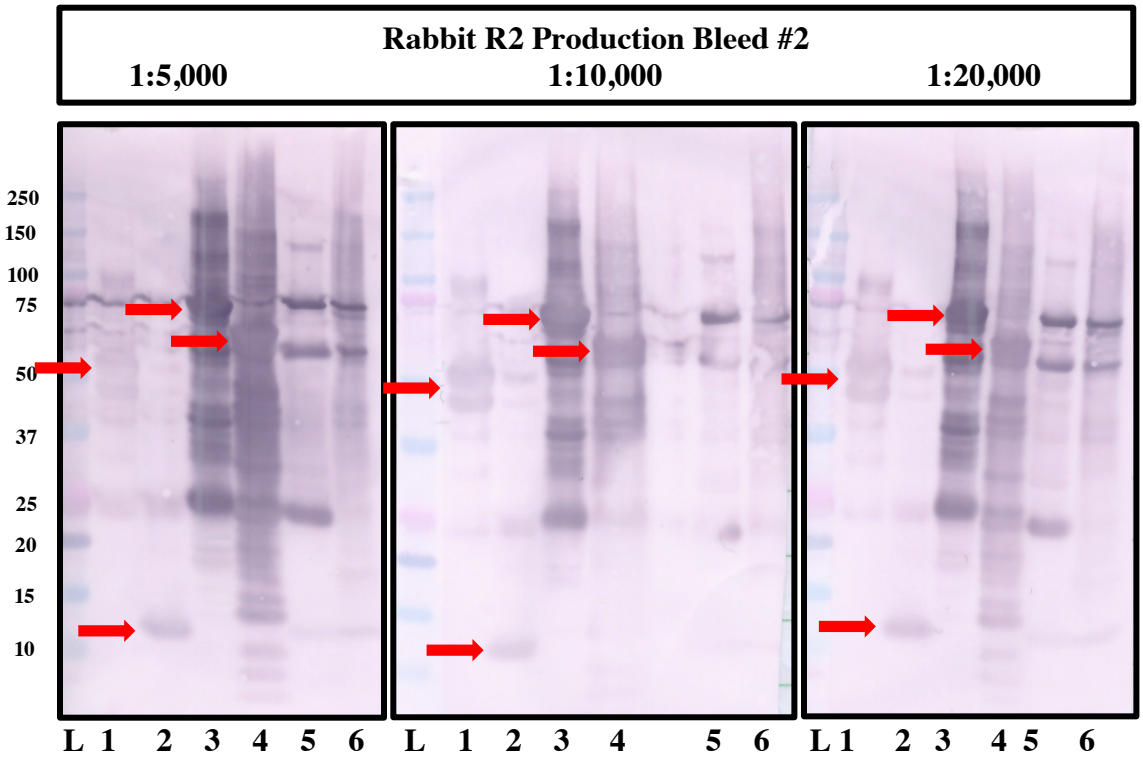
Rabbit R2 Production Bleed #2
1:5,000
1:10,000
1:20,000
250
150
100
75
50
37
25
20
15
10
L 1 2 3 4 5 6
L 1 2 3 4 5 6
L 1 2 3 4 5 6

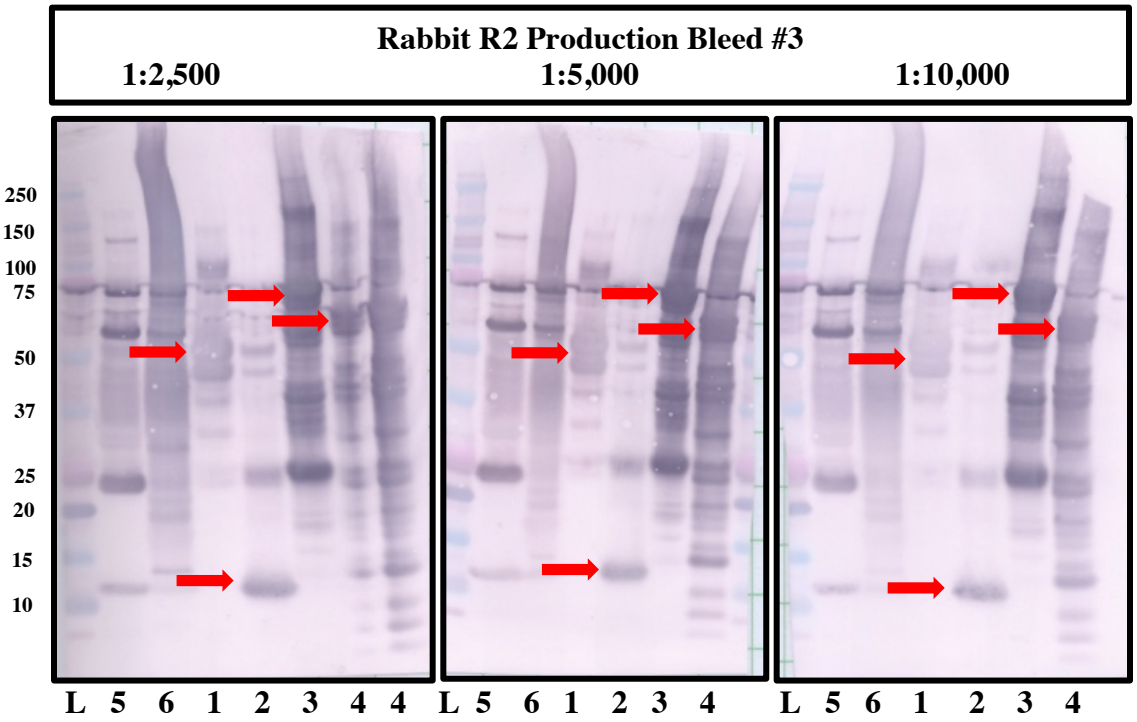

FIGURE 9: Rabbit R2 Production Bleeds #1-3 Serum Western blots
Western blot analysis of rabbit R2 production bleeds #1-3 sera. Description of antigens loaded on blots: (**lane L**) 2 µL protein ladder, (**lane 1**) 1 µg nMpt32, (**lane 2**) 1 µg nGroES, (**lane 3**) 1 µg recDnaK, (**lane 4**) 1 µg recGlnA, (**lane 5**) 5 µg CFP, and (**lane 6**) 5 µg WCL. PAB serum for production bleeds #1 & #2 was tested at dilutions of 1:5,000, 1:10,000, and 1:20,000. PAB serum for production bleed #3 was tested at dilutions of 1:2,500, 1:5,000, and 1:10,000. Dilutions tested are labeled above the corresponding blots. Mpt32 (45 kDa, "hamburger bun" pattern), GroES (10 kDa), DnaK (~67 kDa), and GlnA (~53 kDa) protein bands are indicated by red arrows.

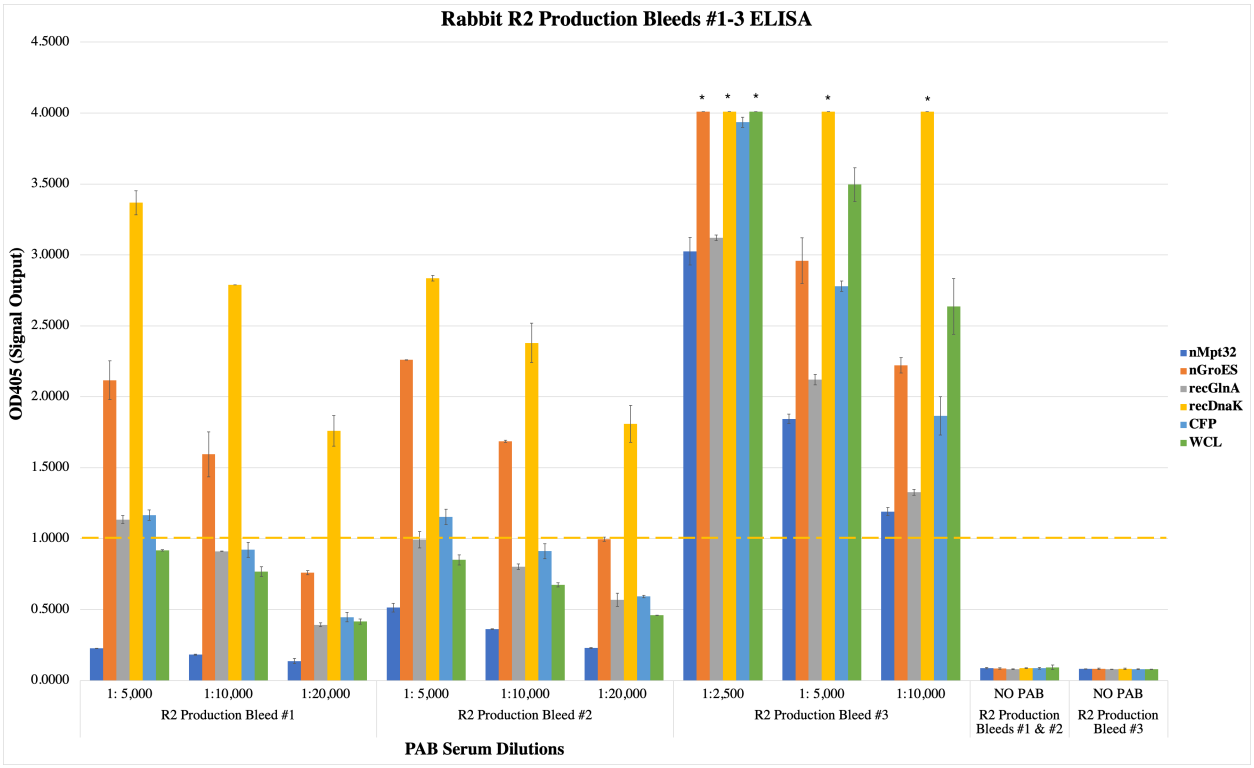

FIGURE 10: Rabbit R2 Production Bleeds #1-3 Serum ELISA

ELISA analysis of rabbit R2 production bleeds #1-3 sera. Production bleeds #1 & #2 were run on the same microplate using the same NO PAB negative controls ("*NO PAB R2 Production Bleeds #1 & #2*" on graph). Production bleed #3 was run on a separate microplate with its own NO PAB negative controls ("*NO PAB R2 Production Bleed #3*" on graph). Averaged *duplicate* OD405 output signals (for "samples" and NO PAB negative controls) are graphed on *Y-axis*. PAB serum dilutions are graphed on the *X-axis*. The colors correspond to the different antigens. The purified antigens (nMpt32, nGroES, recGlnA, recDnaK) were plated at a concentration of 1 µg/100 µL (10,000 ng/mL). The crude *Mtb* fractions CFP and WCL were plated at a concentration of 5 µg/100 µL (50,000 ng/mL). PAB serum was tested at dilutions of 1:5,000, 10,000, and 20,000 for production bleeds #1 and #2, but was tested at dilutions of 1:2,500, 1:5,000, and 1:10,000 for production bleed #3. A dashed-yellow line indicates an OD405 signal of 1.

2.3.5 Polyclonal Antibody Purification

During purification of the R2-1 PAB serum, different aliquots were taken from each step of the process. This sample is now denoted as PR2-1 for differentiation of the purified PAB serum. The denaturing SimplyBlue-stained gel (Figure 11) demonstrates these different purification steps. Lanes 1 and 2 in Figure 11 show a large protein band ~66 kDa (black arrow) that was most likely albumin. This high molecular weight protein seemed to be purified out of the sample in the final PR2-1 product (lanes 6-8). The final PR2-1 product had defined 50 kDa

and 25 kDa bands, representing the heavy and light chains of the antibodies, respectively. There may have been some higher molecular weight bands above 50 kDa. PR2-1 final products were kept in separate fractions until final qualification with SimplyBlue-stained gel (lanes 6-8) and then combined. This qualification gel demonstrated successful purification of a very complex sample such as PAB serum using the purification methods chosen.

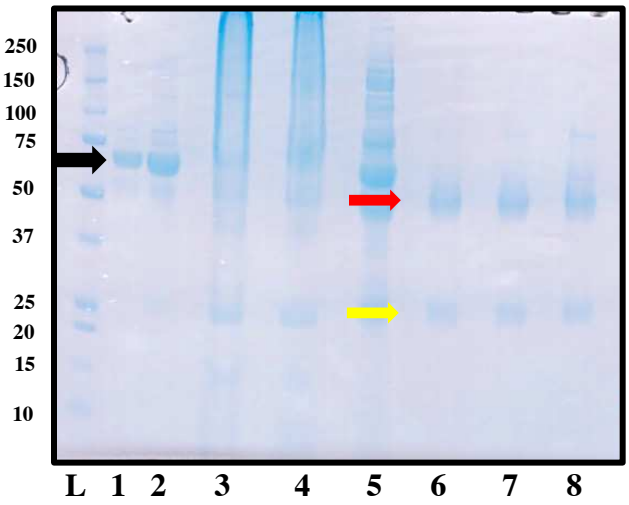

FIGURE 11: Rabbit R2 Production Bleed #1 PAB Serum Purification
Purification of PAB serum from first production bleed of rabbit R2 (indicated as PR2-1) via Melon gel column. Purified PAB serum was subjected to analysis via a denaturing SDS-PAGE gel stained with SimplyBlue stain. SimplyBlue-stained gel is comparing ***un***purified R2-1 PAB serum from the first production bleed, aliquots of different stages of the purification process (ammonium sulfate (AS) precipitation), and the final purified product. Description of different aliquots loaded on gel: (**lane L**) 2 µL protein ladder, (**lane 1**) 1 µg ***un***purified R2-1 PAB serum, (**lane 2**) 5 µg ***un***purified R2-1 PAB serum, (**lane 3**) 7.5 µL AS precipitation fraction (after AS precipitation and before centrifugation), (**lane 4**) 7.5 µL 50% AS precipitation (supernatant fraction), (**lane 5**) 7.5 µL 50% AS precipitation (dialyzed pellet fraction), (**lane 6**) 5 µg Melon gel flow through (FT), (**lane 7**) 5 µg Melon gel washes #1-5 (w1-5), (**lane 8**) 5 µg Melon gel washes #6-10 (w6-10). Lanes #6-8 are the final product from Melon gel column. **Un**purified PAB serum for the gel was from a different aliquot than the combined ones used for purification. Antibody heavy and light chains are indicated by red and yellow arrows, respectively, for last three purified Melon gel fractions. Bands that appear to be albumin (~66 kDa) are indicated by a black arrow. SimplyBlue gel image brightened 40% for ease of visualizing bands.

2.3.6 Monoclonal Antibody Purification

The denaturing SimplyBlue-stained gel (Figure 12) demonstrates the different purification steps for the DnaK MAB. Lanes 1-3 in Figure 12 showed a large protein band ~65 kDa. This high molecular weight band most likely corresponded to albumin. This high molecular weight protein seemed to be purified out of the sample in the final purified MAB product (lanes 4 and 5). The final purified DnaK MAB product has defined 50 kDa and 25 kDa protein bands, representing heavy and light chains of the antibody, respectively. There may be some higher molecular weight bands above 50 kDa, but this sample was deemed pure enough for biotinylation.

Western blot analysis for the purified DnaK MAB demonstrated a dilution of 1:20,000 (Figure 12). More concentrated dilutions of the purified DnaK MAB were performed but the MAB remained incredibly reactive to the recDnaK and crude WCL fraction antigens at a dilution of 1:20,000. The positive control (***un***purified MAB cell culture supernatant) was performed at a dilution of 1:5,000 only and showed a very faint band signal for the recDnaK and crude WCL fraction antigens. Thus, the purification process seemed to not only successfully purify the MAB, but also concentrate the MAB to the point of using a 4-fold less concentrated MAB dilution when compared to the cell culture supernatant control.

Figure 13 demonstrates the ELISA data for the purified DnaK MAB. The purified DnaK MAB was highly reactive at a dilution of 1:5,000 for recDnaK. Reactivity to both crude fractions remained low with signals well below an OD405 of 1. The ***un***purified cell culture supernatant positive control was not reactive on ELISA at a dilution of 1:5,000 (more concentrated dilutions were not tested). This could have been, in part, due to antibody integrity issues created by storing the diluted positive control at -70°C for a couple months. The positive control and the crude

fractions were almost indistinguishable from the NO MAB negative control. The data indicated that the purified DnaK MAB was unable to detect the native DnaK antigen in either crude fraction at any of the dilutions tested. More concentrated dilutions of the purified DnaK MAB would have to be tested against both crude fractions to determine their adequate dilutions for ELISA. Because the desired antigen only makes up a small percentage of the crude sample, an increase in MAB concentration could be needed for detection. However, we still were able to demonstrate that the purified MAB had increased reactivity (with a less concentrated dilution) when compared to the ***un***purified cell culture supernatant (with a more concentrated dilution).

Thus, it seems that the DnaK MAB is able to recognize the linearized recDnaK antigen better than the folded DnaK antigen. This is demonstrated by the fact that the purified MAB is more reactive at a lower dilution via Western blotting than ELISA, respectively.

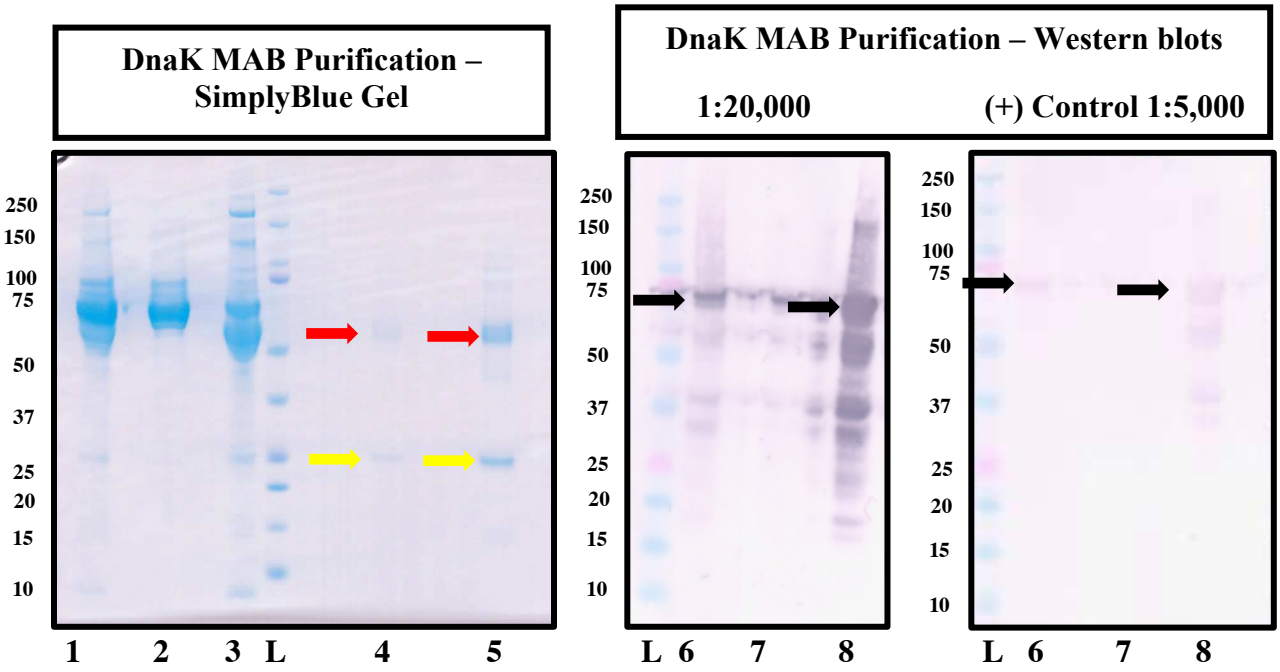

FIGURE 12: DnaK MAB Purification SimplyBlue Gel & Western blot
Purification of DnaK MAB via Melon gel. Purified DnaK MAB was subjected to analysis via Western blotting and a denaturing SDS-PAGE gel stained with SimplyBlue stain. Aliquots of each step in the purification process were saved and loaded on gels. These aliquots were taken from cell culture supernatant, ammonium sulfate (AS) precipitation on the cell culture supernatant (AS supernatant and dialyzed pellet fractions), along with the Melon gel purified products. Description of different aliquots loaded on gel: (**lane L**) 2 µL protein ladder, (**lane 1**) 4 µL cell culture supernatant (before AS precipitation), (**lane 2**) 4 µL AS precipitation (supernatant fraction), (**lane 3**) 4 µL AS precipitation (dialyzed pellet fraction), (**lane 4**) 1 µg purified MAB, and (**lane 5**) 5 µg purified MAB. Description of different aliquots loaded on blots: (**lane L**) protein ladder, (**lane 6**) 5 μg WCL, (**lane 7**) 5 μg CFP, and (**lane 8**) 1 μg recDnaK. The purified DnaK MAB was tested at dilutions of 1:5,000, 1:10,000, and 1:20,000, but only the 1:20,000 dilution blot is shown here. The positive (+) control (DnaK Clone A, ***un***purified cell culture supernatant) was tested at a dilution of 1:5,000. Antibody heavy and light chains are indicated by red and yellow arrows, respectively, on the SimplyBlue-stained gel. DnaK (~67 kDa) protein bands are indicated by black arrows on Western blot. SimplyBlue gel image brightened 40% for visualization of bands.

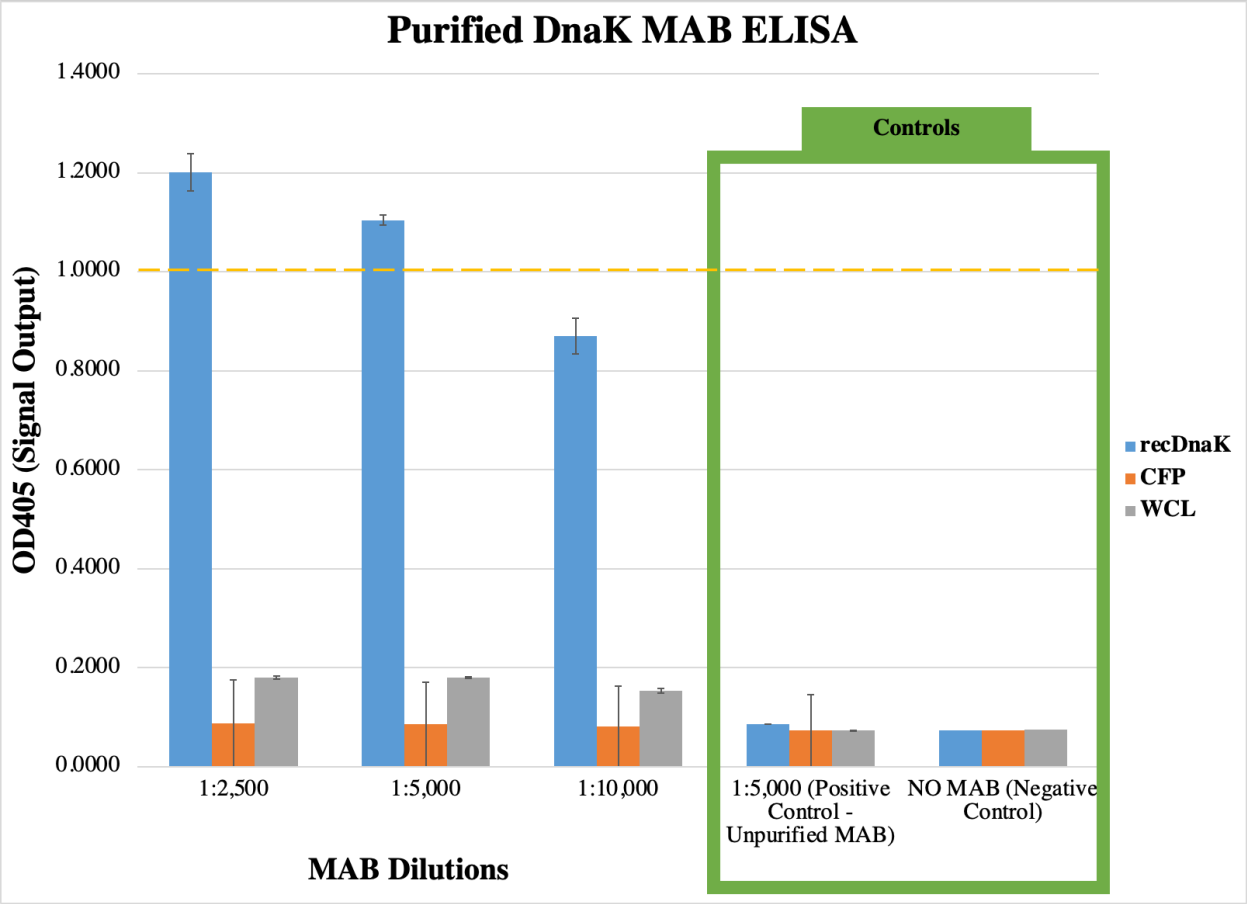

FIGURE 13: DnaK MAB Purification ELISA
Purification of DnaK MAB via Melon gel. Purified DnaK MAB was subjected to analysis via ELISA. Averaged *duplicate* OD405 output signals (for "samples" and positive control) as well as averaged *quadruplicate* OD405 output signals (for NO MAB negative control) are graphed on *Y-axis*. Purified MAB dilutions (for "samples) are graphed on the *X-axis*. The positive control and negative control are also graphed on *X-axis* (in green box). The antigens are graphed according to different colors: recDnaK (blue), CFP (orange), and WCL (grey). RecDnaK antigen was plated at a concentration of 1 µg/100 µL (10,000 ng/mL). The crude *Mtb* fractions CFP and WCL were plated at a concentration of 5 µg/100 µL (50,000 ng/mL). Purified MAB was tested at dilutions of 1:2,500, 1:5,000, and 1:10,000. The positive control (Clone A, ***un***purified cell culture supernatant) was tested at a dilution of 1:5,000. A yellow dotted line is graphed to show OD405 of 1.

The denaturing SimplyBlue-stained gel (Figure 14) demonstrates the different purification steps for the α-GroES (SA-12) MAB. Lanes 1-3 in Figure 14 showed a large protein band ~65 kDa, similar to what was observed for DnaK MAB (Figure 12). This high molecular weight protein seemed to be purified out of the sample in the final purified MAB product (Figure

14: lanes 4 and 5). The final purified MAB product had defined 50 kDa and 25 kDa protein bands, representing heavy and light chains of the antibody, respectively. There were some higher molecular weight bands above 50 kDa, but this sample was deemed pure enough for biotinylation.

Western blot analysis for the purified α-GroES MAB demonstrated a dilution of 1:500 and was reactive against both the nGroES and crude CFP fraction antigens (Figure 14). A less concentrated dilution (1:1,000) could have been performed, as the band signals were dark at a 1:500. This dilution is much more concentrated than the DnaK MAB Western blot dilutions. This could be indicative of the α-GroES MAB having a lower affinity to its protein antigen. The positive control (***un***purified MAB cell culture supernatant) was performed at a dilution of 1:20 only and showed similar reactivity to the purified MAB dilution of 1:500. Thus, the purification process seemed to not only successfully purify but also concentrate the α-GroES MAB to the point of using a 25-fold less concentrated MAB dilution when compared to the cell culture supernatant control.

Figure 15 demonstrates the ELISA data for the purified α-GroES MAB. The purified MAB was reactive at a dilution of 1:100 for nGroES. Less concentrated dilutions were not tested but seeing as though the OD405 signal is close to 1 for the 1:100 dilution, a less concentrated dilution of the MAB may put the signal under the yellow-dashed line (Figure 15). As mentioned previously, these less concentrated dilutions could indicate poor affinity to the protein antigen. The purified α-GroES MAB was less reactive to both crude fractions. More concentrated dilutions would have to be tested to find the optimal dilution for each crude fraction. The positive control (***un***purified MAB cell culture supernatant) was performed at a dilution of 1:20 only and showed poor reactivity compared to the purified α-GroES MAB against all antigens

(nGroES and both crude fractions). It is important to note that the ***un***purified MAB cell culture supernatant was never previously qualified on ELISA and may have a more concentrated dilution. The NO MAB negative control remained low for all antigens.

Thus, it seems that the α-GroES (SA-12) MAB is able to recognize the linearized nGroES antigen better than the folded nGroES antigen. This is demonstrated by the fact that the purified α-GroES MAB is more reactive at a less concentrated dilution via Western blotting than ELISA.

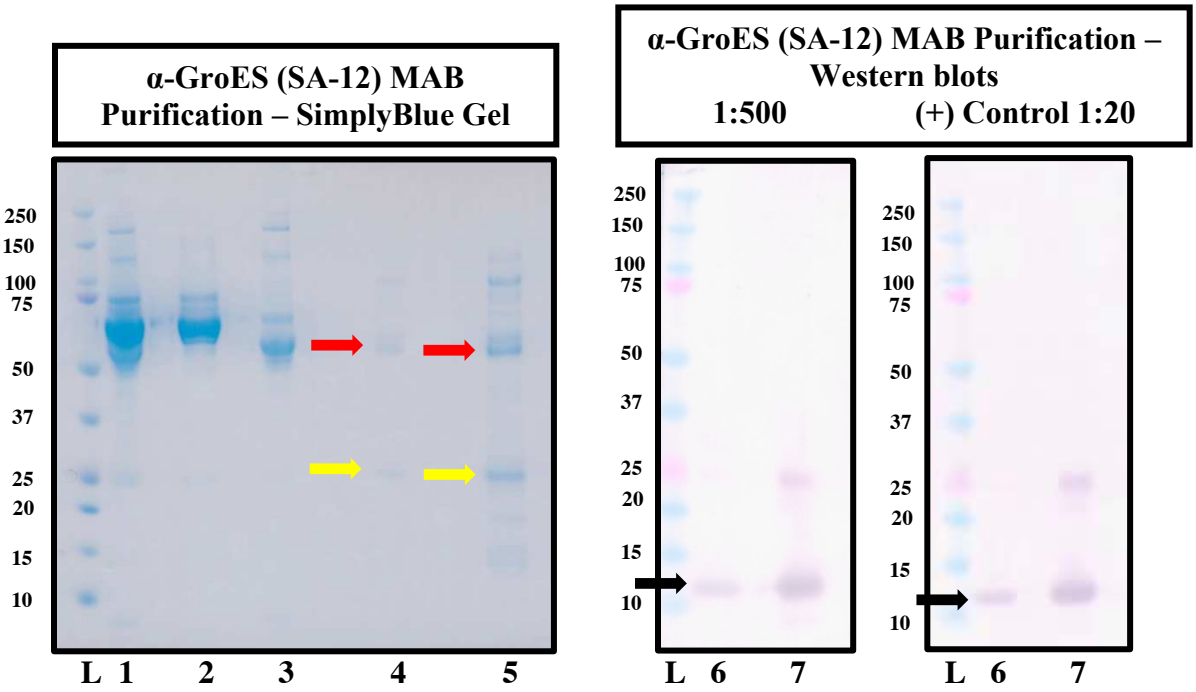

FIGURE 14: α-GroES MAB Purification SimplyBlue Gel & Western blot
Purification of α-GroES MAB via Melon gel. Purified α-GroES MAB was subjected to analysis via Western blotting and a denaturing SDS-PAGE gel stained with SimplyBlue stain. Aliquots of each step in the purification process were saved and loaded on gels. These aliquots were taken from cell culture supernatant, ammonium sulfate (AS) precipitation on the cell culture supernatant (AS supernatant and dialyzed pellet), along with the Melon gel purified products. Description of different aliquots loaded on gel: (**lane L**) 2 µL protein ladder, (**lane 1**) 4 µL cell culture supernatant (before AS precipitation), (**lane 2**) 4 µL AS precipitation (supernatant), (**lane 3**) 7.5 µL AS precipitation (dialyzed pellet *from diluted wash of sample in tube*), (**lane 4**) 1 µg purified MAB, and (**lane 5**) 5 µg purified MAB. Description of different aliquots loaded on blots: (**lane L**) protein ladder, (**lane 6**) 5 µg CFP, and (**lane 7**) 1 µg nGroES. The purified MAB was tested at a dilution of 1:50, 1:100, and 1:500, but only the 1:500 dilution blot is shown here.

The positive (+) control (SA-12, ***un***purified cell culture supernatant) was tested at a dilution of 1:20. Antibody heavy and light chains are indicated by red and yellow arrows, respectively, on the SimplyBlue-stained gel. GroES (10 kDa) protein bands are indicated by a black arrow on Western blot. SimplyBlue image brightened 20% for visualization of bands.

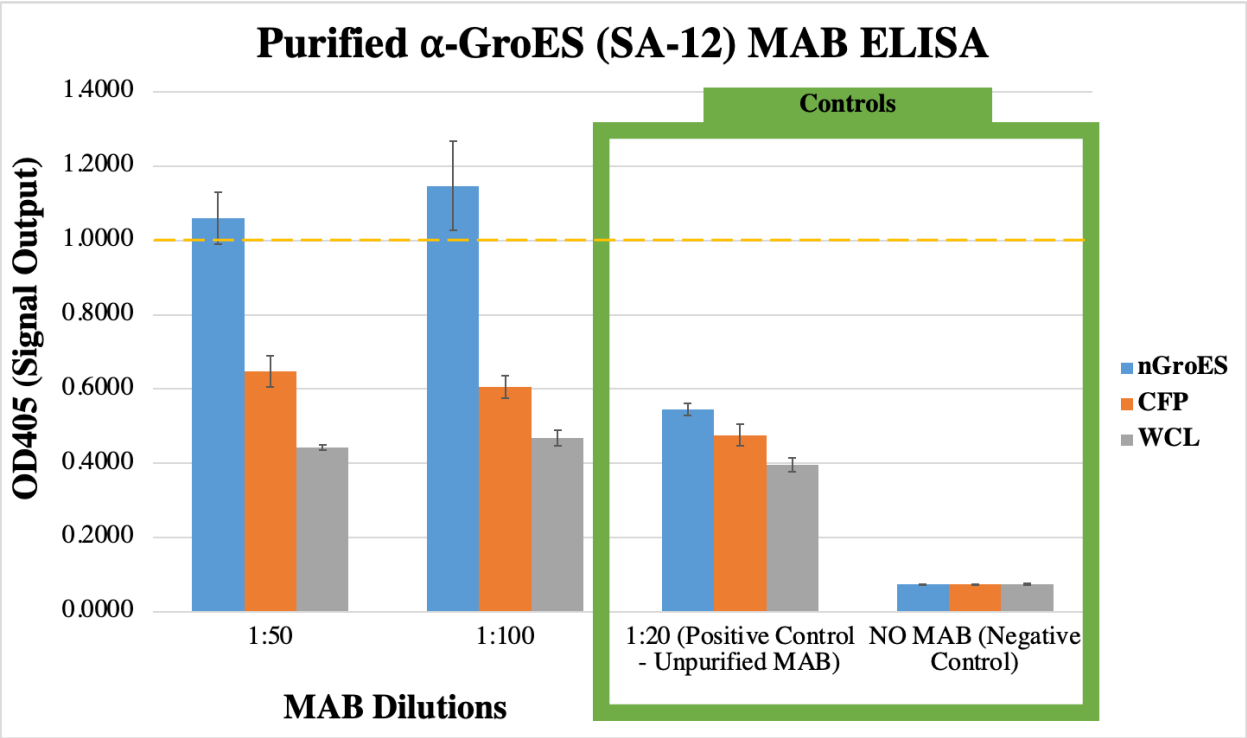

FIGURE 15: α-GroES MAB Purification ELISA
Purification of α-GroES (SA-12) MAB via Melon gel. Purified α-GroES MAB was subjected to analysis via ELISA. Averaged *duplicate* OD405 output signals (for "samples" and positive control) as well as averaged *quadruplicate* OD405 output signals (for NO MAB negative control) are graphed on *Y-axis*. Purified MAB dilutions (for "samples) are graphed on the *X-axis*. The positive control and negative control are also graphed on *X-axis* (in green box). The antigens are graphed according to different colors: nGroES (blue), CFP (orange), and WCL (grey). nGroES antigen was plated at a concentration of 1 µg/100 µL (10,000 ng/mL). The crude *Mtb* fractions CFP and WCL were plated at a concentration of 5 µg/100 µL (50,000 ng/mL). Purified MAB was tested at dilutions of 1:50 and 1:100. The positive control (SA-12, ***un***purified cell culture supernatant) was tested at a dilution of 1:20. A yellow dotted line is graphed to show OD405 of 1.

The denaturing SimplyBlue-stained gel (Figure 16) demonstrates the different purification steps for the Mpt32 MAB. Lanes 1-3 in Figure 16 showed, once again, a large protein band ~65 kDa, possibly albumin. This high molecular weight protein seemed to be purified out of the sample in the final purified Mpt32 MAB products (lanes 4-6). The final

purified Mpt32 MAB products had defined 50 kDa and 25 kDa protein bands, representing heavy and light chains of the antibody, respectively. The Mpt32 MAB was one of the first MABs we attempted to purify. Due to this, more optimization of the purification protocol was needed. The Mpt32 MAB was not as extensively washed as the subsequent DnaK and α-GroES MABs were. Lane 4 was loaded with the initial flow through (FT) and lane 5 was loaded with the washes 1 + 2 fraction (Figure 16). The FT and washes 1+2 were later combined (denoted as "FT/washes 1+2"). However, a third wash (lane 6) was collected separately (denoted as "wash 3"). The purpose of a third wash was to see if any residual antibody remained on the column. The denaturing SimplyBlue-stained gel showed that the "FT/washes 1+2 fraction" (lanes 4 and 5) had more contaminating proteins than the "wash 3" fraction (lane 6). The contaminating bands were anything other than the antibody heavy (50 kDa) and light (25 kDa) chains. We made the decision to keep the "FT/washes 1+2" and "wash 3" fractions separated for downstream qualification and biotinylation.

Western blot analysis for the purified Mpt32 MAB demonstrated a dilution of 1:5,000 for the "FT/washes 1+2" fraction and a dilution of 1:10,000 for the "wash 3" fraction (Figure 16) for both nMp32 and crude CFP fraction. The purified Mpt32 MAB "FT/washes 1+2" fraction blots were not run with a positive control (for no specific reason). The positive control (***un***purified MAB cell culture supernatant) for the purified Mpt32 MAB "wash 3" fraction blots was performed at a dilution of 1:10,000 for both nMpt32 and crude CFP fraction. However, the band signal intensity for this positive control was very faint in comparison to the same dilution performed for the purified MAB. More concentrated dilutions of the positive control would need to be performed for a better comparison to the purified MAB signal (i.e., fold-increase in reactivity of the purified MAB).

Figure 17 demonstrates the ELISA data for the purified Mpt32 MAB (both fractions). Graph A depicts the data for the "FT/washes 1+2" fraction and Graph B depicts the data for the "wash 3" fraction. The purified MAB was reactive at a dilution of 1:1,000 for the "wash 3" fraction against nMpt32. An argument could be made for even less concentrated dilutions (not tested). However, we observed that for the "FT/washes 1+2" fraction, none of the dilutions tested were sufficient for an OD405 signal of 1 for nMpt32. Therefore, more concentrated dilutions would have to be tested. Both Mpt32 MAB fractions performed poorly against the crude CFP fraction. The signal for CFP depicted in Graph A was close to that of the positive control. The signal for CFP depicted in Graph B was ~1/2 that of the nMpt32 antigen. Again, more concentrated dilutions would have to be tested for the crude CFP fraction.

The positive controls for both MAB fractions were tested at a dilution of 1:1,000 only. However, more concentrated dilutions would need to be tested for optimal dilution for the ELISA. The NO MAB negative control was low. Thus, it seems that both Mpt32 MAB fractions were able to recognize the linearized nMpt32 antigen better than the folded nMpt32 antigen. This was demonstrated by the fact that the purified MAB fractions were more reactive at a less concentrated dilution for Western blotting than ELISA.

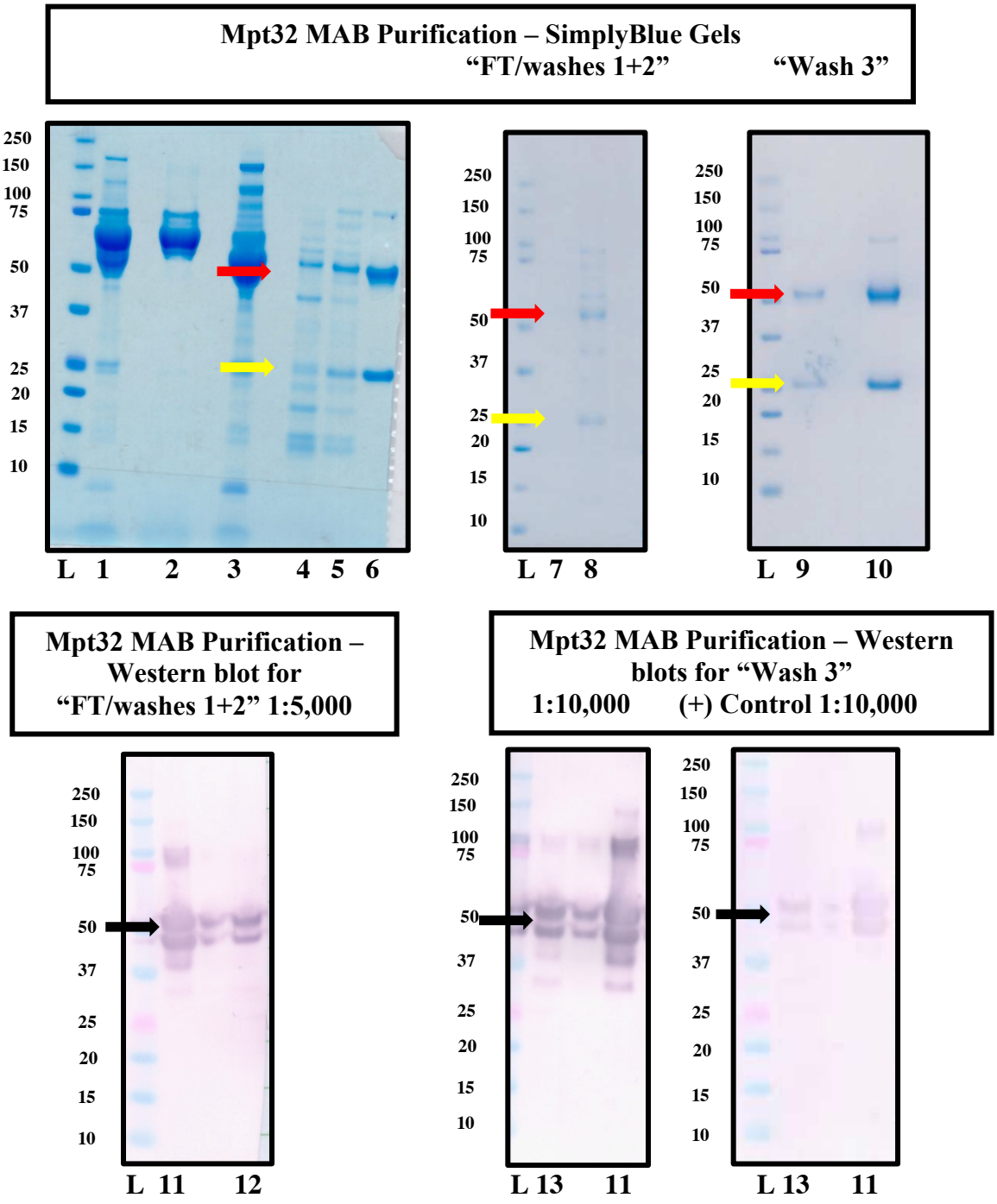

FIGURE 16: Mpt32 MAB Purification SimplyBlue Gel & Western blots
Purification of Mpt32 MAB via Melon gel. Purified Mpt32 MAB was subjected to analysis via Western blotting and a denaturing SDS-PAGE gel stained with SimplyBlue stain. Aliquots of each step in the purification process were saved and loaded onto gels. These aliquots were taken from cell culture supernatant, ammonium sulfate (AS) precipitation on the cell culture supernatant (AS supernatant and dialyzed pellet fractions), along with the Melon gel purified products. Description of different aliquots loaded on gel: (**lane L**) 2 µL protein ladder, (**lane 1**) 4

μL cell culture supernatant (before AS precipitation), (**lane 2**) 4 μL AS precipitation (supernatant fraction), (**lane 3**) 4 μL AS precipitation (dialyzed pellet fraction), (**lane 4**) 4 μL Melon gel FT1 (no washes), (**lane 5**) 4 μL Melon gel washes 1 + 2, (**lane 6**), 4 μL Melon gel wash 3, (**lane 7**) 1 μg purified combined "FT1/washes 1+2" MAB, (**lane 8**) 5 μg purified combined "FT1/washes 1+2" MAB, (**lane 9**) 1 μg purified "wash 3" MAB, and (**lane 10**) 5 μg purified "wash 3" MAB. Description of different aliquots loaded on blots: (**lane L**) 2 μL protein ladder, (**lane 11**) 1 μg nMpt32, (**lane 12**) 4 μg CFP, and (**lane 13**) 5 μg CFP. The purified MAB FT/washes 1+2 sample were tested at dilutions of 1:5,000, 1:10,000, and 1:20,000, but only the 1:5,000 dilution blot is shown here. The purified MAB Wash 3 sample was tested at dilutions of 1:5,000, 1:10,000, and 1:20,000, but only the 1:10,000 dilution blot is shown here. The Mpt32 FT/washes 1+2 blot did not have a positive control. The positive (+) control (Clone B, ***un***purified cell culture supernatant) was tested at a dilution of 1:10,000 for the Mpt32 wash 3 blots. Antibody heavy and light chains are indicated by red and yellow arrows, respectively, on the SimplyBlue-stained gel. Mpt32 (45 kDa) protein bands are indicated by a black arrow on Western blots (typical "hamburger patty" pattern). SimplyBlue image brightened 20% for ease of seeing bands.

A. Purified Mpt32 MAB "FT/washes 1+2" ELISA

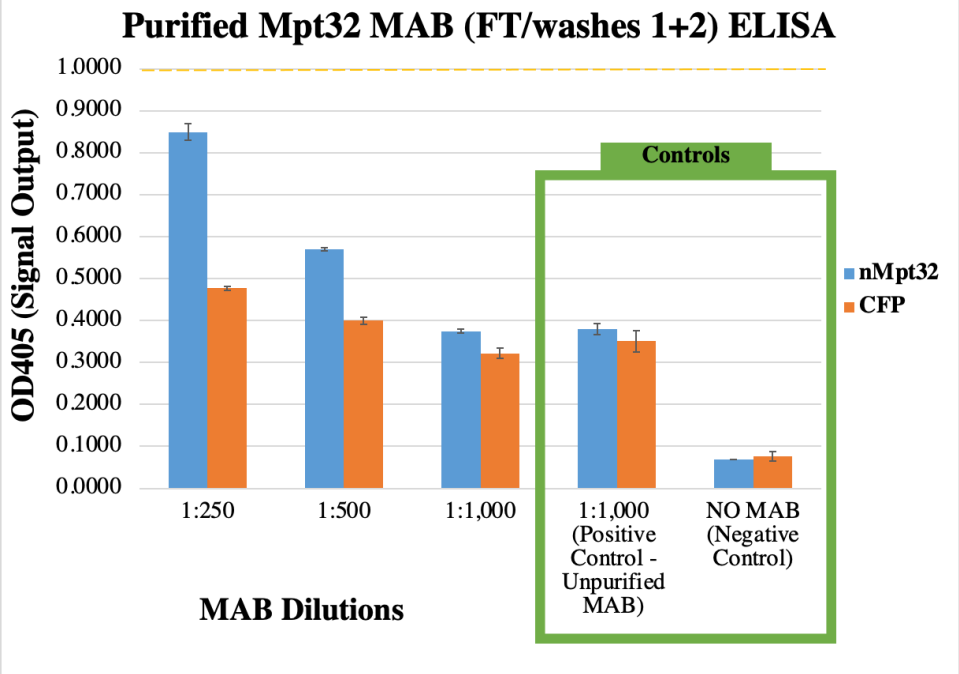

B. Purified Mpt32 MAB "wash 3" ELISA

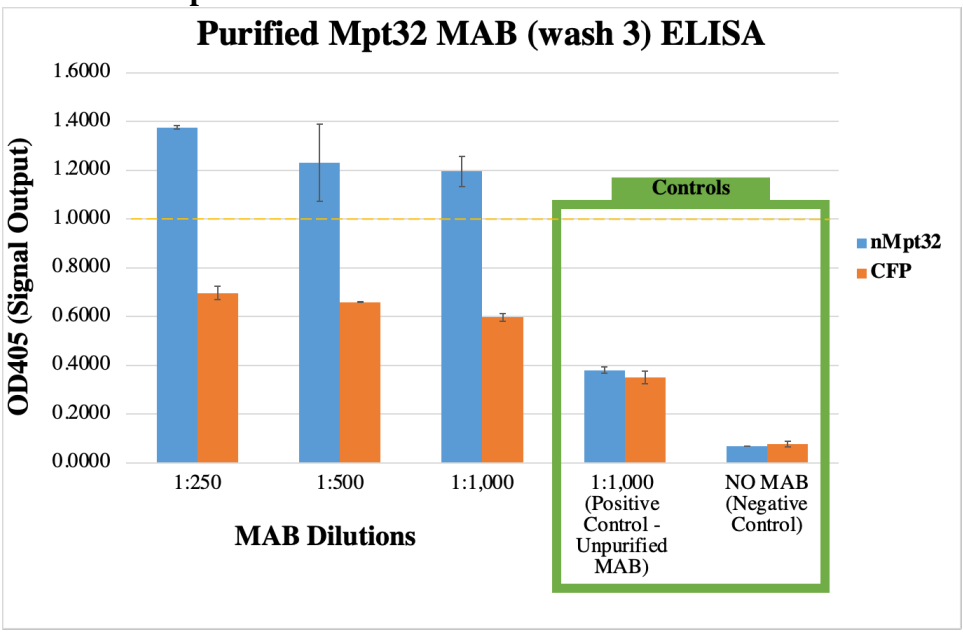

FIGURE 17: Mpt32 MAB Purification ELISA

Purification of Mpt32 MAB via Melon gel. Purified Mpt32 MABs (both **Graph A** "FT/washes 1+2" and **Graph B** "wash 3" fractions) were subjected to analysis via ELISA. Averaged *duplicate* OD405 output signals (for "samples" and controls) are graphed on *Y-axis*. Purified MAB dilutions (for "samples) are graphed on the *X-axis*. The positive control and negative control are also graphed on *X-axis* (in green box). The antigens are graphed according to different colors: nMpt32 (blue) and CFP (orange). nMpt32 antigen was plated at a concentration of 1 μg/100 μL (10,000 ng/mL). The crude *Mtb* fraction CFP was plated at a concentration of 5

μg/100 μL (50,000 ng/mL). Purified MAB was tested at dilutions of 1:250, 1:500, and 1:1,000. The positive control (Clone B, ***un***purified cell culture supernatant) was tested at a dilution of 1:1,000. A yellow dotted line is graphed to show OD405 of 1.

2.3.7 Monoclonal Antibody Biotinylation

Western blot analysis demonstrated successful biotinylation of DnaK, α-GroES (SA-12), and Mpt32 (both fractions) purified MABs (Figures 18-20). Each purified, biotinylated MAB was tested at the same dilution as the purified, ***un***biotinylated MABs. The biotinylated MABs were used with a streptavidin-HRP system instead of an alkaline phosphatase system. More dilutions would need to be tested to determine adequate dilutions for each MAB. However, we wanted to solely demonstrate successful biotinylation and therefore, the dilutions tested were sufficient for our purposes.

For the purified, biotinylated DnaK MAB, we observed strong reactivity to recDnaK at a dilution of 1:20,000 (Figure 18) but weaker to no reactivity to both the crude CFP and WCL fractions. For the purified, biotinylated α-GroES (SA-12) MAB we observed strong reactivity to nGroES at a dilution of 1:500 (Figure 19) and somewhat weaker reactivity to the crude CFP fraction for the same dilution. For the purified, biotinylated Mpt32 MAB we observed strong reactivity to both "FT/washes 1+2" and "wash 3" fractions against nMpt32 (Figure 20) at dilutions of 1:5,000 and 1:10,000, respectively. However, for both Mpt32 MAB fractions, we observed a somewhat weaker reactivity to the crude CFP fraction. It is important to note that the "wash 3" fraction remained more reactive (at least surmised from the Western blot dilutions tested) than the "FT/washes 1+2" fraction for Mpt32. Therefore, we carried forward with using the "wash 3" fraction only for the development and optimization of the sandwich ELISAs.

A negative control (denoted as (-) control with dilution) of purified, ***un***biotinylated MAB was used for the biotinylated Western blots. This negative control for each MAB was carried out

with the same dilution as the corresponding purified, biotinylated MABs. This allowed us to visualize any non-specific binding of the purified, ***un***biotinylated MAB with the strep-HRP conjugate reagent. For each MAB, a high molecular weight band (not characterized) can be seen in the crude CFP and WCL fractions in Figures 18-20.

A TBST negative control (denoted as (-) control TBST in Figure 18 only) was also used. Instead of incubating with the corresponding MAB, TBST was added to the blot for this incubation step. This allowed us to visualize any non-specific binding of the strep-HRP conjugate reagent to the antigen or to the blot. Figure 18 demonstrates that there was some non-specific binding of the strep-HRP reagent to the WCL crude fraction (lane 2).

The Western blots for the purified, biotinylated MABs started developing quickly after the addition of the TMB substrate and were blown out. These blots were a quick checkpoint for successful biotinylation. Since our goal was to use the purified, biotinylated MABs on ELISAs, we did not see a reason to test less concentrated dilutions for these Western blots. The biotinylation reagent that we used, the EZ-Link™ NHS-Biotin, is a "N-Hydroxysuccinimide (NHS) ester" connected to a biotin molecule via a linker arm [112]. This reagent specifically targets "primary amino groups" on proteins, usually "lysines or a polypeptide's N-terminus" region[112]. Antibodies contain many of these target groups for biotinylation [112]. The manufacturer states that ~8-12 biotin moieties are added to one single IgG molecule, this number depended on the amount of excess biotin reagent added[112]. For this project, we chose to biotinylate the MABs on the higher end of molar excess of biotin reagent used.

MAB protein concentrations decreased for all purified, biotinylated MABs when compared to the concentrations of the purified, ***un***biotinylated MABs (see *section 2.2.5 Monoclonal Antibody Biotinylation* for purified, ***un***biotinylated concentrations). For the

purified, biotinylated MABs, the protein concentration was determined after biotinylated MABs were run through 50,000 MWCO amicons. The purified, biotinylated DnaK MAB had a protein concentration of 6.637 mg/mL. The purified, biotinylated α-GroES (SA-12) MAB had a protein concentration of 1.560 mg/mL. The purified, biotinylated Mpt32 MAB fraction "FT/washes 1+2" had a protein concentration of 0.966 mg/mL. The purified, biotinylated Mpt32 MAB fraction "wash 3" had a concentration of 0.907 mg/mL. All samples were in ~1 mL of solution. This demonstrated a loss of product most likely after 50,000 MWCO amicon concentration of the purified, biotinylated MABs.

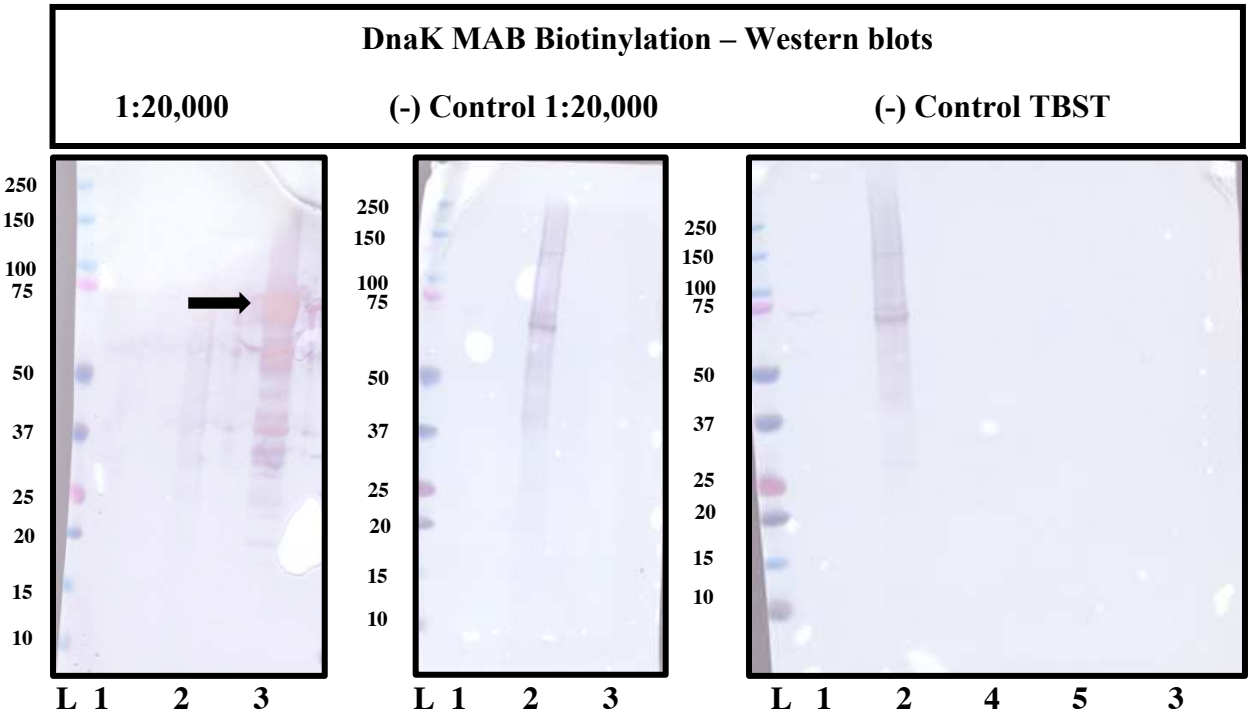

FIGURE 18: Purified DnaK MAB Biotinylation Qualification Western blot
Purified DnaK MAB was subjected to Western blot analysis after biotinylation. Description of antigens loaded on blot: (**lane L**) 2 µL protein ladder, (**lane 1**) 5 µg CFP, (**lane 2**) 5 µg WCL, (**lane 3**) 1 µg recDnaK, (**lane 4**) 1 µg nMpt32, and (**lane 5**) 1 µg nGroES. The purified, biotinylated MAB was tested at a dilution of 1:20,000. A negative control of purified, ***un***biotinylated DnaK MAB was tested at a dilution of 1:20,000. A negative control of TBST in lieu of the MAB was used as well. DnaK protein band (~67 kDa) is indicated by a black arrow. The blots were brightened 20% for ease of seeing bands.

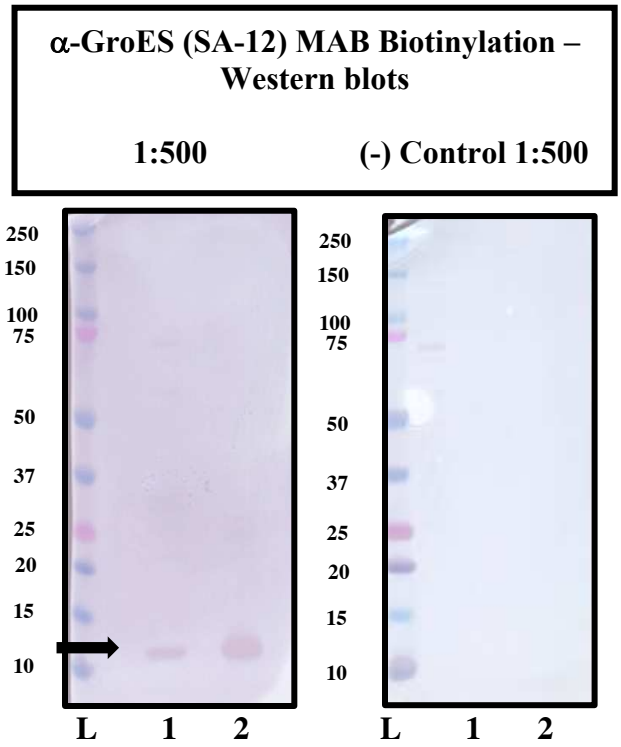

FIGURE 19: Purified α-GroES MAB Biotinylation Qualification Western blot
Purified α-GroES (SA-12) MAB was subjected to Western blot analysis after biotinylation. Description of antigens loaded on blot: (**lane L**) 2 µL protein ladder, (**lane 1**) 5 µg CFP, and (**lane 2**) 1 µg nGroES. The purified, biotinylated MAB was tested at a dilution of 1:500. A negative control of purified, ***un***biotinylated α-GroES MAB was tested at a dilution of 1:500. A negative control of TBST in lieu of the MAB was used as well (see ***Figure 18, (-) Control TBST***). GroES protein band (10 kDa) is indicated by black arrow. The blots were brightened 20% for ease of seeing bands.

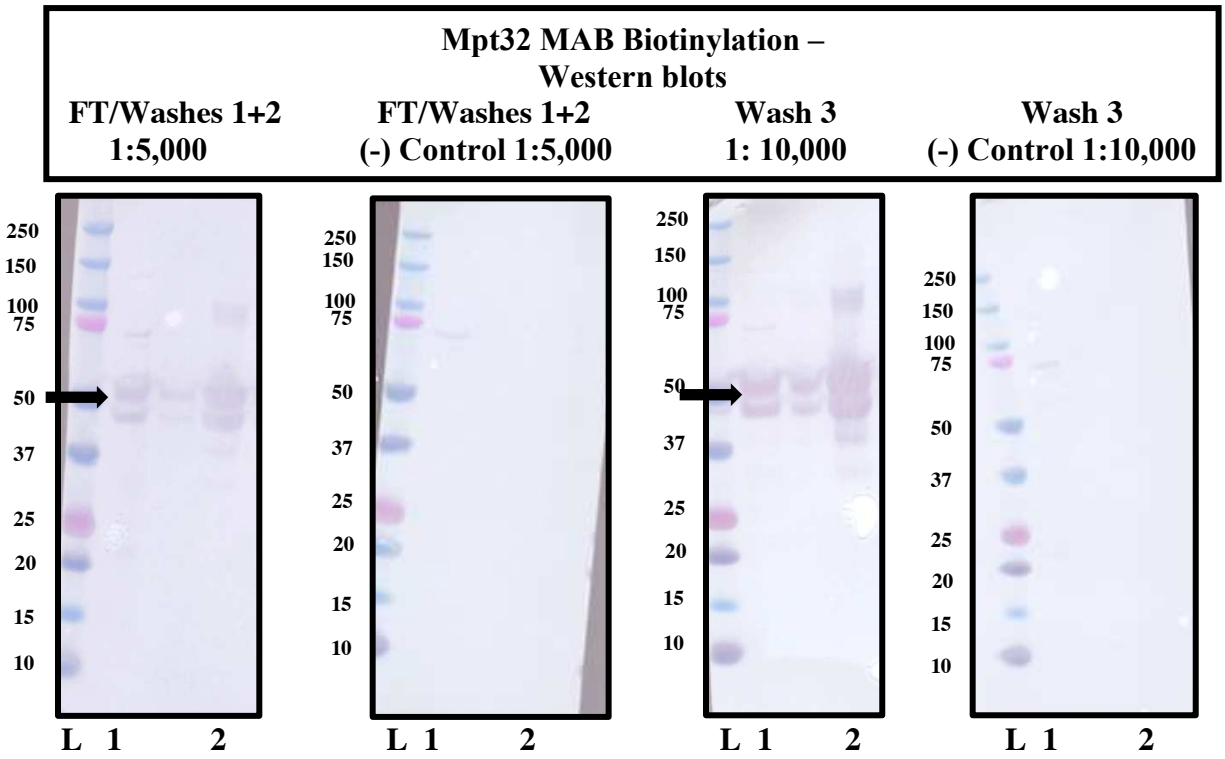

FIGURE 20: Purified Mpt32 MAB Biotinylation Qualification Western blots
Purified Mpt32 MAB was subjected to Western blot analysis after biotinylation. Description of antigens loaded on blots: (**lane L**) 2 µL protein ladder, (**lane 1**) 5 µg CFP, and (**lane 2**) 1 µg nMpt32. The purified, biotinylated MAB was tested at a dilution of 1:5,000 for "FT/washes 1+2" MAB fraction and a dilution of 1:10,000 for "wash 3" MAB fraction. A negative control of purified, ***un***biotinylated Mpt32 MAB fractions were tested at dilutions of 1:5,000 ("FT/washes 1+2") and 1:10,000 ("wash 3"). A negative control of TBST in lieu of the MAB was used as well (see ***Figure 18, (-) Control TBST***). Mpt32 protein band (45 kDa) is indicated by black arrows (typical "hamburger patty" pattern). The blots were brightened 20% for ease of seeing bands.

2.4 Conclusions

The data presented in this chapter demonstrated the successful creation and qualification of the reagents necessary for the development of a sandwich ELISA against *Mtb* proteins.

2.4.1 Polyclonal Antibody Production & Purification

We were able to produce highly reactive PAB serum to all four antigens. The PAB serum (from both rabbits) was reactive for both Western blotting and ELISA immunoassays. In general, the PAB serum seemed to recognize the linearized proteins (Western blotting) better than the

folded proteins (ELISA). This was demonstrated by less concentrated dilutions used with higher reactivity for most of the Western blots compared to ELISA dilutions.

It was also incredible that the rabbits maintained such high reactivity to the purified antigens ~ 3 months post final immunization. Thus, we were able to collect a plethora of serum, a non-renewable reagent, to run experiments for this project and other future projects.

2.4.1.1 Rabbit R1

Due to the inability of the α-GlnA MAB to recognize the folded GlnA protein, rabbit R1 was immunized solely with the recombinant GlnA protein for an abundant production of α-GlnA PAB serum. The goal being that the α-GlnA PAB serum would be used to develop a sandwich ELISA in the future when a new hybridoma cell line could be created that would recognize epitopes on the native GlnA protein or used for an indirect ELISA as a proof of principle. Therefore, GlnA purification data was not presented here and biotinylation was not attempted.

2.4.1.2 Rabbit R2

Rabbit R2 was immunized against native Mpt32, native GroES, recombinant DnaK, and recombinant GlnA. The goal being that this PAB serum would be used to develop the ultrasensitive sandwich ELISA against Mpt32, GroES, DnaK, and GlnA when a MAB is available. The unpurified PAB serum from rabbit R2 will be used to develop and optimize the sandwich ELISA. We have successfully purified a sample of the PAB serum from the first production bleed of rabbit R2 (Figure 11). This purified PAB serum from rabbit R2 could be used in the future for comparison with the unpurified PAB serum on the sandwich ELISA.

2.4.2 Monoclonal Antibody Purification & Biotinylation

We successfully purified the MABs from a very crude hybridoma cell culture supernatant sample. These cultures contained contaminating serum proteins (FBS) that are generally difficult

to remove. The ammonium sulfate precipitation aided in removal of some of these contaminating proteins. However, we demonstrated that the Melon gel column was able to generate an incredibly pure product. The use of amicon ultrafiltration units helped concentrate the final purified products.

We also demonstrated successful biotinylation of the purified MABs. The biotinylation procedure was simple, quick, and efficient. Even though we had product loss after the 50,000 MWCO amicons post-biotinylation, the purified, biotinylated MABs retained high specificity and sensitivity, as demonstrated by the Western blots (Figures 18-20). The dilutions were also low enough that a smaller amount of product could be used for a given assay. After confirmation of biotinylation, we were ready to start optimization trials of the sandwich ELISA using the reagents we had produced.

CHAPTER 3: THE ROLE OF *MYCOBACTERIUM TUBERCULSIS* ANTIGENS IN ELISA DEVELOPMENT

3.1 Introduction

As mentioned previously in Chapter 1 *section 1.9.1 Project Specific Goals*, the study Mehaffy et al., 2020 identified 31 *Mtb* protein peptides in purified serum EVs of individuals with LTBI. The top six peptides identified in this study corresponded to the *Mtb* proteins GlnA, GroES, DnaK, AcpM, GarA, and Mpt32 [86]. For this master's thesis project, GroES, DnaK and Mpt32 proteins will be used to develop an ultrasensitive ELISA.

GroES and DnaK are both crucial heat shock chaperone proteins for *Mtb* [118]. Heat shock proteins are utilized in both times of stress as well as cellular growth [119–122] by both prokaryotes and eukaryotes [123]. Prokaryotes can increase their heat shock protein abundance from "5 to 15%" when they are exposed to stressful environments [117]. One of the main chaperone functions of these heat shock proteins includes folding of cellular proteins, whether in times of stress or no stress [117]. The fact that DnaK and GroES were amongst the top six proteins identified in the Mehaffy et al., 2020 study indicates their function as chaperone proteins could be important to *Mtb* survival during times of latent infection[86].

GroES (10 kDa protein, Rv3418c, protein CPN10) is a secreted chaperonin [124,125] that complexes with another chaperone protein, GroEL [117]. This chaperone complex aids in refolding of denatured proteins [126] as well as "prevent[s] aggregation of polypeptides" that enter this complex [117]. GroES has been identified in both the *Mtb* cytoplasmic space as well as in the culture media [127]. However, GroES is "one of the most abundant proteins found in short-term culture filtrates of logarithmically growing *M. tuberculosis*" [127] and therefore, is generally more recognizable in its secreted form. Like other prokaryotes, GroES is expressed in *Mtb* during

times of stress [128–131,86] and cellular growth [132,86]. GroES is also highly immunogenic and an inducer of T cell activation [117,133].

DnaK (~67 kDa, Rv0350) is another chaperone protein that works closely with a co-chaperone called ClpB [134]. Together, this complex shuttles aggregated and disaggregated proteins back and forth to each other and ultimately, the DnaK chaperone will fold the disaggregated proteins properly [135–138,134]. DnaK has also been found to be a key player for "native protein folding" in *Mycobacterium smegmatis* (*M. smeg*) [139]. One study demonstrated that when DnaK was depleted in *M. smeg* in times of cellular growth, protein aggregates began to form in the cytoplasm [139]. However, in times of stress, DnaK was shown to "re-localize" to aggregated proteins in the cytoplasm for aggregate degradation [139]. This same study also indicated that DnaK depletion could influence cell "membrane integrity" [139]. Literature on the DnaK system in *Mtb* is not as well characterized as in *M. smeg*. However, *M. smeg* plays an important role as a "model organism" for *Mtb* [134]. Therefore, DnaK could play key, if not essential roles in *Mtb* as well [134].

Mpt32 ("Apa – alanine-and proline-rich antigen, 45/47 kDa, Rv1860") is a secreted glycoprotein [140,141]. The native Mpt32 glycoprotein is heavily glycosylated with mannose sugar moieties which serve as strong T lymphocyte stimulators [142,143]. Specifically, amino acid residues within the "proline-rich domains" of the native protein contain these glycosylation sites [141,144]. It has been observed that recombinant Mpt32 proteins produced in *M. smeg* and *Escherichia coli* (*E. coli*) have altered "mannosylation patterns" and amount of "sugar residues" compared to the native proteins (from *Mtb*, *Mycobacterium bovis*, and BCG strains) and lose their ability to promote strong T cell responses [143]. Horn et al., 1999 demonstrated that delayed-type hypersensitivity responses in BCG vaccinated guinea pigs differed with immunization against native (strong response) or recombinant (lower or absent responses) versions of the Mpt32

protein [143]. Horn et al., 1999 also observed a decrease in sensitization *in vitro* when stimulating T cells with the guinea pig serum from the group immunized with the recombinant Mpt32 proteins [143]. Thus, the native Mpt32 glycosylation pattern and amount of "sugar residues" plays a key role in immunogenicity of the antigen[143]. Mpt32 also functions as an adhesin for *Mtb* within the lungs [145,146]. The glycosylated sites of the Mpt32 protein have been shown to influence binding interactions as part of the adhesion action [145,146]. Mpt32 has been shown to bind to the "cell-binding domain" of fibronectin [144]. Fibronectin is an intricate part of the extracellular matrix [147,148,144] that allows *Mtb* to attach to host cells for internalization [149,150,144].

A peptide of GlnA1 was the top peptide identified in the Mehaffy et al., 2020 study. Mehaffy et al., 2020 identified the SVF peptide in 82% of LTBI samples [86]. This peptide showed promise as a biomarker of LTBI, as the response of this peptide in TB-positive patient samples was very low [86]. *Mtb* encodes for multiple *glnA* genes [128]. GlnA1 protein is the most abundantly produced and detectable in "*Mtb* cultures" [128]. GlnA is a glutamine synthetase that utilizes ammonium sources from the environment to produce L-glutamine [86,151]. GlnA is therefore tightly involved in cell-wall synthesis of *Mtb* with the production of "extracellular L-glutamine" [152]. GlnA can also block phagosome-lysosome fusion via increasing the phagosome nitrogen content [152,153]. These functions highlight the indispensable role of GlnA for *Mtb*.

These proteins are important in *Mtb* pathogenesis and survival [86]. These proteins could be potential biomarkers for LTBI diagnosis [86]. The ability to identify these proteins in complex samples (such as serum) could allow for differential diagnosis of LTBI. However, to be able to establish and optimize potential diagnostics, the purified recombinant or native forms of these proteins must be used before complex fluids can be tested. Here, purified native GroES, native Mpt32, and recombinant DnaK will be used to create an ultrasensitive ELISA for the detection of

Mtb antigens as a potential point-of-care diagnostic. Chapter 2 (*2.4.1.1: Rabbit R1*) emphasizes the reasons for the omission of GlnA protein for this master's project.

3.2 Methods

3.2.1 Sandwich ELISA

The following sandwich ELISA protocol followed the ThermoFisher *ELISA Technical Guide and Protocols, Tech Tip #65*, with some modifications [154].

Pierce™ white opaque 96-well polystyrene microplates were used for all chemiluminescent sandwich ELISAs (Fisher Scientific). Seal plate microplate adhesive film was used for all incubations, excluding washes, and changed when wet (Daigger Scientific). PBST buffer was used as a wash buffer as well as the base diluent. Briefly, PBS at a 1X (Corning) or 10X (Invitrogen) stock concentration were used to make a 1X PBST buffer (1X PBS, 0.05% TWEEN®20, pH 7.20) (Fisher Scientific). PBST was stored at 4°C. For all washing steps, 200 µL/well of PBST was added using a multichannel pipetman. Three washes were performed, 5 min each, shaking at room temperature for all incubation steps excluding the strep-HRP conjugate (6 x 5 min washes). All liquids were decanted, and the microplate was tapped 3-4 times on a towel to remove excess liquid. For all incubation steps, an acceptable range for the incubation times was between 1 hr and 1 hr + 10 min. All ELISA incubation steps were performed shaking continuously at 200 rpm using a titer plate shaker (Lab-Line Instruments, Inc., Model #4625) at room temperature, unless otherwise specified. A 49 mM sodium carbonate/sodium bicarbonate coating buffer (pH 9.6, in ultrapure water) was used for PAB serum dilutions for plating [111]. The coating buffer was subsequently filtered and stored at room temperature for no more than one month.

Total ***un***purified PAB serum protein concentration was determined via Pierce™ BCA Protein Assay Kit (ThermoFisher Scientific). For the development and optimization of the sandwich ELISA, ***un***purified R2-1 PAB serum was used.

Checkerboard titration assays were used to find the optimal antibody pairing of the PAB sera and the purified, biotinylated monoclonal antibody (MAB). The final plated concentration of PAB serum (in μg/mL) was specific for each antigen (from optimal pairing). The appropriate PAB serum concentration was diluted in coating buffer. The negative control wells (without PAB serum) were coated with 100 μL/well of coating buffer only. The coated microplate was sealed with a plate sealer and placed at 4°C overnight, rocking. The following day, the coated PAB serum was removed, and the microplate was washed. Blocking solution was plated at 300 μL/well and incubated for 1 hr. The microplate was then washed. Some trials differed in wash steps between blocking and antigen incubations. Some trials had 3 x 5 min and some trials had one brief wash. However, per the original ThermoFisher protocol, a wash in between these steps is not necessary but not harmful [154]. The antigen (purified recDnaK, nMpt32, or nGroES) was diluted in trial specific diluent (all in PBST buffer) for a final concentration of 1 μg/100 μL (10,000 ng/mL), unless otherwise stated for a specific trial. The antigen was incubated for 1 hr. The microplate was then washed. The antigen-specific purified, biotinylated MAB was diluted in trial specific diluent (in PBST) to the appropriate dilution and plated at 100 μL/well. The MAB was incubated for 1 hr. The microplate was then washed. A streptavidin-horseradish peroxidase (streptavidin-HRP) enzyme conjugate (Sigma-Aldrich) was then added at a 2 μg/mL (0.2 μg/100 μL) concentration in the trial specific diluent (in PBST), unless otherwise stated. The diluent for the strep-HRP conjugate was 1/5 of the original dilution (i.e., 0.4%BSA/PBST instead of 2%BSA/PBST for standard diluent), excluding PBST diluent. The strep-HRP conjugate was

incubated for 1 hr. The enzyme conjugate solution was then removed for hazardous waste disposal (along with the first wash). The microplate was washed six times in total. A SuperSignal™ ELISA Pico chemiluminescent substrate (Fisher Scientific) was used for development. This substrate was chosen because it can "detect picogram levels of antigen" in ELISA assays [155]. The sandwich ELISA was developed using the manufacturer's protocol for the substrate [155]. Briefly, a 1:1 solution of the Pico luminol/enhancer and the Pico stable peroxide solution was made and mixed well. The substrate was plated at 100 µL/well. Wells were inspected for bubbles prior to reading. The microplate was immediately placed in a microplate reader (BioTek Multi-Mode Synergy HTX) with the ability to read luminescence (luminometer). The microplate reader was set at ~25°C (room temperature) each run. The plate was agitated for 1 min at 365 cpm (orbital shake) in the microplate reader and three subsequent luminescent reads were taken. Depending on how full the microplate was, some reads took longer than others. Luminescence was measured in relative light units (RLUs). The microplate reader read each well for 1 s. An OVFRLW signal was given for signals >99,999 RLUs (standard dynamic range of 0 to 99,999 RLUs).

3.2.2 Sandwich ELISA Data Analysis

Most data analyses for the sandwich ELISA trials were performed using Microsoft Excel. The two duplicate signal output values were averaged and graphed on the *Y-axis*. To determine the *sample: NO PAB* ratios, the averaged duplicate RLU values for the "sample" were divided by the averaged duplicate RLU values for the corresponding NO PAB negative control. To determine the *sample: NO AG* ratios, the averaged duplicate RLU values for the "sample" were divided by the averaged duplicate RLU values for the corresponding NO AG negative control. These ratios allowed us to determine if the "sample" was more than just background noise and to

what extent. A ratio of 1 indicated that the sample was just background noise. A higher ratio indicated that there was lower background noise. Any OVRFLW values were given a numerical value of 100,000 RLUs for data analysis purposes only.

Standard deviation (SD) for "samples" and negative controls were graphed. Positive and negative SD values were entered. Any signals that received an OVRFLW value could not be calculated, and an asterisk was placed in the table and above the corresponding columns in the graphs.

3.2.3 Direct-Biotinylated ELISA

The following direct-biotinylated ELISA protocol followed the ThermoFisher *ELISA Technical Guide and Protocols, Tech Tip #65*, with some modifications [154].

Much of the protocol for the direct-biotinylated ELISAs remained similar to the protocol for the sandwich ELISAs. The modifications will be briefly mentioned here. One of the main differences was that the purified recombinant or native antigens were coated on the plate instead of the PAB serum. Briefly, the antigens were coated at 1 μg/ 100μL (10,000 ng/mL), unless otherwise stated for a specific trial, in the same coating buffer mentioned in *section 3.2.1 Sandwich ELISA*. Another difference was that all wash steps performed were three, 5 min washes, shaking at room temperature (did not change). The last difference was in the duration of the reads in the microplate reader. For the direct-biotinylated ELISAs, the microplate reader read each well for 20 ms (millisecond), 50 ms, and 1 s, unless stated otherwise. The signal output was also changed to extended dynamic range to read signals 0 to 5,800,000 RLUs, unless otherwise stated. An OVRFLW signal was given for signals >5,800,000 RLUs.

3.2.4 Direct-Biotinylated ELISA Data Analysis

Data analyses for the direct-biotinylated ELISAs were similar to those for the sandwich

ELISAs (*section 3.2.2 Sandwich ELISA Data Analysis*). One difference was that any OVRFLW values (using extended dynamic range) were given a numerical value of 5,800,001 RLUs for data analysis purposes only.

Limit of detection (LOD) and limit of quantification (LOQ) of the direct-biotinylated ELISAs were calculated using linear regression analysis (in Microsoft Excel). In Excel, each step was selected in order: "Data" tab → Data analysis → Regression → Y (averaged duplicate RLU signal output values) & X (antigen concentrations) values entered → 95% confidence level selected → Standard Error calculated ("summary output"). The standard error calculated from this regression analysis was the "standard deviation of the error" [156]. The slope was found when the "equation" was added to the graph. The linear regression analysis was only performed on the graphs with linear trendlines. A polynomial trendline was added to graphs for a better fit comparison when applicable (stated explicitly). LODs and LOQs were calculated using the linear regression analysis for graphs with linear trendlines. For LOD, a 3:1 *signal: background noise* was used. For LOQ, a 10:1 *signal: background noise* was used [157].

LOD Equation = (Standard Error/Slope) x 3

LOQ Equation = (Standard Error/Slope) x 10

A "blank" control was added to the LOD graphs to determine the level of background noise in the assay. The NO AG negative control does not include any antigen, which can be used as a true "blank" for the LOD [157]. The NO AG accounts for any background noise caused by non-specific interactions of other reagents in the system. Therefore, the NO AG average duplicate RLU signal outputs (for MAB of 1:1,000 dilution only) were graphed on the LOD graphs for each antigen. Any "sample" signals that fell below this "blank" signal were considered

background noise. Any “sample” signals that were above this “blank” signal were considered true signals.

3.2.5 Surface Plasmon Resonance (SPR) Using the Biacore System

A T100 Biacore system with T200 sensitivity enhanced was used for all SPR experiments. A Cytiva Series S CM5 chip (Fisher Scientific) was used for all Biacore experiments. A Cytiva amine coupling kit (Fisher Scientific) was used for immobilization of ligand to the CM5 chip. Non-treated, 96-well, U-shaped polystyrene microplates (Greiner Bio-One, VWR) were used for the single-cycle kinetics run. Microplates were sealed with aluminum foil seal plates (provided by previous users).

For the CM5 chip layout, flow cell #1 (Fc-1) was used as the reference channel (blank) and flow cell #2 (Fc-2) was used to immobilize the BSA ligand.

Wizard methods on the Biacore T200 Control Software, version 3.2.1 were used for the entirety of the experiments.

All experiments were performed at 25 °C. PBST was used as the running buffer (1X PBS with 0.05% TWEEN® 20, pH 7.20) and was connected to the “tube A” inlet. Ultrapure (Milli-Q) water was connected to the “water” inlet. All buffers were 0.2 μm filtered and degassed prior to using. TWEEN® 20 was added post-degassing of 1X PBS (pH 7.20) to avoid frothing.

3.2.5.1 pH Scouting for BSA Ligand

10 mM sodium acetate buffers were made at a pH of 4, 4.5, 5, or 5.5. Buffers were stored at room temperature. The day of the pH scouting run, fresh PBST and ultrapure (Milli-Q) water buffers were made (*3.2.5 Surface Plasmon Resonance (SPR) Using the Biacore System*)**.**

A 1 mg/mL BSA in PBST stock solution was made for pH scouting and immobilization. Here, 100 mg of BSA (Gold Biotechnology®) was dissolved in and brought up to 100 mL total volume in PBST.

The Wizard template method used was "Immobilization pH Scouting". For this method, the different 10 mM acetate buffers were tested for pre-concentration. The BSA solution was run at 10 μg/mL. All other parameters were run according to the Wizard method.

3.2.5.2 Immobilization of BSA Ligand

The Biacore machine was left in standby mode overnight from pH scouting. The next day, immobilization of the BSA ligand was performed using an amine coupling kit for the S Series CM5 chip.

The BSA ligand was immobilized in Fc-2. Amine coupling occurred in both Fc-1 (reference channel) and Fc-2 (ligand channel) and a 10 mM sodium acetate pH 4.5 was chosen for this immobilization run. The Fc-1 channel went through the activation and inactivation steps of amine immobilization without any ligand. This created the same surface as the Fc-2 but was used as the "blank" or negative control channel.

The Wizard template method used was "Immobilization". For this method, the T200 Amine immobilization run was selected and a 25 μg/mL BSA (in PBST) solution was used.

3.2.5.3 Single-Cycle Kinetics with BSA Ligand and Purified Protein (nMpt32 & recDnaK) Analytes

A single-cycle kinetics run was performed using purified proteins, native Mpt32 (nMpt32) and recombinant DnaK (recDnaK). For this single-cycle kinetics method, buffer was first injected to create a baseline, nMpt32 was then injected (at five different concentrations), and recDnaK was injected last (at five different concentrations).

Concentration of the purified proteins was determined prior to the single-cycle kinetics run via Pierce™ BCA Protein Assay Kit (ThermoFisher Scientific). Both purified proteins were re-suspended in 1X PBS.

The Wizard template method used was "Method Builder" using the option for single-cycle kinetics. RecDnaK and nMpt32 were run at concentrations of 31.25 nM, 62.5 nM, 125 nM, 250 nM, and 500 nM.

3.2.5.4 Data Analysis for Biacore Methods

The results from the Biacore T200 Control Software, version 3.2.1 were exported for evaluation using the Biacore T200 Evaluation Software 3.2.1. These results were depicted as sensorgrams, with response (in RU – resonance units - values) graphed on the *Y-axis* and time (in seconds) graphed on the *X-axis*.

3.3 Results and Discussion

The type of ELISA we wanted to utilize was the sandwich ELISA. This is due to the fact that the sandwich ELISA is generally thought to be the most sensitive and specific of the ELISA types [98]. However, the sandwich ELISA incorporates the use of more reagents than any other ELISA type. Therefore, extensive optimization was needed to ensure that non-specific interactions were minimized. We performed many optimization trials to increase the *signal: background noise* ratio. Some steps in the sandwich ELISA protocol described in *section 3.2.1 Sandwich ELISA* were altered and were noted appropriately for the specific trial. The sandwich ELISAs were optimized using the purified recombinant or native proteins only, instead of using *Mtb* crude CFP or WCL fractions. However, a handful of trials did include these crude antigens and will be explicitly stated when used.

To begin the optimization process of the sandwich ELISA, we first found the optimal

pairing of the PAB serum and the purified, biotinylated MABs for each antigen. To do this, we used a checkerboard titration assay (*Appendix: Figure 37*). From left to right, one reagent (***un***purified PAB serum) was diluted and from top to bottom, the other reagent (purified, biotinylated MAB) was diluted. The optimal pairing of the PAB serum and the MAB gave the highest readable output signal. This pairing was then used for subsequent sandwich ELISA optimization trials. After the optimal PAB serum and MAB pairings were found, we were able to look at optimizing other reagents within the sandwich ELISA.

Each trial had a "positive control" as well as multiple negative controls, which are described in detail below. The "positive control" will be denoted as the "sample" which includes the full sandwich (PAB serum, blocking solution, antigen, MAB, strep-HRP conjugate, and chemiluminescent substrate). The negative controls were created by taking out one "piece" of the sandwich at a time. We relied on the negative controls to tell us if there were any possible non-specific interactions occurring with any of the reagents. Table 1 depicts the most common negative controls used in the trials. The setup of the table (from left to right) depicts the order of reagent addition during the sandwich ELISA protocol. The NO AG (NO Antigen) negative control is the true negative control. However, other negative controls, like NO PAB, were important in identifying problems within the sandwich ELISAs.

Table 1: Negative Controls for Sandwich ELISA
Y indicates that a particular reagent was added. **N (Diluent)** indicates that a particular reagent was NOT added and instead, the diluent (specific for trial) was incubated in lieu of that reagent. Yellow filled "Negative Control" boxes indicate most frequently used negative controls. *All negative controls received the chemiluminescent substrate*.
**Note: CB = coating buffer*

Negative Control	CB*	PAB serum	Block	Antigen	MAB	Strep-HRP Conjugate
NO AG	**Y**	**Y**	**Y**	**N (Diluent)**	**Y**	**Y**
NO PAB	**Y**	**N (only CB)**	**Y**	**Y**	**Y**	**Y**
NO MAB	**Y**	**Y**	**Y**	**Y**	**N (Diluent)**	**Y**
NO PAB/NO AG	**Y**	**N (only CB)**	**Y**	**N (Diluent)**	**Y**	**Y**
Block (only)	**Y**	**N (only CB)**	**Y**	**N (Diluent)**	**N (Diluent)**	**Y**
PBST (only)	**Y**	**N (only CB)**	**N (PBST only)**	**N (PBST only)**	**N (PBST only)**	**N (PBST only)**
PAB + Strep-HRP	**Y**	**Y**	**Y**	**N (Diluent)**	**N (Diluent)**	**Y**
NO Strep-HRP Conjugate	**Y**	**Y**	**Y**	**Y**	**Y**	**N (1/5th concentration of diluent)**

In this results section, the key results for each antigen are described. Although there were many optimization trials, not all trials were successful. The specific blocking and diluent types will be indicated for each trial (for antigens, MABs, and strep-HRP conjugate). The data presented in the graphs are taken from the first luminescence read only, unless otherwise stated. This is because the earliest sandwich ELISA trial we performed showed that there was not a stark difference between the three luminescence reads (*Appendix: Figure 38*).

3.3.1 Sandwich ELISA Trials

3.3.1.1 Checkerboard Titration Assays

A checkerboard titration assay was used to find the optimal PAB serum and MAB

Pairing for each antigen (recDnaK, nMpt32, & nGroES). For recDnaK, two checkerboard titration assays were performed, months apart. The checkerboard titration assay indicated the optimal PAB serum concentration was 0.5 μg/mL and the optimal MAB dilution was 1:2,500 (*Appendix: Figure 39*). However, when this checkerboard titration assay was repeated later on for recDnaK, the optimal PAB serum concentration was 0.5 μg/mL with an optimal MAB dilution of 1:10,000 (Figure 21). Some DnaK trials were carried out with the 1:2,500 or the 1:10,000 MAB dilution due to when the ELISAs were performed (before or after reproduction of the original checkerboard trial). The MAB dilution for each trial will be explicitly stated.

For nMpt32, the optimal PAB serum concentration was 10 μg/mL and the optimal MAB dilution was 1:500 (Figure 22). For this checkerboard, there were deviations from the original protocol as noted: 200 μL/well of blocking solution was plated, blocking incubation was ~1 hr + 30 min, the blocking solution may have contained thimerosal and TBST, and the antigen incubation was ~48 min. This checkerboard was not repeated because we focused all our efforts on DnaK optimization for reasons that will be discussed in the following sections.

For nGroES, the optimal PAB serum concentration was 0.5 μg/mL and the optimal MAB dilution was 1:40,000 (Figure 23). There were a couple other checkerboard trials prior to this trial (data not shown) with more concentrated dilutions. Only a MAB dilution of 1:20,000 was used for all negative controls. All PAB serum concentrations were accounted for in the negative controls (indicated by colors).

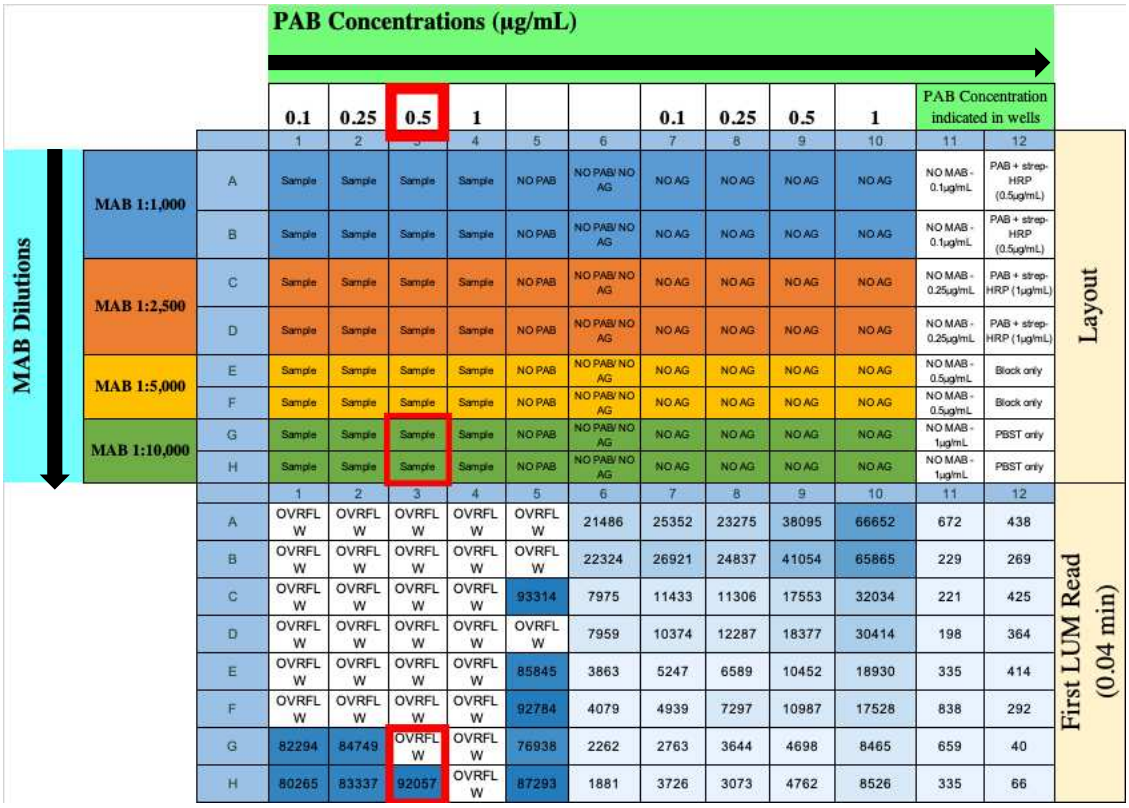

	0.1	0.25	0.5	1			0.1	0.25	0.5	1	PAB Concentration indicated in wells	
	1	2	3	4	5	6	7	8	9	10	11	12
A	Sample	Sample	Sample	Sample	NO PAB	NO PAB/ NO AG	NO AG	NO AG	NO AG	NO AG	NO MAB - 0.1µg/mL	PAB + strep-HRP (0.5µg/mL)
B	Sample	Sample	Sample	Sample	NO PAB	NO PAB/ NO AG	NO AG	NO AG	NO AG	NO AG	NO MAB - 0.1µg/mL	PAB + strep-HRP (0.5µg/mL)
C	Sample	Sample	Sample	Sample	NO PAB	NO PAB/ NO AG	NO AG	NO AG	NO AG	NO AG	NO MAB - 0.25µg/mL	PAB + strep-HRP (1µg/mL)
D	Sample	Sample	Sample	Sample	NO PAB	NO PAB/ NO AG	NO AG	NO AG	NO AG	NO AG	NO MAB - 0.25µg/mL	PAB + strep-HRP (1µg/mL)
E	Sample	Sample	Sample	Sample	NO PAB	NO PAB/ NO AG	NO AG	NO AG	NO AG	NO AG	NO MAB - 0.5µg/mL	Block only
F	Sample	Sample	Sample	Sample	NO PAB	NO PAB/ NO AG	NO AG	NO AG	NO AG	NO AG	NO MAB - 0.5µg/mL	Block only
G	Sample	Sample	Sample	Sample	NO PAB	NO PAB/ NO AG	NO AG	NO AG	NO AG	NO AG	NO MAB - 1µg/mL	PBST only
H	Sample	Sample	Sample	Sample	NO PAB	NO PAB/ NO AG	NO AG	NO AG	NO AG	NO AG	NO MAB - 1µg/mL	PBST only
	1	2	3	4	5	6	7	8	9	10	11	12
A	OVRFLW	OVRFLW	OVRFLW	OVRFLW	OVRFLW	21486	25352	23275	38095	66652	672	438
B	OVRFLW	OVRFLW	OVRFLW	OVRFLW	OVRFLW	22324	26921	24837	41054	65865	229	269
C	OVRFLW	OVRFLW	OVRFLW	OVRFLW	93314	7975	11433	11306	17553	32034	221	425
D	OVRFLW	OVRFLW	OVRFLW	OVRFLW	OVRFLW	7959	10374	12287	18377	30414	198	364
E	OVRFLW	OVRFLW	OVRFLW	OVRFLW	85845	3863	5247	6589	10452	18930	335	414
F	OVRFLW	OVRFLW	OVRFLW	OVRFLW	92784	4079	4939	7297	10987	17528	838	292
G	82294	84749	OVRFLW	OVRFLW	76938	2262	2763	3644	4698	8465	659	40
H	80265	83337	92057	OVRFLW	87293	1881	3726	3073	4762	8526	335	66

Figure 21: DnaK Blocking Trial #9 (Checkerboard)
Checkerboard titration assay for recDnaK. The unpurified, R2-1 PAB serum was diluted from left to right (indicated by the black arrow at the top of the graph) at concentrations of 0.1, 0.25, 0.5, and 1 µg/mL. The purified, biotinylated MAB (DnaK Clone A) was diluted from top to bottom (indicated by the black arrow on the left side of the graph) at dilutions of 1:1,000, 1:2,500, 1:5,000, and 1:10,000. The colors coordinate with the MAB dilutions. Negative controls are indicated in columns #5-12 (with PAB serum concentrations indicated in wells of MAB and PAB + Strep-HRP negative controls). The entire microplate was blocked with a 3% BSA (in PBST) blocking solution. The antigen and MAB were both diluted in a 2%BSA/PBST "standard diluent". The final concentration of the recDnaK antigen for the entire microplate was 1 µg/100µL (10,000 ng/mL). The strep-HRP conjugate was diluted at 2 µg/mL in a 0.4%BSA/PBST diluent. Red boxes indicate optimal PAB serum and MAB pairing.

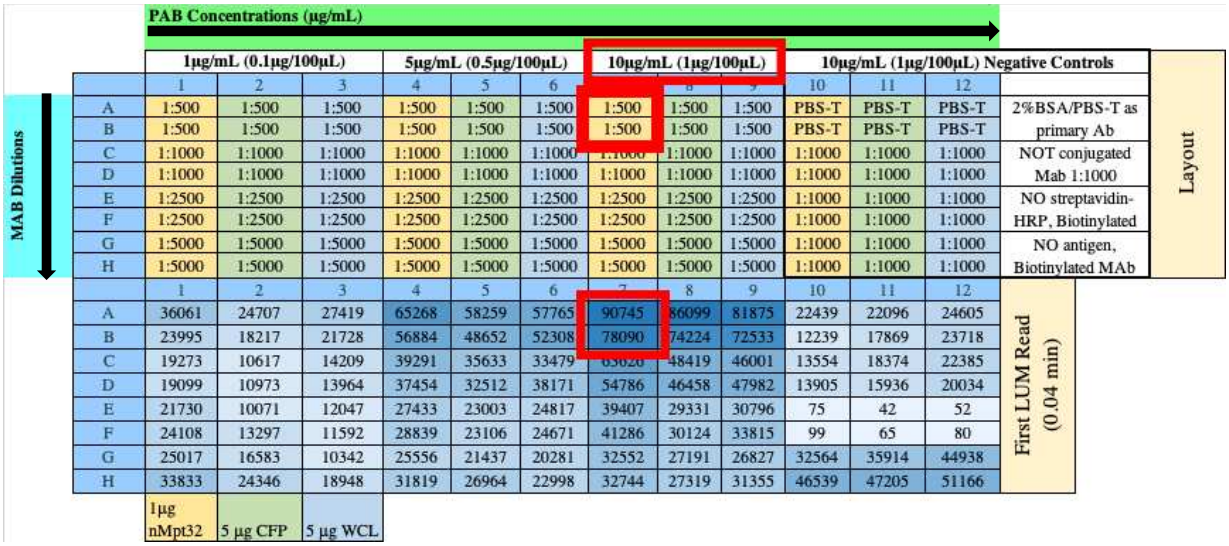

PAB Concentrations (µg/mL)

MAB Dilutions

	1µg/mL (0.1µg/100µL)			5µg/mL (0.5µg/100µL)			10µg/mL (1µg/100µL)			10µg/mL (1µg/100µL) Negative Controls			Layout
	1	2	3	4	5	6	7	8	9	10	11	12	
A	1:500	1:500	1:500	1:500	1:500	1:500	1:500	1:500	1:500	PBS-T	PBS-T	PBS-T	2%BSA/PBS-T as primary Ab
B	1:500	1:500	1:500	1:500	1:500	1:500	1:500	1:500	1:500	PBS-T	PBS-T	PBS-T	
C	1:1000	1:1000	1:1000	1:1000	1:1000	1:1000	1:1000	1:1000	1:1000	1:1000	1:1000	1:1000	NOT conjugated Mab 1:1000
D	1:1000	1:1000	1:1000	1:1000	1:1000	1:1000	1:1000	1:1000	1:1000	1:1000	1:1000	1:1000	
E	1:2500	1:2500	1:2500	1:2500	1:2500	1:2500	1:2500	1:2500	1:2500	1:1000	1:1000	1:1000	NO streptavidin-HRP, Biotinylated
F	1:2500	1:2500	1:2500	1:2500	1:2500	1:2500	1:2500	1:2500	1:2500	1:1000	1:1000	1:1000	
G	1:5000	1:5000	1:5000	1:5000	1:5000	1:5000	1:5000	1:5000	1:5000	1:1000	1:1000	1:1000	NO antigen, Biotinylated MAb
H	1:5000	1:5000	1:5000	1:5000	1:5000	1:5000	1:5000	1:5000	1:5000	1:1000	1:1000	1:1000	

	1	2	3	4	5	6	7	8	9	10	11	12	First LUM Read (0.04 min)
A	36061	24707	27419	65268	58259	57765	90745	86099	81875	22439	22096	24605	
B	23995	18217	21728	56884	48652	52308	78090	74224	72533	12239	17869	23718	
C	19273	10617	14209	39291	35633	33479	63020	48419	46001	13554	18374	22385	
D	19099	10973	13964	37454	32512	38171	54786	46458	47982	13905	15936	20034	
E	21730	10071	12047	27433	23003	24817	39407	29331	30796	75	42	52	
F	24108	13297	11592	28839	23106	24671	41286	30124	33815	99	65	80	
G	25017	16583	10342	25556	21437	20281	32552	27191	26827	32564	35914	44938	
H	33833	24346	18948	31819	26964	22998	32744	27319	31355	46539	47205	51166	
	1µg nMpt32	5 µg CFP	5 µg WCL										

Figure 22: Mpt32 Checkerboard Trial #1

Checkerboard titration assay for nMpt32. The unpurified, R2-1 PAB serum was diluted from left to right (indicated by the black arrow at the top of the graph) at concentrations of 1, 5, and 10 µg/mL. The purified, biotinylated MAB (Mpt32 Clone B, "wash 3") was diluted from top to bottom (indicated by the black arrow on the left side of the graph) at dilutions of 1:500, 1:1,000, 1:2,500, and 1:5,000. The colors (in layout) coordinate with the different antigens used in this specific trial. Negative controls are indicated in columns #10-12, all with PAB serum at a concentration of 10 µg/mL. The negative controls used for this trial (different than most trials) are labeled appropriately to the right of column #12. The entire plate was blocked with a 3% BSA (in PBST) blocking solution. The antigen and MAB were both diluted in a 2%BSA/PBST "standard diluent". The final concentration of nMpt32 antigen for the entire microplate was 1 µg/100µL (10,000 ng/mL). The final concentration of crude *Mtb* fractions, CFP (culture filtrate protein) and WCL (whole cell lysate), for the entire microplate was 5 µg/100µL (50,000 ng/mL). The strep-HRP was diluted at 2 µg/mL in a 0.4%BSA/PBST diluent. Red boxes indicate optimal PAB serum and MAB pairing.

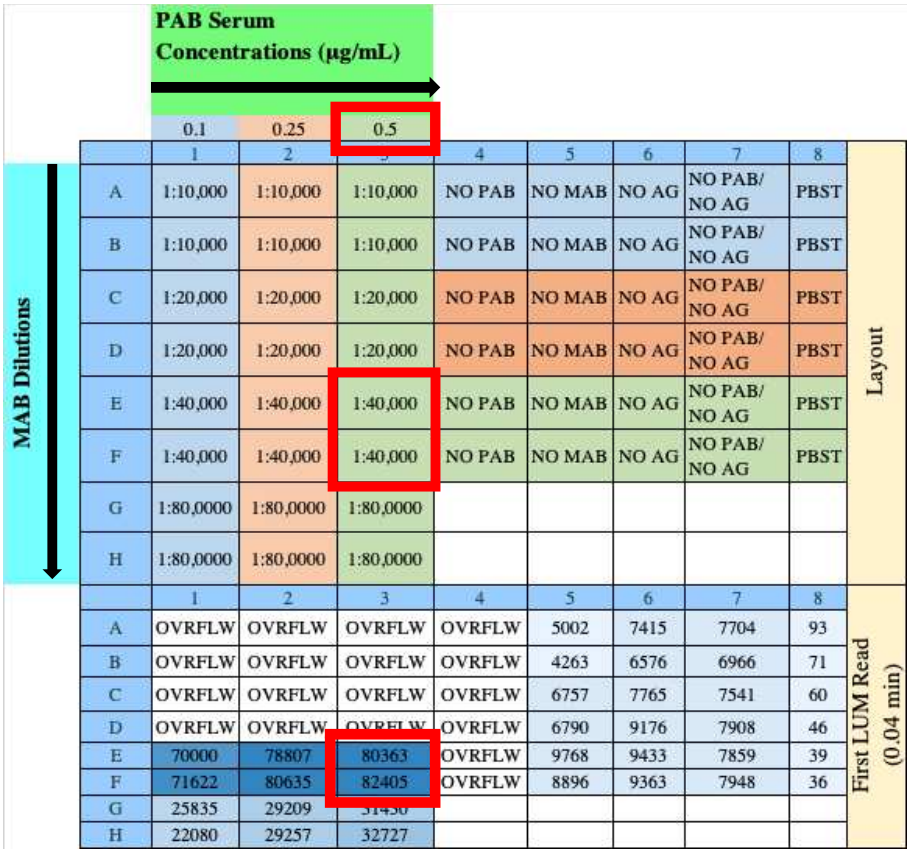

	1	2	3	4	5	6	7	8
A	1:10,000	1:10,000	1:10,000	NO PAB	NO MAB	NO AG	NO PAB/ NO AG	PBST
B	1:10,000	1:10,000	1:10,000	NO PAB	NO MAB	NO AG	NO PAB/ NO AG	PBST
C	1:20,000	1:20,000	1:20,000	NO PAB	NO MAB	NO AG	NO PAB/ NO AG	PBST
D	1:20,000	1:20,000	1:20,000	NO PAB	NO MAB	NO AG	NO PAB/ NO AG	PBST
E	1:40,000	1:40,000	1:40,000	NO PAB	NO MAB	NO AG	NO PAB/ NO AG	PBST
F	1:40,000	1:40,000	1:40,000	NO PAB	NO MAB	NO AG	NO PAB/ NO AG	PBST
G	1:80,0000	1:80,0000	1:80,0000					
H	1:80,0000	1:80,0000	1:80,0000					

	1	2	3	4	5	6	7	8
A	OVRFLW	OVRFLW	OVRFLW	OVRFLW	5002	7415	7704	93
B	OVRFLW	OVRFLW	OVRFLW	OVRFLW	4263	6576	6966	71
C	OVRFLW	OVRFLW	OVRFLW	OVRFLW	6757	7765	7541	60
D	OVRFLW	OVRFLW	OVRFLW	OVRFLW	6790	9176	7908	46
E	70000	78807	80363	OVRFLW	9768	9433	7859	39
F	71622	80635	82405	OVRFLW	8896	9363	7948	36
G	25835	29209	31430					
H	22080	29257	32727					

Figure 23: GroES Checkerboard Trial #3
Checkerboard titration assay for nGroES. The unpurified, R2-1 PAB serum was diluted from left to right (indicated by the black arrow at the top of the graph) at concentrations of 0.1, 0.25, and 0.5 µg/mL. The purified, biotinylated MAB (α-GroES, SA-12) was diluted from top to bottom (indicated by the black arrow on the left side of the graph) at dilutions of 1:10,000, 1:20,000, 1:40,000, and 1:80,000. The colors (in layout) coordinate with the different PAB serum concentrations used. Negative controls are indicated in columns #4-8. The negative controls reflect all PAB serum concentrations (colors), but all had a single MAB dilution of 1:20,000. The entire plate was blocked with a 3% BSA (in PBST) blocking solution. The antigen, MAB, and strep-HRP conjugate were all diluted in a PBST "standard diluent". The final concentration of nGroES antigen for the entire plate was 1 µg/100µL (10,000 ng/mL). The strep-HRP was diluted at a final concentration of 2 µg/mL in PBST diluent. Red boxes indicate optimal PAB serum and MAB pairing. Data presented in graph are from the first luminescence read only.

3.3.1.2 DnaK Preliminary Limit of Detection Trials

Prior to performing any optimization trials for the sandwich ELISA, we decided to attempt a limit of detection trial using recDnaK (Figure 24). We also added in the two crude *Mtb* fractions, CFP and WCL. This trial was to preliminarily see how sensitive the sandwich ELISA

was with the optimal PAB serum and MAB pairing. In the first LOD trial, we observed a decrease in the signal output as the recDnaK antigen concentration decreased (Figure 24). However, curiously the CFP and WCL signal outputs plateaued at lower antigen concentrations (Figure 24). This could have been the result of reaching the detection limit for DnaK for these crude samples. We observed poor linearity for all antigens (Figure 24).

It is also important to note that this trial had a couple of inconsistencies. The MAB dilutions were different for the crude fractions and the recDnaK protein. These original MAB dilutions were determined from an earlier checkerboard trial for DnaK (*Appendix: Figure 39*). It would have been better to have kept the same parameters for all proteins, especially when we could not determine how much of the DnaK protein was in the crude fractions. The MAB incubation parameters were also changed: the MAB was incubated normally for 1 hr, shaking at room temperature and then placed at 4°C for ~3 hr due to extraneous circumstances. The sandwich ELISA was then finished normally.

We attempted a second LOD trial with recDnaK (Figure 25). For this trial, we eliminated some of the problems from the first attempt. First, we performed a 1:2 serial dilution for all antigens (recDnaK, CFP, and WCL). Second, we used the same concentration of PAB serum (0.5 μg/mL) and MAB dilution (1:2,500) for all three antigens. Third, the incubation parameters for the MAB were carried out as described in *section 3.2.1 Sandwich ELISA*. Lastly, we increased the concentration of both the crude samples from 50,000 ng/mL to 200,000 ng/mL to see if we could observe a decreasing trend instead of a plateau. Since DnaK makes up such a small percentage of the crude samples, increasing the crude samples could allow for better detection. However, sometimes this can offer the opposite affect where too much crude sample hinders detection.

For this LOD trial, we still observed a plateauing of the two crude fractions at lower concentrations of antigens (Figure 25). Again, this indicated that maybe the limit of detection for DnaK was reached in the crude fractions. What concerned us more was that the recDnaK demonstrated a plateauing as well at the lower antigen concentrations (Figure 25). We still observed poor linearity for all antigens (Figure 25), similar to what we saw in the first LOD trial (Figure 24). The recDnaK antigen R-squared value decreased in this second LOD trial as well.

We also added in the NO PAB negative control for the first time in this trial. This negative control for recDnaK was very high, with an average duplicate signal output value of 64,973.5 RLUs. However, the same negative control for the crude fractions was very low at 5,789 RLUs for CFP and 7,808.5 RLUs for WCL (raw data not shown). Therefore, this trial demonstrated to us that the sandwich ELISA needed further extensive optimization before we could accurately run an LOD and suggested that the recDnaK antigen may be binding non-specifically to the plate or to other reagents.

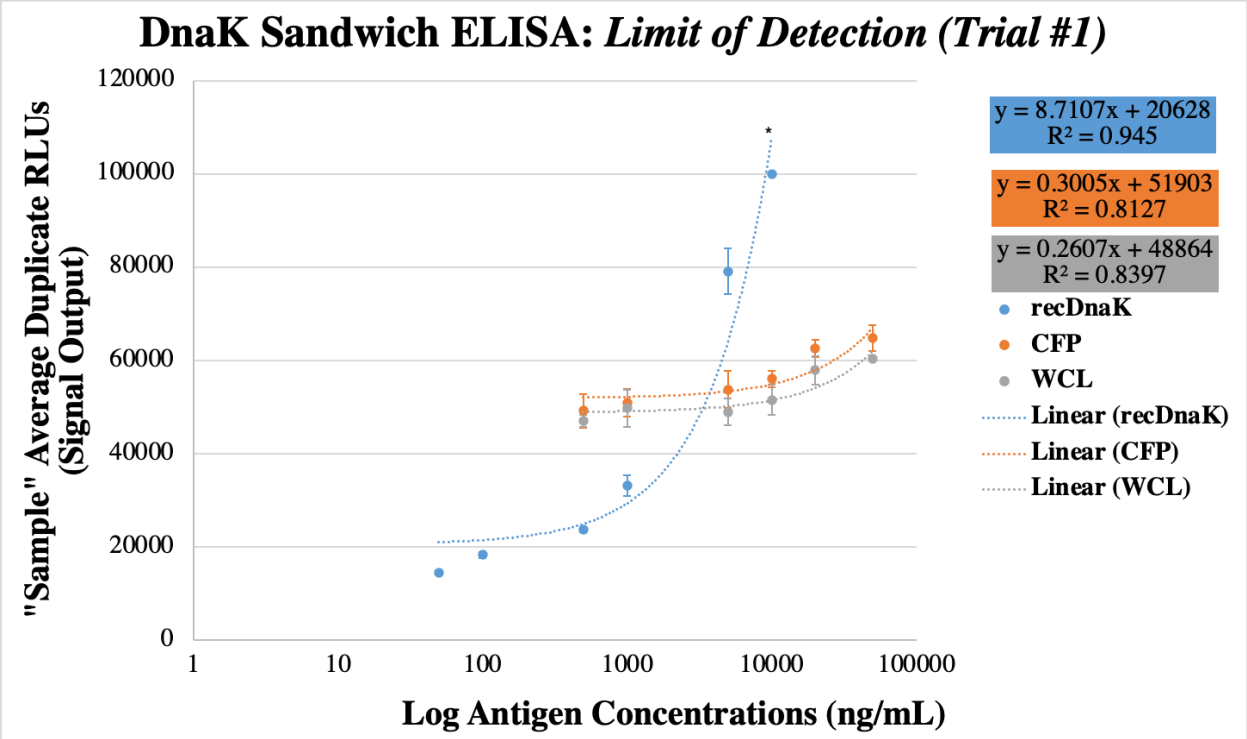

Figure 24: DnaK LOD Trial #1

Limit of detection trial (#1) for recDnaK. The "sample" average duplicate signal output (RLUs) was graphed on the *Y-axis*. The antigen concentrations were graphed on the *X-axis*. The *X-axis* was converted to logarithmic scale (base 10). The unpurified, R2-1 PAB serum was diluted at 0.5 µg/mL for recDnaK and at 1 µg/mL for crude *Mtb* fractions, CFP (culture filtrate protein) and WCL (whole cell lysate). The MAB (purified, biotinylated DnaK Clone A) was diluted at 1:2,500 for recDnaK and 1:1000 for CFP and WCL fractions. The entire plate was blocked with a 3% BSA (in PBST) blocking solution. The blocking solution may have contained thimerosal and TBST. 2%BSA/PBST diluent was used as the "standard diluent". The antigen and MAB were both diluted in the "standard diluent". The final concentrations of recDnaK antigen were 50, 100, 500, 1,000, 5,000, and 10,000 ng/mL (not a serial dilution). The final concentrations of CFP and WCL crude fractions were 500, 1,000, 5,000, 10,000, 20,000, and 50,000 ng/mL (not a serial dilution). The strep-HRP was diluted at a final concentration of 2 µg/mL in 0.4%BSA/PBST diluent. An asterisk is placed at the very top blue dot, corresponding to the recDnaK antigen concentration of 10,000 ng/mL with an OVRFLW "sample" value (100,000 RLUs). Linear trendlines were added for each antigen data plots and the R-squared and line equation are displayed (color coordinated).

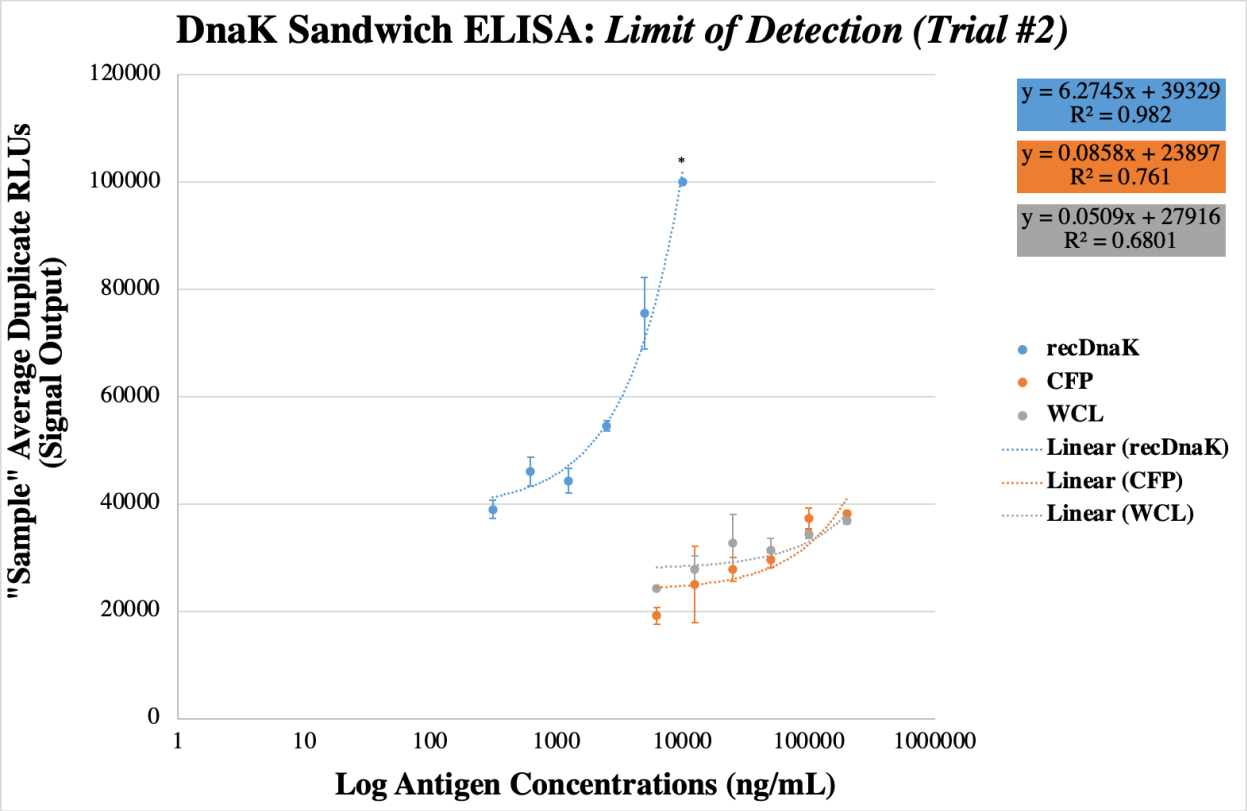

Figure 25: DnaK LOD Trial #2 Graph
Limit of detection trial (#2) for recDnaK. The "sample" average duplicate signal output (RLUs) was graphed on the *Y-axis*. The antigen concentrations were graphed on the *X-axis*. The *X-axis* was converted to logarithmic scale (base 10). The unpurified, R2-1 PAB serum was diluted at 0.5 µg/mL for all antigens (recDnaK, CFP, and WCL fractions). The purified, biotinylated DnaK MAB (Clone A) was diluted at 1:2500 for all three antigens. The entire plate was blocked with a 3% BSA (in PBST) blocking solution. The blocking solution may have contained thimerosal and TBST. The antigen and MAB were both diluted in 2%BSA/PBST standard diluent. The final concentrations of recDnaK antigen were 312.5, 625, 1,250, 2,500, 5,000, and 10,000 ng/mL (1:2 serial dilution). The final concentrations of CFP and WCL crude fractions were 6,250, 12,500, 25,000, 50,000, 100,000, and 20,0000 ng/mL (1:2 serial dilution). The strep-HRP was diluted at a final concentration of 2 µg/mL in 0.4%BSA/PBST diluent. Linear trendlines were added for each antigen data plots and the R-squared and line equation are displayed (color coordinated).

3.3.1.3 DnaK Blocking Trials (BSA & Milk)

To rule out binding of the recDnaK antigen to the plate, we performed several trials using different blocking buffers, different concentrations of blocking solutions, and other parameters relating to blocking. The first couple of trials were comparing blocking incubation parameters (1 hr, shaking at room temperature versus overnight, rocking at 4°C) as well as comparing bovine

serum albumin (BSA) and milk as blocking types (Figure 26). The BSA was a purified reagent (Gold Biotechnology), and the milk was a non-fat dry milk powder (Walmart). 10% solutions (in PBST) of each blocking type were made as stock solutions. The NO PAB and NO AG negative control signals were added for comparison in Figure 26.

Figure 26 demonstrates that there was not a stark difference between the % blocking solution (1, 3, or 5%) for either block type. Although, for BSA, an argument could be made that the 1%BSA blocking solution had slightly better "sample" signals (for either incubation parameter). We also observed a severe decrease in signal overall when looking at milk as the block ("sample" and negative controls). We cannot definitively say that incubation of the block overnight, rocking at 4°C was better than the 1 hr, shaking at room temperature incubation. Therefore, we decided to stick with 1 hr, shaking at room temperature incubation parameters for future trials.

We found it curious that the NO PAB negative control signal in these trials (Figure 26) was ~3/4 of the "sample" signal. This concerned us because it indicated that there were non-specific interactions occurring within the sandwich ELISA which could have created a false positive signal. When we tried milk as the blocking solution, we did generally see a decrease overall for the NO PAB negative control when compared to the "sample" signal. We did observe that the NO AG negative control signal was relatively quite low throughout these trials.

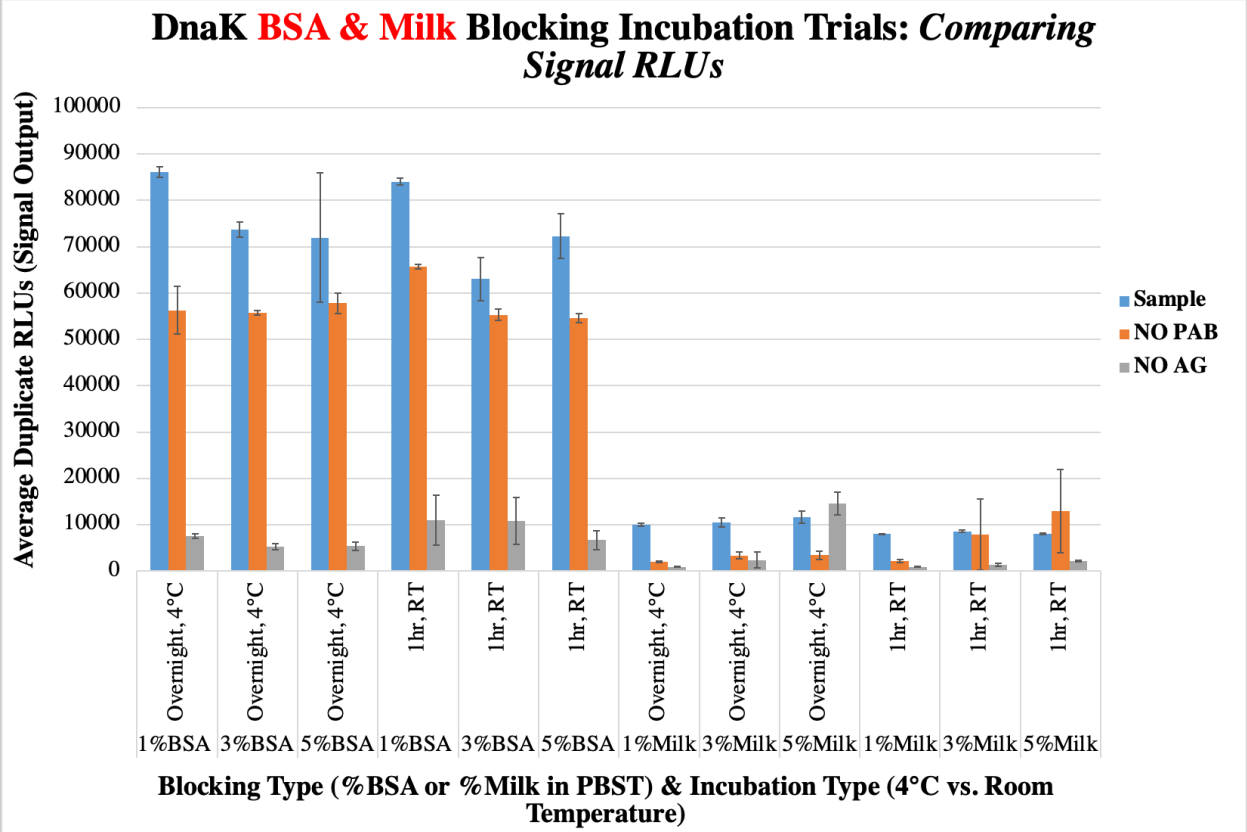

Figure 26: DnaK BSA & Milk Blocking (Incubation) Trials #1 and #2 *Comparing Signal RLUs*

Blocking trials for recDnaK looking at BSA and Milk as blocking solutions with different incubation parameters. The signal outputs in RLUs from averaged duplicate RLU values (corresponding to each sample or negative control) are graphed on the *Y-axis*. The %BSA or %Milk blocking solutions (1, 3, and 5%) as well as the incubation parameters, either overnight, rocking at 4°C or 1 hr, shaking at RT are graphed on the *X-axis*. The "sample" (blue), the NO PAB (orange), and the NO AG (grey) negative controls are graphed. 2%BSA/PBST (for BSA blocking solution) and 2%Milk/PBST (for milk blocking solution) were used as the "standard diluents". The antigen and MAB were diluted in the "standard diluents". The unpurified, R2-1 PAB serum was diluted to a final concentration of 0.5 µg/mL in coating buffer for both trials. The final concentration of the recDnaK antigen was 1 µg/100µL (10,000 ng/mL) for both trials. The MAB dilution was at 1:2,500 for both trials. The strep-HRP conjugate was diluted at 2 µg/mL in 0.4%BSA/PBST or 0.4%Milk/PBST diluents, respective of their blocking solutions.

Because the milk obliterated the "sample" signal, we focused on optimizing BSA as the blocking reagent. Since it appeared that there was high background from the NO PAB negative control using BSA as the blocking solution, we decided to carry out different trials looking at different diluents, still with BSA as the block. It is important to note that the graph presented in

Figure 27, Graph A is made up of multiple BSA blocking trials. These data were put together for comparison purposes, even if not performed on the same ELISA plate. Combining the data from all the trials allowed us to look for general trends for each of the antigens.

It is important to note that there were reproducibility issues between ELISA plates (*Appendix: Figure 39*). As noted previously, the original checkerboard (*Appendix: Figure 39*) for recDnaK had a more concentrated MAB dilution than the second checkerboard carried out (Figure 21). This difference could be attributed to different batches of strep-HRP conjugate used. Another source of error could have been that a 10%BSA + thimerosal stock solution was used for dilution of the blocking solution (for checkerboard trial #2 only). The only stock solution in the lab with thimerosal was a 10%BSA in TBST solution. The tris-based solution could have changed the interactions within the sandwich ELISA reagents when compared to using PBST.

For these BSA blocking trials, PBST, 2%BSA/PBST, and 2%Milk/PBST were tested as "standard diluents". Figure 27, Graph A demonstrates a high NO PAB negative control background for BSA block with both PBST and 2%BSA/PBST as the diluents. The 2%Milk/PBST diluent aided in decreasing the NO PAB negative control background, but there was still a severe decrease in overall "sample" signal. The PBST diluent also increased the NO AG negative control signal for that group. Looking at the RLU signal output values allowed us to compare the different diluent signals overall but to directly compare the background noise from the NO PAB negative control to the sample signal, we had to look at the *sample: NO PAB* ratios. Calculations for finding the ratios can be found in *section 3.2.2 Sandwich ELISA Data Analysis*.

Figure 27, Graph B demonstrates the *sample: NO PAB* ratios. PBST and 2%BSA/PBST diluents both had poor ratios *at* values of 1 or *close to* 1, respectively. This indicated to us that the "sample" was not much more than just background noise coming from non-specific

interactions occurring within the sandwich ELISA. Even though the 2%Milk/PBST diluent decreased the signal overall, the ratios were much higher than the PBST and 2%BSA/PBST diluents.

A. Comparing Signal RLUs

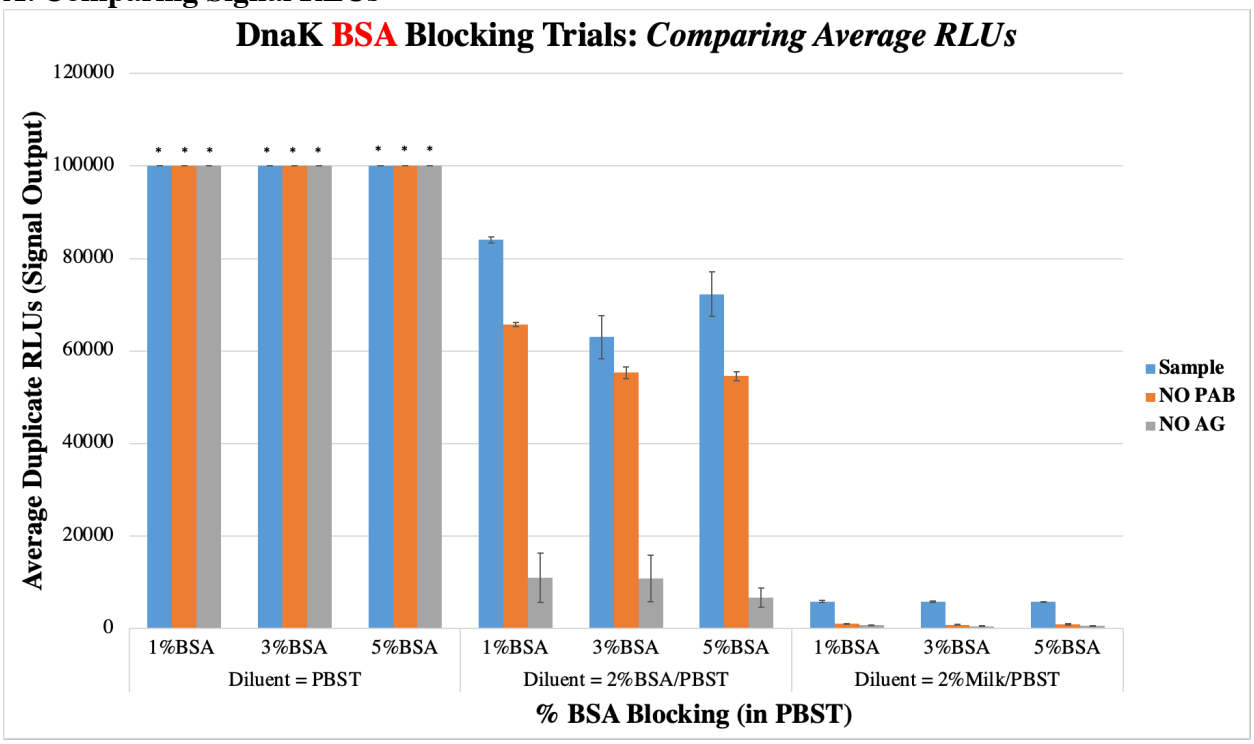

B. Comparing *Sample: NO PAB* Ratios

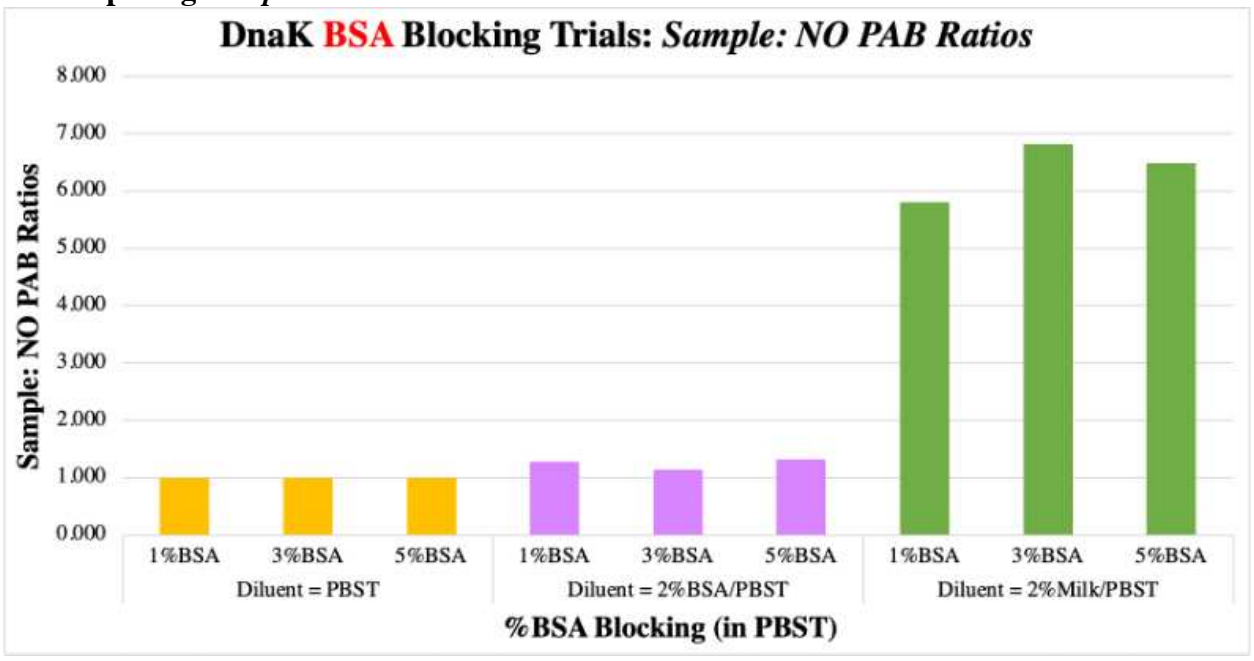

Figure 27: DnaK BSA Blocking Trials (#2 & #11)
Blocking trials for recDnaK looking at BSA as sole blocking solution with different diluents. **Graph A)** The signal output in RLUs from averaged duplicate RLU values (corresponding to each sample or negative control) are graphed on the *Y-axis*. The %BSA blocking solutions (1, 3, and 5%) are graphed on the *X-axis* and are grouped according to the corresponding diluents. The diluents are labeled appropriately under each group. The "sample" (blue), the NO PAB (orange), and the NO AG (grey) negative controls are graphed. **Graph B)** Ratios of the "sample" signals divided by the NO PAB negative control signals. Ratio values are graphed on the *Y-axis*. The different %BSA blocking solutions in PBST (1, 3, 5%) are graphed on the *X-axis* and are grouped according to the corresponding diluents. The diluents are depicted in different colors. Data from the group with 2%BSA/PBST diluent originated from BSA blocking trial #2. Data from groups with PBST and 2%Milk/PBST diluents originated from BSA blocking trial #11. The unpurified, R2-1 PAB serum was diluted for a final concentration of 0.5 μg/mL in coating buffer for both trials. The antigen and MAB were diluted in the "standard diluents" (PBST, 2%BSA/PBST, or 2%Milk/PBST) corresponding to the respective group in the graph. The recDnaK antigen was diluted at 1 μg/100 μL (10,000 ng/mL) for both trials. Trial #2 had a MAB (purified, biotinylated DnaK Clone A) dilution of 1:2,500 and trial #11 had a MAB dilution of 1:10,000. The strep-HRP conjugate was diluted at a concentration of 2 μg/mL in PBST, 0.4%BSA/PBST, or 0.4%Milk/PBST diluents, corresponding to the respective group in the graph.

Since the 2%Milk/PBST diluent from the BSA blocking trials (Figures 26 & 27) showed promise in lowering the NO PAB background noise, we decided to perform trials with milk as the blocking solution. We also included PBST and 2%BSA/PBST diluents for comparison. Figure 40, Graph A (*Appendix)* as expected, demonstrates that all "sample" signals, for all diluents, are lower for milk block than those of the BSA blocking trials (Figure 27, Graph A). Figure 40, Graph A (*Appendix)* also demonstrates the lowering of the NO PAB negative control background noise using milk as a blocking solution with 2%BSA/PBST and 2%Milk/PBST as the diluents. The NO PAB background is ~ 2/3 the "sample" signal for PBST diluent and ~1/3-1/2 the "sample" signal for 2%BSA/PBST diluent (*Appendix: Figure 40, Graph A*). This is compared to BSA blocking solution with a 2%BSA/PBST diluent where was observed the NO PAB signal to be ~3/4 of the "sample" signal (Figure 27, Graph A). Since the PBST signals ("sample" and NO PAB) were in OVRFLW for the BSA blocking trials, we could not accurately compare these signals with the milk blocking trials. Figure 40, Graph B (*Appendix*) demonstrates

that milk as a blocking solution and diluent produced the best *sample: NO PAB* ratio. Since the overall *sample: NO PAB* ratios improved with milk as a blocking solution (for all three diluents) when compared to BSA as a blocking solution, these data also suggest that a reagent in the sandwich ELISA was binding non-specifically to the BSA block.

3.3.1.4 Identification of Non-Specific Binding Interactions in the DnaK Sandwich ELISA

To determine which reagents were binding non-specifically to the BSA block, we looked at previous negative controls used across multiple DnaK sandwich ELISA trials to try to eliminate possible interactions within the NO PAB negative control. Figure 28 depicts a pseudo sandwich ELISA layout. A negative control that would eliminate a specific reagent is labeled under each reagent.

Refer to Table 1 for a description of each negative control mentioned. If we are looking at the NO PAB negative control specifically, the PAB serum was never plated so we could eliminate the PAB serum as the culprit. We have had a NO PAB/NO AG negative control and it was relatively low (demonstrated in Figure 21). Therefore, if the MAB was binding to the plate directly (insufficient blocking) or binding to the BSA block, there would be an increase in signal for this negative control. We observed some increase in the signal with the MAB at a too concentrated of a dilution (1:1,000) (demonstrated in Figure 21). We also had different %BSA blocking solutions (1, 3, 5%) for multiple trials (demonstrated in Figures 26, Graph A and 27, Graph A) and there was not a stark difference between the NO PAB signals for different %BSA blocking solutions. Therefore, if there was insufficient blocking of the plate, an increase in the %BSA blocking solution should have decreased the NO PAB negative control background noise. This was not the case and insufficient blocking of the plate could be eliminated as the culprit. In one of the earliest trials, we used a NO Strep-HRP Conjugate negative control and the averaged

duplicate values (for recDnaK) were ~150 RLUs (data not shown). The chemiluminescent substrate does not produce a light response without the HRP enzyme present. Therefore, we could eliminate the substrate as the culprit. We also had a "block only" negative control for multiple trials which had been relatively low (demonstrated in Figure 21). Therefore, we could eliminate the strep-HRP conjugate as the culprit because the block only negative control included blocking solution, strep-HRP conjugate, and the chemiluminescent substrate. This left us with a hypothesis that the non-specific interaction was occurring between the BSA block and the recDnaK antigen (indicated by a purple box in Figure 28).

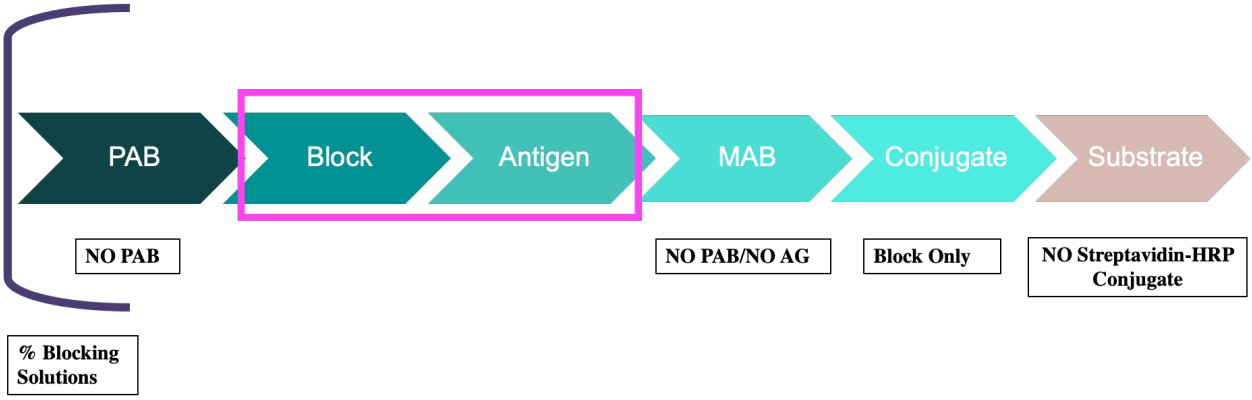

Figure 28: The NO PAB Negative Control Dilemma
Pseudo sandwich ELISA layout depicting possible non-specific interactions within the DnaK sandwich ELISA using BSA as the block. The "standard diluent" in this scenario is 2%BSA/PBST. The negative controls eliminating each reagent as the culprit are labeled under the corresponding reagent. The purple box indicates the identified possible non-specific interaction between the BSA block and the recDnaK antigen.

To support this possible non-specific binding interaction, Figure 29 depicts the relationship between the NO PAB negative control signal and recDnaK antigen concentration. This trial was originally looking at different strep-HRP conjugate dilutions but demonstrated an interesting trend. For this comparison, the same strep-HRP conjugate dilution was 1:2,500 only. Figure 29 demonstrates that an increase in antigen resulted in a higher NO PAB signal, even though there was not any PAB serum plated. This indicated that the background signal was

coming from a non-specific interaction of one reagent with the recDnaK antigen. As mentioned previously (Figure 28), the non-specific interaction was hypothesized to be occurring between the recDnaK antigen and the BSA block.

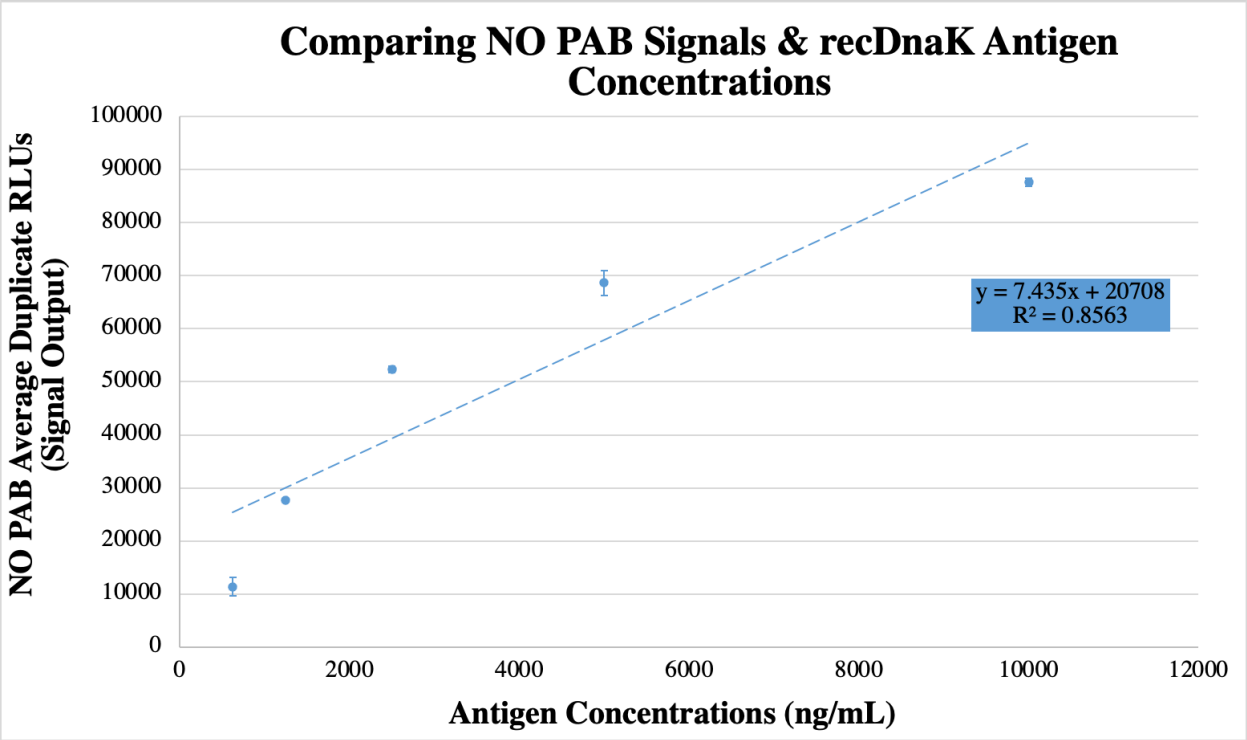

Figure 29: DnaK (BSA) LOD Trial #4 (Checkerboard) – Comparing NO PAB Signals & recDnaK Antigen Concentrations

Depiction of the relationship between the NO PAB negative background signal and the recDnaK antigen concentration. The NO PAB average duplicate RLU values (signal output) are graphed on the *Y-axis*. The recDnaK antigen concentrations are graphed on the *X-axis* in ng/mL. The entire microplate was blocked with a 3%BSA (in PBST) blocking solution. The unpurified R2-1 PAB serum was diluted to a final concentration of 0.5 µg/mL in coating buffer. 2%BSA/PBST was used as the "standard diluent". The antigen and MAB were diluted in the "standard diluent". The recDnaK antigen was diluted using a 1:2 serial dilution series, starting at 10,000 ng/mL (1 µg/100 µL). The MAB (purified, biotinylated DnaK Clone A) had a dilution of 1:2,500. The strep-HRP conjugate (for these data) was at a dilution of 1:2,500 in a 0.4%BSA/PBST diluent.

3.3.1.5 DnaK Blocking Trials Continued (Addition of Other Blocking Solutions)

To try and alleviate the problem of the non-specific binding occurring between recDnaK and BSA blocking solution, we performed other blocking trials using different blocking types. Because milk lowered the "sample" signal drastically, we were hoping different blocking

solutions would help increase this signal but also maintain a low background noise level. The different blocks included ovalbumin, casein buffer, and a protein-free block. For each of these blocking trials, different diluents were tested: PBST, 2%BSA/PBST, and/or the block specific protein in PBST. The only exclusion to this was the protein-free blocking trial which only utilized 2%BSA/PBST as the diluent. Generally, 1, 3, and 5% protein block solutions in PBST were tested. However, for the casein buffer trials, 1X, 3X, and 5X solutions were tested (prepared from stock solution). The casein buffer came ready to use in a stock solution (SurModics, Inc.). The protein-free block was used undiluted as a block (neat) per the manufacturer's directions [158]

First, we looked at using ovalbumin (OVA) as another protein block (*Appendix: Figure 41*). The OVA protein came as a crude reagent of albumin from chicken egg whites (Sigma). According to the manufacturer, "ovalbumin make[s] 75% of the total egg white protein" (*Albumin from Chicken Egg White (A5253)*, n.d.). A 10%OVA (in PBST) stock solution was prepared for the blocking trials. This reagent was difficult to dissolve completely into solution. Stirring overnight at 4°C (trial #2) aided in dissolving the crude OVA into solution (although chunks remained). When PBST or 2%BSA/PBST diluents were used, the NO PAB signal was in OVRFLW along with the "sample" signals (*Appendix: Figure 41, Graph A*). When looking at the *sample: NO PAB* ratios (*Appendix: Figure 41, Graph B*), we saw that the OVA block performed poorly for all diluent types. The 3%OVA (in PBST) blocking solution with a 2%OVA/PBST diluent *sample: NO PAB* ratio was deceiving because although the ratio was high, the "sample" signals were incredibly low (*Appendix: Figure 41, Graphs A and B*).

We were given a sample of casein buffer from SurModics, Inc. to try as a blocking buffer (*Appendix: Figure 42, Graph A*). For this trial, it was recommended by the manufacturer to

dilute the casein buffer in ultrapure water (as a blocking solution and as a diluent) and use a 1X casein buffer solution for a diluent [160]. We noticed a similar trend with this protein block as with the OVA. However, the casein buffer solution as a block and diluent increased all signals slightly when compared to OVA as both a block and a diluent. There was no improvement to background signal of the NO PAB negative control as demonstrated by the *signal: NO PAB* ratios (*Appendix: Figure 42, Graph B*).

One final blocking solution we tried was the Pierce™ Protein-Free T20 blocking buffer in PBS (Fisher Scientific). This buffer was made in PBS, pH 7.4 with Tween®20 added to a final concentration of 0.05% [158]. The protein-free buffer "contain[s] a protein-free compound" but the manufacturer did not provide details on the composition of the compound [158]. For this trial, 3%BSA/PBST block was compared on the same microplate as the protein-free block (*Appendix: Figure 43*). We had hoped that using a protein-free block would eliminate the non-specific interactions occurring between the BSA protein block and the recDnaK protein antigen. However, as demonstrated in *Appendix: Figure 43*, the protein-free buffer still maintained a high NO PAB negative control background noise.

PBST as a diluent increased the NO PAB background noise (and in some instances, the NO AG background noise) for multiple blocking trials. However, even with different blocking solutions, the NO PAB background noise was still high with the use of the 2%BSA/PBST diluent. This could mean that the recDnaK could have been binding to the BSA in the diluent to some extent. However, for the milk blocking trials, there was a decrease in NO PAB background noise for the 3% and 5% milk blocking solutions with a 2%BSA/PBST diluent (*Appendix: Figure 40, Graph A*). This indicated that an increase in %Milk block could alleviate this interaction with BSA in the diluent. For the OVA, casein buffer, and the protein-free blocking

trials, since the NO PAB signals were all OVRFLW for the 2%BSA/PBST diluent, we could not explicitly make this comparison. The addition of the different proteins (specific for the blocking type) to the diluent tended to lower the "sample" signal along with the NO PAB background signal overall. 2%Milk/PBST as the diluent produced the highest *sample: NO PAB* ratios, when used in tandem with milk (*Appendix: Figure 40, Graph B*) or BSA (Figure 27, Graph B) as the block. This could be due to the fact that milk is made up of a slew of different proteins [161] that could aid in blocking the recDnaK antigen from binding non-specifically to the blocking solution.

These blocking trials demonstrated to us that there could be something in the function of the DnaK protein antigen that could aid in its ability to bind non-specifically to BSA as well as other protein (and protein-free) blocks. Since chaperone proteins tend to be sticky, we hypothesized that the chaperone function of DnaK allowed the protein to bind non-specifically to the BSA block and in turn, created high background in the sandwich ELISA system. To support this hypothesis, we decided to look at another antigen, Mpt32, which is not a chaperone protein, to see if this high NO PAB background trend continued.

3.3.1.6 Mpt32 Sandwich ELISA Trials

Even though we did not attempt as many blocking trials with nMpt32, we performed one with 1, 3, and 5% BSA (in PBST) blocking solutions and the protein-free block. What we observed with Mpt32 sandwich ELISA was the opposite of the DnaK sandwich ELISA. The Mpt32 blocking trial (Figure 30, Graph A) showed a near depletion of the NO PAB negative control background signal. Therefore, this demonstrated that the nMpt32 antigen was not binding to the BSA block like recDnaK was.

However, The NO AG negative control background noise increased, and the NO AG signal was ~2/3 that of the "sample" signal. We also observed that there was not a noticeable difference between block type or 1, 3, 5% BSA blocking solutions for the "sample" signals or the NO AG negative control signals. This was also reflected in the *sample: NO AG* ratios (Figure 30, Graph B). Therefore, another problem was occurring within the Mpt32 sandwich ELISA.

A. Comparing Signal RLUs

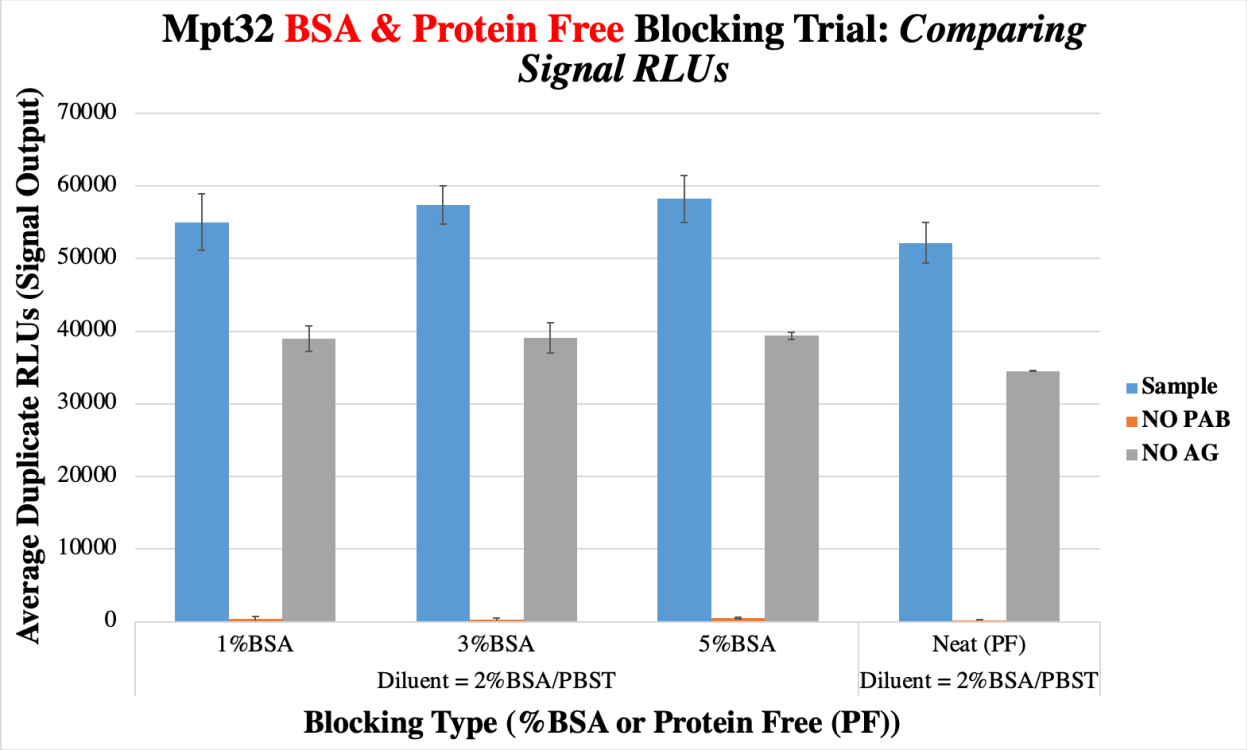

B. Comparing *Sample: NO PAB* Ratios

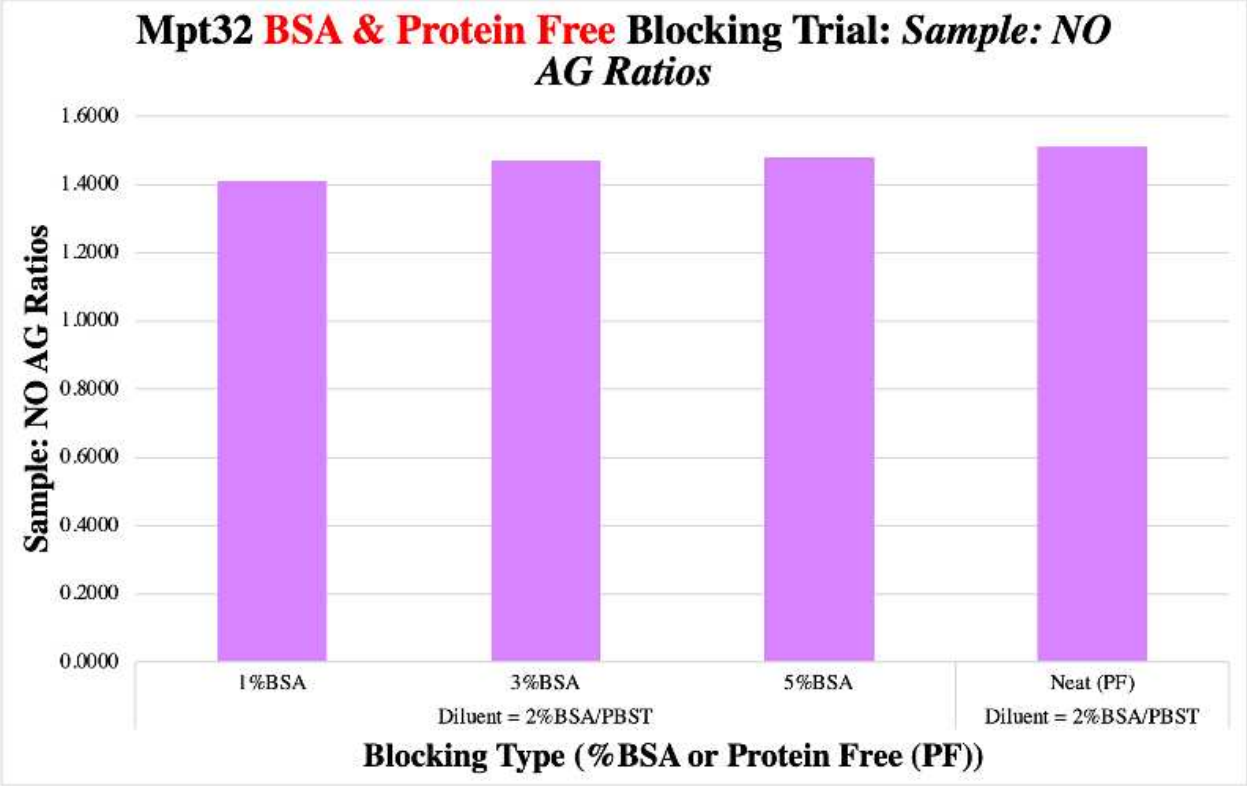

Figure 30: Mpt32 BSA & Protein-Free Blocking Trial (#1)

Blocking trial (#1) for nMpt32 looking at BSA and protein-free block as blocking solutions. **Graph A)** The signal output in RLUs from averaged duplicate RLU values (corresponding to each sample or negative control) are graphed on the *Y-axis*. The %BSA in PBST (1, 3, and 5%) and undiluted (neat) protein-free blocking solutions are graphed on the *X-axis*. The "sample" (blue), the NO PAB (orange), and the NO AG (grey) negative controls are graphed. **Graph B)** Ratios of the "sample" signals divided by the NO AG negative control signals. Ratio values are graphed on the *Y-axis*. The different %BSA in PBST (1, 3, 5%) and undiluted protein-free (neat) blocking solutions are graphed on the *X-axis*. 2%BSA/PBST diluent was used for this trial as the "standard diluent". The antigen and MAB were diluted in the "standard diluent". The final concentration for the nMpt32 antigen was 1 μg/100 μL (10,000 ng/mL). The MAB (purified, biotinylated Mpt32 Clone B, "wash 3") had a dilution of 1:500. The strep-HRP conjugate was diluted at a concentration of 2 μg/mL in 0.4%BSA/PBST diluent.

3.3.1.7 GroES Sandwich ELISA Trials

Because the Mpt32 blocking trial showed a different trend than the DnaK blocking trials, we decided to look at the last antigen, nGroES, another chaperone protein. If GroES trials produced a high NO PAB negative control background signal, and a low NO AG negative control background (like we observed for DnaK), then this would help support our hypothesis further, that the chaperone function of DnaK (and GroES) protein was influencing the protein to bind to the BSA block. Indeed, the trend for nGroES mirrored that of recDnaK (Figure 23). The GroES checkerboard titration assay included a checkboard of the PAB serum and the MAB dilutions, but we also added in the corresponding negative controls (all PAB serum concentrations, only a MAB dilution of 1:20,000). Because we did not include all MAB dilutions for the negative controls, another checkerboard would need to be performed with the additional MAB dilutions to confirm optimal pairing.

Even though we do not have the data for the negative controls at a 1:40,000 MAB dilution (from optimal pairing), Figure 23 demonstrates clearly a very high NO PAB background signal (in OVRFLW) (Column #4, Rows A-F) and a low NO AG background signal (Column #6, Rows A-F) at a 1:20,000 MAB dilution. Multiple NO PAB negative controls were plated, even though they were all the same, only one duplicate was needed. The "sample" signal for the

MAB dilution of 1:20,000 was also in OVRFLW for all PAB serum concentrations. The other negative controls (NO MAB, NO PAB/NO AG, and PBST) remained low. Therefore, this GroES trial helped further support our hypothesis that the non-specific binding to the BSA block was chaperone specific.

3.3.2 Optimization and Use of Surface Plasmon Resonance Technology

Surface plasmon resonance (SPR) technology using the Biacore system was utilized to look at protein-protein interactions on a more sensitive platform. This technology was used to support the hypothesis that the chaperone proteins were binding to the BSA block. For the Biacore, BSA (in PBST) was used as the ligand. pH scouting and immobilization using an amine coupling kit were used to determine best immobilization buffer/conditions and to permanently fix the BSA ligand to the Series S CM5 chip, respectively. A single-cycle kinetics method was used to look at binding and interactions between the analytes (nMpt32 and recDnaK) with the BSA ligand. Refer to footnote [1] on page 119 for more information on the Biacore instrument and SPR technology.

3.3.2.1 pH Scouting for BSA Ligand

For the pH scouting method, 10 mM sodium acetate solutions with a pH of 4, 4.5, 5, or 5.5 were chosen as the pre-concentration buffer. Figure 44 (*Appendix*) depicts the results for this pH scouting method. The different colors correspond to each buffer pH. The buffer with a pH of 4.5 had the highest response (indicated by the black arrow on the sensorgram) and was chosen for future experiments. This means that the BSA protein ligand had the strongest "attraction" (positive charge) to the dextran matrix (negative charge) at this pH [162].

3.3.2.2 Immobilization of BSA Ligand

For immobilization, Both Fc-1 and Fc-2 were exposed to the amine coupling reagents, but Fc-2 was immobilized with the BSA protein ligand. Figure 45 (*Appendix*) depicts the sensorgram results for the immobilization of BSA for the trial that worked (with a BSA concentration of 25 μg/mL used). The immobilized amount of BSA is the baseline level (blue arrow) subtracted from the immobilization level (red arrow). Figure 46 (*Appendix*) depicts the response values given for Fc-1 reference channel and the Fc-2 BSA ligand channel. The final response value for Fc-1 was 61.9 RU and for Fc-2 was 8,266.4 RU. This indicated how much BSA ligand was successfully bound to Fc-2. The Fc-1 reference channel final response value acts as a background noise reference.

Because the final response value was so high, it was unlikely we could extrapolate kinetics data from this ligand channel. The T100 manual suggested that a lower R_{max} is better for kinetics while a higher R_{max} can be used for concentration determination [162]. The fact that we immobilized a large amount of BSA protein to the chip surface was advantageous for us as we wanted to visualize binding of the recDnaK analyte to the BSA ligand. Kinetics data could allow us to understand how strong the non-specific binding interactions were, but they were not as crucial as qualitatively confirming the non-specific binding interactions.

3.3.2.3 Single Cycle Kinetics with BSA Ligand and Purified Protein (nMpt32 & recDnaK) Analytes

After immobilization of the BSA ligand, we tried a single-cycle kinetics method. For this method we injected five "blank concentrations" of buffer (PBST), then five concentrations of nMpt32 analyte (45,000 Da), and lastly, five concentrations (same as nMpt32) of recDnaK (67,000 Da) analyte. The single-cycle kinetics method injected the lowest concentration first, and then increasing concentrations (method specific). The five concentrations (nM) of the analytes

(in PBST buffer) we used were made as a 1:2 serial dilution series: 31.25, 62.5, 125, 250, and 500.

Figure 31 depicts the results of this single-cycle kinetics run as overlayed sensorgrams of all the cycles: startup injections of buffer (cycles 1-3), five buffer injections (cycle 4), five nMpt32 injections (cycle 5), and five recDnaK injections (cycle 6). The overlayed sensorgrams were zoomed in to show the classic single-cycle kinetics binding shape. The data presented on the sensorgrams are normalized to the Fc-1 reference channel: Fc2-1, the reference channel data (Fc-1) subtracted from the BSA ligand channel data (Fc-2).

Here we saw that we could qualitatively determine that the recDnaK protein bound BSA and it did so in a concentration dependent manner. The concentrations are indicated on the sensorgram. As the concentration increased, so did the response of the binding between analyte (recDnaK) and ligand (BSA). We also observed that the nMpt32 response stayed stagnant and at baseline (with buffer only injections). This indicated that the nMpt32 analyte did not bind to the BSA ligand. This analyte was injected prior to the recDnaK analyte to act as an internal negative control. Therefore, these results helped support our hypothesis that the chaperone protein recDnaK was binding non-specifically to the BSA block.

This reflected the trend we saw in the sandwich ELISAs. nMpt32 antigen did not bind to the BSA block and did not give a high background signal for the NO PAB negative control. Whereas recDnaK antigen did bind the BSA block and thus, increased the background signal of the NO PAB negative control.

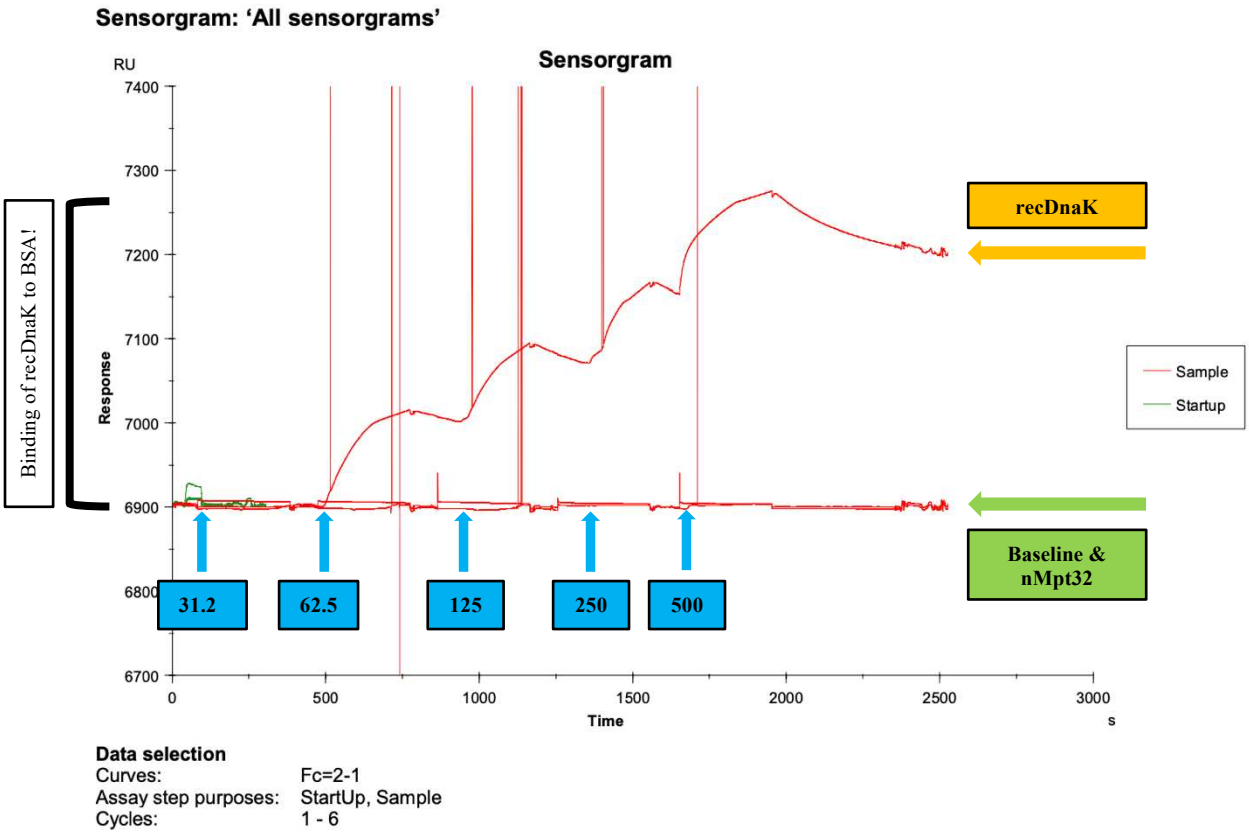

Figure 31: Sensorgrams from Single-Cycle Kinetics Run (Overlay of all 6 cycles – startup, buffer, nMpt32, and recDnaK)
Single-cycle kinetics sensorgram results data. All cycle sensorgrams (including startup, (PBST) buffer only injections, nMpt32 injections, and recDnaK injections) are overlayed. Blue arrows indicate injection of the different analyte concentrations. The corresponding analyte concentration (nanomolar, nM) are indicated in the blue boxes under the appropriate arrows (31.25, 62.5, 125, 250, & 500). The green arrow and corresponding box indicate the baseline (PBST buffer only) and the nMpt32 response lines. The orange arrow and corresponding box indicate the recDnaK response line.

3.3.3 Direct-Biotinylated ELISA Trials

3.3.3.1 Optimization of the Direct-Biotinylated ELISA Using DnaK

The sandwich ELISA trials for all three antigens demonstrated that the sandwich ELISA type was not ideal for the chaperone proteins, due their binding to BSA. Therefore, a direct ELISA, using the purified, biotinylated MABs (from here recognized as "direct-biotinylated ELISA") was attempted. Coating the antigen would allow for more adsorption of the antigen directly onto the microplate. Therefore, more antigen would be "captured" and we should see an

increase in “sample” signal and a decrease in background noise. Even though there still could be non-specific binding interactions between the chaperone protein antigens and the BSA protein block, the increase in successful antigen bound may help increase the *sample: background noise* ratios. Finally, less reagents used in an ELISA assay means less opportunities for non-specific interactions to occur between multiple reagents.

The direct-biotinylated ELISA utilized similar negative controls as those for the sandwich ELISA. Table 2 includes the different negative controls used for the direct-biotinylated ELISA. The direct-biotinylated ELISAs were all performed with a 3%BSA/PBST blocking solution only. However, for the blocking trials, we tested three different diluents: PBST, 2%BSA/PBST, and 2%Milk/PBST. The blocking trials for the direct-biotinylated ELISA were only performed using recDnaK. These trials were labeled as “blocking trials” to differentiate between the LOD trials.

Table 2: Negative Controls for Direct-Biotinylated ELISA
Y indicates that a particular reagent was added. **N (Diluent)** indicates that a particular reagent was NOT added and instead, the diluent (specific for trial) was incubated in lieu of that reagent. *All negative controls received the chemiluminescent substrate.*

**Note: CB = coating buffer*

Negative Control	CB*	Antigen	Block	MAB	Strep-HRP Conjugate
NO AG	**Y**	**N (only CB)**	**Y**	**Y**	**Y**
NO MAB	**Y**	**Y**	**Y**	**N (Diluent)**	**Y**
Block (only)	**Y**	**N (only CB)**	**Y**	**N (Diluent)**	**Y**
PBST (only)	**Y**	**N (only CB)**	**N (PBST only)**	**N (PBST only)**	**N (PBST only)**

The first blocking trial we performed using the direct-biotinylated ELISA, the MAB dilutions were too concentrated. Once the chemiluminescent substrate was added, a dark brown color was produced. Figure 47, A (*Appendix*) shows the layout for this first trial and Figure 47, B (*Appendix*) shows an image of the microplate taken after the microplate was read. At first, we thought this could have been due to too much strep-HRP enzyme, as this can cause the "oxidized and inactive portion" of the HRP enzyme to appear as a brown color on Western blots [163]. We thought that this same phenomenon could have been translated to the ELISA platform. However, when we looked at the NO MAB negative control (for all diluents), there was no color change. Therefore, we attributed the dark brown color to possibly a too concentrated dilution of the biotinylated MAB. We also observed a titration of the dark brown color for the "sample" as the MAB was diluted.

Therefore, for the second blocking trial using the direct-biotinylated ELISA for recDnaK, we diluted the MAB further. We also changed some of the microplate reader program parameters. We first read the plate with the normal parameters (standard dynamic range, 1 s reads per well), but all the "samples" were in OVRFLW. We then re-read the plate and changed the signal output to include an "extended dynamic range" with reads at 20 ms per well. The extended dynamic range allowed us to capture the signal output values ≤ 5,800,000 RLUs. The

quicker (20 ms) reads per well allowed us to capture intense signal outputs, as the sensor was not saturated with light as it would have been at 1 s reads per well.

Figure 32 depicts the results from the second direct-biotinylated ELISA blocking trial for recDnaK. Even though the NO AG negative control signals were graphed, they were so low in comparison to the "sample" signals that they were not visible. The way the graph is set up demonstrates a large *sample: background noise* ratio. The graph also clearly demonstrates the proportionate decrease of the "sample" signal as the MAB was diluted further. Figure 32 demonstrates how sensitive this direct-biotinylated ELISA was, with a signal of ~1.3 million RLUs for the lowest dilution of the MAB of 1:160,000 (for all three diluents). We also did not see a stark difference between the diluent types when looking at the "sample" signals. This was different than what we observed with the sandwich ELISA type where there was a discrepancy between the diluents. The 1:160,000 MAB dilution was the only dilution with clear "sample" wells on the microplate. Figure 48, A (*Appendix*) shows the layout for this second trial and Figure 48, B (*Appendix*) shows an image of the microplate taken after the microplate was read. There may have been a *slight* yellowing of the wells for the 2%BSA/PBST and PBST diluents. However, this dilution was used for a subsequent LOD trial. The NO MAB negative control wells were clear for all diluents (*Appendix: Figure 48, B*).

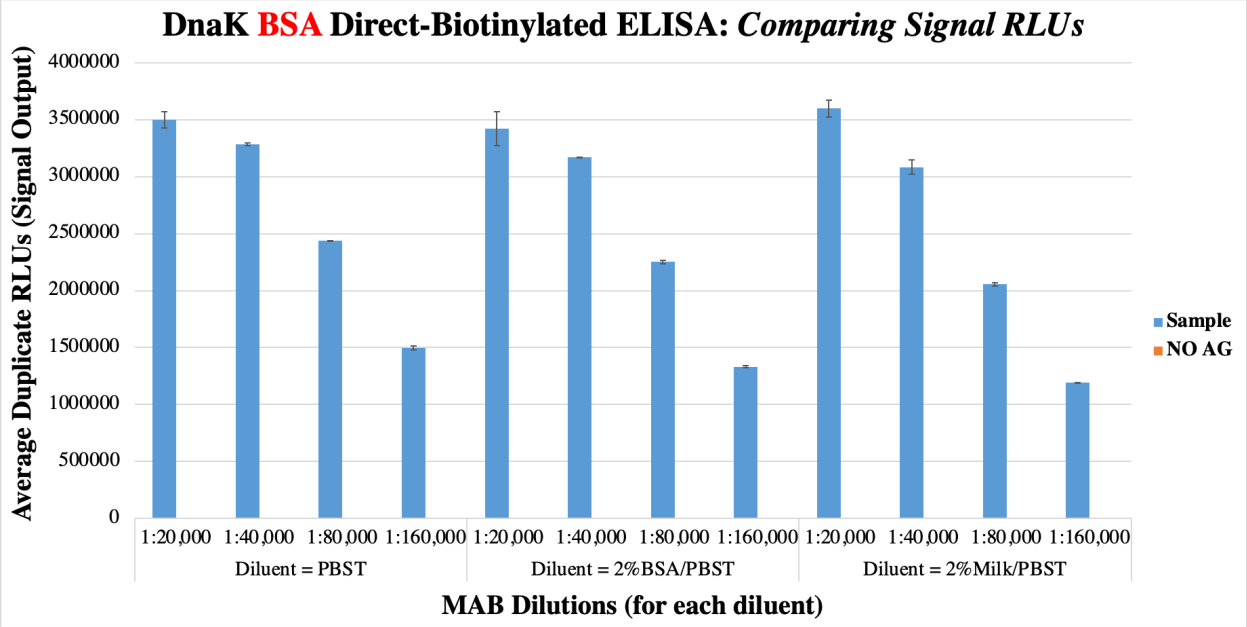

Figure 32: DnaK BSA Direct-Biotinylated ELISA Blocking Trial (#2) *Comparing Signal RLUs*

Direct-biotinylated ELISA blocking trial #2 for recDnaK. The averaged duplicate signal output values in RLUs for the "sample" (blue) and the NO AG negative control (orange) are graphed on the *Y-axis*. The MAB dilutions are graphed on the *X-axis*. The entire microplate was blocked with a 3%BSA (in PBST) blocking solution. PBST, 2%BSA/PBST, and 2%Milk/PBST were used as the "standard diluents". The diluents are labeled appropriately under each group of four MAB dilutions. A serial 1:2 dilution series (starting at 1:10,000) was performed for the MAB (purified, biotinylated DnaK Clone A) dilutions (1:20,000, 1:40,000, 1:80,000, and 1:160,000) in all three diluent types. The strep-HRP conjugate was diluted at a final concentration of 2 µg/mL in PBST, 0.4%BSA/PBST, and 0.4%Milk/PBST diluents (corresponding to respective "standard diluent" type). Only the first read (20 ms) data was used for graph.

3.3.3.2 Direct-Biotinylated Limit of Detection ELISA Trials (For All Antigens)

The first LOD, with the MAB at a dilution of 1:160,000, had a sensitivity of 10 ng/mL (*Appendix: Figure 49*). However, this trial produced a poor linear curve with a 1:10 serial dilution series of recDnaK (*Appendix: Figure 49*). A polynomial curve fit the data better for this trial, but regression analysis was not performed. Another checkerboard titration assay was attempted with more concentrated MAB dilutions and a 1:2 serial dilution series of recDnaK (*Appendix: Figure 50*), Most of the "sample" signals were in OVRFLW and the recDnaK

antigen concentration was too high (~ 3,220,000 RLUs for the last antigen concentration) (*Appendix: Figure 50*).

Therefore, for the third and final LOD trial for recDnaK, a checkerboard titration assay was performed with even more concentrated MAB dilutions and even more dilute recDnaK antigen concentrations. Figure 33 (Graphs A and B) demonstrates the "sample" signals for the 1:1,000 MAB dilution only. This MAB dilution was chosen for the detection of the lowest concentration of antigen (*Appendix: Table 6*). The recDnaK antigen concentrations were diluted using a 1:2 dilution series.

Figure 33 (Graph A) demonstrates a high degree of linearity with an R-squared value of 0.9943. However, the lower data points created an irregular curve prior to the linear portion of the data (highlighted in the green box in Figure 33, Graph B). Figure 33, Graph B demonstrates a polynomial trendline. This DnaK LOD trial would need to be repeated to determine if 1) this irregular curve persisted and 2) a polynomial regression model would be the best fit for these data. Thus, the data points within the irregularly curved area of the graph for this LOD trial were inaccurate data and a regression model for the polynomial trendline was not calculated. Since the linear portion of the data was above the LOD, a linear regression model could be used for these data. The linear regression model was then used for determination of the LOD and LOQ for the DnaK antigen.

For this trial, a readable signal at 1.2207 ng/mL of the recDnaK antigen was detected (*Appendix: Table 6*). This was the lowest concentration that had a signal above background noise (NO AG). The calculated LOD for this trial was 6.310 ng/mL and the LOQ was 21.032 ng/mL (Table 3).

A. Linear Trendline

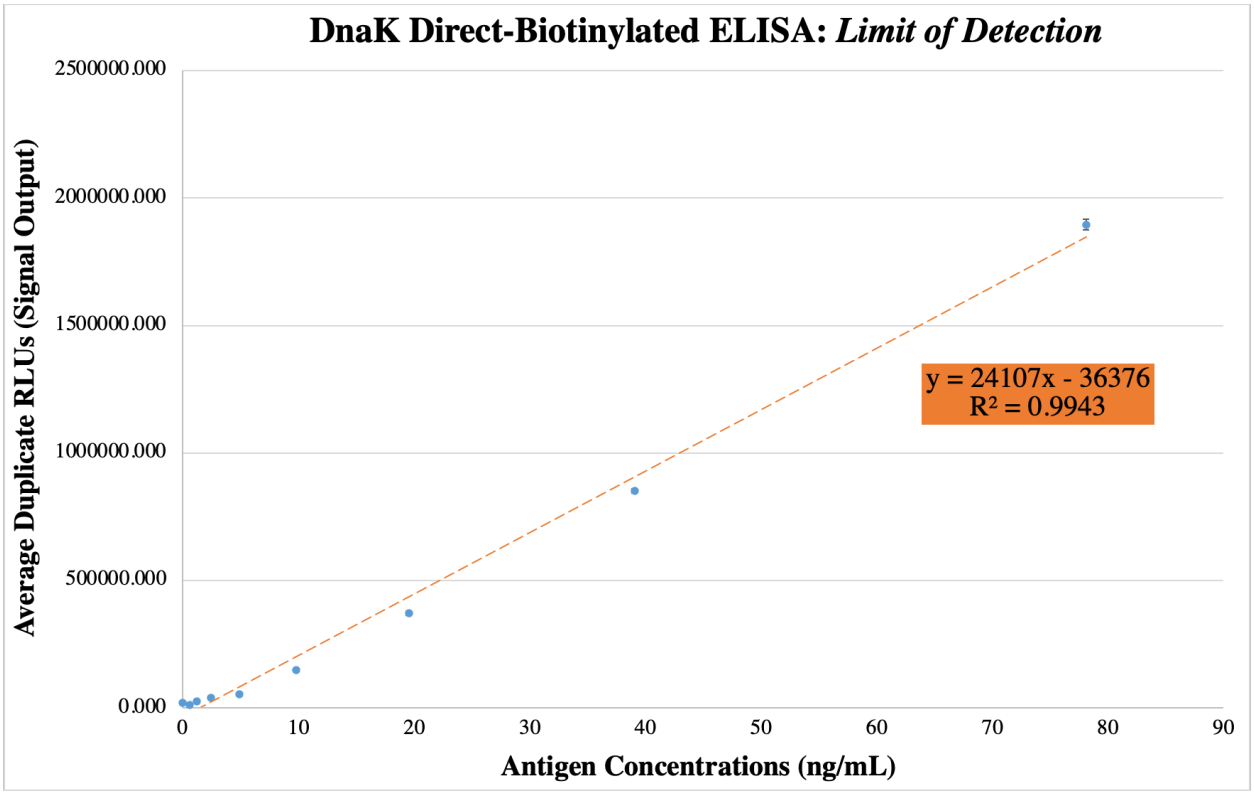

B. Polynomial Trendline

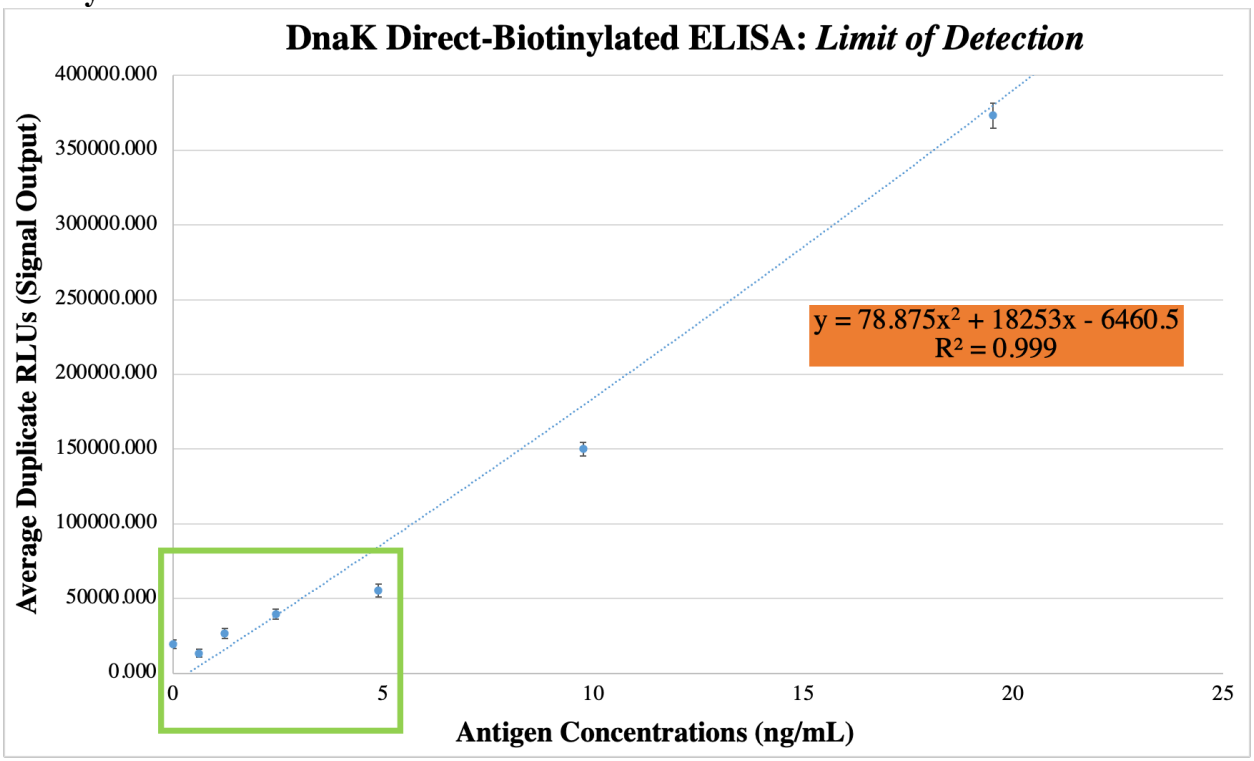

Figure 33: DnaK Direct-Biotinylated ELISA LOD Trial (#3)

Direct-biotinylated ELISA LOD trial (#3) for recDnaK. The average duplicate RLU signal output values for the "sample" (for MAB dilution at 1:1,000 only) are graphed on the *Y-axis*. The recDnaK antigen concentrations are graphed on the *X-axis* in ng/mL. **Graph A)** a linear trendline was added and **Graph B)** a polynomial trendline was added and the lower antigen concentration data points were zoomed in on, as highlighted in the green box. The recDnaK antigen was diluted in coating buffer using a 1:2 serial dilution series, starting at 78.125 ng/mL. The entire microplate was blocked with a 3%BSA (in PBST) blocking solution. 2%BSA/PBST was used as the "standard diluent". The MAB (purified, biotinylated DnaK Clone A) was diluted in the "standard diluent". The strep-HRP conjugate was diluted at a final concentration of 2 µg/mL in 0.4%BSA/PBST diluent. Only the first read (20 ms) data was used for graph.

Table 3: LOD & LOQ of Direct-Biotinylated ELISA for DnaK
Calculated LOD and LOQ values for DnaK direct-biotinylated ELISA. Data were taken from **Graph A** only and calculated with a linear regression model. Final values are expressed in ng/mL. The equations, standard errors (from linear regression), and slope (from graph equation) are given.

DnaK Direct-Biotinylated ELISA LOD & LOQ			
Equation	**Standard Error (SE)**	**Slope**	**Value (ng/mL)**
LOD = (SE/Slope)*3	50701.620	24107.000	6.310
LOQ = (SE/Slope)*10	50701.620	24107.000	21.032

For Mpt32, we performed the same LOD checkerboard titration assay as DnaK (trial #3). Figure 34 demonstrates the "sample" signals for the 1:1,000 MAB dilution only. This MAB dilution was chosen for the detection of the lowest concentration of antigen (*Appendix: Table 7*). The nMpt32 antigen concentrations were diluted using a 1:2 dilution series. Figure 34 also demonstrates a high degree of linearity with and R-squared value of 0.9995.

For this trial, a readable signal at 0.61035 ng/mL of the nMpt32 antigen was detected. However, considering the NO AG negative control signal was so low (145 RLUs) (*Appendix: Table 7),* a lower antigen dilution could have theoretically been attempted to see if the LOD decreased further. The calculated LOD of this trial was 1.884 ng/mL and the LOQ was 6.278 ng/mL (Table 4). It seems this direct-biotinylated ELISA platform performed better for the nMpt32 antigen than the recDnaK antigen.

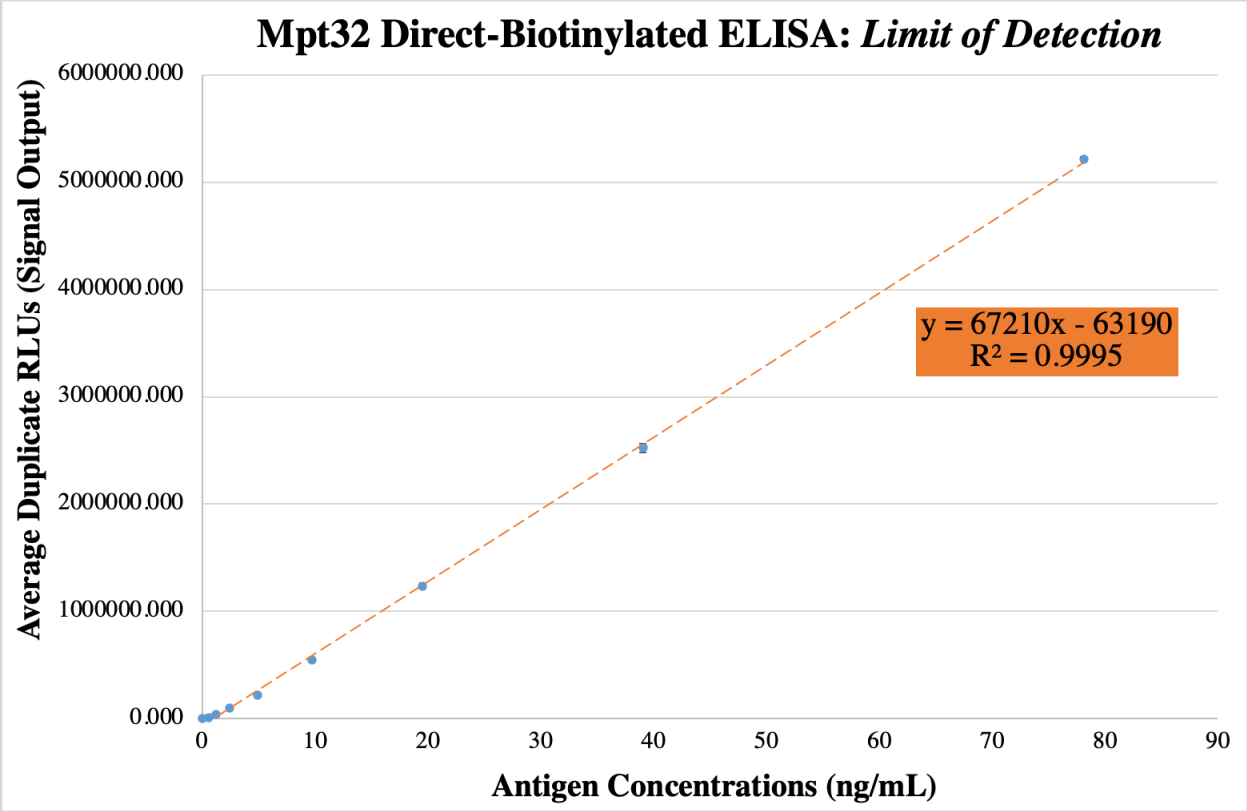

Figure 34: Mpt32 Direct-Biotinylated ELISA LOD Trial #1
Direct-biotinylated ELISA LOD trial for nMpt32. The average duplicate RLU signal output values for the "sample" (for MAB dilution at 1:1,000 only) are graphed on the *Y-axis*. The nMpt32 antigen concentrations are graphed on the *X-axis* in ng/mL. The nMpt32 antigen was diluted in coating buffer using a 1:2 serial dilution series, starting at 78.125 ng/mL. The entire plate was blocked with a 3%BSA (in PBST) blocking solution. 2%BSA/PBST was used as the "standard diluent". The MAB (purified, biotinylated Mpt32 Clone B, "wash 3") was diluted in the "standard diluent". The strep-HRP conjugate was diluted at a final concentration of 2 µg/mL in 0.4%BSA/PBST diluent. Only the first read (20 ms) data was used for graph.

Table 4: LOD & LOQ of Direct-Biotinylated ELISA for Mpt32
Calculated LOD and LOQ values for Mpt32 direct-biotinylated ELISA. Final values are expressed in ng/mL. The equations, standard errors (from linear regression), and slope (from graph equation) are given.

Mpt32 Direct-Biotinylated ELISA LOD & LOQ			
Equation	**Standard Error (SE)**	**Slope**	**Value (ng/mL)**
LOD = (SE/Slope)*3	42197.357	67210.000	1.884
LOQ = (SE/Slope)*10	42197.357	67210.000	6.278

For GroES, we performed the same LOD checkerboard titration assay as DnaK (trial #3). Figure 35 demonstrates the "sample" signals for the 1:1,000 MAB dilution only. This MAB dilution was chosen for the detection of the lowest concentration of antigen (*Appendix: Table 8*).

The nGroES antigen concentrations were diluted using a 1:2 dilution series. Figure 35 also demonstrates a high degree of linearity with an R-squared value of 0.9995.

For this trial, a readable signal at 0.61035 ng/mL of the nGroES antigen was detected. However, considering the NO AG negative control signal was so low (~3,000 RLUs), (*Appendix: Table 8*), a lower antigen dilution could have theoretically been attempted to see if the LOD decreased further. The calculated LOD for this trial was 1.959 ng/mL and the LOQ was 6.531 ng/mL (Table 5). It seems this direct-biotinylated ELISA platform performed better for the nGroES antigen than the recDnaK antigen but about the same as the nMpt32 antigen**.**

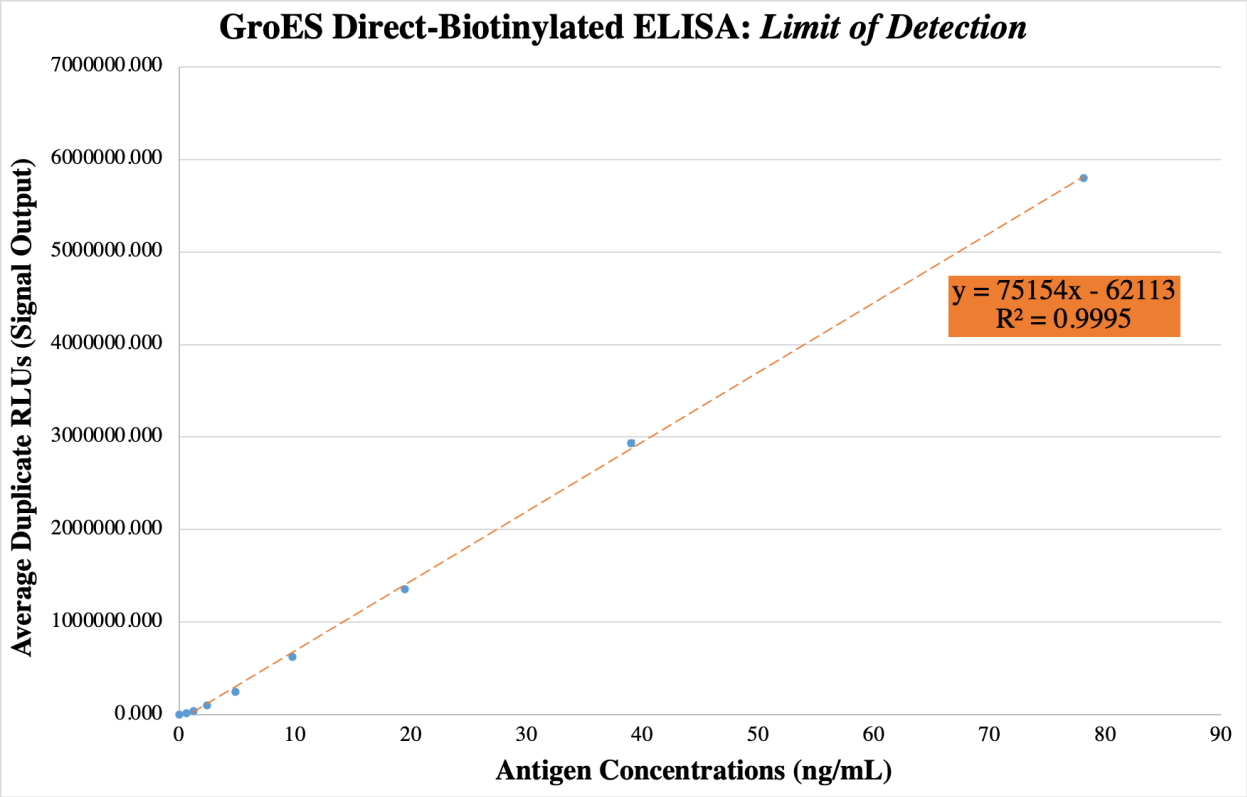

Figure 35: GroES Direct-Biotinylated ELISA LOD Trial #1
Direct-biotinylated ELISA LOD trial for nGroES. The average duplicate RLU signal output values for the "sample" (for MAB dilution at 1:1,000 only) are graphed on the *Y-axis*. The nGroES antigen concentrations are graphed on the *X-axis* in ng/mL. The nGroES antigen was diluted in coating buffer using a 1:2 serial dilution series, starting at 78.125 ng/mL. The entire plate was blocked with a 3%BSA (in PBST) blocking solution. 2%BSA/PBST was used as the "standard diluent". The MAB (purified, biotinylated α-GroES, SA-12) was diluted in the "standard diluent". The strep-HRP conjugate was diluted at a final concentration of 2 µg/mL in 0.4%BSA/PBST diluent. Only the first read (20 ms) data was used for graph.

Table 5: LOD & LOQ of Direct-Biotinylated ELISA for GroES
Calculated LOD and LOQ values for nGroES direct-biotinylated ELISA. Final values are expressed in ng/mL. The equations, standard errors (from linear regression), and slope (from graph equation) are given.

GroES Direct-Biotinylated ELISA LOD & LOQ			
Equation	**Standard Error (SE)**	**Slope**	**Value (ng/mL)**
LOD = (SE/Slope)*3	49079.794	75154.000	1.959
LOQ = (SE/Slope)*10	49079.794	75154.000	6.531

3.4 Conclusions

3.4.1 Direct-Biotinylated ELISA Assay Sensitivity

The LOD trials using the direct-biotinylated ELISA platform demonstrated a highly sensitive assay for all three antigens. Literature is very limited for direct-biotinylated ELISA assay detection limits and ranges. However, one study developed a chemiluminescent direct ELISA that was able to reach an LOD of 0.5 ng/mL [164]. The setup differed from ours as they plated serum antibodies as their "antigen" of interest [164]. However, this study demonstrates how sensitive a simpler ELISA format can be. The LOD results from our study were slightly less sensitive in comparison, with LODs of ~ 2 ng/mL for both Mpt32 and GroES and ~ 6 ng/mL for DnaK direct-biotinylated ELISAs. However, we demonstrated that this type of ELISA with a biotin-strep-HRP conjugate complex and a chemiluminescent substrate can be very sensitive, which is a promising feat.

The nMpt32 and nGroES antigens produced a more sensitive assay than recDnaK, although all had LOD values < 10 ng/mL. The LOQs for Mpt32 and GroES demonstrated that the "reliable detection" [157] of these two antigens for this direct ELISA platform was more sensitive and could detect lower concentrations of antigen. The LOQ for DnaK was a little more than three times higher than the LOQs of Mpt32 and GroES. However, an LOQ of 21.032 ng/mL on a direct-biotinylated ELISA assay is still sensitive.

We demonstrated that the purification and biotinylation methods for the monoclonal antibodies produced a high-quality reagent that aided in increasing ELISA assay sensitivity. The resultant of the development and production of highly specific MAB reagents to detect *Mtb* polypeptides was the subsequent development of an ultrasensitive direct-biotinylated ELISA. This direct-biotinylated ELISA helped circumvent the non-specific binding interactions of the chaperone proteins and the BSA block whilst still maintaining a highly sensitive assay. We were able to lower the background noise levels and produce relatively high sample signals (when compared to the NO AG negative controls). Thus, we demonstrated successful development and optimization of this direct-biotinylated ELISA platform for these three antigens.

3.4.2 SPR Analysis Using the Biacore Instrument

The Biacore system is based on surface plasmon resonance (SPR) technology. This can be used to characterize binding interactions among a ligand and an analyte, including protein-protein interactions [165]. The Biacore is the instrument that is used to measure this SPR phenomenon [165].

Kinetics data was not extrapolated due to the need for further optimization of the ligand and analytes. The 1:1 binding fit model (surface bound) indicated a poor fit for both analytes (data not shown) for the single-cycle kinetics method. One of the most important indicators for calculating accurate kinetics data, the Chi-squared value, determines "the quality of fit" for the "experimental data" compared to the software algorithm analyses [166]. The experimental data indicated a Chi-squared value of 95 (RU^2) for nMpt32 analyte and 199 (RU^2) for recDnaK analyte. It is recommended the Chi-squared value be < 10 (Ru^2) [166].

The binding level of recDnaK was also low (413 RU) compared to how much BSA ligand was immobilized (8,266.4 RU). The amount of ligand bound originally was also too much

to calculate accurate kinetics data and led to inaccurate readings from inappropriate analyte interactions with the surface [166,167]. There were high bulk contributions for both analytes, which has to do with the difference in composition of the running buffer and analyte buffer [168]. The analytes were originally in 1X PBS (without Tween®20) but such a small volume was used to create the analyte solutions. Therefore, it is possible the Tween®20 in the running buffer added to these bulk contributions.

Even though kinetics data could not be extrapolated from this run, the data, as previously mentioned, still qualitatively demonstrated the binding of the recDnaK analyte to the BSA ligand. This qualitative data helped support what was observed in the sandwich ELISAs between the recDnaK antigen and the BSA block. Further optimization of these Biacore methods is needed to determine binding kinetics between recDnaK with BSA, as well as to look at binding interactions of nGroES and BSA.

3.4.3 Other Considerations for ELISA Optimization

The sandwich ELISA failed to produce reliable, reproducible results. The high background noise from the NO PAB negative control created a problem within the assay that was difficult to resolve for the chaperone proteins. Therefore, we were unable to fully optimize this ELISA type and in turn, were not able to determine the sensitivity of this assay (LOD & LOQ). The trials performed for the sandwich ELISA demonstrated the difficulty in designing and developing an assay, even one as "simple" as an ELISA. This sandwich ELISA, if used in the future, would need further, extensive optimization.

The trials described in *sections 3.3.1 Sandwich ELISA Trials* and *3.3.3 Direct-Biotinylated ELISA Trials* demonstrated how difficult it is to develop an ELISA assay. Fine tuning the ELISA system requires optimal pairing of reagents to create a highly reproducible

assay. However, the ELISA may need to be optimized to a certain antigen, which can cause problems in different ELISA assay types (sandwich versus direct), as demonstrated in this chapter. The background problem could be amplified with the addition of complex samples like serum or serum EVs. The trials presented in this chapter are not an exhaustive list of all the trials performed. Other optimization trials included dialyzed milk as a blocking solution and diluent, different strep-HRP conjugate dilutions, different washing steps between blocking and antigen incubations, higher salt PBST as the diluent (2X), incubation parameters (time and temperature), cross-contamination, and other milk blocking trials. These trials did not directly pertain to the story told so are not detailed here; however, they demonstrated the complex process of trial and error of designing and developing an ELISA assay.

[1]

[1] The Biacore instrument includes a liquid flow and injection system (for buffers and samples, respectively), a gold-plated sensor chip, a light source, and a monitoring system [165]. There are four flow cells (Fc) within each sensor chip. The glass plate within each sensor chip is coated on one side with "a gold film" [165]. A chip-specific matrix is then applied to the gold-coated side of the sensor chip [165]. The Biacore system defines the ligand as the molecule of choice that is bound to the matrix on the surface of the chip. The Series S CM5 sensor chip was used. This chip includes a matrix of "carboxymethylated dextran" to aid in the immobilization of proteaceous ligands via covalent bonds [162]. The dextran matrix also aids in ligand-analyte interactions by "provid[ing] a hydrophilic environment" [162].

On the opposite side of the glass plate, a light source is directed through a prism and is reflected at a specific angle after reaching the glass plate [169,170]. The light source excites the electrons within the gold film which subsequently begin to move in a wave-like pattern across the gold film [171]. This wave of electrons is referred to as the "plasmon" in the SPR [169,170]. This directed light is partially absorbed in the plasmon but some of it is reflected [169,170]. There is a "dip" in reflected light intensity as the light is lost to the plasmon (Nguyen et al., 2015). This specific angle of reflection is known as the SPR angle [171]. The change in SPR angle is a reflection of what is occurring on the opposite side (gold-plated) of the glass plate. The refractive index of a molecule binding on the surface influences the SPR angle [169,170]. In other words, as an analyte passes through the flow cell and binds to the ligand, the increase in mass at the surface of the plate increases the SPR angle [171]. The detector picks up on the change of SPR angle as molecules interact and the change is measured in response units (RU) [173]. A sensorgram is used to depict the change in SPR angle versus time [172]. A "baseline" SPR angle is created (with ligand immobilized and buffer running through) [172] this is also known as the "starting critical angle" [173].

The sensorgram then depicts different phases of the ligand-analyte interactions. The association phase depicts the interaction of the ligand and analyte [168]. An equilibrium phase is encountered when the analyte concentration saturates the system [172]. When the analyte ceases to be injected (only buffer), the dissociation phase begins and a loss of mass on the gold side of the plate creates a decrease in SPR angle, which is reflected in the sensorgram [172]. Regeneration of the surface can be performed to remove any leftover analyte bound to the ligand [172].

CHAPTER FOUR: FUTURE DIRECTIONS & CONCLUDING REMARKS

4.1 Study Summary

Diagnostic tests for TB have fallen short in differentially diagnosing active TB and LTBI. The current TST and IGRA tests for LTBI only provide a tentative diagnosis. However, with the advancement in different molecular technologies, there has been an outpouring of research dedicated to biomarker discovery. Biomarker discovery not only allows researchers to identify and characterize host-derived and pathogen-derived products that are produced during *Mtb* infection, but it also allows for the possibility of creating highly specific and sensitive diagnostic tools. Especially where diagnostic tests are lacking for LTBI, biomarker discovery could aid in fewer miss-diagnoses as well as aid in creating diagnostics with higher positive predicative values [9] for the progression of LTBI to the active phase of disease. Discovery of pathogen-specific biomarkers for TB diagnosis is complicated by the fact that host-derived serum proteins are in an overabundance [174,88,51] compared to pathogen-derived proteins [51]. However, sensitive technologies like mass spectrometry have allowed for the identification of "low abundance" pathogen-specific proteins in purified serum EVs [92]. Concentration of potential *Mtb* biomarkers using different purification methods provides an opportunity to detect hidden protein signatures [92] that could aid in identification of certain subclinical states of TB. As previously mentioned, these highly sensitive technologies are great for the biomarker discovery phase but fall short for implementation as feasible diagnostic tests in resource-limited areas.

Here, we have attempted to combine sensitive technologies that identified potential biomarker candidates for LTBI with a simple diagnostic ELISA platform. This proof-of-concept study allowed us to create a highly sensitive ELISA that could potentially be used as a POC diagnostic for LTBI. Although sandwich ELISAs are generally thought to be the more specific

and sensitive of the ELISA types [98], we demonstrated that this type of ELISA can be complicated by high background from reagent incompatibility. We also demonstrated that the function of the antigens, in this case, chaperones, could affect assay development and performance.

The addition of a more complex fluid, like serum EVs, could complicate the sandwich ELISA by further increasing the background noise. Thus, distinguishing between low abundance pathogen-specific protein biomarkers, complex serum matrix background, and assay background may be a challenge. These assay complications were highlighted in our studies (Chapter 3). To circumvent the high assay background that was observed in the sandwich ELISA trials, we chose to attempt a simpler ELISA type. We demonstrated that by purifying and biotinylating the monoclonal antibodies in tandem with a streptavidin-HRP system using a chemiluminescent substrate, we were able to ultimately create a highly sensitive direct-biotinylated ELISA against purified *Mtb* recombinant and native proteins.

This chapter will highlight some of the future directions for this project.

4.2 Serum EVs

One future direction for this study includes testing the optimized ultrasensitive direct-biotinylated ELISA on purified serum EV samples from individuals with active TB and LTBI, as well as healthy donor controls. This would allow us to determine if the ultrasensitive ELISA could not only detect pathogen-specific protein biomarkers but also differentiate between disease states and healthy controls. Before testing the direct-biotinylated ELISA on serum EV samples from individuals with active TB and LTBI, we would first want to determine if comparable LODs and LOQs are found when the *Mtb* antigens are spiked into a more complex matrix (such as serum from healthy donors).

We would also like to compare sensitivity of the fully optimized ELISA to the MRM-MS methods. Previously, our lab determined that the MRM-MS methods used could detect "low femtomolar range…of mycobacterial products in serum" [92]. Even though it is unlikely the chemiluminescent ELISA could be as sensitive as a targeted mass spectrometry method, comparing these two methods is the first step in evaluating the ELISA as a point-of-care tool.

4.3 POC Implementation

If we are able to detect these three protein signatures using serum EVs on the developed ELISA, we would need to further optimize the ELISA so that it could be implemented in resource-limited settings. Some settings may not have access to expensive microplate readers. Therefore, we would need to look for alternative technology to read the ELISA. There has been recent work by Bergua et al. to provide a "portable plate reader" that utilizes "cheaper" alternatives to the microplate reader design, detection materials, and software [175]. These devices incorporated everything a researcher would need for a typical ELISA: plate space, smartphone for signal detection, and a motor for orbital shaking [175]. These devices provided "comparable sensitivity" for colorimetric ELISAs performed in a microplate reader [175]. Bergua et al. did not test their devices on chemiluminescent substrates but did for fluorescence [175]. Bergua et al. was able to develop these devices for under $300 [175]. This could be an interesting device for comparative studies with a microplate reader for chemiluminescent substrates. This highlights a promising development for the implementation of some of these higher costing, highly sought-after immunoassays as POC tools.

Another technology that has been implemented at the POC is the lateral flow assay (LFA). LFAs are "…the cheapest, fastest, and easiest to use paper-based POC tests" [176,173,177–180]. An LFA can be utilized for many different "sample types" [178]. There are a couple of different

setups for the LFA, but in general, a sample moves through different sections of the LFA via "capillary action" [178]. Each section (pads and membranes) provides manipulation of the sample with other reagents for capture and detection [179]. A positive control is added at the end of the LFA to capture excess "labeled detector" reagents for "assay validation" [176]. Even though the setup and cost of LFAs are enticing, the "sensitivity and specificity" of these tests can often be subpar when compared to traditional (more expensive) assays [180]. However, researchers are attempting to circumvent these issues through the use of better detection reagents [178], "sample pre-enrichment" [180], and different LFA readers for different detection schemes [179] . Overall, LFAs show promise as low cost, low-tech POC tools. The reagents produced in our study could potentially be utilized in this type of LFA platform as an alternative to the ELISA platform for a POC diagnostic.

The other technical problem for the potential POC diagnostic ELISA would be determining the best method for serum EV purification. In previous studies from our lab, centrifugation and Exoquick (Systems Biosciences, Inc., Mountain View, CA) were utilized for serum EV purification [51,86,92]. However, the high cost of a centrifuge alone is a glaring problem. Therefore, other methods of serum EV purification need to be discovered or optimized before implementing the ELISA as a POC diagnostic as to limit the amount of materials needed for the serum purification as well as the cost of expensive laboratory equipment.

4.4 The GlnA Challenge

Another future direction would be to successfully purify native (n) GlnA. Since GlnA was the top protein identified in serum EVs of individuals with LTBI in the Mehaffy et al., 2020 study, creating a better antigen (nGlnA) and a high-affinity MAB is of interest [86]. These results indicate that GlnA is a potential target for differential "diagnosis of LTBI" [86]. Therefore,

developing an ultrasensitive ELISA for nGlnA could produce a POC diagnostic specific for LTBI.

GlnA has been detected (proteomic analyses) in the whole cell lysate (and subcellular fractions) as well as the culture filtrates of *Mtb* [181]. Therefore, an appropriate starting material with the highest concentration of nGlnA protein would need to be determined first. From here, we could look at fractionation methods to enrich for nGlnA. These fractions could be created using high speed centrifugation, ammonium sulfate precipitation, high-performance liquid chromatography (HPLC) columns, or a combination of all.

We attempted and failed to replicate nGlnA purification using a protocol from Harth et al., 1994 [152]. This protocol utilized ammonium sulfate precipitation, ion exchange chromatography (DEAE-Sepharose CL-6B), covalent chromatography (thiopropyl-Sepharose6B) [182], and size exclusion chromatography (Sepharose 6B), respectively [152]. It would be better to eliminate multiple different types of chromatography, due to the potential loss of product, especially if starting concentration of the native protein is low. This purification of the native protein would be beneficial for two reasons: 1) the recombinant GlnA reagent used had gone through denaturation steps to remove the protein from possible inclusion bodies in the *E. coli* production model and so eliminating the need to use this recombinant protein system would remove this problem (data not shown) and 2) the recombinant protein had many different subunit or breakdown products, which is not ideal for antibody production.

The successful purification of nGlnA would allow us to then create a MAB specific to the native version of this protein. We could immunize the mice with the native version, create stable hybridoma cell lines that produce highly reactive antibodies to the native protein, as well as develop ELISAs that utilize a folded protein. We could also look at utilizing recombinant

antibody technology to create "highly specific" antibodies to the native protein [183]. We could use phage display libraries, mammalian cells to generate different fragmented antibodies [183,184] or other "expression systems" to generate recombinant antibodies [184,185]. Recombinant antibody technology may offer more benefits than using hybridoma technology. For one, hybridoma generation takes a couple of months from the beginning of immunizations to the establishment of stable hybridoma cell lines. There are also suggestions that hybridoma-generated MABs offer "low-affinity in conventional assays" [184]. Therefore, exploring new technologies may aid in increasing antibody affinities [184].

4.5 Mpt32 Sandwich ELISA

A final future goal would be to determine and resolve the problem surrounding the Mpt32 sandwich ELISA. Since Mpt32 showed a different trend than what was observed with the chaperone proteins, we attempted a few other trials to resolve this problem. These trials included using less concentrated MAB dilutions, testing different diluents, utilizing a more reactive PAB serum batch (from production bleed #3 for rabbit R2) against nMpt32, and utilizing the purified R2-1 PAB serum. However, most of them were not successful and demonstrated the need for more extensive optimization of the sandwich ELISA for the nMpt32 antigen.

4.6 Concluding Thoughts

We were able to design and develop an ultrasensitive direct-biotinylated ELISA for the detection of purified *Mtb* proteins. Further, we demonstrated that the function of the antigen target (i.e., chaperone) can interfere with the development of a sandwich ELISA. The future directions of this project could pave a way to the creation of a potential POC diagnostic for LTBI. This potential POC diagnostic ELISA could not only help identify certain *Mtb* protein biomarkers in serum EV samples and differentially diagnose LTBI from active TB, but it could

also provide a low-cost, low-tech, highly accessible tool for areas where resources are limited. However, as with all diagnostic tests, there are many mountains to climb before a highly sensitive and highly reproducible product can be provided. The ultimate goal of this study and subsequent master's thesis was to provide a possible diagnostic tool to aid in the eradication of TB. No step is too small when it comes to ending a truly devastating disease.

REFERENCES

1. Global Tuberculosis Report 2021. Published online 2021. https://www.who.int/publications/i/item/9789240037021

2. Jilani TN, Avula A, Gondal AZ, Siddiqui AH. *Active Tuberculosis*. StatPearls Publishing; 2022. https://www.ncbi.nlm.nih.gov/books/NBK513246/

3. Hayward S, Harding RM, McShane H, Tanner R. Factors influencing the higher incidence of tuberculosis among migrants and ethnic minorities in the UK. *F1000Research*. 2018;7:461-461. doi:10.12688/f1000research.14476.2

4. Ogbuoji O, Qi J, Olson ZD, et al. Annual Rates of Decline in Child, Maternal, Tuberculosis, and Noncommunicable Disease Mortality across 109 Low- and Middle-Income Countries from 1990 to 2015. In: *Disease Control Priorities: Improving Health and Reducing Poverty*. 3rd ed. Chapter 5. ; 2017. https://www.ncbi.nlm.nih.gov/books/NBK525288/ doi: 10.1596/978-1-4648-0527-1_ch5

5. Romha G, Gebru G, Asefa A, Mamo G. Epidemiology of Mycobacterium bovis and Mycobacterium tuberculosis in animals: Transmission dynamics and control challenges of zoonotic TB in Ethiopia. *Prev Vet Med*. 2018;158:1-17. doi:10.1016/j.prevetmed.2018.06.012

6. Behr MA, Gagneux S. 24 - The Rise and Fall of the Mycobacterium tuberculosis Complex. In: Tibayrenc M, ed. *Genetics and Evolution of Infectious Disease*. Elsevier; 2011:651-667. doi:10.1016/B978-0-12-384890-1.00024-8

7. Saelens JW, Viswanathan G, Tobin DM. Mycobacterial Evolution Intersects With Host Tolerance. *Front Immunol*. 2019;10. https://www.frontiersin.org/article/10.3389/fimmu.2019.00528

8. Drain Paul K., Bajema Kristina L., Dowdy David, et al. Incipient and Subclinical Tuberculosis: a Clinical Review of Early Stages and Progression of Infection. *Clin Microbiol Rev*. 2018;31(4):e00021-18. doi:10.1128/CMR.00021-18

9. Migliori GB, Ong CWM, Petrone L, D'Ambrosio L, Centis R, Goletti D. The definition of tuberculosis infection based on the spectrum of tuberculosis disease. *Breathe*. 2021;17(3):210079. doi:10.1183/20734735.0079-2021

10. Latent TB Infection and TB Disease. Published online November 11, 2020. https://www.cdc.gov/tb/topic/basics/tbinfectiondisease.htm#:~:text=TB%20bacteria%20become%20active%20if,spend%20time%20with%20every%20day.

11. WHO consolidated guidelines on tuberculosis: tuberculosis preventive treatment. Published online 2020. https://apps.who.int/iris/bitstream/handle/10665/331170/9789240001503-eng.pdf

12. Liu CH, Liu H, Ge B. Innate immunity in tuberculosis: host defense vs pathogen evasion. *Cell Mol Immunol*. 2017;14(12):963-975. doi:10.1038/cmi.2017.88

13. Gengenbacher M, Kaufmann SHE. Mycobacterium tuberculosis: success through dormancy. *FEMS Microbiol Rev*. 2012;36(3):514-532. doi:10.1111/j.1574-6976.2012.00331.x

14. Goletti D, Petruccioli E, Joosten SA, Ottenhoff THM. Tuberculosis Biomarkers: From Diagnosis to Protection. *Infect Dis Rep*. 2016;8(2):6568-6568. doi:10.4081/idr.2016.6568

15. Heemskerk D, Caws M, Marais B, Farrar J. Tuberculosis in Adults and Children. In: Chapter 4, Diagnosis. Springer; 2015. https://www.ncbi.nlm.nih.gov/books/NBK344401/

16. Shin SS, J Seung K. 39 - Tuberculosis. In: Magill AJ, Hill DR, Solomon T, Ryan ET, eds. *Hunter's Tropical Medicine and Emerging Infectious Disease (Ninth Edition)*. W.B. Saunders; 2013:416-432. doi:10.1016/B978-1-4160-4390-4.00039-4

17. Facciuolo A, Mutharia LM. Mycobacterial glycoproteins: a novel subset of vaccine candidates. *Front Cell Infect Microbiol*. 2014;4. https://www.frontiersin.org/article/10.3389/fcimb.2014.00133

18. Maehira Y, Spencer RC. Harmonization of Biosafety and Biosecurity Standards for High-Containment Facilities in Low- and Middle-Income Countries: An Approach From the Perspective of Occupational Safety and Health. *Front Public Health*. 2019;7:249-249. doi:10.3389/fpubh.2019.00249

19. MacGregor-Fairlie M, Wilkinson S, Besra GS, Goldberg Oppenheimer P. Tuberculosis diagnostics: overcoming ancient challenges with modern solutions. *Emerg Top Life Sci*. 2020;4(4):435-448. doi:10.1042/ETLS20200335

20. Helb D, Jones M, Story E, et al. Rapid detection of Mycobacterium tuberculosis and rifampin resistance by use of on-demand, near-patient technology. *J Clin Microbiol*. 2010;48(1):229-237. doi:10.1128/JCM.01463-09

21. Lawn SD, Nicol MP. Xpert® MTB/RIF assay: development, evaluation and implementation of a new rapid molecular diagnostic for tuberculosis and rifampicin resistance. *Future Microbiol*. 2011;6(9):1067-1082. doi:10.2217/fmb.11.84

22. Raja S, Ching J, Xi L, et al. Technology for Automated, Rapid, and Quantitative PCR or Reverse Transcription-PCR Clinical Testing. *Clin Chem*. 2005;51(5):882-890. doi:10.1373/clinchem.2004.046474

23. Diagnostic Standards and Classification of Tuberculosis in Adults and Children. *Am J Respir Crit Care Med*. 2000;161(4 Pt 1):1376-1395.

24. Chegou NN, Heyckendorf J, Walzl G, Lange C, Ruhwald M. Beyond the IFN-γ horizon: biomarkers for immunodiagnosis of infection with Mycobacterium tuberculosis. *Eur Respir J*. 2014;43(5):1472. doi:10.1183/09031936.00151413

25. Kiazyk S, Ball TB. Latent tuberculosis infection: An overview. *Can Commun Dis Rep Releve Mal Transm Au Can*. 2017;43(3-4):62-66. doi:10.14745/ccdr.v43i34a01

26. Lin PL, Flynn JL. Understanding Latent Tuberculosis: A Moving Target. *J Immunol*. 2010;185(1):15. doi:10.4049/jimmunol.0903856

27. Barry CE 3rd, Boshoff HI, Dartois V, et al. The spectrum of latent tuberculosis: rethinking the biology and intervention strategies. *Nat Rev Microbiol*. 2009;7(12):845-855. doi:10.1038/nrmicro2236

28. Schwander S, Dheda K. Human lung immunity against Mycobacterium tuberculosis: insights into pathogenesis and protection. *Am J Respir Crit Care Med*. 2011;183(6):696-707. doi:10.1164/rccm.201006-0963PP

29. Huynh KK, Joshi SA, Brown EJ. A delicate dance: host response to mycobacteria. *Host Pathog Senescence*. 2011;23(4):464-472. doi:10.1016/j.coi.2011.06.002

30. Cáceres N, Tapia G, Ojanguren I, et al. Evolution of foamy macrophages in the pulmonary granulomas of experimental tuberculosis models. *Tuberculosis*. 2009;89(2):175-182. doi:10.1016/j.tube.2008.11.001

31. Kim MJ, Wainwright HC, Locketz M, et al. Caseation of human tuberculosis granulomas correlates with elevated host lipid metabolism. *EMBO Mol Med*. 2010;2(7):258-274. doi:10.1002/emmm.201000079

32. Peyron P, Vaubourgeix J, Poquet Y, et al. Foamy Macrophages from Tuberculous Patients' Granulomas Constitute a Nutrient-Rich Reservoir for M. tuberculosis Persistence. *PLOS Pathog*. 2008;4(11):e1000204. doi:10.1371/journal.ppat.1000204

33. Silva Miranda M, Breiman A, Allain S, Deknuydt F, Altare F. The Tuberculous Granuloma: An Unsuccessful Host Defence Mechanism Providing a Safety Shelter for the Bacteria? Shevach E, ed. *Clin Dev Immunol*. 2012;2012:139127. doi:10.1155/2012/139127

34. Pai M, Behr MA, Dowdy D, et al. Tuberculosis. *Nat Rev Dis Primer*. 2016;2(1):16076. doi:10.1038/nrdp.2016.76

35. Carranza C, Pedraza-Sanchez S, de Oyarzabal-Mendez E, Torres M. Diagnosis for Latent Tuberculosis Infection: New Alternatives. *Front Immunol*. 2020;11. https://www.frontiersin.org/article/10.3389/fimmu.2020.02006

36. Latent tuberculosis infection: updated and consolidated guidelines for programmatic management. Published online 2018. https://apps.who.int/iris/bitstream/handle/10665/260233/9789241550239-eng.pdf

37. Yang H, Kruh-Garcia NA, Dobos KM. Purified protein derivatives of tuberculin — past, present, and future. *FEMS Immunol Med Microbiol*. 2012;66(3):273-280. doi:10.1111/j.1574-695X.2012.01002.x

38. Flaherty DK, ed. Chapter 19 - Delayed-Type Hypersensitivity Reactions. In: *Immunology for Pharmacy*. Mosby; 2012:152-161. doi:10.1016/B978-0-323-06947-2.10019-7

39. Stöppler MC. Tuberculosis Skin Test (PPD Skin Test). Shiel WC, ed. Published online March 30, 2022. https://www.medicinenet.com/tuberculosis_skin_test_ppd_skin_test/article.htm

40. The T-SPOT.TB test technology. Published online 2022. https://www.tspot.com/why-the-t-spot-tb-test/technology/

41. Barcellini L, Borroni E, Brown J, et al. First evaluation of QuantiFERON-TB Gold Plus performance in contact screening. *Eur Respir J*. 2016;48(5):1411. doi:10.1183/13993003.00510-2016

42. Pai Madhukar, Denkinger Claudia M., Kik Sandra V., et al. Gamma Interferon Release Assays for Detection of Mycobacterium tuberculosis Infection. *Clin Microbiol Rev*. 2014;27(1):3-20. doi:10.1128/CMR.00034-13

43. van Ingen J, de Zwaan R, Dekhuijzen R, Boeree M, van Soolingen D. Region of difference 1 in nontuberculous Mycobacterium species adds a phylogenetic and taxonomical character. *J Bacteriol*. 2009;191(18):5865-5867. doi:10.1128/JB.00683-09

44. Wang MS, Wang JL, Wang XF. The performance of interferon-gamma release assay in nontuberculous mycobacterial diseases: a retrospective study in China. *BMC Pulm Med*. 2016;16(1):163-163. doi:10.1186/s12890-016-0320-3

45. Redelman-Sidi G, Sepkowitz KA. IFN-γ Release Assays in the Diagnosis of Latent Tuberculosis Infection among Immunocompromised Adults. *Am J Respir Crit Care Med*. 2013;188(4):422-431. doi:10.1164/rccm.201209-1621CI

46. Abubakar I, Drobniewski F, Southern J, et al. Prognostic value of interferon-γ release assays and tuberculin skin test in predicting the development of active tuberculosis (UK PREDICT TB): a prospective cohort study. *Lancet Infect Dis*. 2018;18(10):1077-1087. doi:10.1016/S1473-3099(18)30355-4

47. Correia-Neves M, Fröberg G, Korshun L, et al. Biomarkers for tuberculosis: the case for lipoarabinomannan. *ERJ Open Res*. 2019;5(1):00115-02018. doi:10.1183/23120541.00115-2018

48. Hargreaves NJ, Kadzakumanja O, Whitty C, Salaniponi F, Harries A, Squire S. 'Smear-negative' pulmonary tuberculosis in a DOTS programme: poor outcomes in an area of high HIV seroprevalence. *Int Union Tuberc Lung Dis*. 2021;5(Number 9):847-854(8).

49. Shingadia D, Novelli V. Diagnosis and treatment of tuberculosis in children. *Lancet Infect Dis*. 2003;3(10):624-632. doi:10.1016/S1473-3099(03)00771-0

50. Siddiqi K, Lambert ML, Walley J. Clinical diagnosis of smear-negative pulmonary tuberculosis in low-income countries: the current evidence. *Lancet Infect Dis*. 2003;3(5):288-296. doi:10.1016/S1473-3099(03)00609-1

51. Kruh-Garcia NA, Wolfe LM, Chaisson LH, et al. Detection of Mycobacterium tuberculosis Peptides in the Exosomes of Patients with Active and Latent M. tuberculosis Infection Using MRM-MS. *PLOS ONE*. 2014;9(7):e103811. doi:10.1371/journal.pone.0103811

52. Sia IG, Wieland ML. Current concepts in the management of tuberculosis. *Mayo Clin Proc*. 2011;86(4):348-361. doi:10.4065/mcp.2010.0820

53. Dutta NK, Karakousis PC. Latent tuberculosis infection: myths, models, and molecular mechanisms. *Microbiol Mol Biol Rev MMBR*. 2014;78(3):343-371. doi:10.1128/MMBR.00010-14

54. Mack U, Migliori GB, Sester M, et al. LTBI: latent tuberculosis infection or lasting immune responses to M. tuberculosis? A TBNET consensus statement. *Eur Respir J*. 2009;33(5):956. doi:10.1183/09031936.00120908

55. Sarrazin H, Wilkinson KA, Andersson J, et al. Association between Tuberculin Skin Test Reactivity, the Memory CD4 Cell Subset, and Circulating FoxP3-Expressing Cells in HIV-Infected Persons. *J Infect Dis*. 2009;199(5):702-710. doi:10.1086/596735

56. World Health Organization. *High Priority Target Product Profiles for New Tuberculosis Diagnostics: Report of a Consensus Meeting, 28-29 April 2014, Geneva, Switzerland*. World Health Organization; 2014. https://apps.who.int/iris/handle/10665/135617

57. DHEDA K, RUHWALD M, THERON G, PETER J, YAM WC. Point-of-care diagnosis of tuberculosis: Past, present and future. *Respirology*. 2013;18(2):217-232. doi:10.1111/resp.12022

58. Grewal R, Swanepoel C, Snyders C, Isaacs S, Abayomi E. Biomarker discovery for diagnosis and treatment of tuberculosis: a role for biobanking? *J Biorepository Sci Appl Med*. Published online October 1, 2015:47. doi:10.2147/BSAM.S64571

59. Hamasur B, Bruchfeld J, Haile M, et al. Rapid diagnosis of tuberculosis by detection of mycobacterial lipoarabinomannan in urine. *J Microbiol Methods*. 2001;45(1):41-52. doi:10.1016/S0167-7012(01)00239-1

60. Connelly JT, Andama A, Grant BD, et al. Field evaluation of a prototype tuberculosis lipoarabinomannan lateral flow assay on HIV-positive and HIV-negative patients. *PLOS ONE*. 2021;16(7):e0254156. doi:10.1371/journal.pone.0254156

61. Dheda K, Davids V, Lenders L, et al. Clinical utility of a commercial LAM-ELISA assay for TB diagnosis in HIV-infected patients using urine and sputum samples. *PloS One*. 2010;5(3):e9848-e9848. doi:10.1371/journal.pone.0009848

62. Minion J, Leung E, Talbot E, Dheda K, Pai M, Menzies D. Diagnosing tuberculosis with urine lipoarabinomannan: systematic review and meta-analysis. *Eur Respir J*. 2011;38(6):1398. doi:10.1183/09031936.00025711

63. Esmail Aliasgar, Pooran Anil, Sabur Natasha F., et al. An Optimal Diagnostic Strategy for Tuberculosis in Hospitalized HIV-Infected Patients Using GeneXpert MTB/RIF and Alere Determine TB LAM Ag. *J Clin Microbiol*. 2020;58(10):e01032-20. doi:10.1128/JCM.01032-20

64. Peter JG, Theron G, van Zyl-Smit R, et al. Diagnostic accuracy of a urine lipoarabinomannan strip-test for TB detection in HIV-infected hospitalised patients. *Eur Respir J*. 2012;40(5):1211-1220. doi:10.1183/09031936.00201711

65. Sabur NF, Esmail A, Brar MS, Dheda K. Diagnosing tuberculosis in hospitalized HIV-infected individuals who cannot produce sputum: is urine lipoarabinomannan testing the answer? *BMC Infect Dis*. 2017;17(1):803-803. doi:10.1186/s12879-017-2914-7

66. ClinicalTrials.gov. https://clinicaltrials.gov/

67. Verma I, Kaur K. Omics in Tuberculosis Diagnosis: Today and Tomorrow. In: Sobti RC, Sobti A, eds. *Biomedical Translational Research: Technologies for Improving Healthcare*. Springer Nature Singapore; 2022:181-200. doi:10.1007/978-981-16-4345-3_13

68. Boehme CC, Nicol MP, Nabeta P, et al. Feasibility, diagnostic accuracy, and effectiveness of decentralised use of the Xpert MTB/RIF test for diagnosis of tuberculosis and multidrug resistance: a multicentre implementation study. *Lancet Lond Engl*. 2011;377(9776):1495-1505. doi:10.1016/S0140-6736(11)60438-8

69. Chakravorty Soumitesh, Simmons Ann Marie, Rowneki Mazhgan, et al. The New Xpert MTB/RIF Ultra: Improving Detection of Mycobacterium tuberculosis and Resistance to Rifampin in an Assay Suitable for Point-of-Care Testing. *mBio*. 8(4):e00812-17. doi:10.1128/mBio.00812-17

70. Tucci P, González-Sapienza G, Marin M. Pathogen-derived biomarkers for active tuberculosis diagnosis. *Front Microbiol*. 2014;5:549-549. doi:10.3389/fmicb.2014.00549

71. Steingart KR, Flores LL, Dendukuri N, et al. Commercial serological tests for the diagnosis of active pulmonary and extrapulmonary tuberculosis: an updated systematic review and meta-analysis. *PLoS Med*. 2011;8(8):e1001062-e1001062. doi:10.1371/journal.pmed.1001062

72. World Health Organization: Policy Update Automated Realtime Nucleic Acid Amplification Technology for Rapid and Simultaneous Detection of Tuberculosis and Rifampicin Resistance: Xpert MTB/RIF System. Published online 2013. https://apps.who.int/iris/bitstream/handle/10665/112472/9789241506335_eng.pdf

73. Wergeland I, Pullar N, Assmus J, et al. IP-10 differentiates between active and latent tuberculosis irrespective of HIV status and declines during therapy. *J Infect*. 2015;70(4):381-391. doi:10.1016/j.jinf.2014.12.019

74. Farber JM. Mig and IP-10: CXC chemokines that target lymphocytes. *J Leukoc Biol*. 1997;61(3):246-257. doi:10.1002/jlb.61.3.246

75. Luster AD, Unkeless JC, Ravetch JV. γ-Interferon transcriptionally regulates an early-response gene containing homology to platelet proteins. *Nature*. 1985;315(6021):672-676. doi:10.1038/315672a0

76. Ruhwald M, Aabye MG, Ravn P. IP-10 release assays in the diagnosis of tuberculosis infection: current status and future directions. *Expert Rev Mol Diagn*. 2012;12(2):175-187. doi:10.1586/erm.11.97

77. Biraro IA, Kimuda S, Egesa M, et al. The Use of Interferon Gamma Inducible Protein 10 as a Potential Biomarker in the Diagnosis of Latent Tuberculosis Infection in Uganda. *PloS One*. 2016;11(1):e0146098-e0146098. doi:10.1371/journal.pone.0146098

78. Kaplan G, Luster AD, Hancock G, Cohn ZA. The expression of a gamma interferon-induced protein (IP-10) in delayed immune responses in human skin. *J Exp Med*. 1987;166(4):1098-1108. doi:10.1084/jem.166.4.1098

79. Orme IM, Cooper AM. Cytokine/chemokine cascades in immunity to tuberculosis. *Immunol Today*. 1999;20(7):307-312. doi:10.1016/S0167-5699(98)01438-8

80. Aggerbeck H, Ruhwald M, Hoff ST, et al. C-Tb skin test to diagnose Mycobacterium tuberculosis infection in children and HIV-infected adults: A phase 3 trial. *PloS One*. 2018;13(9):e0204554-e0204554. doi:10.1371/journal.pone.0204554

81. Ruhwald M, Aggerbeck H, Gallardo RV, et al. Safety and efficacy of the C-Tb skin test to diagnose Mycobacterium tuberculosis infection, compared with an interferon γ release assay and the tuberculin skin test: a phase 3, double-blind, randomised, controlled trial. *Lancet Respir Med*. 2017;5(4):259-268. doi:10.1016/S2213-2600(16)30436-2

82. Knight GM, Dodd PJ, Grant AD, Fielding KL, Churchyard GJ, White RG. Tuberculosis prevention in South Africa. *PloS One*. 2015;10(4):e0122514-e0122514. doi:10.1371/journal.pone.0122514

83. TB Diagnostics Market Analysis. Market assessment of tuberculosis diagnostics in South Africa, 20122013. *Int J Tuberc Lung Dis*. 2015;19(Number 2):216-222(7). doi:oi:10.5588/ijtld.14.0565

84. Wang S, He L, Wu J, et al. Transcriptional Profiling of Human Peripheral Blood Mononuclear Cells Identifies Diagnostic Biomarkers That Distinguish Active and Latent Tuberculosis. *Front Immunol*. 2019;10. https://www.frontiersin.org/article/10.3389/fimmu.2019.02948

85. Hessvik NP, Llorente A. Current knowledge on exosome biogenesis and release. *Cell Mol Life Sci CMLS*. 2018;75(2):193-208. doi:10.1007/s00018-017-2595-9

86. Mehaffy C, Kruh-Garcia NA, Graham B, et al. Identification of Mycobacterium tuberculosis Peptides in Serum Extracellular Vesicles from Persons with Latent Tuberculosis Infection. *J Clin Microbiol*. 2020;58(6):e00393-20. doi:10.1128/JCM.00393-20

87. Théry C, Witwer KW, Aikawa E, et al. Minimal information for studies of extracellular vesicles 2018 (MISEV2018): a position statement of the International Society for Extracellular Vesicles and update of the MISEV2014 guidelines. *J Extracell Vesicles*. 2018;7(1):1535750-1535750. doi:10.1080/20013078.2018.1535750

88. Schorey JS, Bhatnagar S. Exosome Function: From Tumor Immunology to Pathogen Biology. *Traffic*. 2008;9(6):871-881. doi:10.1111/j.1600-0854.2008.00734.x

89. O'Brien A. D., Beatty Wandy L., Russell David G. Identification of Mycobacterial Surface Proteins Released into Subcellular Compartments of Infected Macrophages. *Infect Immun*. 2000;68(12):6997-7002. doi:10.1128/IAI.68.12.6997-7002.2000

90. Bhatnagar S, Shinagawa K, Castellino FJ, Schorey JS. Exosomes released from macrophages infected with intracellular pathogens stimulate a proinflammatory response in vitro and in vivo. *Blood*. 2007;110(9):3234-3244. doi:10.1182/blood-2007-03-079152

91. Giri PK, Kruh NA, Dobos KM, Schorey JS. Proteomic analysis identifies highly antigenic proteins in exosomes from M. tuberculosis-infected and culture filtrate protein-treated macrophages. *Proteomics*. 2010;10(17):3190-3202. doi:10.1002/pmic.200900840

92. Mehaffy C, Dobos KM, Nahid P, Kruh-Garcia NA. Second generation multiple reaction monitoring assays for enhanced detection of ultra-low abundance Mycobacterium tuberculosis peptides in human serum. *Clin Proteomics*. 2017;14:21-21. doi:10.1186/s12014-017-9156-y

93. Yalow RS, Berson SA. Immunoassay of endogenous plasma insulin in man. *J Clin Invest*. 1960;39(7):1157-1175. doi:10.1172/JCI104130

94. Aydin S. A short history, principles, and types of ELISA, and our laboratory experience with peptide/protein analyses using ELISA. *Festschr Highlight Career Abba J Kastin Found Ed Res Educ Pept Field*. 2015;72:4-15. doi:10.1016/j.peptides.2015.04.012

95. Van Weemen BK, Schuurs AHWM. Immunoassay using antigen—enzyme conjugates. *FEBS Lett*. 1971;15(3):232-236. doi:10.1016/0014-5793(71)80319-8

96. Engvall E, Perlmann P. Enzyme-linked immunosorbent assay (ELISA) quantitative assay of immunoglobulin G. *Immunochemistry*. 1971;8(9):871-874. doi:10.1016/0019-2791(71)90454-X

97. What is an ELISA? Published online 2022. https://www.rndsystems.com/resources/what-is-an-elisa-and-elisa-types

98. Overview of ELISA. Accessed March 20, 2022. https://www.thermofisher.com/us/en/home/life-science/protein-biology/protein-biology-learning-center/protein-biology-resource-library/pierce-protein-methods/overview-elisa.html

99. Tips for Reducing ELISA Background. Published online October 8, 2012. Accessed March 7, 2022. https://www.biocompare.com/Bench-Tips/122704-Tips-for-Reducing-ELISA-Background/

100. Avidin-biotin Interaction. https://www.thermofisher.com/us/en/home/life-science/protein-biology/protein-biology-learning-center/protein-biology-resource-library/pierce-protein-methods/avidin-biotin-interaction.html

101. Ringler DH, Newcomer CE. *The Biology of the Laboratory Rabbit*. Academic press; 2014.

102. Leenaars M, Hendriksen CFM. Critical Steps in the Production of Polyclonal and Monoclonal Antibodies: Evaluation and Recommendations. *ILAR J*. 2005;46(3):269-279. doi:10.1093/ilar.46.3.269

103. Ascoli CA, Aggeler B. Overlooked benefits of using polyclonal antibodies. *BioTechniques*. 2018;65(3):127-136. doi:10.2144/btn-2018-0065

104. Hau J, Hendriksen CFM. Refinement of Polyclonal Antibody Production by Combining Oral Immunization of Chickens with Harvest of Antibodies from the Egg Yolk. *ILAR J*. 2005;46(3):294-299. doi:10.1093/ilar.46.3.294

105. Lipman NS, Jackson LR, Trudel LJ, Weis-Garcia F. Monoclonal Versus Polyclonal Antibodies: Distinguishing Characteristics, Applications, and Information Resources. *ILAR J*. 2005;46(3):258-268. doi:10.1093/ilar.46.3.258

106. Bergmann-Leitner ES, Mease RM, Duncan EH, Khan F, Waitumbi J, Angov E. Evaluation of immunoglobulin purification methods and their impact on quality and yield of antigen-specific antibodies. *Malar J*. 2008;7(1):129. doi:10.1186/1475-2875-7-129

107. Melon™ gel IgG Purification Kit. Accessed March 7, 2022. https://www.thermofisher.com/order/catalog/product/45212?SID=srch-srp-45212

108. Lopez E, Scott NE, Wines BD, et al. Low pH Exposure During Immunoglobulin G Purification Methods Results in Aggregates That Avidly Bind Fcγ Receptors: Implications for Measuring Fc Dependent Antibody Functions. *Front Immunol*. 2019;10. https://www.frontiersin.org/article/10.3389/fimmu.2019.02415

109. Giese G, Myrold A, Gorrell J, Persson J. Purification of antibodies by precipitating impurities using Polyethylene Glycol to enable a two chromatography step process. *J Chromatogr B*. 2013;938:14-21. doi:10.1016/j.jchromb.2013.08.029

110. Percent (%) Solutions Calculator. Published online December 23, 2017. https://www.physiologyweb.com/calculators/percent_solutions_calculator.html

111. Sandwich ELISA protocol with streptavidin-biotin detection: Bio-rad.

112. Instructions EZ-Link® NHS-Biotin Reagents. Accessed May 7, 2022. https://www.thermofisher.com/document-connect/document-connect.html?url=https%3A%2F%2Fassets.thermofisher.com%2FTFS-Assets%2FLSG%2Fmanuals%2FMAN0011206_EZ_NHS_Biotin_Reag_UG.pdf

113. 3,3',5,5'-Tetramethylbenzidine (TMB) Liquid Substrate System for Membranes Product Information. Published online 2019. Accessed June 2, 2022. https://www.sigmaaldrich.com/deepweb/assets/sigmaaldrich/product/documents/164/519/t0565bul.pdf

114. Kaliste E, Linnainmaa M, Meklin T. Airborne contaminants in conventional laboratory rabbit rooms. *Lab Anim*. 2002;36(1):43-50. doi:10.1258/0023677021911759

115. Environmental Monitoring Technical Bulletin. Published online 2005. Accessed March 7, 2022. https://www.criver.com/sites/default/files/resources/rm_rm_r_environmental_monitoring.pdf

116. Kaufmann S. H. E., Rosenkrands Ida, Weldingh Karin, et al. Differential T-Cell Recognition of Native and Recombinant Mycobacterium tuberculosis GroES. *Infect Immun*. 1999;67(11):5552-5558. doi:10.1128/IAI.67.11.5552-5558.1999

117. Qamra R, Mande SC, Coates ARM, Henderson B. The unusual chaperonins of Mycobacterium tuberculosis. *TB Res India*. 2005;85(5):385-394. doi:10.1016/j.tube.2005.08.014

118. Lupoli TJ, Vaubourgeix J, Burns-Huang K, Gold B. Targeting the Proteostasis Network for Mycobacterial Drug Discovery. *ACS Infect Dis*. 2018;4(4):478-498. doi:10.1021/acsinfecdis.7b00231

119. Aligue R, Akhavan-Niak H, Russell P. A role for Hsp90 in cell cycle control: Wee1 tyrosine kinase activity requires interaction with Hsp90. *EMBO J*. 1994;13(24):6099-6106. doi:10.1002/j.1460-2075.1994.tb06956.x

120. Knauf U, Bielka H, Gaestel M. Over-expression of the small heat-shock protein, hsp25, inhibits growth of Ehrlich ascites tumor cells. *FEBS Lett*. 1992;309(3):297-302. doi:10.1016/0014-5793(92)80793-G

121. Spector NL, Samson W, Ryan C, et al. Growth arrest of human B lymphocytes is accompanied by induction of the low molecular weight mammalian heat shock protein (Hsp28). *J Immunol*. 1992;148(6):1668.

122. Jolly C, Morimoto RI. Role of the Heat Shock Response and Molecular Chaperones in Oncogenesis and Cell Death. *JNCI J Natl Cancer Inst*. 2000;92(19):1564-1572. doi:10.1093/jnci/92.19.1564

123. Kim WS, Jung ID, Kim JS, et al. Mycobacterium tuberculosis GrpE, A Heat-Shock Stress Responsive Chaperone, Promotes Th1-Biased T Cell Immune Response via TLR4-Mediated Activation of Dendritic Cells. *Front Cell Infect Microbiol*. 2018;8. https://www.frontiersin.org/article/10.3389/fcimb.2018.00095

124. Sonnenberg MG, Belisle JT. Definition of Mycobacterium tuberculosis culture filtrate proteins by two-dimensional polyacrylamide gel electrophoresis, N-terminal amino acid sequencing, and electrospray mass spectrometry. *Infect Immun*. 1997;65(11):4515-4524. doi:10.1128/iai.65.11.4515-4524.1997

125. Kumar CMS, Mande SC, Mahajan G. Multiple chaperonins in bacteria--novel functions and non-canonical behaviors. *Cell Stress Chaperones*. 2015;20(4):555-574. doi:10.1007/s12192-015-0598-8

126. Roberts Michael M., Coker Alun R., Fossati Gianluca, Mascagni Paolo, Coates Anthony R. M., Wood Steve P. Mycobacterium tuberculosis Chaperonin 10 Heptamers Self-Associate through Their Biologically Active Loops. *J Bacteriol*. 2003;185(14):4172-4185. doi:10.1128/JB.185.14.4172-4185.2003

127. Fossati G, Izzo G, Rizzi E, et al. Mycobacterium tuberculosis chaperonin 10 is secreted in the macrophage phagosome: is secretion due to dissociation and adoption of a partially helical structure at the membrane? *J Bacteriol*. 2003;185(14):4256-4267. doi:10.1128/JB.185.14.4256-4267.2003

128. Harth G, Masleša-Galić S, Tullius MV, Horwitz MA. All four Mycobacterium tuberculosis glnA genes encode glutamine synthetase activities but only GlnA1 is abundantly expressed and essential for bacterial homeostasis. *Mol Microbiol*. 2005;58(4):1157-1172. doi:10.1111/j.1365-2958.2005.04899.x

129. Kremer L, Nampoothiri KM, Lesjean S, et al. Biochemical Characterization of Acyl Carrier Protein (AcpM) and Malonyl-CoA:AcpM Transacylase (mtFabD), Two Major Components ofMycobacterium tuberculosis Fatty Acid Synthase II *. *J Biol Chem*. 2001;276(30):27967-27974. doi:10.1074/jbc.M103687200

130. Schaeffer ML, Agnihotri G, Kallender H, Brennan PJ, Lonsdale JT. Expression, purification, and characterization of the Mycobacterium tuberculosis acyl carrier protein, AcpM. *Biochim Biophys Acta BBA - Mol Cell Biol Lipids*. 2001;1532(1):67-78. doi:10.1016/S1388-1981(01)00116-0

131. Tullius MV, Harth G, Horwitz MA. High extracellular levels of Mycobacterium tuberculosis glutamine synthetase and superoxide dismutase in actively growing cultures are due to high expression and extracellular stability rather than to a protein-specific export mechanism. *Infect Immun*. 2001;69(10):6348-6363. doi:10.1128/IAI.69.10.6348-6363.2001

132. Schubert OT, Ludwig C, Kogadeeva M, et al. Absolute Proteome Composition and Dynamics during Dormancy and Resuscitation of Mycobacterium tuberculosis. *Cell Host Microbe*. 2015;18(1):96-108. doi:10.1016/j.chom.2015.06.001

133. Barnes PF, Mehra V, Rivoire B, et al. Immunoreactivity of a 10-kDa antigen of Mycobacterium tuberculosis. *J Immunol*. 1992;148(6):1835.

134. Lupoli TJ, Fay A, Adura C, Glickman MS, Nathan CF. Reconstitution of a Mycobacterium tuberculosis proteostasis network highlights essential cofactor interactions with chaperone DnaK. *Proc Natl Acad Sci U S A*. 2016;113(49):E7947-E7956. doi:10.1073/pnas.1617644113

135. Doyle SM, Hoskins JR, Wickner S. Collaboration between the ClpB AAA+ remodeling protein and the DnaK chaperone system. *Proc Natl Acad Sci U S A*. 2007;104(27):11138-11144. doi:10.1073/pnas.0703980104

136. Reidy M, Sharma R, Shastry S, et al. Hsp40s specify functions of Hsp104 and Hsp90 protein chaperone machines. *PLoS Genet*. 2014;10(10):e1004720-e1004720. doi:10.1371/journal.pgen.1004720

137. Rosenzweig Rina, Moradi Shoeib, Zarrine-Afsar Arash, Glover John R., Kay Lewis E. Unraveling the Mechanism of Protein Disaggregation Through a ClpB-DnaK Interaction. *Science*. 2013;339(6123):1080-1083. doi:10.1126/science.1233066

138. Schlieker C, Tews I, Bukau B, Mogk A. Solubilization of aggregated proteins by ClpB/DnaK relies on the continuous extraction of unfolded polypeptides. *FEBS Lett*. 2004;578(3):351-356. doi:10.1016/j.febslet.2004.11.051

139. Fay A, Glickman MS. An essential nonredundant role for mycobacterial DnaK in native protein folding. *PLoS Genet*. 2014;10(7):e1004516-e1004516. doi:10.1371/journal.pgen.1004516

140. Dobos K M, Swiderek K, Khoo K H, Brennan P J, Belisle J T. Evidence for glycosylation sites on the 45-kilodalton glycoprotein of Mycobacterium tuberculosis. *Infect Immun*. 1995;63(8):2846-2853. doi:10.1128/iai.63.8.2846-2853.1995

141. Dobos K M, Khoo K H, Swiderek K M, Brennan P J, Belisle J T. Definition of the full extent of glycosylation of the 45-kilodalton glycoprotein of Mycobacterium tuberculosis. *J Bacteriol*. 1996;178(9):2498-2506. doi:10.1128/jb.178.9.2498-2506.1996

142. Tan MCAA, Mommaas AM, Drijfhout JW, et al. Mannose receptor-mediated uptake of antigens strongly enhances HLA class II-restricted antigen presentation by cultured dendritic cells. *Eur J Immunol*. 1997;27(9):2426-2435. doi:10.1002/eji.1830270942

143. Horn C, Namane A, Pescher P, et al. Decreased Capacity of Recombinant 45/47-kDa Molecules (Apa) of Mycobacterium tuberculosis to Stimulate T Lymphocyte Responses Related to Changes in Their Mannosylation Pattern *. *J Biol Chem*. 1999;274(45):32023-32030. doi:10.1074/jbc.274.45.32023

144. Kuo CJ, Gao J, Huang JW, et al. Functional and structural investigations of fibronectin-binding protein Apa from Mycobacterium tuberculosis. *Biochim Biophys Acta BBA - Gen Subj*. 2019;1863(9):1351-1359. doi:10.1016/j.bbagen.2019.06.003

145. Ragas A, Roussel L, Puzo G, Rivière M. The Mycobacterium tuberculosis Cell-surface Glycoprotein Apa as a Potential Adhesin to Colonize Target Cells via the Innate Immune System Pulmonary C-type Lectin Surfactant Protein A *. *J Biol Chem*. 2007;282(8):5133-5142. doi:10.1074/jbc.M610183200

146. Módolo DG, Horn CS, Soares JSM, et al. Transgenic Nicotiana tabacum seeds expressing the Mycobacterium tuberculosis Alanine- and Proline-rich antigen. *AMB Express*. 2018;8(1):178. doi:10.1186/s13568-018-0708-y

147. Middleton AM, Chadwick MV, Nicholson AG, et al. Interaction of Mycobacterium tuberculosis with human respiratory mucosa. *Tuberculosis*. 2002;82(2):69-78. doi:10.1054/tube.2002.0324

148. Ratliff TL, Mcgarr JA, Abou-zeid C, et al. Attachment of Mycobacteria to Fibronectin-coated Surfaces. *Microbiology*. 1988;134(5):1307-1313. doi:https://doi.org/10.1099/00221287-134-5-1307

149. Kuroda K, Brown EJ, Telle WB, Russell DG, Ratliff TL. Characterization of the internalization of bacillus Calmette-Guerin by human bladder tumor cells. *J Clin Invest*. 1993;91(1):69-76. doi:10.1172/JCI116202

150. Schorey J S, Li Q, McCourt D W, et al. A Mycobacterium leprae gene encoding a fibronectin binding protein is used for efficient invasion of epithelial cells and Schwann cells. *Infect Immun*. 1995;63(7):2652-2657. doi:10.1128/iai.63.7.2652-2657.1995

151. Gouzy A, Poquet Y, Neyrolles O. Nitrogen metabolism in Mycobacterium tuberculosis physiology and virulence. *Nat Rev Microbiol*. 2014;12(11):729-737. doi:10.1038/nrmicro3349

152. Harth G, Clemens DL, Horwitz MA. Glutamine synthetase of Mycobacterium tuberculosis: extracellular release and characterization of its enzymatic activity. *Proc Natl Acad Sci U S A*. 1994;91(20):9342-9346. doi:10.1073/pnas.91.20.9342

153. Gordon AH, D'Arcy Hart P, Young MR. Ammonia inhibits phagosome–lysosome fusion in macrophages. *Nature*. 1980;286(5768):79-80. doi:10.1038/286079a0

154. ELISA technical guide and protocols, Tech Tip #65. Published online 2010. http://tools.thermofisher.com/content/sfs/brochures/TR0065-ELISA-guide.pdf

155. SuperSignal® ELISA Pico Chemiluminescent Substrate (Instructions). Published online 2011. https://assets.fishersci.com/TFS-Assets/LSG/manuals/MAN0011318_SupSig_ELISA_Pico_Chemilum_Subs_UG.pdf

156. Mathematics of simple regression. https://people.duke.edu/~rnau/mathreg.htm

157. Armbruster DA, Pry T. Limit of blank, limit of detection and limit of quantitation. *Clin Biochem Rev*. 2008;29 Suppl 1(Suppl 1):S49-S52.

158. Pierce™ Protein-Free Blocking Buffers - Thermo Scientific User Guide. Published online September 7, 2021. Accessed May 18, 2022. https://www.thermofisher.com/document-connect/document-connect.html?url=https%3A%2F%2Fassets.thermofisher.com%2FTFS-Assets%2FLSG%2Fmanuals%2FMAN0011566_Pierce_ProteinFree_Block_Buff_UG.pdf

159. Albumin from chicken egg white (A5253). Accessed May 20, 2022. https://www.sigmaaldrich.com/US/en/product/sigma/a5253

160. BioFX™ Phosphate Buffered Saline/Casein Block and Diluent-5X Concentrate - Product Insert. Published online May 18, 2020. https://d163axztg8am2h.cloudfront.net/static/doc/58/4d/74902adb747fec34a086153068dd.pdf

161. Vogt RV, Phillips DL, Omar Henderson L, Whitfield W, Spierto FW. Quantitative differences among various proteins as blocking agents for ELISA microtiter plates. *J Immunol Methods*. 1987;101(1):43-50. doi:10.1016/0022-1759(87)90214-6

162. Biacore® T100 Getting Started (Manual, Version 2). Published online April 2005. https://www2.helsinki.fi/sites/default/files/atoms/files/gettingstartedt100.pdf

163. Alegria-Schaffer A, Lodge A, Vattem K. Chapter 33 Performing and Optimizing Western Blots with an Emphasis on Chemiluminescent Detection. In: Burgess RR, Deutscher MP, eds. *Methods in Enzymology*. Vol 463. Academic Press; 2009:573-599. doi:10.1016/S0076-6879(09)63033-0

164. Samsonova J, Bashkurov M, Ivanova N, Rubtsova MY, Egorov A. ELISA of streptomycin in buffer and milk: Effect of reagents' structure and analysis format on assay performance. *Food Agric Immunol*. 2005;16(1):47-57.

165. Hashimoto S. Principles of BIACORE. In: Nagata K, Handa H, eds. *Real-Time Analysis of Biomolecular Interactions: Applications of BIACORE*. Springer Japan; 2000:23-30. doi:10.1007/978-4-431-66970-8_3

166. Zhang X, Oglesbee M. Use of surface plasmon resonance for the measurement of low affinity binding interactions between HSP72 and measles virus nucleocapsid protein. *Biol Proced Online*. 2003;5:170-181. doi:10.1251/bpo59

167. Myszka DG. Kinetic analysis of macromolecular interactions using surface plasmon resonance biosensors. *Curr Opin Biotechnol*. 1997;8(1):50-57. doi:10.1016/S0958-1669(97)80157-7

168. Biacore™ Assay Handbook (Edition AA). Published online May 2012. https://shared-resources.dhvi.duke.edu/sites/shared-resources.dhvi.duke.edu/files/Biacore%20Assay%20Handbook.pdf

169. Tang Y, Zeng X, Liang J. Surface Plasmon Resonance: An Introduction to a Surface Spectroscopy Technique. *J Chem Educ*. 2010;87(7):742-746. doi:10.1021/ed100186y

170. Surface Plasmon Resonance. https://www.lino-biotech.com/surface-plasmon-resonance-spr/

171. Surface Plasmon Resonance. https://www.cytivalifesciences.com/en/us/solutions/protein-research/knowledge-center/surface-plasmon-resonance/surface-plasmon-resonance

172. Schasfoort RBM. Chapter 1 Introduction to Surface Plasmon Resonance. In: *Handbook of Surface Plasmon Resonance (2)*. The Royal Society of Chemistry; 2017:1-26. doi:10.1039/9781788010283-00001

173. Nguyen HH, Park J, Kang S, Kim M. Surface plasmon resonance: a versatile technique for biosensor applications. *Sensors*. 2015;15(5):10481-10510. doi:10.3390/s150510481

174. Mahanty S, Bausch DG, Thomas RL, et al. Low Levels of Interleukin-8 and Interferon-Inducible Protein–10 in Serum Are Associated with Fatal Infections in Acute Lassa Fever. *J Infect Dis*. 2001;183(12):1713-1721. doi:10.1086/320722

175. Bergua JF, Álvarez-Diduk R, Idili A, et al. Low-Cost, User-Friendly, All-Integrated Smartphone-Based Microplate Reader for Optical-Based Biological and Chemical Analyses. *Anal Chem*. 2022;94(2):1271-1285. doi:10.1021/acs.analchem.1c04491

176. Hu J, Wang S, Wang L, et al. Advances in paper-based point-of-care diagnostics. *Biosens Bioelectron*. 2014;54:585-597. doi:10.1016/j.bios.2013.10.075

177. Nguyen VT, Song S, Park S, Joo C. Recent advances in high-sensitivity detection methods for paper-based lateral-flow assay. *Biosens Bioelectron*. 2020;152:112015. doi:10.1016/j.bios.2020.112015

178. Soh JH, Chan HM, Ying JY. Strategies for developing sensitive and specific nanoparticle-based lateral flow assays as point-of-care diagnostic device. *Nano Today*. 2020;30:100831. doi:10.1016/j.nantod.2019.100831

179. Ye H, Liu Y, Zhan L, Liu Y, Qin Z. Signal amplification and quantification on lateral flow assays by laser excitation of plasmonic nanomaterials. *Theranostics*. 2020;10(10):4359-4373. doi:10.7150/thno.44298

180. Liu Y, Zhan L, Qin Z, Sackrison J, Bischof JC. Ultrasensitive and Highly Specific Lateral Flow Assays for Point-of-Care Diagnosis. *ACS Nano*. 2021;15(3):3593-3611. doi:10.1021/acsnano.0c10035

181. Mycobrowser: Gene Rv2220 (glnA) in Mycobacterium tuberculosis H37Rv. Accessed June 8, 2022. https://mycobrowser.epfl.ch/genes/Rv2220

182. Bradshaw TP, Dunlap RB. Characterization of the covalent chromatography of thymidylate synthase on thiopropyl-Sepharose 6B. *Biochim Biophys Acta BBA - Protein Struct Mol Enzymol*. 1993;1163(2):165-175. doi:10.1016/0167-4838(93)90178-T

183. Frenzel A, Hust M, Schirrmann T. Expression of Recombinant Antibodies. *Front Immunol*. 2013;4. https://www.frontiersin.org/article/10.3389/fimmu.2013.00217

184. Saeed AFUH, Wang R, Ling S, Wang S. Antibody Engineering for Pursuing a Healthier Future. *Front Microbiol*. 2017;8. https://www.frontiersin.org/article/10.3389/fmicb.2017.00495

185. Kamionka M. Engineering of therapeutic proteins production in Escherichia coli. *Curr Pharm Biotechnol*. 2011;12(2):268-274. doi:10.2174/138920111794295693

186. ELISA Development and Optimization. Accessed May 16, 2022. https://www.thermofisher.com/us/en/home/life-science/protein-biology/protein-biology-learning-center/protein-biology-resource-library/pierce-protein-methods/overview-elisa/elisa-development-optimization.html

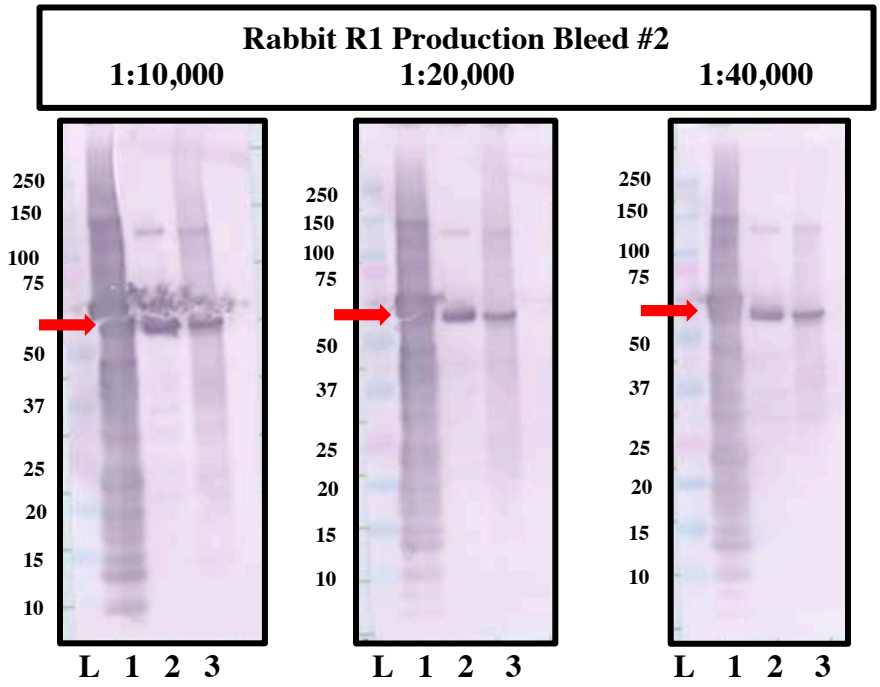

FIGURE 36: Rabbit R1 Production Bleed #2 Serum Western blots
Western blot analysis of rabbit R1 production bleed #2 serum. Description of antigens loaded on blots: (**lane L**) 2 µL protein ladder, (**lane 1**) 1 µg recGlnA, (**lane 2**) 5 µg CFP, and (**lane 3**) 5 µg WCL. The PAB serum was tested at dilutions of 1:10,000, 1:20,000, and 1:40,000. Dilutions tested are labeled above the corresponding blots. GlnA protein band (~53 kDa) is indicated by red arrows.

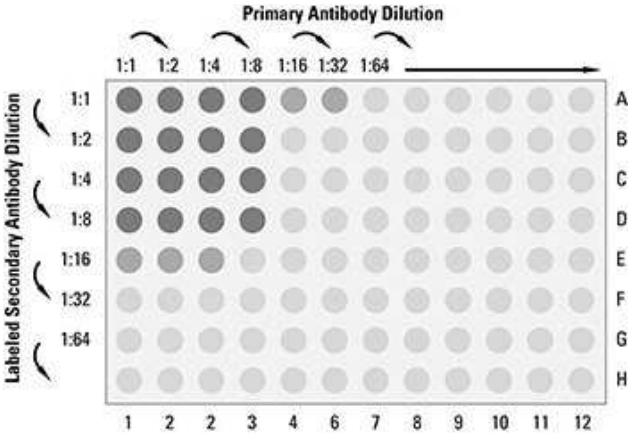

Figure 37: Checkerboard Titration Assay (ThermoFisher)
This image depicts a checkerboard titration assay [186]. For the sandwich ELISA layout, the ***un***purified R2-1 PAB serum concentration would correspond to the "primary antibody dilution" (diluted from left to right). The purified, biotinylated MABs would correspond to the "labeled

secondary antibody dilution" (diluted from top to bottom). The highest readable signal output values of these two reagents will be considered the optimal pairing.

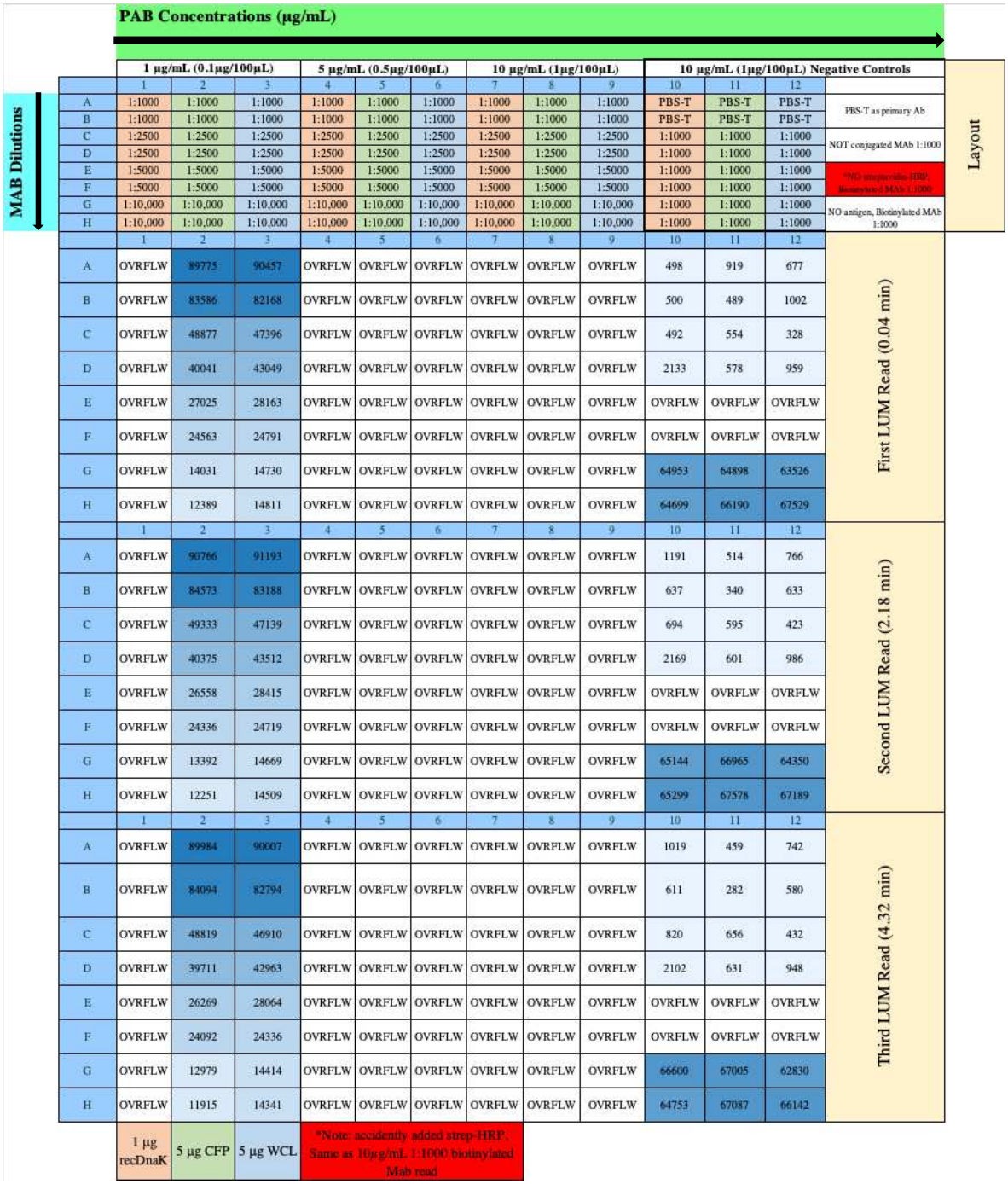

PAB Concentrations (µg/mL)

MAB Dilutions

	1 µg/mL (0.1µg/100µL)			5 µg/mL (0.5µg/100µL)			10 µg/mL (1µg/100µL)			10 µg/mL (1µg/100µL) Negative Controls			Layout
	1	2	3	4	5	6	7	8	9	10	11	12	
A	1:1000	1:1000	1:1000	1:1000	1:1000	1:1000	1:1000	1:1000	1:1000	PBS-T	PBS-T	PBS-T	PBS-T as primary Ab
B	1:1000	1:1000	1:1000	1:1000	1:1000	1:1000	1:1000	1:1000	1:1000	PBS-T	PBS-T	PBS-T	
C	1:2500	1:2500	1:2500	1:2500	1:2500	1:2500	1:2500	1:2500	1:2500	1:1000	1:1000	1:1000	NOT conjugated MAb 1:1000
D	1:2500	1:2500	1:2500	1:2500	1:2500	1:2500	1:2500	1:2500	1:2500	1:1000	1:1000	1:1000	
E	1:5000	1:5000	1:5000	1:5000	1:5000	1:5000	1:5000	1:5000	1:5000	1:1000	1:1000	1:1000	*NO streptavidin-HRP, Biotinylated MAb 1:1000
F	1:5000	1:5000	1:5000	1:5000	1:5000	1:5000	1:5000	1:5000	1:5000	1:1000	1:1000	1:1000	
G	1:10,000	1:10,000	1:10,000	1:10,000	1:10,000	1:10,000	1:10,000	1:10,000	1:10,000	1:1000	1:1000	1:1000	NO antigen, Biotinylated MAb 1:1000
H	1:10,000	1:10,000	1:10,000	1:10,000	1:10,000	1:10,000	1:10,000	1:10,000	1:10,000	1:1000	1:1000	1:1000	

	1	2	3	4	5	6	7	8	9	10	11	12	First LUM Read (0.04 min)
A	OVRFLW	89775	90457	OVRFLW	OVRFLW	OVRFLW	OVRFLW	OVRFLW	OVRFLW	498	919	677	
B	OVRFLW	83586	82168	OVRFLW	OVRFLW	OVRFLW	OVRFLW	OVRFLW	OVRFLW	500	489	1002	
C	OVRFLW	48877	47396	OVRFLW	OVRFLW	OVRFLW	OVRFLW	OVRFLW	OVRFLW	492	554	328	
D	OVRFLW	40041	43049	OVRFLW	OVRFLW	OVRFLW	OVRFLW	OVRFLW	OVRFLW	2133	578	959	
E	OVRFLW	27025	28163	OVRFLW	OVRFLW	OVRFLW	OVRFLW	OVRFLW	OVRFLW	OVRFLW	OVRFLW	OVRFLW	
F	OVRFLW	24563	24791	OVRFLW	OVRFLW	OVRFLW	OVRFLW	OVRFLW	OVRFLW	OVRFLW	OVRFLW	OVRFLW	
G	OVRFLW	14031	14730	OVRFLW	OVRFLW	OVRFLW	OVRFLW	OVRFLW	OVRFLW	64953	64898	63526	
H	OVRFLW	12389	14811	OVRFLW	OVRFLW	OVRFLW	OVRFLW	OVRFLW	OVRFLW	64699	66190	67529	

	1	2	3	4	5	6	7	8	9	10	11	12	Second LUM Read (2.18 min)
A	OVRFLW	90766	91193	OVRFLW	OVRFLW	OVRFLW	OVRFLW	OVRFLW	OVRFLW	1191	514	766	
B	OVRFLW	84573	83188	OVRFLW	OVRFLW	OVRFLW	OVRFLW	OVRFLW	OVRFLW	637	340	633	
C	OVRFLW	49333	47139	OVRFLW	OVRFLW	OVRFLW	OVRFLW	OVRFLW	OVRFLW	694	595	423	
D	OVRFLW	40375	43512	OVRFLW	OVRFLW	OVRFLW	OVRFLW	OVRFLW	OVRFLW	2169	601	986	
E	OVRFLW	26558	28415	OVRFLW	OVRFLW	OVRFLW	OVRFLW	OVRFLW	OVRFLW	OVRFLW	OVRFLW	OVRFLW	
F	OVRFLW	24336	24719	OVRFLW	OVRFLW	OVRFLW	OVRFLW	OVRFLW	OVRFLW	OVRFLW	OVRFLW	OVRFLW	
G	OVRFLW	13392	14669	OVRFLW	OVRFLW	OVRFLW	OVRFLW	OVRFLW	OVRFLW	65144	66965	64350	
H	OVRFLW	12251	14509	OVRFLW	OVRFLW	OVRFLW	OVRFLW	OVRFLW	OVRFLW	65299	67578	67189	

	1	2	3	4	5	6	7	8	9	10	11	12	Third LUM Read (4.32 min)
A	OVRFLW	89984	90007	OVRFLW	OVRFLW	OVRFLW	OVRFLW	OVRFLW	OVRFLW	1019	459	742	
B	OVRFLW	84094	82794	OVRFLW	OVRFLW	OVRFLW	OVRFLW	OVRFLW	OVRFLW	611	282	580	
C	OVRFLW	48819	46910	OVRFLW	OVRFLW	OVRFLW	OVRFLW	OVRFLW	OVRFLW	820	656	432	
D	OVRFLW	39711	42963	OVRFLW	OVRFLW	OVRFLW	OVRFLW	OVRFLW	OVRFLW	2102	631	948	
E	OVRFLW	26269	28064	OVRFLW	OVRFLW	OVRFLW	OVRFLW	OVRFLW	OVRFLW	OVRFLW	OVRFLW	OVRFLW	
F	OVRFLW	24092	24336	OVRFLW	OVRFLW	OVRFLW	OVRFLW	OVRFLW	OVRFLW	OVRFLW	OVRFLW	OVRFLW	
G	OVRFLW	12979	14414	OVRFLW	OVRFLW	OVRFLW	OVRFLW	OVRFLW	OVRFLW	66600	67005	62830	
H	OVRFLW	11915	14341	OVRFLW	OVRFLW	OVRFLW	OVRFLW	OVRFLW	OVRFLW	64753	67087	66142	

1 µg recDnaK	5 µg CFP	5 µg WCL	*Note: accidently added strep-HRP. Same as 10µg/mL 1:1000 biotinylated Mab read

Figure 38: DnaK Checkerboard Trial #1 – Luminescence Read Comparison
First sandwich ELISA performed – checkerboard titration assay for recDnaK. Figure depicting difference between signal output values for first, second, and third luminescence reads. The microplate was read using standard dynamic range with reads at 1 sec per well. The entire microplate was blocked with a 3%BSA (in PBST) blocking solution. The ***un***purified PAB serum was diluted from left to right (indicated by the black arrow at the top of the graph) at

concentrations of 1, 5, and 10 µg/mL. The MAB (purified, biotinylated DnaK Clone A) was diluted from top to bottom (indicated by the black arrow on the left-side of the graph) at dilutions of 1:1,000, 1:2,500, 1:5,000, and 1:10,000. The colors (in layout) coordinate with the different antigens used. The recDnaK antigen was diluted at 1 µg/100 µL (10,000 ng/mL) (orange). The crude *Mtb* fractions, CFP and WCL, were diluted at 5 µg/100 µL (50,000 ng/mL) (green and blue, respectively). *The antigen incubation ran long, ~ 1 hr + 30 min*. Negative controls are indicated in columns #10-12, with descriptions of negative controls used to the right of column #12. The negative controls reflect an ***un***purified PAB serum concentration of 10 µg/mL. 2%BSA/PBST was used as the "standard diluent". The antigen and MAB were both diluted in the "standard diluent". The strep-HRP was diluted at a final concentration of 2 µg/mL in 0.4%BSA/PBST diluent. The strep-HRP conjugate was added to one of the negative controls (indicated by a red box).

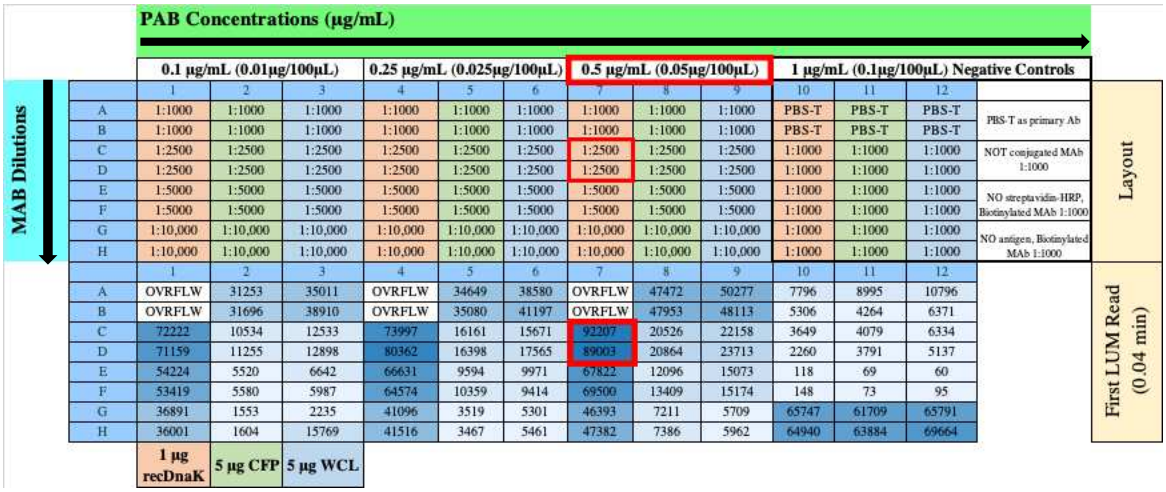

PAB Concentrations (µg/mL)

MAB Dilutions

	0.1 µg/mL (0.01µg/100µL)			0.25 µg/mL (0.025µg/100µL)			0.5 µg/mL (0.05µg/100µL)			1 µg/mL (0.1µg/100µL) Negative Controls			Layout
	1	2	3	4	5	6	7	8	9	10	11	12	
A	1:1000	1:1000	1:1000	1:1000	1:1000	1:1000	1:1000	1:1000	1:1000	PBS-T	PBS-T	PBS-T	PBS-T as primary Ab
B	1:1000	1:1000	1:1000	1:1000	1:1000	1:1000	1:1000	1:1000	1:1000	PBS-T	PBS-T	PBS-T	
C	1:2500	1:2500	1:2500	1:2500	1:2500	1:2500	1:2500	1:2500	1:2500	1:1000	1:1000	1:1000	NOT conjugated MAb 1:1000
D	1:2500	1:2500	1:2500	1:2500	1:2500	1:2500	1:2500	1:2500	1:2500	1:1000	1:1000	1:1000	
E	1:5000	1:5000	1:5000	1:5000	1:5000	1:5000	1:5000	1:5000	1:5000	1:1000	1:1000	1:1000	NO streptavidin-HRP, Biotinylated MAb 1:1000
F	1:5000	1:5000	1:5000	1:5000	1:5000	1:5000	1:5000	1:5000	1:5000	1:1000	1:1000	1:1000	
G	1:10,000	1:10,000	1:10,000	1:10,000	1:10,000	1:10,000	1:10,000	1:10,000	1:10,000	1:1000	1:1000	1:1000	NO antigen, Biotinylated MAb 1:1000
H	1:10,000	1:10,000	1:10,000	1:10,000	1:10,000	1:10,000	1:10,000	1:10,000	1:10,000	1:1000	1:1000	1:1000	

	1	2	3	4	5	6	7	8	9	10	11	12	First LUM Read (0.04 min)
A	OVRFLW	31253	35011	OVRFLW	34649	38580	OVRFLW	47472	50277	7796	8995	10796	
B	OVRFLW	31696	38910	OVRFLW	35080	41197	OVRFLW	47953	48113	5306	4264	6371	
C	72222	10534	12533	73997	16161	15671	92207	20526	22158	3649	4079	6334	
D	71159	11255	12898	80362	16398	17565	89003	20864	23713	2260	3791	5137	
E	54224	5520	6642	66631	9594	9971	67822	12096	15073	118	69	60	
F	53419	5580	5987	64574	10359	9414	69500	13409	15174	148	73	95	
G	36891	1553	2235	41096	3519	5301	46393	7211	5709	65747	61709	65791	
H	36001	1604	15769	41516	3467	5461	47382	7386	5962	64940	63884	69664	
	1 µg recDnaK	5 µg CFP	5 µg WCL										

Figure 39: DnaK Checkerboard Titration Assay Trial #2 (Original) for Reproducibility Issues

Original checkerboard titration assay for recDnaK. The ***un***purified PAB serum was diluted from left to right (indicated by the black arrow at the top of the graph) at concentrations of 0.1, 0.25, and 0.5 µg/mL. RecDnaK antigen was tested along with crude *Mtb* fractions, CFP and WCL. The MAB (purified, biotinylated DnaK Clone A) was diluted from top to bottom (indicated by the black arrow on the left side of the graph) at dilutions of 1:1,000, 1:2,500, 1:5.000, and 1:10,000. The colors coordinate with the MAB dilutions. Negative controls are indicated in columns #10-12 and have a PAB serum concentration of 1µg/mL. Descriptions of the negative controls are to the right of the negative control layout to the right of column #12. The entire microplate was blocked with a 3% BSA (in PBST) blocking solution. 2%BSA/PBST was used as the "standard diluent". The antigen and MAB were both diluted in the "standard diluent". The final concentration of the recDnaK antigen was 1 µg/100µL (10,000 ng/mL). The final concentration of the crude fractions, CFP and WCL, antigens was 5 µg/100µL (50,000 ng/mL). The strep-HRP conjugate was diluted at 2 µg/mL in a 0.4%BSA/PBST diluent. Red boxes indicate optimal PAB serum and MAB pairing.

A. Comparing Signal RLUs

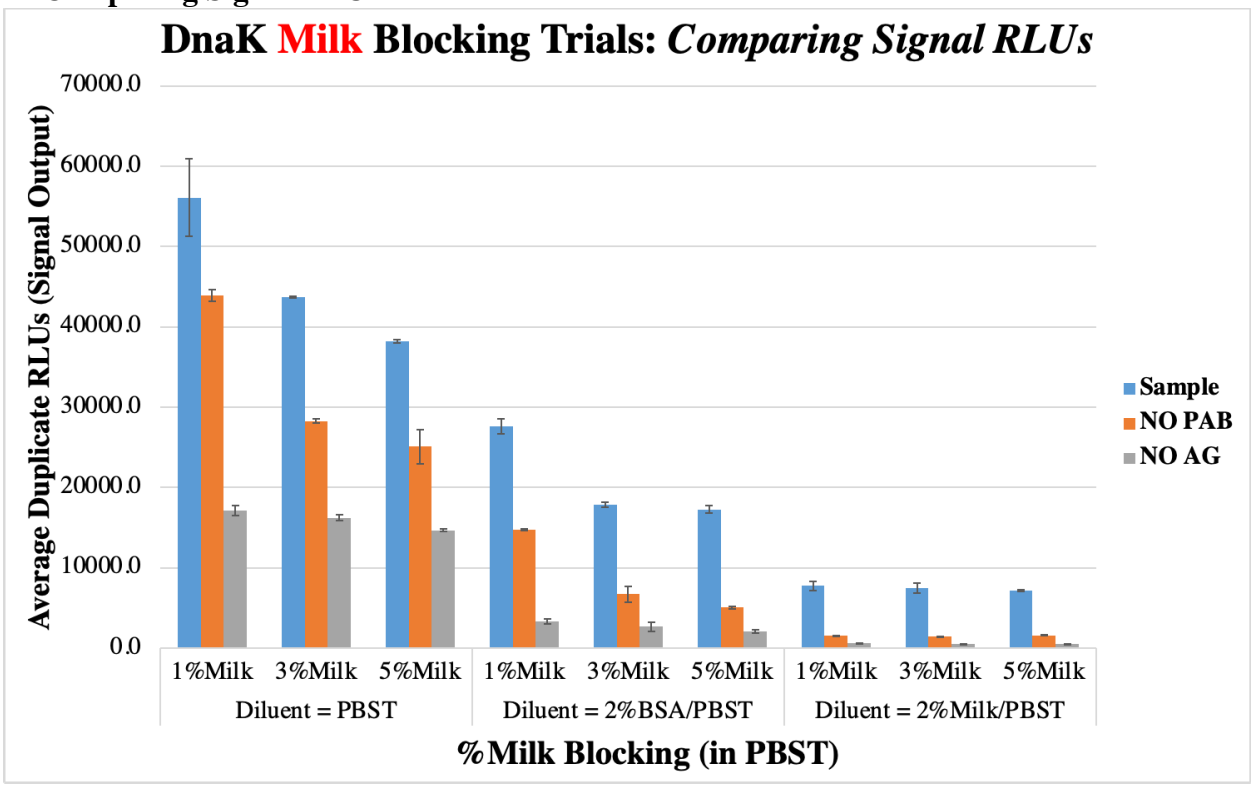

B. Comparing *sample: NO PAB* Ratios

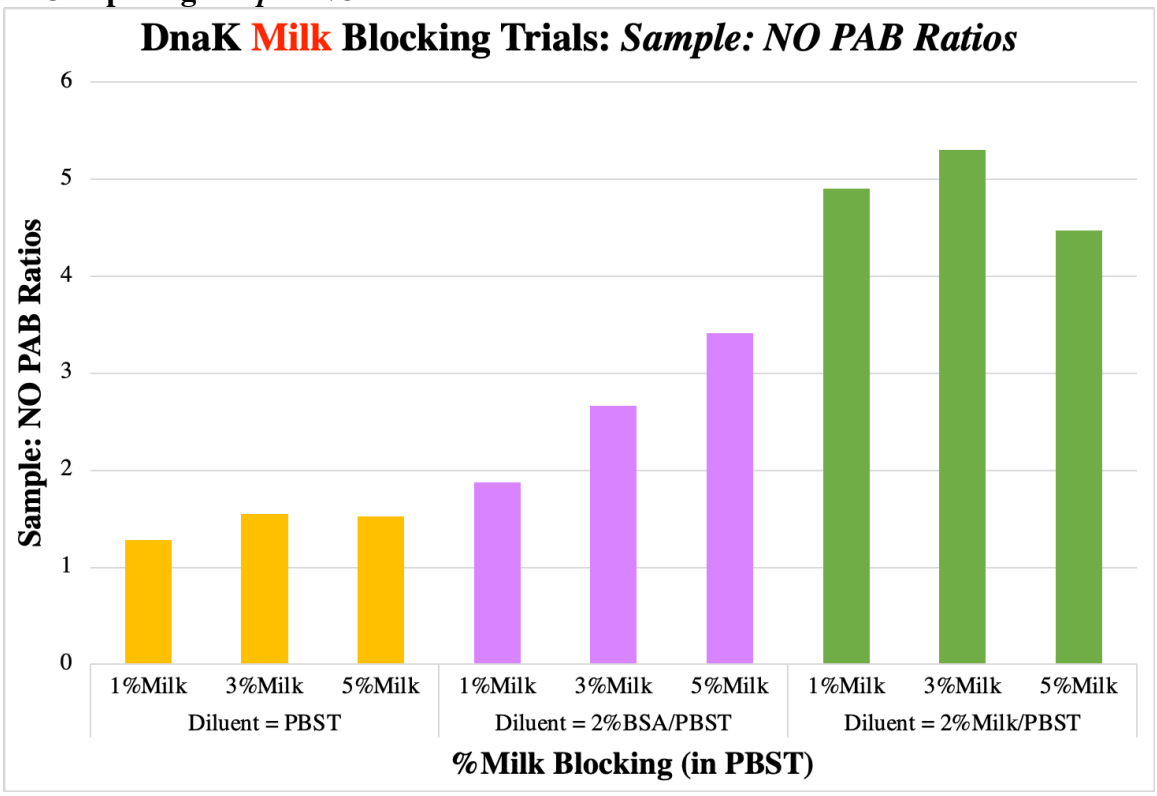

Figure 40: DnaK Milk Blocking Trials (#4 and #6)

Blocking trials (#4 & #6) for DnaK looking at milk as sole blocking solution with different "standard diluents", PBST, 2%BSA/PBST, and 2%Milk/PBST. **Graph A)** The signal output, in RLUs (averaged duplicates), corresponding to each "sample" and negative control are graphed on the *Y-axis*. The %Milk blocking solutions (1, 3, and 5%) are graphed on the *X-axis* and are grouped according to the corresponding diluents. The diluents are labeled appropriately under each group of three. The "sample" (blue), the NO PAB (orange), and the NO AG (grey) negative controls are graphed. **Graph B)** Ratios of the "sample" signals divided by the NO PAB negative control signals. Ratio values are graphed on the *Y-axis*. The different %Milk blocking solutions in PBST (1, 3, 5%) are graphed on the *X-axis* and are grouped according to the corresponding diluents. The diluents are depicted in different colors. Data from group with PBST and 2%BSA/PBST diluents originated from trial #4. Data from group with 2%Milk/PBST diluent originated from trial #6. The unpurified, R2-1 PAB serum was diluted for a final concentration of 0.5 μg/mL in coating buffer for both trials. The antigen and MAB were diluted in the "standard diluents". The recDnaK antigen was diluted at 1 μg/100 μL (10,000 ng/mL) for both plates. Trial #4 had a MAB (purified, biotinylated DnaK Clone A) dilution of 1:2,500 and trial #6 had a MAB dilution of 1:10,000. The strep-HRP conjugate was diluted at a concentration of 2 μg/mL in PBST, 0.4%BSA/PBST, or 0.4%Milk/PBST diluents, corresponding to the respective diluent group.

A. Comparing Signal RLUs

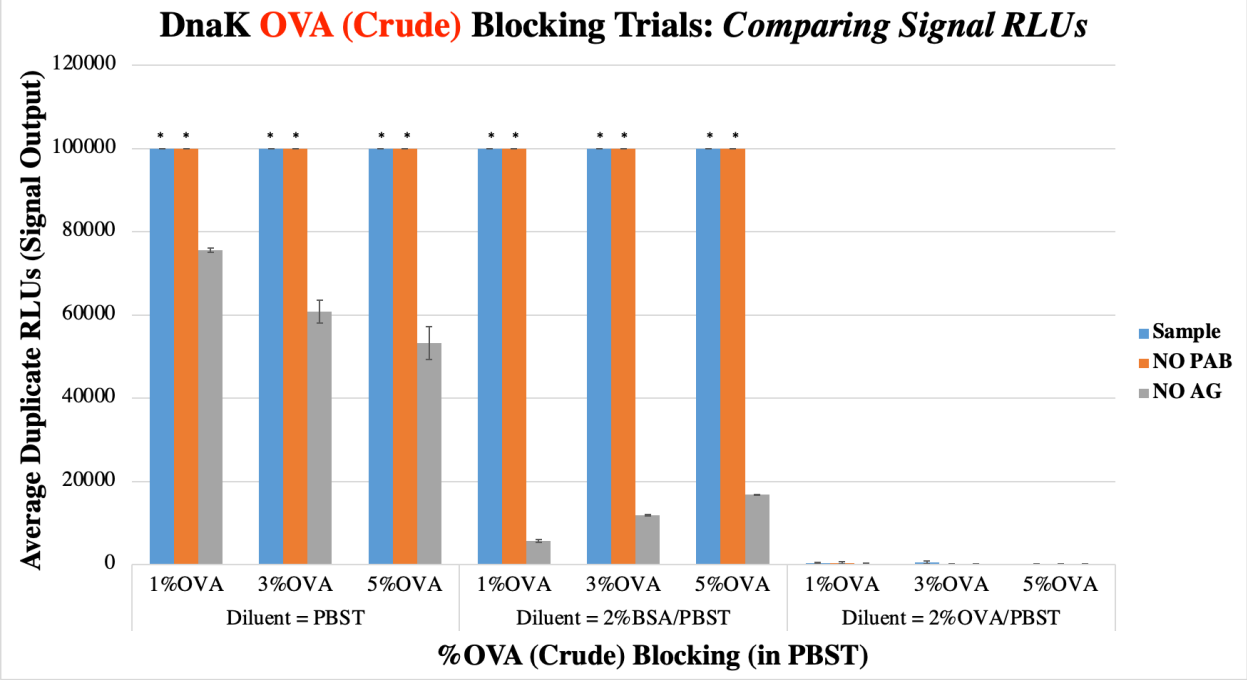

B. Comparing *sample: NO PAB* Ratios

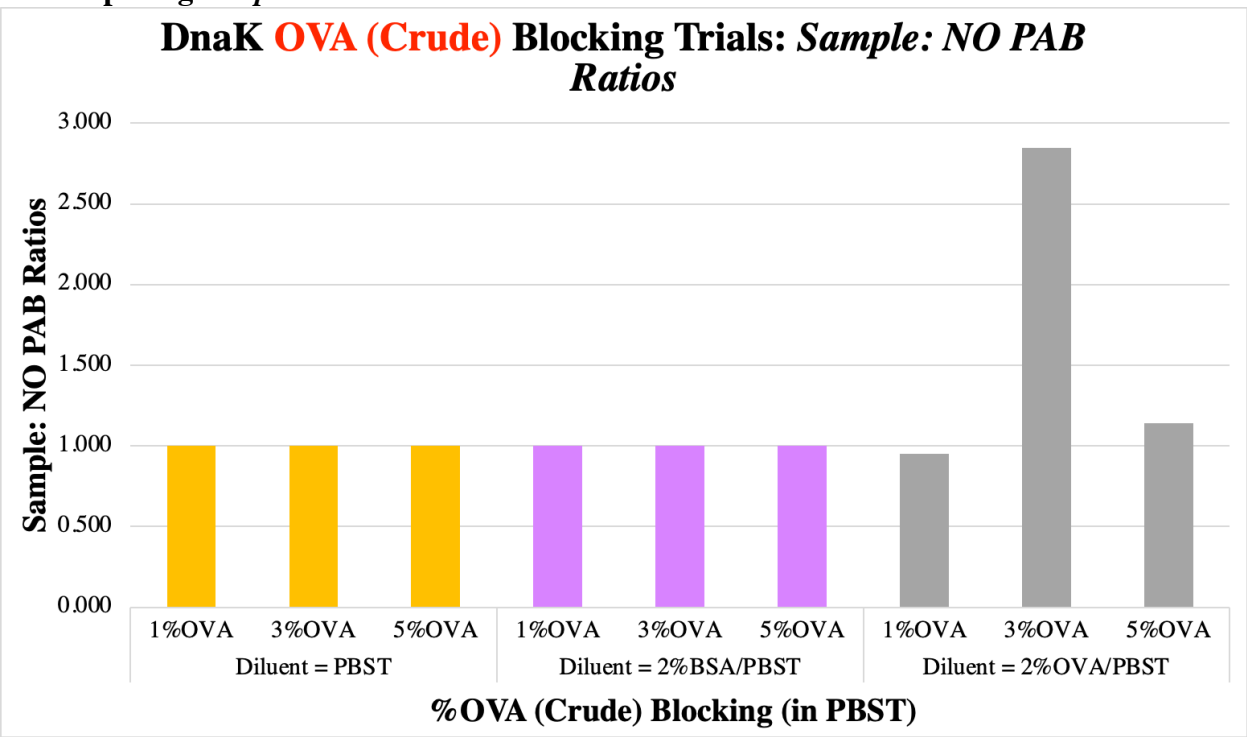

Figure 41: DnaK OVA (Crude) Blocking Trials (#1 & #2) *Comparing Signal RLUs*
Blocking trials for DnaK looking at crude ovalbumin (OVA) protein as sole blocking solution with different diluents (trials #1 & #2). The OVA protein came from a crude reagent of albumin from chicken eggs. **Graph A)** The signal output, in RLUs (averaged duplicates), corresponding to each "sample" and negative control are graphed on the *Y-axis*. The %OVA blocking solutions

(1, 3, and 5%) are graphed on the *X-axis* and are grouped according to the corresponding diluents. The diluents are labeled appropriately under each group of three %blocking solutions. The "sample" (blue), the NO PAB (orange), and the NO AG (grey) negative controls are graphed. **Graph B)** Ratios of the "sample" signals divided by the NO PAB negative control signals. Ratio values are graphed on the *Y-axis*. The different %OVA blocking solutions in PBST (1, 3, 5%) are graphed on the *X-axis* and are grouped according to the corresponding diluents. The diluents are depicted in different colors. Data from group with PBST diluent are from OVA blocking trial #1. Data from group with 2%BSA/PBST and 2%OVA/PBST diluents originated from OVA blocking trial #2. The unpurified, R2-1 PAB serum was diluted for a final concentration of 0.5 μg/mL in coating buffer for both trials. The antigen and MAB were diluted in the "standard diluents" (PBST, 2%BSA/PBST, or 2%OVA/PBST) corresponding to the respective group in the graph. The recDnaK antigen was diluted at 1 μg/100 μL (10,000 ng/mL) for both trials. Trial #1 had a MAB (purified, biotinylated DnaK Clone A) dilution of 1:2,500 and trial #2 had a MAB dilution of 1:10,000. The strep-HRP conjugate was diluted at a concentration of 2 μg/mL in PBST, 0.4%BSA/PBST, or 0.4%Milk/PBST diluents, corresponding to the respective group in the graph.

A. Comparing Signal RLUs

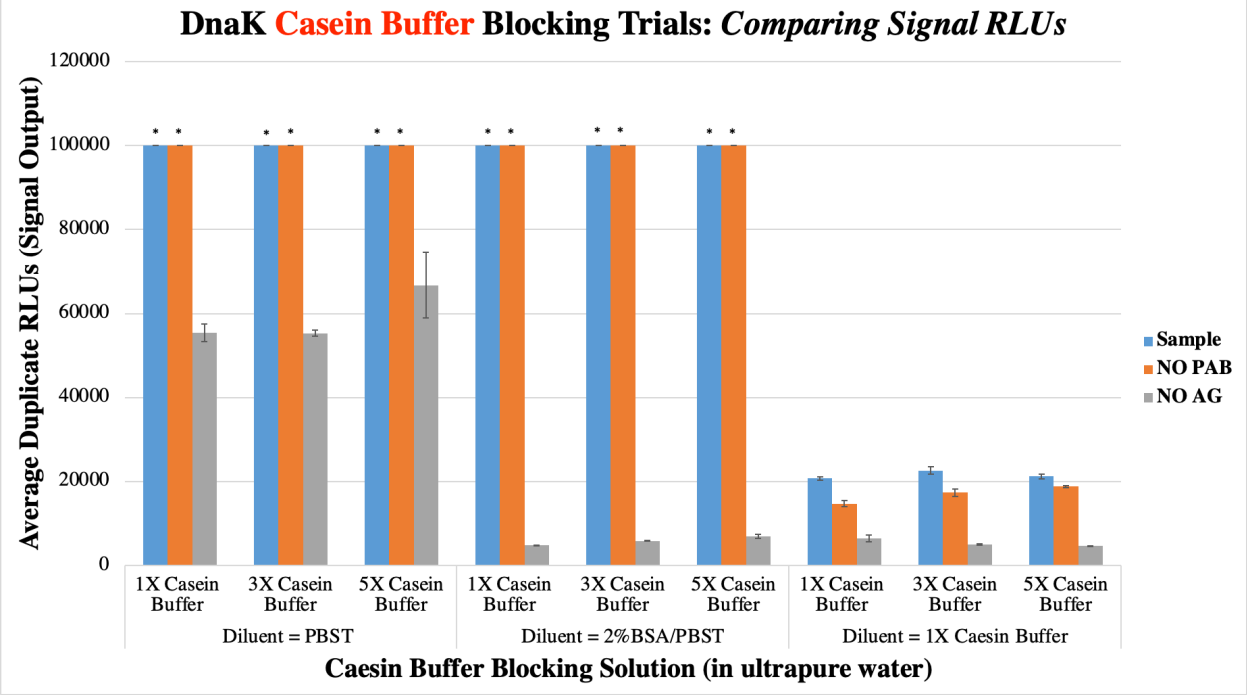

B. Comparing *sample: NO PAB* Ratios

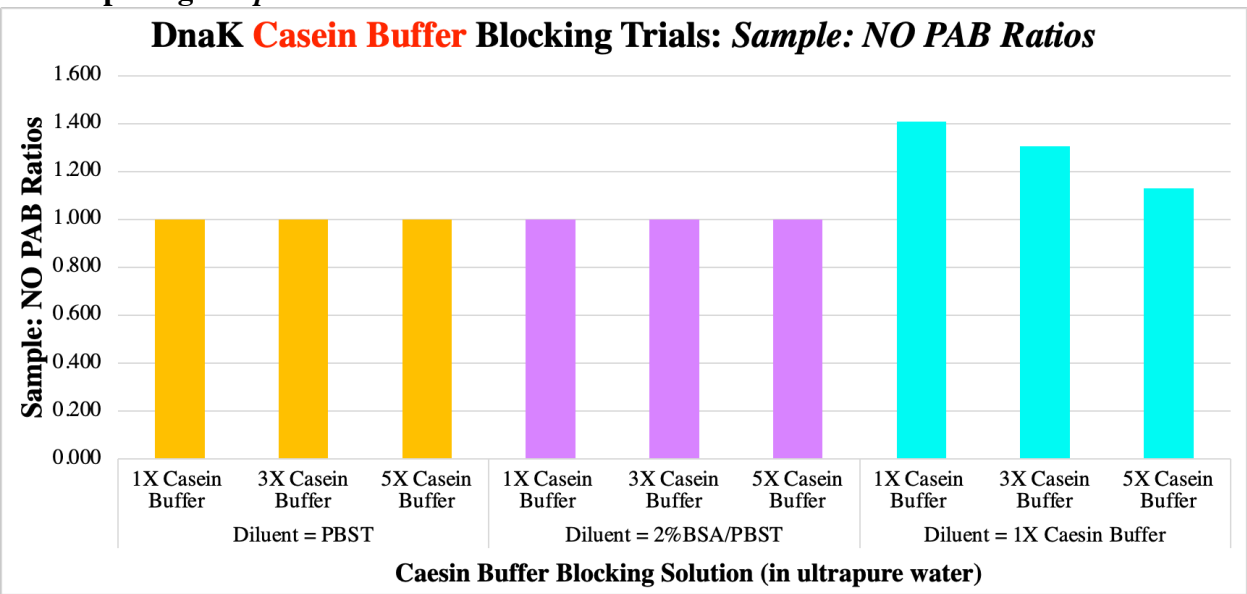

Figure 42: DnaK Casein Buffer Blocking Trials (#1, 2, & 3)
Blocking trials for DnaK looking at casein protein (casein buffer) as sole blocking solution with different diluents (trials #1, 2, & 3). The casein protein came as a ready-to-use buffer from SurModics, Inc. The dilutions from the stock solution (5X concentration) are indicated as 1X, 3X, or 5X. Casein buffer specific blocking solutions and diluents were made in ultrapure water. **Graph A)** The signal output, in RLUs (averaged duplicates), corresponding to each "sample" and negative control are graphed on the *Y-axis*. The casein buffer blocking solutions (1, 3, and 5X) are graphed on the *X-axis* and are grouped according to the corresponding diluents. The

diluents are labeled appropriately under each group of three blocking solution concentrations. The "sample" (blue), the NO PAB (orange), and the NO AG (grey) negative controls are graphed. **Graph B)** Ratios of the "sample" signals divided by the NO PAB negative control signals. Ratio values are graphed on the *Y-axis*. The different casein buffer blocking solutions (1, 3, 5X) are graphed on the *X-axis* and are grouped according to the corresponding diluents. The diluents are depicted in different colors. Data from group with 2%BSA/PBST diluent originated from casein buffer blocking trial #1. Data from group with 1X casein buffer diluent originated from casein buffer blocking trial #2. Data from group with PBST diluent originated from casein buffer blocking trial #3. The unpurified, R2-1 PAB serum was diluted for a final concentration of 0.5 µg/mL in coating buffer for all trials. The antigen and MAB were diluted in the "standard diluents" (PBST, 2%BSA/PBST, or 1X casein buffer) corresponding to the respective group in the graph. The recDnaK antigen was diluted at 1 µg/100 µL (10,000 ng/mL) for all plates. All trials had a MAB (purified, biotinylated DnaK Clone A) dilution of 1:10,000. The strep-HRP conjugate was diluted at a concentration of 2 µg/mL in PBST, 0.4%BSA/PBST, or 0.2X casein buffer (in water) diluents, corresponding to the respective group in the graph.

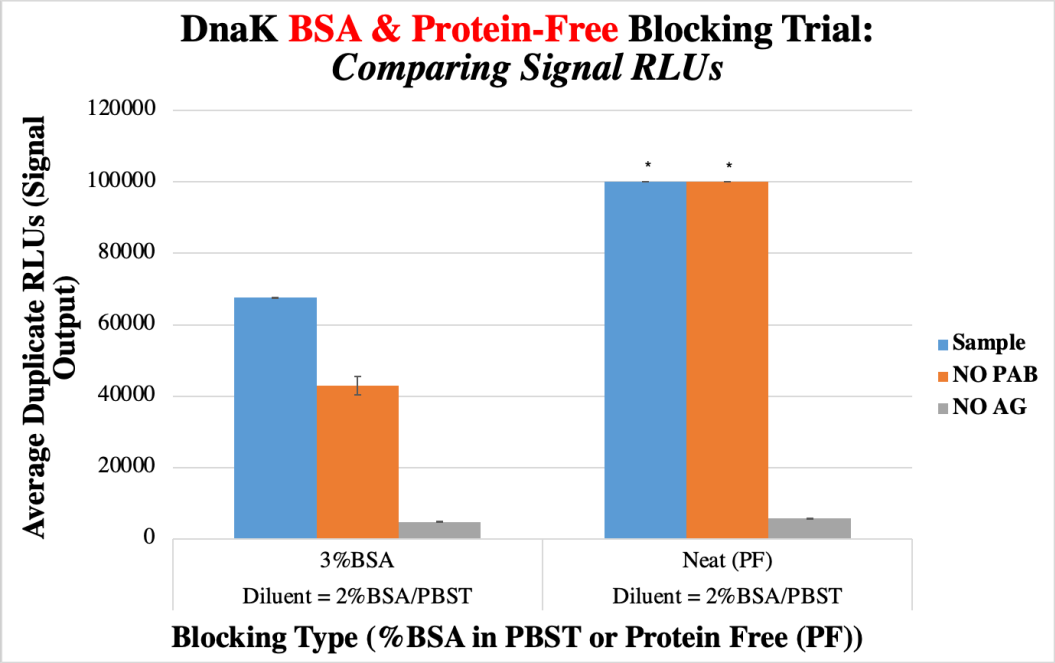

Figure 43: DnaK BSA & Protein-Free Blocking Trial (#7) *Comparing Signal RLUs*
Blocking trial for DnaK looking at BSA vs protein-free blocking solutions. The signal output, in RLUs (averaged duplicates), corresponding to each "sample" and negative control are graphed on the *Y-axis*. The 3%BSA (in PBST) blocking solution and protein-free (neat) are graphed on the *X-axis*. 2%BSA/PBST diluent was used as the "standard diluent" for both blocking solutions. The "sample" (blue), the NO PAB (orange), and the NO AG (grey) negative controls are graphed. The unpurified, R2-1 PAB serum was diluted for a final concentration of 0.5 µg/mL in coating buffer. The antigen and MAB were diluted in the "standard diluent". The recDnaK antigen was diluted at 1 µg/100 µL (10,000 ng/mL). The MAB (purified, biotinylated DnaK Clone A) dilution was 1:2,500. The strep-HRP conjugate was diluted at a final concentration of 2 µg/mL in 0.4%BSA/PBST diluent.

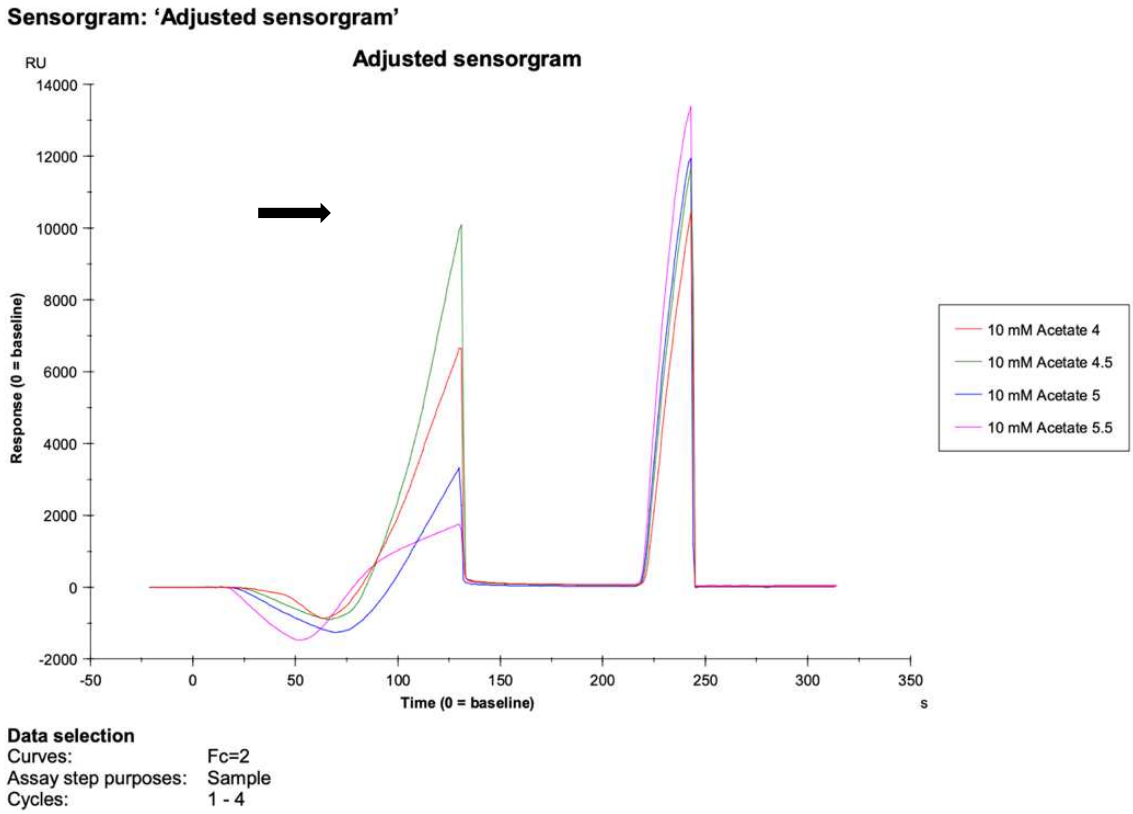

Figure 44: BSA pH Scouting Sensorgram Results (Overlay of All Cycles – All pH)
10 mM sodium acetate buffers, pH 4, 4.5, 5, and 5.5, were tested using the immobilization pH scouting Wizard method on the Biacore T200 Control Software, version 3.2.1. The sensorgram is shown for flow cell #2 with response units on *Y-axis* and time on *X-axis*. All cycles (different pH) were overlayed on sensorgram. Colors correspond to the different buffer pH. A black arrow indicates pre-concentration buffer pH chosen for BSA ligand. 10 µg/mL of BSA (in PBST) was used for this method.

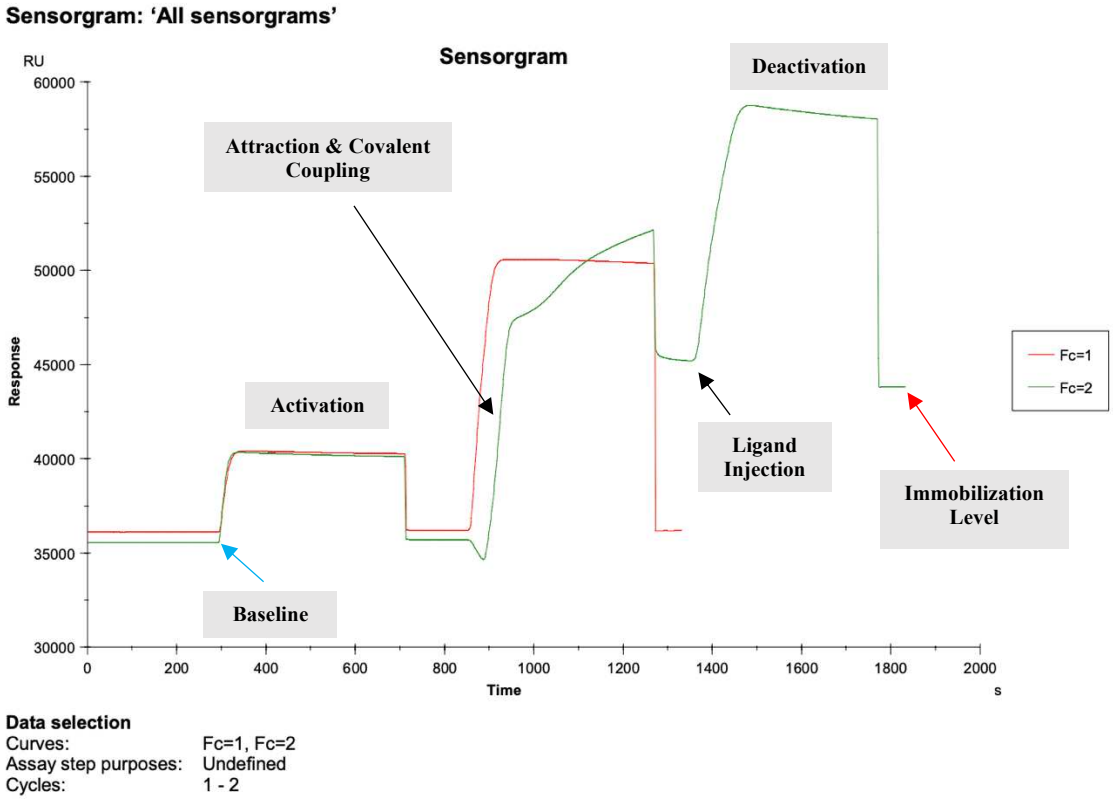

Figure 45: Immobilization of BSA Ligand Sensorgram Results (Overlay of All Cycles – Both Flow Cells)

Immobilization of the BSA ligand to the surface of the CM5 chip, Fc-2. The sensorgrams of the reference channel (Fc-1, red) and the ligand (BSA) channel (Fc-2, green) are overlayed. 25 µg/mL of BSA (in PBST) was used for immobilization. For the immobilization method, the contact time was set to 420 s and the flow rate was set at 10 µL/min. An amine coupling kit was used for immobilization of BSA. Descriptions of each step of the immobilization process are added above corresponding peak (grey boxes) or via an arrow . The blue arrow indicates the baseline for the Fc-2 channel and the red arrow indicates the immobilization level of the Fc-2 channel. The reference channel (Fc-1, red) is shown having an activation peak, followed by attraction and covalent coupling, then a deactivation (no ligand to inject or immobilize).

Immobilization Wizard results

Chip: CM5
Flow cells per cycle: 1

Flow cell	Procedure	Method	Ligand	Response Bound (RU)	Response Final (RU)
1	Blank	Amine			61.9
2	Time and flow	Amine	BSA	9526.0	8266.4

Figure 46: Immobilization of BSA Ligand Results
Result values (RU) recorded for the BSA immobilization run. The response final (RU) reflects how much ligand was bound successfully to the chip surface (Fc-2). The response final (RU) of Fc-1 reflects the baseline response.

A. Layout

		2%BSA/PBST			PBST Only			2%Milk/PBST		
		1	2	3	4	5	6	7	8	9
MAB 1:2500	A	Sample	NO AG	NO MAB	Sample	NO AG	NO MAB	Sample	NO AG	NO MAB
	B	Sample	NO AG	NO MAB	Sample	NO AG	NO MAB	Sample	NO AG	NO MAB
MAB 1:5000	C	Sample	NO AG	Block Only	Sample	NO AG	Block Only	Sample	NO AG	Block Only
	D	Sample	NO AG	Block Only	Sample	NO AG	Block Only	Sample	NO AG	Block Only
MAB 1:10,000	E	Sample	NO AG		Sample	NO AG		Sample	NO AG	
	F	Sample	NO AG		Sample	NO AG		Sample	NO AG	
MAB 1:20,000	G	Sample	NO AG		Sample	NO AG		Sample	NO AG	
	H	Sample	NO AG		Sample	NO AG		Sample	NO AG	

B. Microplate

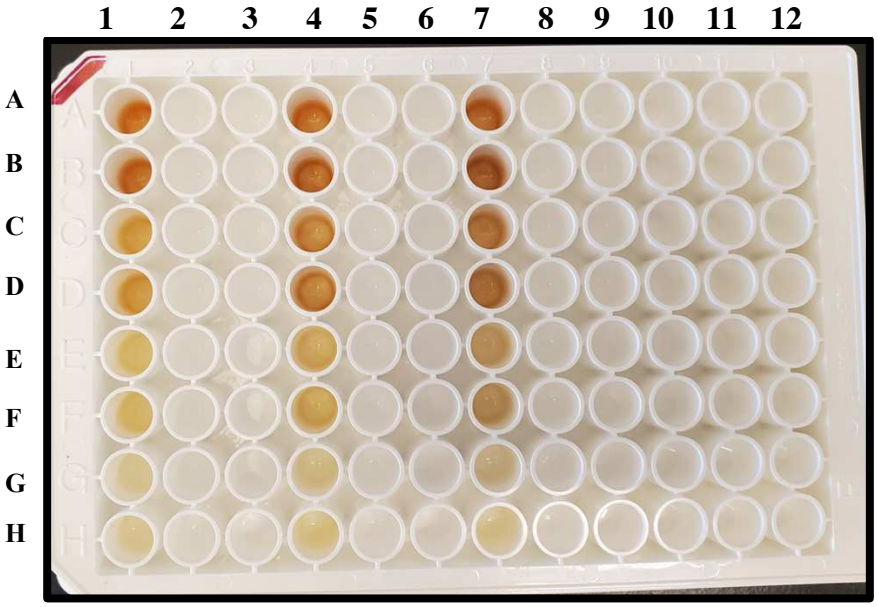

Figure 47: DnaK Direct-Biotinylated ELISA Blocking Trial (#1)

Direct-biotinylated ELISA Blocking trial (#1) for recDnaK. **A)** layout of microplate, **B)** microplate image. Depicting brown color change with dilution of MAB and inactive strep-HRP conjugate. Microplate read at 1 s per well, standard dynamic range.

A. Layout

		2%BSA/PBST			PBST Only			2%Milk/PBST		
		1	2	3	4	5	6	7	8	9
MAB 1:20,000	A	Sample	NO AG	NO MAB	Sample	NO AG	NO MAB	Sample	NO AG	NO MAB
	B	Sample	NO AG	NO MAB	Sample	NO AG	NO MAB	Sample	NO AG	NO MAB
MAB 1:40,000	C	Sample	NO AG	Block Only	Sample	NO AG	Block Only	Sample	NO AG	Block Only
	D	Sample	NO AG	Block Only	Sample	NO AG	Block Only	Sample	NO AG	Block Only
MAB 1:80,000	E	Sample	NO AG		Sample	NO AG		Sample	NO AG	
	F	Sample	NO AG		Sample	NO AG		Sample	NO AG	
MAB 1:160,000	G	Sample	NO AG		Sample	NO AG		Sample	NO AG	
	H	Sample	NO AG		Sample	NO AG		Sample	NO AG	

B. Microplate

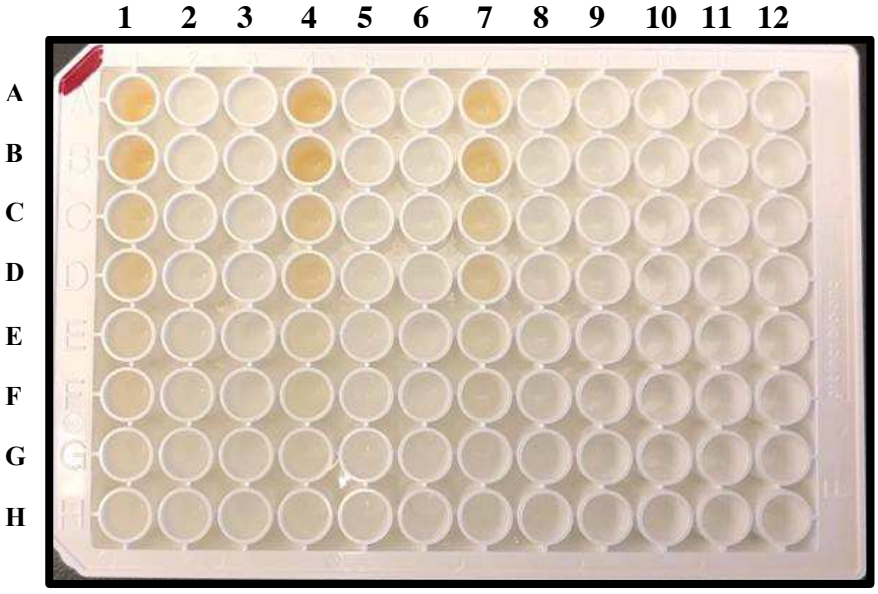

Figure 48: DnaK Direct-Biotinylated ELISA Blocking Trial (#2)
Direct-biotinylated ELISA Blocking trial (#2) for recDnaK. **A)** layout of microplate, **B)** microplate image. Depicting brown color change with dilution of MAB and inactive strep-HRP conjugate. Microplate read at 20 ms per well, extended dynamic range.

A. Linear Trendline

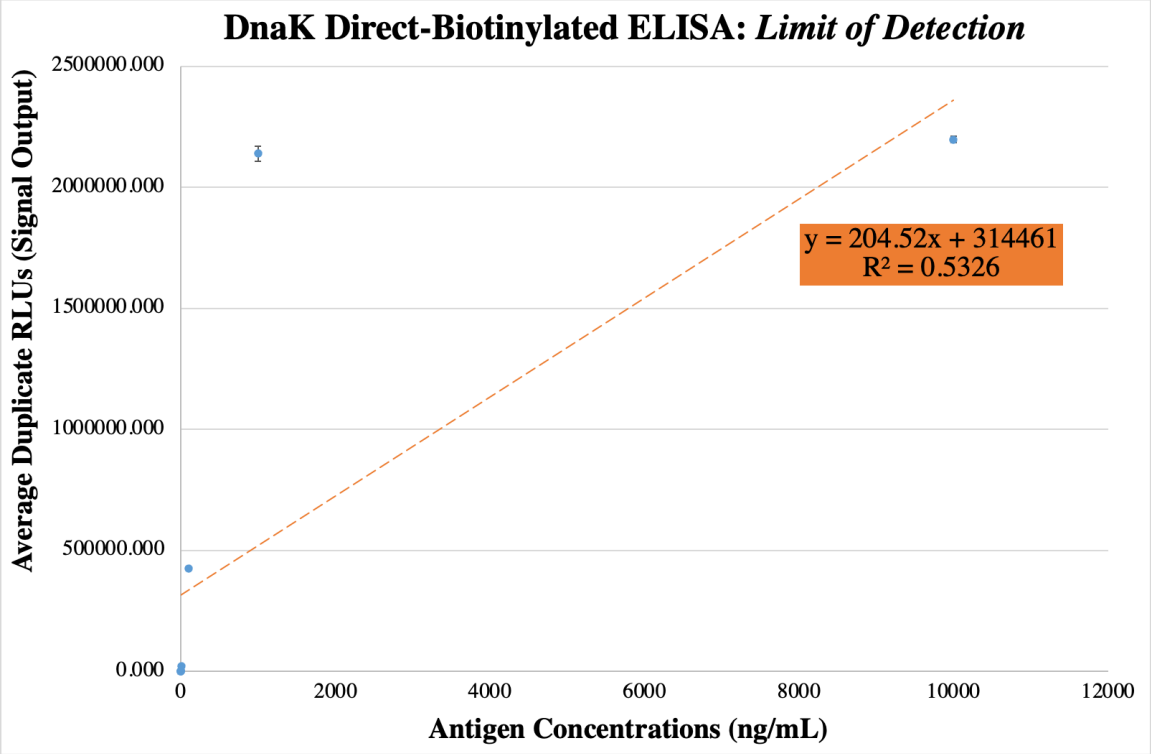

B. Polynomial Trendline

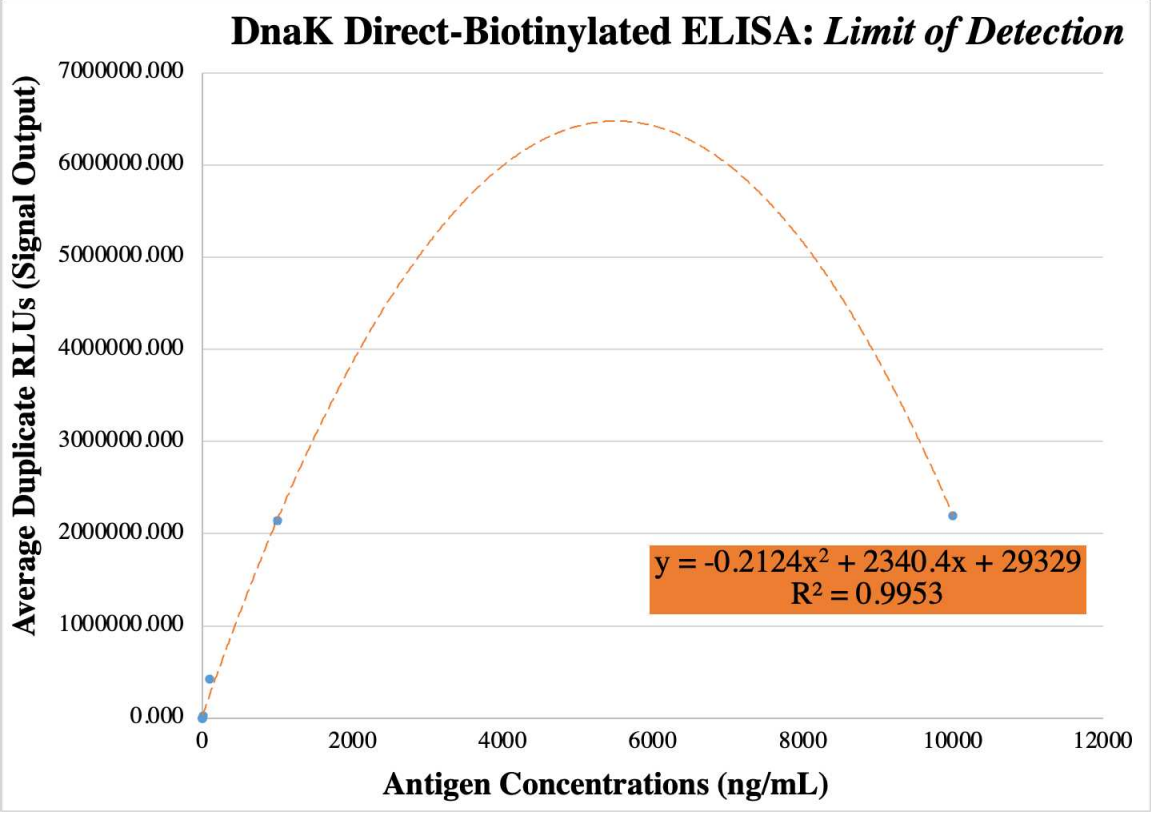

Figure 49: DnaK Direct-Biotinylated LOD Trial #1
Direct-biotinylated ELISA LOD trial (#1) for recDnaK. The average duplicate RLU signal output values for the "sample" are graphed on the *Y-axis*. The recDnaK antigen concentrations are graphed on the *X-axis* in ng/mL. **Graph A)** a linear trendline was added and **Graph B)** a polynomial trendline was added. The recDnaK antigen was diluted in coating buffer using a 1:10 serial dilution series, starting at 10,000 ng/mL. The entire plate was blocked with a 3%BSA (in PBST) blocking solution. 2%BSA/PBST was used as the "standard diluent". The MAB (purified, biotinylated DnaK Clone A) was diluted in the "standard diluent" at a dilution of 1:160,000. The strep-HRP conjugate was diluted at a final concentration of 2 µg/mL in 0.4%BSA/PBST diluent. Only the first read (20 ms) data was used for graph. Microplate shook at 282 cpm instead of 365 cpm by accident.

		Antigen Concentrations (ng/mL)											
		2500		1250		625		312.5		156.25			
		1	2	3	4	5	6	7	8	9	10	11	12
MAB Dilutions	MAB 1:2500 A	Sample	NO MAB	Sample	NO MAB	Sample	NO MAB	Sample	NO MAB	Sample	NO MAB	NO AG	Block
	MAB 1:2500 B	Sample	NO MAB	Sample	NO MAB	Sample	NO MAB	Sample	NO MAB	Sample	NO MAB	NO AG	Block
	MAB 1:5000 C	Sample		Sample		Sample		Sample		Sample		NO AG	PBST
	MAB 1:5000 D	Sample		Sample		Sample		Sample		Sample		NO AG	PBST
	MAB 1:10,00 E	Sample		Sample		Sample		Sample		Sample		NO AG	
	MAB 1:10,00 F	Sample		Sample		Sample		Sample		Sample		NO AG	
	MAB 1:20,000 G	Sample		Sample		Sample		Sample		Sample		NO AG	
	MAB 1:20,000 H	Sample		Sample		Sample		Sample		Sample		NO AG	
Layout													
		1	2	3	4	5	6	7	8	9	10	11	12
First LUM Read (20 ms)	A	OVRFLW	14810	OVRFLW	12598	OVRFLW	8669	OVRFLW	4544	3224175	2514	5352	322
	B	OVRFLW	16562	OVRFLW	13076	OVRFLW	9029	OVRFLW	4807	3225484	2909	4371	310
	C	OVRFLW		OVRFLW		OVRFLW		OVRFLW		2735129		2158	171
	D	OVRFLW		OVRFLW		OVRFLW		OVRFLW		2686372		3421	223
	E	OVRFLW		OVRFLW		OVRFLW		4364153		2076538		2237	203
	F	OVRFLW		OVRFLW		OVRFLW		4258427		1985165		1390	179
	G	OVRFLW		OVRFLW		OVRFLW		3064471		1396647		712	159
	H	OVRFLW		OVRFLW		OVRFLW		2986235		1383461		846	127

Figure 50: DnaK Direct-Biotinylated LOD Trial #2
Direct-biotinylated ELISA LOD trial (#2) for recDnaK. The recDnaK antigen concentrations were plated from left to right (indicated by top black arrow), in decreasing concentration. The recDnaK antigen was diluted in coating buffer using a 1:2 serial dilution series, starting at 2,500 ng/mL. The entire plate was blocked with a 3%BSA (in PBST) blocking solution. 2%BSA/PBST was used as the "standard diluent". The MAB (purified, biotinylated DnaK Clone A) was diluted in the "standard diluent". The MAB dilutions were added from top to bottom (indicated by left side black arrow) at dilutions of 1:2,500, 1:5,000, 1:10,000, and 1:20,000 (1:2 serial dilution series). The strep-HRP conjugate was diluted at a final concentration of 2 µg/mL in 0.4%BSA/PBST diluent. Only the first read (20 ms) data are presented.

Table 6: DnaK Direct-Biotinylated ELISA LOD Trial #3 Raw Data
Raw data "sample" values for direct-biotinylated ELISA LOD trial (#3) for DnaK. All antigen concentrations are shown in µg/ 100 µL (top colored row) and ng/mL (bottom colored row). The recDnaK antigen was diluted in coating buffer using a 1:2 serial dilution series, starting at 78.125 ng/mL. The MAB (purified, biotinylated DnaK Clone A) dilutions (1:1,000, 1:2,500, 1:5,000,

and 1:10,000) are indicated as well. The table depicts a checkerboard titration assay of the recDnaK antigen and MAB dilutions. Only the first read (20 ms) data was used for table.

		Antigen Concentrations									
		0.0078125	0.00390625	0.001953125	0.000976563	0.000488281	0.000244141	0.00012207	0.000061035	Blank (NO AG)	µg/100µL
		78.125	39.0625	19.53125	9.76563	4.88281	2.44141	1.2207	0.61035	0	ng/mL
MAB Dilutions	1:1000	1896014.500	850625.500	373253.000	150047.000	55430.000	39546.500	26681.000	13432.500	19556.500	
	1:2500	1525062.000	663996.500	291101.000	114126.500	39127.000	21564.000	12498.500	6811.000		
	1:5000	1196721.000	529141.000	241957.000	89639.500	29785.000	16390.000	7421.000	3481.500		
	1:10,000	1032492.500	447150.500	187810.000	74312.500	22159.500	10257.000	4471.000	1731.000		

Table 7: Mpt32 Direct-Biotinylated ELISA LOD Trial #1 Raw Data

Raw data "sample" values for direct-biotinylated ELISA LOD trial for Mpt32. All antigen concentrations are shown in µg/ 100 µL (top colored row) and ng/mL (bottom colored row). The nMpt32 antigen was diluted in coating buffer using a 1:2 serial dilution series, starting at 78.125 ng/mL. The MAB (purified, biotinylated Mpt32 Clone B, "wash 3") dilutions (1:1,000, 1:2,500, 1:5,000, and 1:10,000) are indicated as well. The table depicts a checkerboard titration assay of the nMpt32 antigen and MAB dilutions. Only the first read (20 ms) data was used for table.

		Antigen Concentrations									
		0.0078125	0.00390625	0.001953125	0.000976563	0.000488281	0.000244141	0.00012207	0.000061035	Blank (NO AG)	µg/100µL
		78.125	39.0625	19.53125	9.76563	4.88281	2.44141	1.2207	0.61035	0	ng/mL
MAB Dilutions	1:1000	5218346.500	2523592.000	1237025.000	546045.000	218748.500	98639.500	37717.000	11632.000	145.000	
	1:2500	4438220.500	2161082.000	1043349.000	468096.500	192214.000	85528.000	32317.500	10171.000		
	1:5000	3401375.000	1631340.500	793811.000	344309.000	153806.500	65146.500	24893.500	8033.000		
	1:10,000	2474507.500	1184908.000	572535.500	252821.500	103494.000	42304.500	15793.000	5188.500		

Table 8: GroES Direct-Biotinylated ELISA LOD Trial #1 Raw Data

Raw data "sample" values for direct-biotinylated ELISA LOD trial for nGroES. All antigen concentrations are shown in µg/ 100 µL (top colored row) and ng/mL (bottom colored row). The nGroES antigen was diluted in coating buffer using a 1:2 serial dilution series, starting at 78.125 ng/mL. The MAB dilutions (1:1,000, 1:2,500, 1:5,000, and 1:10,000) are indicated as well. The table depicts a checkerboard titration assay of the nGroES antigen and MAB dilutions. Only the first read (20 ms) data was used for table. Purple highlighted box indicates an OVRFLW value (> 5,800 000 RLUs).

		Antigen Concentrations									
		0.0078125	0.00390625	0.001953125	0.000976563	0.000488281	0.000244141	0.00012207	0.000061035	Blank (NO AG)	µg/100µL
		78.125	39.0625	19.53125	9.76563	4.88281	2.44141	1.2207	0.61035	0	ng/mL
MAB Dilutions	1:1000	5800001.000	2933973.500	1360326.500	622200.000	251564.000	106301.000	43721.500	16805.000	3066.500	
	1:2500	4360192.000	2277244.500	1053806.000	480793.500	200778.000	80257.500	30941.000	12762.000		
	1:5000	2762796.000	1601945.500	739262.000	343851.500	140525.000	54045.500	20255.000	7391.000		
	1:10,000	1603571.000	952007.500	463554.500	207073.000	87466.000	33260.000	11670.500	4413.000		